Chemistry

BULLETIN
OF THE
CHEMICAL SOCIETY OF JAPAN

CHEMISTRY HALL LIBRARY

Vol. 32 No. 4 April 1959

CONTENTS

General and Physical

A. SHIMADA: Crystal Structure and Lattice Energy of *i*-Erythritol. I. Crystal Structure of *i*-Erythritol 325

A. SHIMADA: Crystal Structure and Lattice Energy of *i*-Erythritol. II. Lattice and Hydrogen Bond Energies for *i*-Erythritol. 330

C. V. SURYANARAYANA and S. ALAMELU: Electrical Conductance of Concentrated Aqueous Solutions of Copper Sulfate 333

M. NAKAGAKI and K. OSAGAWA: Penetration of Liquids into Filter Paper Used in Paper Chromatography 344

K. KODERA and Y. ONISHI: The Molecular Cross-sectional Areas for the Determination of Specific Surface Areas of Solids. I. Carbon Black 356

H. TAKAHASHI: Effects of Dry Grinding on Talc 374

H. TAKAHASHI: Wet Grinding on Kaolin Minerals 381

K. TAKIYAMA: Formation and Aging of Precipitates. XI. An Electron Micro-Diffraction Study on Nucleation of Barium Sulfate Precipitate from Homogeneous Solution 387

M. MURAMATSU: Studies on the Interaction of Surface Films with Solute in Solution. V. Deposition of Monolayers of Several Amphipathic Compounds from Surface of Aqueous Solutions of Congo Red and Crystal Violet 391

N. MATAGA, K. NISHIMOTO and S. MATAGA: Remarks on the Molecular Calculation of Naphthalene and Anthracene 395

R. MATUURA, H. KIMIZUKA, S. MIYAMOTO, R. SHIMOZAWA and K. YATSUNAMI: The Study of Adsorption of Detergents at a Solution-Air Interface by Radiotracer Method. II. The Kinetics of Adsorption of Sodium Alkyl Sulfates. 404

Analytical and Inorganic

N YAMAGATA, T YAMAGATA and S. MATSUDA: The Different Distribution of Rubidium and Cesium in Natural Plants 407

Organic and Biological

T. ABE: Substituent Effects on the Ultraviolet Absorption Spectrum of 1,3,5-Trinitrobenzene in Some Solvents 339

S. KAKIMOTO: The Aconite Alkaloids. XXIV. Oxidation of Miyaconitine and Miyaconitinone. 349

H. SUGINOME and S. KAKIMOTO: The Aconite Alkaloids. XXV. Selenium Dehydrogenation of Miyaconitinone and Lucidusculine 352

H. SUGINOME and S. FURUSAWA: The Aconite Alkaloids. XXVI. On Lucaconine and Monoacetyllucaconine 354

(Continued on inside cover)

Published by the Chemical Society of Japan

THE CHEMICAL SOCIETY OF JAPAN

(NIPPON KAGAKUKAI)

Founded in 1948

Successor to the former Chemical Society of Japan founded in 1878 and to the Society of Chemical Industry, Japan founded in 1898.

OFFICERS

Munio KOTAKE, *President*, Osaka University, Osaka
Shin-ichiro FUJISE, *Vice-President*, Tohoku University, Sendai
Taro HAYASHI, *Vice-President*, Ochanomizu Women's University, Tokyo
Tokuichi TSUMAKI, *Vice-President*, Kyushu University, Fukuoka
Kenichi YAMAMOTO, *Vice-President*, Waseda University, Tokyo

BULLETIN OF THE CHEMICAL SOCIETY OF JAPAN

Editor: Yoshiyuki URUSHIBARA, The University of Tokyo, Tokyo
Assistant Editor: Kazuo SAITO, The University of Tokyo, Tokyo
Editorial Board:

Rempei GOTOH	Kei MATSUZAKI	Tadao SHIBA
Hiroshi HAMAGUCHI	Saburo NAGAKURA	Osamu SIMAMURA
Genjiro HAZATO	Hiroshi NOZAKI	Mutsuaki SHINAGAWA
Isao ICHISHIMA	Seizo OKAMURA	Tatsuo TAKESHIMA
Masaji KUBO	Tunetaka SASAKI	Sumio UMEZAWA
Hisao KUROYA	Tetsuro SEIYAMA	

(*Continued from outside cover*)

K. NAIKI: Studies on 3-(Anthraquinon-1-yl)oxazolidin-2-ones. I. 3-(Methylanthraquinon-1-yl)oxazolidin-2-ones and Their Related Compounds 331
S. NAGAHAMA, H. KOBAYASHI and **S. AKIYOSHI**: Polyterpenes. II. Oxidation of Thujopsene with Lead Tetra-acetate 363
M. FUJIMOTO: Phenothiazine Derivatives. V. Synthesis of Hydroxyphenothiazines. 371
S. FURUSAWA: The Aconite Alkaloids. XXVII. On Lucaconine 399
K. MORITA: Stereochemistry of Some Steroidal Ketones. 411

Applied

S. MOCHIDA, I. KAWASAKI and **Y. NISHIMURA**: Changes of Dynamic Properties of Some Kaolin Minerals by Heat-treatment 319
Y. TSUDA: Heat of Solution of Methanolized Cellulose 372

Short Communications

K. NARITA and **K. MORI**: Crystal Structures of Silicon Nitride 417
H. SHIMIZU, M. KATAYAMA and **S. FUJIWARA**: Chemical Shifts of Proton Resonance and Mesomeric Effects in Substituted Benzene. 419
T. FUKUDA: The Poisoning Effect of Lead Acetate and Quinoline 420
T. AMIYA: Isomerization of Luciculine 421
N. SHIBATA and **K. YOSHIHARA**: Preparation of Chromium-51 of a High Specific Activity by the Szilard-Chalmers Process 422
H. HIRAOKA: Self-diffusion of Benzene under Pressure 423

CHEMISTRY HALL LIBRARY

Changes of Dynamic Properties of Some Kaolin Minerals by Heat-treatment

By Shigeru MOCHIDA, Isao KAWASAKI and Yoichi NISHIMURA

(Received July 18, 1958)

In general, ceramic products are made by heating clay mineral at a high temperature in order to utilize its strength and hardness. In some cases, however, moderate abrasion as well as strength and hardness are required where clay mineral is used at the meta-stable state in the process of its structural changes, different from the general conception of ceramic products. It is therefore, important to study changes of dynamic properties of clay mineral when it is heated at a relatively low temperature region, and this study aims at clarifying the characteristics of the results of heat-treatment in air-tight and carbon dioxide atmosphere.

Mutual relationship between changes of dynamic properties, densities and structures of some kaolin minerals was investigated when they were heated in a closed vessel. On the dynamic properties, the Young's modulus and bending strength, and on the physical properties, bulk density and density were measured.

At the same time, the relationship between changes of dynamic properties and structures was partly tested by X-ray diffraction method. The results of Kibushi-clay heated in a closed vessel were compared with the results when it was heated in the open air.

Samples.—The following kaolin minerals were used in this study: Shidare-Kibushi clay from Shidare, Gifu, Japan; Yagusa-Kibushi clay from Yagusa, Aichi, Japan; Naegi-Kaolin from Naegi, Gifu, Japan; and Hongkong-Kaolin from Hongkong.

By the X-ray diffraction method, any of them excepting Hongkong-Kaolin is a kaolin mineral of fireclay type[1] and contains a small quantity of quartz in spite of being elutriated. Shidare-Kibushi clay contains a small quantity of organic matter as an impurity. Hongkong-Kaolin is halloysite with a high crystallinity[2]. The results of chemical analysis of the four samples which have been elutriated are shown in Table I.

In differential thermal analysis curves of all samples, the endothermic peak was reached due to the loss of inter-layer water between 100 and 200°C and to the loss of structural water between 400 and 500°C. The exothermic peak was reached at about 950°C corresponding to the structural change to mullite.

TABLE I
CHEMICAL ANALYSIS OF SOME KAOLIN MINERALS

Component	Shidare-Kibushi	Yagusa-Kibushi	Naegi-Kaolin	Hongkong-Kaolin
SiO_2	48.76	50.29	47.48	46.78
TiO_2	0.77	0.23	0.01	tr.
Al_2O_3	34.53	33.13	37.59	35.62
Fe_2O_3	1.50	2.10	0.40	0.46
MnO	0.00	tr.	0.00	tr.
CaO	0.27	0.24	0.11	0.81
MgO	0.20	0.64	0.02	0.63
K_2O	0.34	1.51	1.61	1.16
Na_2O	0.19	0.58	0.16	1.11
Ig·Loss	13.43	11.40	12.45	13.27
Total	99.99	99.82	99.83	99.84

All samples were elutriated, roll-milled with a proper amount of water and extruded into rods of about 3.5 mm. in diameter by a press. Each sample prepared as mentioned above was dried at 100°C in a drying oven for 24 hours. The samples were heated in an air-tight graphite crucible, the temperature of which is raised by 5°C per minute in an electric furnace with siliconit heaters, and then they were cooled down naturally in the crucible taken out of the furnace after having constantly been heated therein at a given temperature for an hour. In the case of heat-treatment in the open air, samples were heated in a porcelain crucible with many holes under the same conditions as in the case of the air-tight crucible. The temperatures of heat-treatment in both cases were 500, 800, 900, 1000, 1050, 1100, 1150, 1200 and 1250°C.

Experimental

Young's Modulus. — Young's modulus was measured in a cramp-free state by loading at a non-fixed end. It was calculated by the following equation[3]:

$$\text{Young's modulus} = (4l^3/\pi a^4 e)\,P/3$$

where l, distance between the fixed point and the loaded point = 10 cm.; P, load = 980 dynes; a, radius of sample (cm.); and e, length of strain (cm.).

1) G. W. Brindley and K. Robinson, *Trans. Faraday Soc.*, **42B**, 198 (1946).
2) G. Honjo and K. Mihama, *Acta Cryst.*, **7**, 511 (1954), and H. Takahashi, This Bulletin, **31**, 275 (1958).
3) Y. Tani, "Experimental Elasticity", (Iwanami Koza) V. F. 30 (1939).

TABLE II
BULK DENSITY OF SOME KAOLIN MINERALS

Temp. °C	Shidare-Kibushi		Yagusa-Kibushi	Naegi-Kaolin	Hongkong-Kaolin
100	1.72	open	1.92	1.86	1.68
500	1.64	1.58	1.88	1.78	1.63
800	1.64	1.61	1.80	1.72	1.55
900	1.72	1.76	1.95	1.88	1.63
1000	1.74	1.82	2.04	1.92	1.65
1050	1.86	2.03	2.37	2.14	1.74
1100	2.02	2.49	2.43	2.31	1.88
1150	2.34	2.46	2.43	2.44	2.13
1200	2.37	2.45	2.08	2.50	2.15
1250	2.44	2.39	—	—	—

TABLE III
DENSITY OF SOME KAOLIN MINERALS

Temp. °C	Shidare-Kibushi		Yagusa-Kibushi	Naegi-Kaolin	Hongkong-Kaolin
100	2.629	open	2.629	2.61	2.58
500	2.537	2.505	2.598	2.59	2.57
800	2.572	2.574	2.577	2.56	2.58
900	2.591	2.687	2.685	2.66	2.61
1000	2.672	2.695	2.716	2.68	2.66
1050	2.670	2.699	2.671	2.70	2.67
1100	2.675	2.688	2.647	2.66	2.68
1150	2.651	2.654	2.684	2.64	2.69
1200	2.662	2.669	2.613	2.66	2.69
1250	2.637	2.653	—	—	—

TABLE IV
YOUNG'S MODULUS ($\times 10^{11}$ dyne/cm^2)

Temp. °C	Shidare-Kibushi		Yagusa-Kibushi	Naegi-Kaolin	Hongkong-Kaolin
100	0.525	open	—	—	—
500	1.66	1.78	1.88	1.75	1.02
800	1.63	2.01	2.34	2.00	1.10
900	2.19	2.98	3.25	2.65	1.47
1000	2.52	3.58	4.40	2.83	1.56
1050	3.68	4.82	5.00	3.44	2.01
1100	4.85	5.91	5.92	5.08	2.85
1150	5.75	6.80	6.20	5.78	4.50
1200	6.05	7.18	5.92	6.53	4.27
1250	6.62	6.00	—	—	—

TABLE V
BENDING STRENGTH (g./mm^2)

Temp. °C	Shidare-Kibushi		Yagusa-Kibushi	Naegi-Kaolin	Hongkong-Kaolin
100	1300	open	1620	1490	470
500	2320	5140	2660	3260	1050
800	5100	6490	6950	5990	2570
900	5950	7970	8210	8110	3840
1000	7030	7720	8960	7720	4240
1050	8360	8130	12600	9040	6000
1100	10770	12900	17690	11130	6860
1150	12030	12920	17670	14600	9770
1200	13800	13350	11390	17500	9300
1250	14600	12600	—	—	—

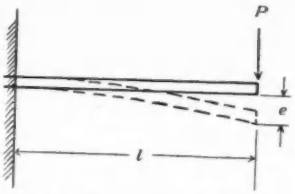

Fig. 1. Measuring procedure of Young's modulus.

Bending Strength. — Although a bending strength does, in an exact sense, not always mean a physical value, it is practically used as a breaking strength in industries. By supporting a sample on two knife edges, continuously loading on the middle of the sample and reading the weight of the load just breaking the sample the bending strength was calculated by the following equation[4]:

$$\text{bending strength} = 8Pl/\pi d^3$$

where P, weight of load just breaking the sample (g.); l, distance between two supporters 60 mm. and d, diameter of sample (mm.).

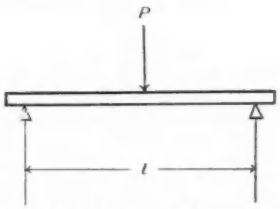

Fig. 2. Measuring procedure of bending strength.

Density. — The sample was ground into a powder finer than 200-mesh and its density was measured by a picnometer in mono-chlorbenzene at 25°C.

Results

Bulk Density.—The value of bulk density is shown in Table II and Fig. 3, and there is the minimum point at about 800°C in each curve, except that the temperature corresponding to the minimum point of bulk density of Shidare-Kibushi clay heated in the open air moves down to about 500°C and its maximum point appears at about 1150°C.

Density.—As shown in Table III and Fig. 4, there is a minimum point between 500 and 800°C and a maximum point at about 1000°C in each curve of the density. Beyond 1000°C the density decreases gradually.

Young's Modulus.—As shown in Table IV and Fig. 5, the Young's modulus increases rapidly beyond 800°C and a maximum value is shown between 1100 and 1200°C.

Bending Strength.—As shown in Table V and Fig. 6, beyond 800°C the bending strength increases gradually and beyond 1000°C, it increases

4) Japanese Industrial Standard (JIS), S-6005, 4 (1955).

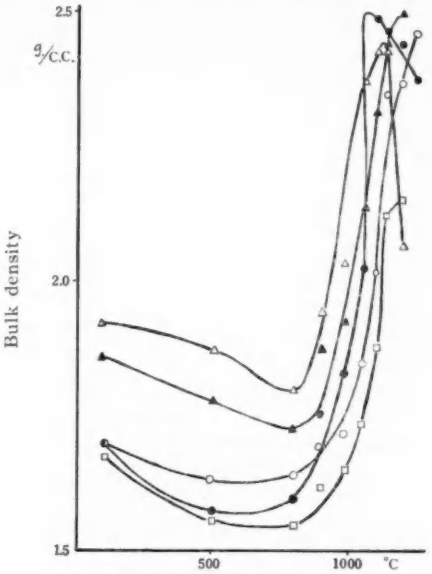

Treated temperature

Fig. 3. Curves showing the changes of bulk density in the various stages of heat-treatment.

- ○ Shidare-Kibushi
- ● Shidare-Kibushi (open)
- △ Yagusa-Kibushi
- ▲ Naegi-Kaolin
- □ Hongkong-Kaolin

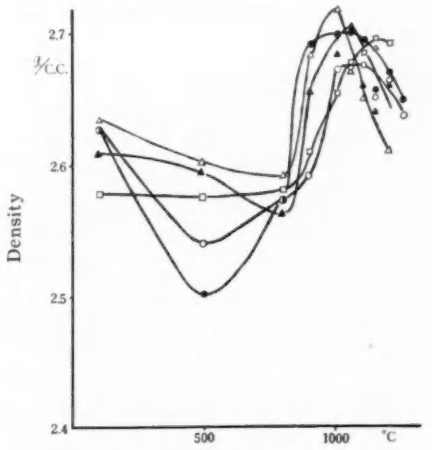

Treated temperature

Fig. 4. Curves showing the changes of density in the various stages of heat-treatment.

- ○ Shidare-Kibushi
- ● Shidare-Kibushi (open)
- △ Yagusa-Kibushi
- ▲ Naegi-Kaolin
- □ Hongkong-Kaolin

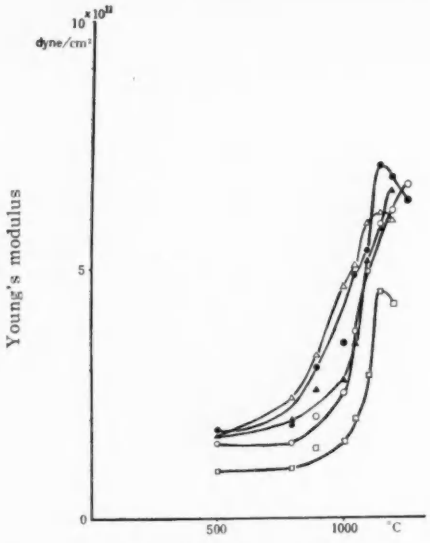

Treated temperature

Fig. 5. Curves showing the changes of Young's modulus in the various stages of heat-treatment.
- ○ Shidare-Kibushi
- ● Shidare-Kibushi (open)
- △ Yagusa-Kibushi
- ▲ Naegi-Kaolin
- □ Hongkong-Kaolin

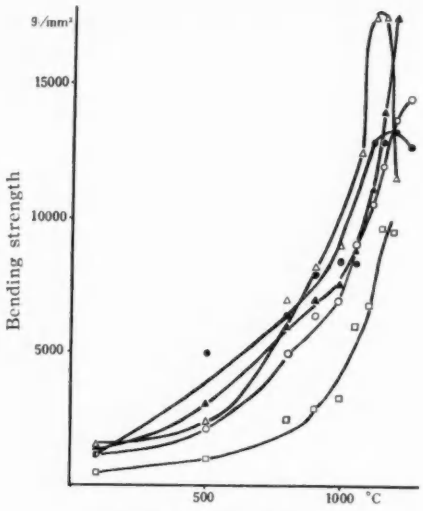

Treated temperature

Fig. 6. Curves showing the changes of bending strength in the various stages of heat-treatment.
- ○ Shidare-Kibushi
- ● Shidare-Kibushi (open)
- △ Yagusa-Kibushi
- ▲ Naegi-Kaolin
- □ Hongkong-Kaolin

rapidly. In both cases, there are maximum values and, after reaching the maximum values, it decreases rapidly.

Discussion

Even clay minerals, which belong to the same "kaolin" group, differ from one another according to their kinds in regard to the bending strength and Young's modulus. There are many factors, for example, particle sizes, structural characteristics, impurities, etc., which influence the dynamic properties of kaolin minerals.

As only four samples were experimented with in regard to their dynamic properties, it is difficult to discuss and to relate the results of their dynamic properties with the results of chemical analysis. The effects of the impurity contained in kaolin mineral on the dynamic properties are studied now and their results will be reported in future.

In this paper, some relationships between the dynamic properties and the structural characteristics are discussed. The changes of the dynamic properties by heat-treatment beyond a certain temperature are not continuative but are abrupt. In the heat-treated specimens of Yagusa-Kibushi clay, for example, the bending strength increases to only 2000 g./mm² between 800 and 1000°C and as much as 8000 g./mm² between 1000 and 1100°C, but decreases rapidly between 1100 and 1200°C. Also, the Young's modulus and even density take a similar tendency. These phenomena seem to be attributed to the changes of crystal structures in clay minerals. Therefore, those causes which affect the changes of dynamic properties may be due to the following:

1. Change of plasticity of kaolin mineral by heating at an early stage.
2. Change of crystal structure of kaolin mineral and transformation of its macrostructure caused by the change of crystal structure by heating at a later stage.
3. Sintering.

Now, the value expressed by percentage which is obtained by dividing a bulk density by a density is called "filling ratio". The dynamic properties and the filling ratio will be discussed. As shown in Table VI and Fig. 7, the minimum value of filling ratio appears, generally speaking at the temperatures between 500 and 800°C. The changes of the filling ratio

TABLE VI
FILLING RATIO (PERCENTAGE)

Temp. °C	Shidare-Kibushi		Yagusa-Kibushi	Naegi-Kaolin	Hongkong-Kaolin
100	65.3	open	73.9	72.0	65.2
500	64.4	63.2	71.8	68.2	63.3
800	64.0	62.6	70.0	67.2	60.2
900	66.2	65.8	72.5	70.7	63.9
1000	65.2	67.7	74.9	71.7	62.1
1050	70.0	75.2	88.8	79.3	65.0
1100	75.5	92.5	91.7	86.8	72.5
1150	88.0	92.5	90.5	91.6	79.2
1200	89.0	91.8	82.7	93.8	80.6
1250	92.6	90.2	—	—	—

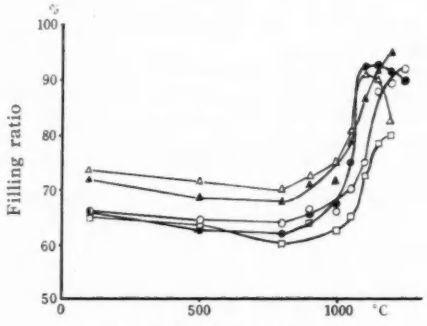

Fig. 7. Curves showing the changes of filling ratio in the various stages of heat-treatment.
○ Shidare-Kibushi
● Shidare-Kibushi (open)
△ Yagusa-Kibushi
▲ Naegi-Kaolin
□ Hongkong-Kaolin

may be due to the following. In the early stage of heating, the sample loses interlayer water. At the temperatures between 500 and 800°C, it has the minimum filling ratio, because it becomes porous owing to the loss of structural water while the shrinkage caused by sintering does not keep pace with it. Beyond 800°C, it is in the state of "meta-kaolin" and its filling ratio is recovered gradually between 800 and 1000°C, because the shrinkage by sintering is larger than the loss of structural water.

The Young's modulus changes a little until it reaches 800°C, but as soon as the temperature exceeds 800°C, the Young's modulus begins to increase in company with filling ratio. This indicates that the Young's modulus increase is accompanied by the sintering. The filling ratio increases rapidly beyond 1000°C which may be due not only to the sintering but also to the commencement of the structural changes of the kaolin minerals[5]. This rapid increase of the filling ratio has influence on the bending strength and the Young's modulus.

The temperature at which crystallization begins varies a little according to the kinds of kaolin mineral. That is to say, in the case of Yagusa-Kibushi clay, the Young's modulus begins to increase just beyond 1000°C, but in the case of Shidare-Kibushi clay and Naegi-Kaolin, it does at higher temperature. In the case of Hongkong-Kaolin, it begins to increase rapidly beyond 1050°C. However, when the temperature of heat-treatment rises up to a certain point along with the development of crystallization, the filling ratio does not increase but begins to decrease and, at the same time, the bending strength and the Young's modulus also are inclined to decrease. This may be explained as follows.

In the case of Shidare-Kibushi clay, the filling ratio continues to increase until 1250°C together with the bending strength and Young's modulus, which may be caused, to a great extent, by the sintering and the commencement of crystallization. Crystals of mullite and α-cristobalite do not yet grow at 1050°C, but they appear at 1200°C. In the case of Yagusa-Kibushi clay, the Young's modulus increases rapidly beyond 1000°C, and reaches the maximum value between 1100 and 1200°C. However, at 1200°C the Young's modulus apparently starts to decrease according to the decrease of the filling ratio. Moreover, the characteristics of the sample heated at 1200°C shows a distinguished expansion in diameter.

X-ray diffraction data will be discussed below. As shown in Fig. 8, in the case of Shidare-Kibushi clay, mullite begins to

5) W. F. Bradley and R. E. Grim, *Am. Mineral*, **36**, 182 (1951).

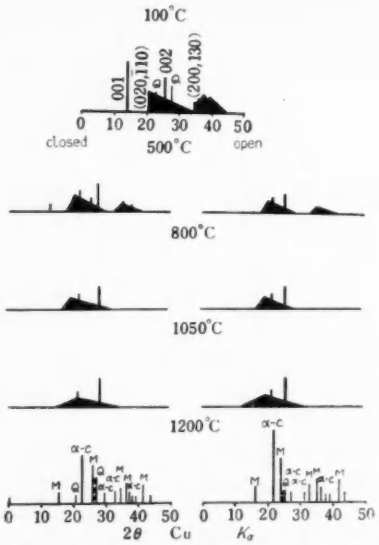

M: mullite, α-c: α-cristobalite, Q: quartz

Fig. 8. Schematic drawings of the X-ray diffractometer traces of heat-treated specimens of Shidare-Kibushi clay.

grow at about 1050°C. At about 1200°C, the crystallization to mullite is distinguishable and the quartz of impurity changes to α-cristobalite. Therefore, it is considered that when this clay begins to crystallize and its filling ratio increases rapidly owing to sintering, both the bending strength and the Young's modulus increase together. However, when the crysrallizations to mullite and α-cristobalite are remarkable, cracks grow along the crystals, and therefore, the filling ratio and bending strength together with the Young's modulus are reduced.

The difference between the heat-treatment in a closed vessel and in the open air will be discussed. In general, Kibushi clay changes at the lower temperature when heated in the open air. This may be clearly seen from the X-ray diffraction diagrams of the heat-treated specimens of Shidare-Kibushi clay shown in Fig. 8. That is, in the heat-treatment in a closed vessel, two reflections, (001) and (002), are clearly left at 500°C although their intensities are weaker, while in the heat-treatment in the open air, the reflections are thoroughly extinguished at the same temperature. The X-ray diffraction diagram of the 1100°C heat-treated specimen in the open air is almost exactly similar to that of the specimen heated at 1200°C in a closed vessel.

Summary

When kaolin mineral is heat-treated at a relatively low temperature region, its density has the minimum value between 500 and 800°C and the maximum at about 1000°C.

The value of dynamic properties of kaolin mineral increases slightly until about 800°C but increases rapidly beyond 1000°C to reach the maximum value. Then, the value is inclined to decrease rapidly beyond the temperatures, at which the maximum value is yielded. Similarly, the filling ratio also has the minimum value at about 800°C and increases rapidly beyond 1000°C to reach the maximum value. This indicates that when kaolin mineral is heat-treated at a relatively low temperature region, its dynamic properties have a close relation with its filling ratio. It is considered that these phenomena are due not only to the sintering of clay mineral by heat-treatment but also to the structural changes as shown in X-ray diffraction data.

The changes of dynamic and physical properties and of the structures of kaolin mineral heated in a closed vessel take place later than those heated in the open air. It may be due to the fact that the oxidation of the organic matters contained in kaolin mineral is oppressed in a closed vessel.

The writers wish to express their sincere thanks to Dr. Hiroshi Takahashi of the University of Tokyo for his valuable advice and assistance throughout this work.

Tombow Pencil Mfg. Co., Ltd.
Toshima, Kita-ku, Tokyo

*Crystal Structure and Lattice Energy of i-Erythritol. I. Crystal Structure of i-Erythritol**

By Akira SHIMADA

(Received August 13, 1958)

i-Erythritol ($CH_2OH \cdot C^*HOH \cdot C^*HOH \cdot CH_2OH$) is one of the polyalcohols, which has a close relationship with carbohydrates. Hence a knowledge of its stereochemical configuration would be of great interest and importance to the chemistry of carbohydrates. The molecule of this compound is built up of two and, in a sense, identical groups, each of which has an asymmetric carbon atom, C*, as indicated in the above chemical formula. It has already been reported that in the crystal of this substance these two identical groups are related to each other by a center of symmetry[1,2]. However, the detailed spatial configuration of this molecule still remains unexplored.

Interesting roles of the hydrogen bond have been elucidated for pentaerythritol in connection with its thermal and electrical properties[3-8]. Therefore, it seems highly promising to make an attempt to find out what types of hydrogen bond are linking molecules together in the crystal of *i*-erythritol, in order to understand some physical properties of this crystal.

Experimental

i-Erythritol crystallizes in the tetragonal bipyramidal class. Crystals were prepared by the slow evaporation of the solution in a mixture of ethyl alcohol and water. They were ground to cylindrical rods, elongated parallel to the [001] or [010] axis; their diameters are less than 0.4 mm. All photographs were taken with Cu K_α radiation. The crystal has been shown by the previous workers[1,2] to possess the space group symmetry $C_{4h}^6-I4_1/a$, with eight molecules in the unit cell. This assignment of the space group was verified by oscillation and Weissenberg photographs in the present experiment, and a redetermination of the unit cell dimensions gave the following values.

$$a=12.81\pm0.03\ \text{Å} \qquad c=6.81\pm0.02\ \text{Å}$$

The axial ratio $c/a=0.532\pm0.003$ as deduced from these lattice constants will give $c/\sqrt{2}\ a=0.376\pm0.002$ if we refer to the old choice of the crystallographic axes*, which is in excellent agreement with the goniometric value 0.3762[9]. Assuming eight molecules in the unit cell with the dimensions given above, the density is calculated to be 1.45 ± 0.01 g./cc., which is in good harmony with the value, 1.450 g./cc., reported by Schröder[10].

The ($hk0$) and ($h0l$) intensity data were estimated visually from multiple-film Weissenberg photographs. They were corrected for the Lorentz and polarization factors, using Cochran's chart[11]. Correction was applied to the absorption in the usual way, although this was found to be very small (absorption coefficient $\mu=12.7$ cm^{-1}). The observed structure ampliudes were first set on to an absolute scale using Wilson's method[12] which were further improved during the later stages of refinement.

Structure Determination

The unit cell contains only eight molecules, that is, sixteen C, sixteen C*, sixteen O_1 and sixteen O_2 atoms, suggesting that the center of gravity of each molecule must occupy a special position in the unit cell. In accord with the conclusion[1,2] already derived from a preliminary consideration of intensities of certain principal planes, it was confirmed that each molecule was situated at a center of symmetry. Hence each atom occupies the general positions given by,

* The major part of this paper was read at the 7th Annual Meeting of the Chemical Society of Japan, April, 1954. A short communication is now in press in Acta Crystallographica, and the present account describes the structure analysis in detail.

1) W. G. Burgers, *Phil. Mag.*, (7) **1**, 289 (1926).
2) N. Schönfeldt, K. Hermann und O. Hassel, *Z. physik. Chem.* (A) **124**, 305 (1926).
3) I. Nitta and T. Watanabé, *Nature*, **140**, 365 (1937); *Sci. Papers Inst. Phys. Chem. Research*, **34**, 1669 (1938).
4) F. J. Llewllyn, E. G. Cox and T. H. Goodwin, *J. Chem. Soc.*, **1937**, 883.
5) I. Nitta, S. Seki and M. Momotani, *Proc. Japan Acad.*, **26**, (9) 25 (1950).
6) I. Nitta, S. Seki, M. Momotani, K. Suzuki and S. Nakagawa, ibid., **26**, (10) 11 (1950).
7) I. Nitta, T. Watanabé, S. Seki and M. Momotani, ibid., **26**, (10) 19 (1950).
8) R. Kiriyama, S. Yabumoto and I. Nitta, This Bulletin, **27**, 115 (1954).
9) P. Groth, "Chemische Krystallographie", Engelmann, Leipzig (1906), part III, p. 240.

* The old axes are such that the z axis is unchanged and the x axis is the diagonal of the basal plane of the new unit cell.

10) Schröder, *Ber.*, **12**, 562 (1879).
11) W. Cochran, *J. Sci. Instr.*, **25**, 253 (1948).
12) A. J. C. Wilson, *Nature*, **150**, 152 (1942).

$$(0,0,0;\ 1/2,1/2,1/2)+$$
$$x,y,z;\ \bar{x},1/2-y,z;\ 3/4-y,1/4+x,1/4+z;$$
$$1/4+y,1/4-x,1/4+z;$$
$$\bar{x},\bar{y},\bar{z};\ x,1/2+y,\bar{z};\ 1/4+y,3/4-x,3/4-z;$$
$$3/4-y,3/4+x,3/4-z$$

Because of the short c axis, it was expected that an approximate structure might appear in an electron density projection on the (001) plane, without complication due to overlappings of atoms. Since a molecule contains only lighter atoms, a Patterson projection $P(uv)$ on the (100) plane, shown in Fig. 1, did not give any useful information about the location of each atom. Hence, an attempt was made to solve the structure with a minimum function[13] derived from this Patterson projection. In order to get a minimum function, a location of rotation peaks must be determined and various minimum functions were tried, regarding acceptable peaks in the Patterson function as the possible image-seeking vectors. The location of rotation peaks, marked by a cross in the Patterson function, gave the most promising minimum function $M_4(xy)$ as shown in Fig. 2. Another approarch to the clue to an approximate structure was obtained by the inequality method[14] using Sakurai's chart[15], and the signs of five out of fifty-two observed reflections could be determined. The first Fourier map prepared with these terms, given in Fig. 3, shows a good resemblance to the minimum function $M_4(xy)$.

Based on these two promising figures, an effort was made to locate each atom at each peak by trial and error method. Starting from the approximate structure projected on the (001) plane, the structure was refined by successive Fourier syntheses with the aid of difference syntheses at later stages. The final Fourier

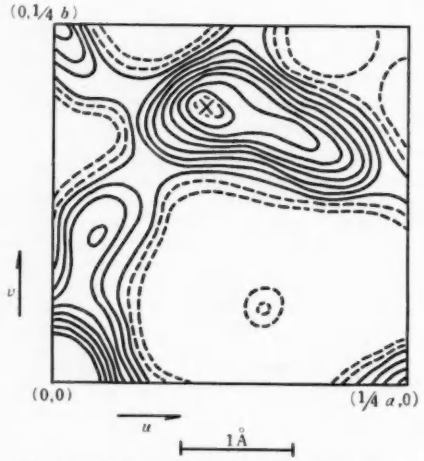

Fig. 1. Patterson projection $P(uv)$ onto (001) with contours at arbitrary intervals.

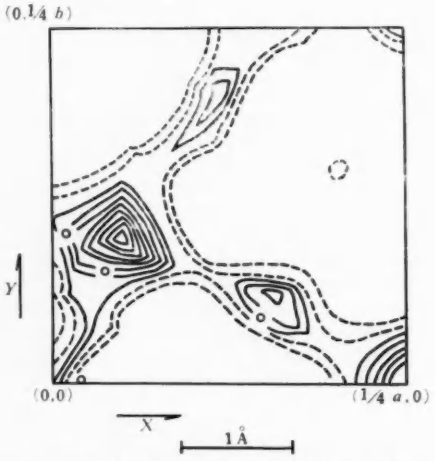

Fig. 2. Minimum function $M_4(xy)$ with contours at arbitrary intervals. Circles indicate the location of atoms corresponding to Fig. 4.

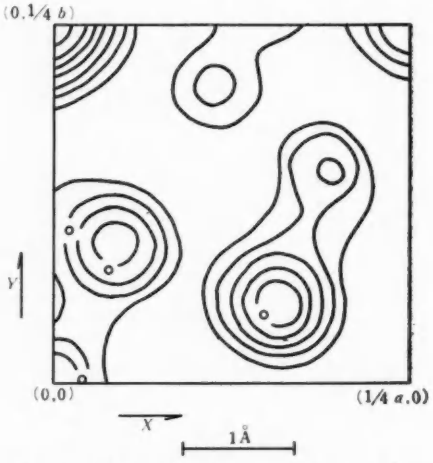

Fig. 3. First Fourier projection onto (001) prepared by inequality method with contours at arbitrary intervals. Circles indicate the location of atoms corresponding to Fig. 4.

13) M. J. Burger, *Acta Cryst.*, **4**, 531 (1951).
14) D. Harker and J. S. Kasper, ibid., **1**, 70 (1948).
15) K. Sakurai, ibid., **5**, 546 (1952).

projection on the (001) plane is shown in Fig. 4. The reliability index $R=(\Sigma||F_o|-|F_c||)/\Sigma|F_o|$ for $(hk0)$ spectra is reduced to 16.5%, the contributions from hydrogen atoms being excluded. Several plausible configurations of the molecule were derived from the Fourier projection on the (001) plane with the aid of the Patterson projection $P(uw)$ on the (010) plane, which is shown in Fig. 5. They were put to the test by the comparison of observed and calculated structure factors for $(h0l)$ spectra. One of these configurations led to an approximately good agreement between the observed and the calculated structure factors, so as to give an approximate value of z for each atom. Since the symmetry of the crystal is high, there are considerable overlappings of atoms in the (010) projection which make it difficult to refine x, y and z values by successive Fourier syntheses alone. We were able to overcome this difficulty by preparing difference syntheses with the coefficients F_o-F_c', where F_c' stands for the structure factor calculated by means of the coordinates of the atoms, the peaks of which were well resolved but equivalent peaks were overlapped by other atoms by the symmetry operations. The usual difference syntheses were also tried at later stages to refine the structure. The electron density projection on the (010) plane is shown in Fig. 6. The reliability index R for $(h0l)$ spectra is found to be 13.3%*, the contributions from

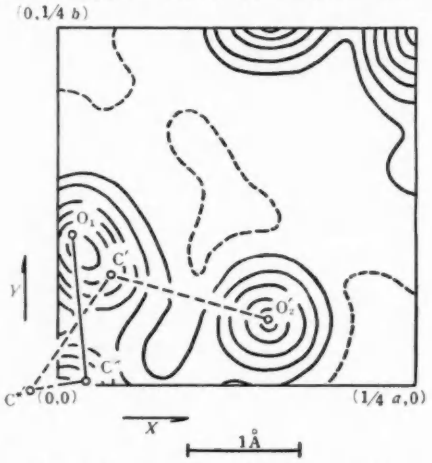

Fig. 4. Final electron density projection onto (001). Contours at intervals of 2 e.Å^{-2} with the lowest solid contour at 3 e.Å^{-2}.

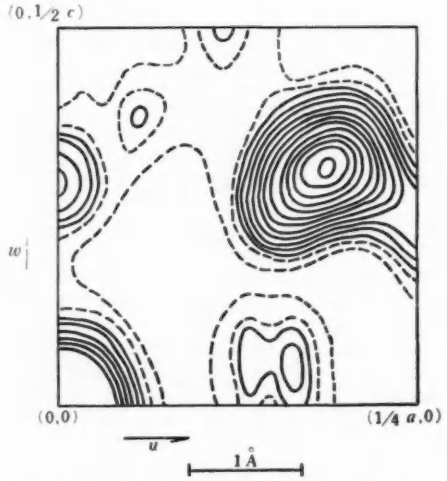

Fig. 5. Patterson projection onto (010) with contours at arbitrary intervals.

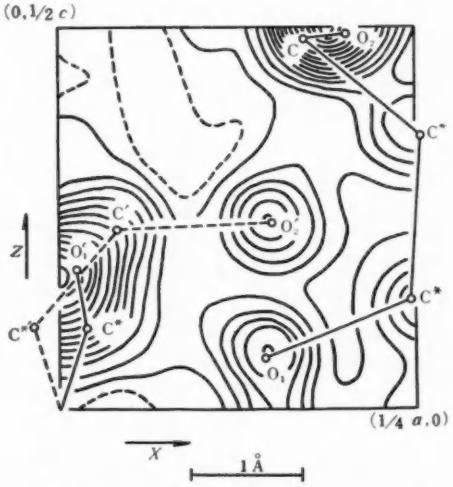

Fig. 6. Final electron density projection onto (010). Contours at intervals of 2 e.Å^{-2} with the lowest solid contour at 3 e.Å^{-2}.

TABLE I

ATOMIC COORDINATES

	x/a	y/b	z/c
C*	0.019	0.001	0.108
C	−0.039	−0.080	0.236
O_1	0.011	0.108	0.185
O_2	−0.148	−0.049	0.243

* The reliability indices for $(hk0)$ and $(h0l)$ spectra were reduced mainly because of the more careful measurement of intensity after the short communication was sent to Acta Crystallographica. The author hopes at some more favorable time to refine the structure by the use of I. B. M. computor which will be provided at his university in the near future.

TABLE II
VALUES OF CALCULATED AND OBSERVED STRUCTURE FACTORS

($hk0$)

h	k	$1/8(F_o)$	$1/8(F_c)$	h	k	$1/8(F_o)$	$1/8(F_c)$	h	k	$1/8(F_o)$	$1/8(F_c)$	h	k	$1/8(F_o)$	$1/8(F_c)$
2	0	1.0	−0.8	2	4	11.8	−14.8	2	8	5.7	−4.5	2	12	2.5	2.1
4	0	6.8	5.6	4	4	8.2	−7.5	4	8	10.0	10.5	4	12	1.4	0.6
6	0	12.8	14.2	6	4	2.1	2.1	6	8	1.8	2.3	6	12	0.9	0.3
8	0	4.6	5.3	8	4	3.5	−3.1	8	8	2.1	2.7	8	12	0	−0.7
10	0	2.7	−2.6	10	4	6.3	−6.3	10	8	2.4	2.8	10	12	0.5	−0.5
12	0	1.2	0.7	12	4	2.3	2.9	12	8	1.9	1.6				
14	0	0	0.7	14	4	1.5	−1.9	14	8	0.8	1.0	2	14	2.3	2.3
16	0	0.4	−0.3									4	14	0.7	−1.0
				2	6	3.2	2.2	2	10	5.2	5.0	6	14	1.3	−1.6
2	2	15.4	13.9	4	6	0.8	2.0	4	10	4.4	4.9	8	14	0	−0.4
4	2	4.3	−4.4	6	6	2.6	−2.1	6	10	2.6	2.1				
6	2	5.1	5.2	8	6	1.2	0.3	8	10	0	−0.3	2	16	1.2	1.1
8	2	5.8	−6.8	10	6	1.5	1.5	10	10	4.1	3.6				
10	2	0.9	0.1	12	6	1.4	1.7	12	10	0	−0.5				
12	2	1.4	−1.7	14	6	0	0.8								
14	2	0.7	−0.8												
16	2	1.6	−1.3												

($h0l$)

h	l	$1/8(F_o)$	$1/8(F_c)$	h	l	$1/8(F_o)$	$1/8(F_c)$	h	l	$1/8(F_o)$	$1/8(F_c)$	h	l	$1/8(F_o)$	$1/8(F_c)$
2	2	13.1	−12.2	2	6	2.4	−2.1	1	1	7.1	7.3	1	5	1.3	−0.4
4	2	3.3	−3.6	4	6	3.0	3.2	3	1	9.7	9.9	3	5	4.6	4.8
6	2	0.4	0.0	6	6	0	−0.6	5	1	4.9	−4.1	5	5	1.5	−1.6
8	2	4.2	−4.2	8	6	1.2	−1.1	7	1	8.0	8.3	7	5	0.8	1.1
10	2	2.9	2.6	10	6	2.2	3.3	9	1	0.9	1.4	9	5	0.8	0.6
12	2	0	−0.6	12	6	1.0	1.2	11	1	2.7	−2.2	11	5	0	−0.3
14	2	0	0.1					13	1	2.2	1.7	13	5	0.8	0.5
				0	8	2.0	2.0	15	1	0.5	0.3				
0	4	5.3	6.8	2	8	1.0	−1.4					1	7	2.1	−2.5
2	4	3.3	−3.2	4	8	0.4	0.5	1	3	10.8	−9.0	3	7	2.3	2.3
4	4	4.2	−4.6	6	8	0	0.0	3	3	0.9	−0.5	5	7	1.5	−1.5
6	4	4.3	4.1					5	3	8.2	−9.3	7	7	0.4	−0.8
8	4	4.4	−3.8					7	3	0	−0.3	9	7	0.6	0.6
10	4	0	−0.4					9	3	1.4	−1.2				
12	4	1.4	−1.6					11	3	2.4	−2.1				
14	4	0.6	0.6					13	3	0.9	0.2				
								15	3	0	−0.1				

hydrogen atoms being excluded. The atomic coordinates detemined in this way are listed in Table I. The observed and the calculated structure factors for ($hk0$) and ($h0l$) spectra are given in Table II. In the above calculation of structure factors, McWeeny's[16] scattering curves of "valence states" for carbon atom and of $f=1/3(f^{\parallel}+2f^{\perp})$ for oxygen atom were used with the isotropic temperature factor $B=2.17$ Å^2.

Discussion of the Structure

Since the molecule lies at the center of symmetry, two identical $CH_2OH\cdot C^*HOH$ groups constituting each half of the molecule are in the *trans*-position to each other, and the zig-zag chain of the four carbon atoms lies exactly in a plane, one of the C* atoms being of the nature *d* and the other *l*. All the valency angles for the carbon atoms are found to be approximately tetrahedral. Hence the configuration of the molecule as a whole can be described, only if we refer to the relative orientation of the outer C–O_2 bond with regard to the outer C*–C bond in each half of the molecule. The configuration of the molecule can be easily understood from Fig. 7, which shows the perspective view of a molecule in the C*–C bond direction. Intramolecular bond distances and bond angles are also listed in Table III. The plane of the C*–C–O_2

16) R. McWeeny, ibid., **4**, 513 (1951).

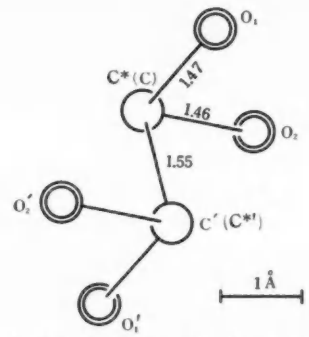

Fig. 7. *i*-Erythritol molecule projected on a plane at right angles to the C*–C bond. Intramolecular bond distances are given in Ångstrom units.

TABLE III
INTRAMOLECULAR BOND DISTANCES AND BOND ANGLES

C*–C	1.54 Å	∠C*'–C*–C	110°
C*–C*'	1.55 Å	∠C*'–C*–O_1	110°
C*–O_1	1.47 Å	∠C–C*–O_1	113°
C–O_2	1.46 Å	∠C*–C–O_2	108°

group forms a dihedral angle of 59° with the plane of the C–C*–O_1 group and an angle of 65° with that of the zig-zag chain of carbon atoms. In other words, the directions of the outer C–O_2 bond and the C*–C*' bond make the *gauche*-configuration with respect to the C*–C bond, and the two hydroxyl oxygen atoms in each half of the molecule are also in the *gauche*-positions around the C*–C bond. It is interesting to note that this relative configuration of the two hydroxyl groups with respect to the C*–C bond agrees with that found in tartaric acid and tartrate ion[17-21]. This mode of linkage is known to exist in carbohydrates. It must also be added that this configuration should be compared with the molecular configurations reported on ethylene glycol and glycerol on the basis of an electron diffraction study[22].

Fig. 8 gives the view of the crystal structure along the *c* axis. In this structure, important roles of two types of hydrogen bonds in the cohesion of the crystal can not be overlooked. The outer hydroxyl oxygen atom is linked to two oxygen atoms of the outer hydroxyl groups of the neighboring molecules, above and below, with a distance 2.66 Å forming a spiral chain arrangement of hydrogen bonds along the *c* axis. The inner hydroxyl oxygen atom, on the other hand, is linked to two oxygen atoms of the inner hydroxyl groups of the neighboring molecules. They form a distorted square of the side length 2.77 Å around the position given by the symmetry $\bar{4}$. They are making a lateral linkage, in a way, but at the same time they are uniting molecules within the same chain mentioned above. Thus, the crystal structure is held together by a three-dimensional net work of these hydrogen bonds, in which all the available hydrogen atoms and all the oxygen atoms also are joining, in agreement with the fact that this crystal has no cleavage.

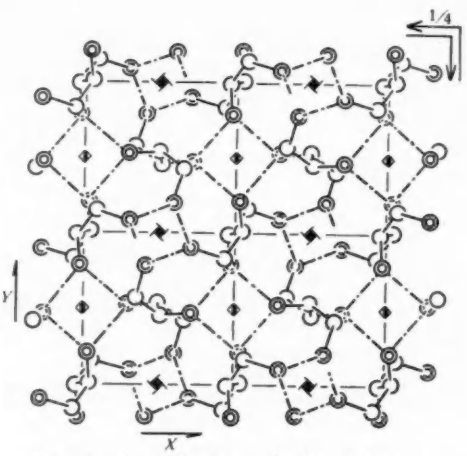

Fig. 8. A projection of the structure along the *c* axis of the crystal.

The author is indebted to Professor I. Nitta, and Professor T. Watanabé for their helpful advice.

Department of Chemistry
Faculty of Science
Konan University
Higashinada-ku, Kobe

17) C. A. Beevers and W. Hughes, *Nature*, **146**, 96 (1940); *Proc. Roy. Soc.* A177, 251 (1941).
18) F. Stern and C. A. Beevers, *Acta Cryst.*, **3**, 341 (1950).
19) R. Sadanaga, ibid., **3**, 416 (1950).
20) G. S. Parry, ibid., **4**, 131 (1951).
21) A. J. van Bommel and J. M. Bijvoet, ibid., **11**, 61 (1958).
22) O. Bastiansen, *Acta chem. scand.*, **3**, 415 (1949).

Crystal Structure and Lattice Energy of i-Erythritol. II. Lattice and Hydrogen Bond Energies for i-Erythritol

By Akira SHIMADA

(Received August 13, 1958)

There have been already reported many studies on the lattice energy of crystalline substances, but most of them are dealing with crystals which are composed of ions. Viewed from the standpoint of the fact that the most powerful force capable of holding ions together is the electrostatic one, this situation seems to be very natural. On the other hand, there have been reported few studies on the lattice energy of crystals composed of more or less complicated molecules. Among these studies, a detailed calculation of the lattice energy has been already carried out for pentaerythritol[1], which gave a satisfactory result in comparison with the observed heat of sublimation. Of *i*-erythritol ($CH_2OH \cdot C^*HOH \cdot C^*HOH \cdot CH_2OH$), which is also a member of tetrahydric alcohols, various physical properties have been already reported and related to those of pentaerythritol[2,3]. Now that the crystal structure of *i*-erythritol has recently been determined by X-ray analysis[4], it was attempted to calculate the lattice energy and compare it with the observed heat of sublimation[2].

Calculation of the Lattice Energy.—The crystal of *i*-erythritol was found to belong to the tetragonal system with $a=12.81$ Å, $c=6.81$ Å and the space group $C_{4h}^6-I4_1/a$[5]. There are eight centro-symmetrical molecules in the unit cell. The structure projected on the (001) plane is shown in Fig. 1, in which the Roman numerals are given for the sake of convenience in the following calculations. The interesting feature of this structure is that two different types of hydrogen bonds, as shown in Fig. 1, link all the molecules firmly in a three-dimensional way*. One of these two types of the hydrogen bond, with a distance 2.77 Å, connects two CHOH groups of adjoining molecules while the other, with a distance 2.66 Å, connects two CH_2OH groups of adjoining molecules. The coordinates of atoms determined by X-ray analysis[4] were used in the following calculations.

The calculations of the lattice energy was carried out in the same way as in the case of pentaerythritol. This energy was supposed to be composed mainly of the van der Waals and electrostatic energies. Slater-Kirkwood's formula was applied to get the former energy, splitting the molecule into three kinds of force center; they are the CH, the CH_2 and the OH group. The polarizability α of each atomic group used in Slater-Kirkwood's formula is shown in Table I. They were

TABLE I
MOLECULAR REFRACTION AND POLARIZABILITY

Group	M_∞	$\alpha \times 10^{24}$ cc.
OH	2.48	0.981
CH	3.41	1.350
CH_2	4.32	1.709

esimated from the molecular refractions M_∞ at infinite wave length[1]. As for the molecules the centers of which lie within about 10 Å from the molecule 0 at the origin, the minus sixth power of distance between force centers was computed one by one and summed up. As for the molecules lying apart beyond 10 Å from the molecule 0, the summation was replaced by integration, assuming the uniform distribution of the force centers. The result of calculation is given in Table II, showing that the contribution of the integral part is found to be very small. The obtained value 20.42 kcal./mol. is somewhat greater than that of pentaerythritol (17.62 kcal./mol.) and this is possibly related to the

1) I. Nitta, S. Seki and K. Suzuki, This Bulletin, **24**, 63 (1951).
2) I. Nitta, S. Seki, M. Momotani, K. Suzuki and S. Nakagawa, *Proc. Japan Acad.*, **26**, (10) 11 (1950).
3) S. Seki and K. Suzuki, This Bulletin, **26**, 63 (1953).
4) A. Shimada, This Bulletin, **32**, 325 (1959).
5) For a detailed explanation of the crystallographic data, see "International Tables for X-ray Crystallography", Kynoch Press, Birmingham, England (1952).

* A preliminary infrared study on *i*-erythritol crystal shows that there is no marked band at the frequency of the unbonded OH stretching mode (3700 cm^{-1}), but at 3210cm^{-1} is observed a broad band which can be ascribed to the stretching modes of the hydrogen-bonded OH. Further study is now in progress.

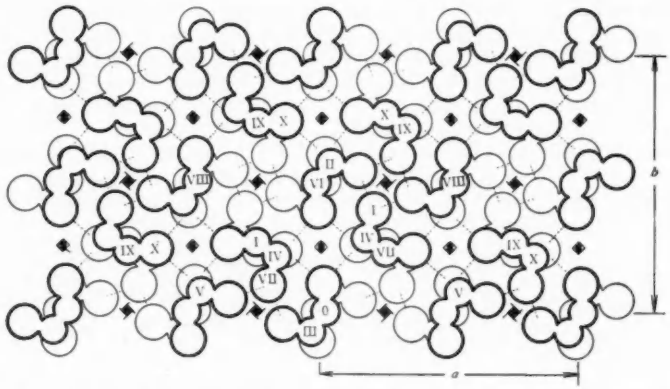

Fig. 1. View of molecular arrangement projected on (001) plane. The upper half of the centro-symmetrical molecule is shown by the broad outline, the large circle standing for OH group and the small one for CH and CH_2 groups. Dashed line indicates the hydrogen bond between the molecules.

TABLE II

VAN DER WAALS ATTRACTION ENERGY BETWEEN DIFFERENT ATOMIC GROUPS

Sort of molecule	van der Waals energy (cal./mol.)						
	CH∼CH	CH_2∼CH	CH_2∼CH_2	OH∼CH	OH∼CH_2	OH∼OH	Total
I	409.0	732.2	406.0	2393.7	3090.4	6168.9	13200.2
II	33.9	113.5	153.5	84.4	133.5	114.2	633.0
III	41.5	182.5	188.5	205.5	534.3	219.0	1371.3
IV	62.7	427.0	821.5	514.9	990.6	356.9	3173.6
V	35.5	102.4	59.4	273.7	264.2	376.4	1011.6
VI	7.6	27.5	22.6	23.8	45.6	36.7	163.8
VII	6.9	16.3	10.3	31.3	37.1	38.1	140.0
VIII	10.1	25.5	22.2	36.5	58.1	54.3	206.7
IX	1.4	14.3	11.1	25.2	35.5	27.7	115.2
Part of sum	608.6	1641.2	1695.1	3589.0	5189.3	7292.2	20015.4
Part of integral	38.1	48.1	59.6	64.4	81.3	112.0	403.5
			Total van der Waals energy:				20418.9

TABLE III

ELECTROSTATIC ENERGY BETWEEN DIFFERENT MOLECULES, USING DIFFERENT NET CHARGES

Sort of molecule	Distance from molecule 0 (Å)	Number of molecules	Electrostatic energy (kcal./mol.)		
			A	B	C
I	4.74	4	−16.687	−19.199	−21.711
II	6.41	2	− 1.260	− 1.809	− 2.344
III	6.81	2	0.166	0.192	0.226
IV	6.83	4	− 3.174	− 3.655	− 4.033
V	7.25	4	1.654	1.781	2.045
VI	9.35	4	− 0.412	− 0.769	− 1.065
VII	9.64	4	0.165	0.231	0.403
VIII	9.68	8	7.894	8.803	9.966
IX	9.94	8	− 0.522	− 0.531	− 0.545
X	11.05	8	0.364	0.435	0.508
		Total:	−11.812	−14.521	−16.550

difference of the packing in the two compounds (molecular volume: *i*-erythritol 84.2 cc./mol. and pentaerythritol 97.5 cc./mol. at room temperature).

In the calculation of electrostatic energy for this crystal, the point charge model was adopted, putting a net charge ε on the nuclear positions of the carbon atoms in CH and CH_2 groups, ε' on the hydrogen atoms in OH groups and $-(\varepsilon+\varepsilon')$ on the oxygen atoms. The positions of hydrogen atoms in OH groups were assumed to lie approximately on the line connecting two oxygen atoms at a distance 0.96 Å from the oxygen atom. A value 0.551×10^{-10} e. s. u. was assigned to the charge ε, and values 1.726 (Case A), 1.870 (Case B) and 2.015 (Case C)$\times10^{-10}$ e. s. u. were given for the charge ε', as in the case of pentaerythritol. These three cases correspond respectively to the three degrees of ionic characters 36, 39 and 42% of the OH bonds. The result of calculation is shown in Table III. In this calculation, the summation is taken over a sphere with its origin at the center of the molecule 0 and a radius of about 11 Å. The contribution of the outer part is neglected, in consideration of a possibility that it will decrease at least with the third power of distance. In fact, it can be shown by the Taylor's theorem that the electrostatic energy between each pair of molecules with no resultant permanent dipole moment will decrease at least with the fifth power of distance, and the number of pairs of molecules will increase with the second power of distance. Summing up the van der Waals and the electrostatic energies, the following three values are obtained, 32.23, 34.94 and 36.97 kcal./mol., corresponding respectively to the case A, B and C. The first value is in good agreement with the experimental value: 32.3± 0.2 kcal./mol[2]. It will be seen that for *i*-erythritol a good agreement is obtained for the case A, whereas the case B or C stands good for the case of pentaerythritol.

Estimation of the Hydrogen Bond Energy.—A part of the lattice energy may be attributed to the four hydrogen bonds, which are formed between a molecule of *i*-erythritol and its nearest neighbors. However, it is not easy to define and calculate that part of energy in this case, because in this complicated structure are appreciable the contributions of distant neighbors especially to the electrostatic energy and, furthermore, there is a rather even distribution of the hydrogen bonds, in contrast to the case of pentaerythritol where the hydrogen bonds connect the molecules to construct a typical layer lattice. Hence, in this case, the hydrogen bond energy is tentatively defined as the interaction energy between two OH groups directly linked together by the hydrogen bond. The van der Waals energies for the hydrogen bonds between two CHOH and two CH_2OH groups come out to be 1.35 and 1.65 kcal./mol. respectively. The corresponding electrostatic energies are computed, for the case A, to be 2.90 and 4.73 kcal./mol. Summing up these values, the hydrogen bond energies are to be 4.3 and 6.4 kcal./mol. The average value of these energies (5.4 kcal./mol.) seems to be somewhat larger than that of pentaerythritol (4.68 kcal./mol. for the case B or 5.16 kcal./mol. for the case C), although the definition of the hydrogen bond is somewhat different between these two compounds[1]. However, it is noteworthy to point out that a reasonable correlation of hydrogen bond energies (4.3 and 6.4 kcal./mol.) with hydrogen bond distances (2.77 and 2.66 Å) has been found in this calculation on the ground of rather simple model, while the model suggested by Lippincott[6] gives the values of hydrogen bond energies, 4.2 and 6.7 kcal./mol., corresponding to these two hydrogen bond distances.

Suzuki et al.[7] suggested another way for estimating hydrogen bond energy. This is to compare the heat of sublimation of the hydrogen-bonded substance with that of a reference substance, which is composed of isoelectronic molecules having similar configuration but no ability of hydrogen-bonding. This method was also applied to the cases of *i*-erythritol and pentaerythritol. The suitable reference substance chosen were 3,4-dimethylhexane and 3,3-diethylpentane each for these two compounds. The heat of sublimation of the reference substance was obtained by adding the heat of fusion[8] and that of vaporization. Since the heat of fusion of 3,4-dimethylhexane is not yet known, it was estimated by adding the difference between the heat of fusion of 2,3-dimethylbutane (0.194 kcal./mol.) and that of

6) E. R. Lippincott and R. Schroeder, *J. Chem. Phys.*, **23**, 1099 (1955).

7) K. Suzuki, S. Ōnishi, T. Koide and S. Seki, This Bulletin, **29**, 127 (1956).

8) F. D. Rossini, K. S. Pitzer, R. L. Arnett, R. M. Braun and G. C. Pimental, "Selected Values of Physical and Thermodynamical Properties of Hydrocarbons and Related Compounds", Carnegie Press, Pittsburgh, U. S. A. (1953).

n-butane (1.114 kcal./mol.) to that of *n*-hexane (3.114 kcal./mol.). The heat of vaporization was calculated from the temperature variation of vapor pressure[8] near the melting point. Table IV gives the latent heats associated with the phase

TABLE IV
HEAT OF PHASE CHANGE FOR THE REFERENCE SUBSTANCE (kcal./mol.)

	Reference substance	
	3,4-Dimethyl-hexane	3,3-Diethyl-pentane
Heat of fusion	2.19	2.35
Heat of vaporization	9.53	10.50
Heat of sublimation	11.7	12.9

changes for the reference substances. From these values, the hydrogen bond energies of 5.2 and 4.6 kcal./mol. have been estimated for *i*-erythritol and pentaerythritol respctively. These values are found to be in good agreement with the average values mentioned in the preceding paragraph.

At any rate, it seems likely that the average hydrogen bond energy for *i*-erythritol is larger than that for pentaerythritol, since the two methods of calculation gave parallel results. The values obtained above can be compared with those obtained on other alcohols[9]. Although in the calculation of the lattice energy mentioned above certain assumptions are involved, and the repulsive and other higher terms are ignored[10], it is noteworthy that the reasonable values for the lattice and hydrogen bond energies are obtained, based on the crystal structure.

The author wish to thank Professor I. Nitta, Professor T. Watanabé and Dr. S. Seki for their continued encouragement and Dr. K. Suzuki for his helpful discussion on the calculation of the lattice energy.

Department of Chemistry
Faculty of Science
Konan University
Higashinada-ku, Kobe

9) I. Nitta and S. Seki, *J. Chem. Soc. Japan, Pure Chem. Sec.* (*Nippon Kagaku Zasshi*), **69**, 143 (1948).
10) In the case of iodine crystal, these two terms were found to cancel out with each other. The agreement of the observed heat of sublimation with the lattice energy calculated by the use of Slater-Kirkwood's formula in many examples seems to indicate that these two terms cancel out with each other. See, I. Nitta and S. Seki, ibid., **64**, 475 (1943).

Electrical Conductance of Concentrated Aqueous Solutions of Copper Sulfate

By C. V. Suryanarayana and S. Alamelu

(Received September 19, 1958)

Numerous attempts have been made to extend the Debye-Hückel theory to electrolyte solutions of higher concentrations than 0.1 N. The attempts of Falkenhagen and Leist[1], Robinson and Stokes[2], Wishaw and Stokes[3], and Leist[4], are the most notable contributions in recent times in this direction.

Suryanarayana and Venkatesan[5,6] recently formulated the equation,

$$\Lambda_c = \Lambda_s + A\frac{(1-c_p)}{\eta_p} \qquad (1)$$

where

$$\Lambda_c = \frac{\text{specific conductance } (K_c)\times 1000}{c_p}$$

Λ_s = specific conductance at saturation $(K_s)\times 1000$

$$c_p = \frac{\text{mole fraction at a given concn.}}{\text{mole fraction at saturation at the same temp.}}$$

of course, at saturation $c_p = 1$

$$\eta_p = \frac{\text{viscosity at a given concn.}}{\text{viscosity at saturation}}$$

1) H. Falkenhagen and M. Leist, *Naturwiss.*, **41**, 570 (1954).
2) R. A. Robinson and R. H. Stokes, *J. Am. Chem. Soc.*, **76**, 1991 (1954).
3) B. F. Wishaw and R. H. Stokes, ibid., **76**, 2065 (1954).
4) M. Leist, *Z.phys.Chem.*, **205**, 16 (1955).
5) C. V. Suryanarayana and V. K. Venkatesan, *Nature*, **178**, 1461 (1956).
6) C. V. Suryanarayana and V. K. Venkatesan, *Acta. Chim. Hung.*, **17**, 327 (1958).

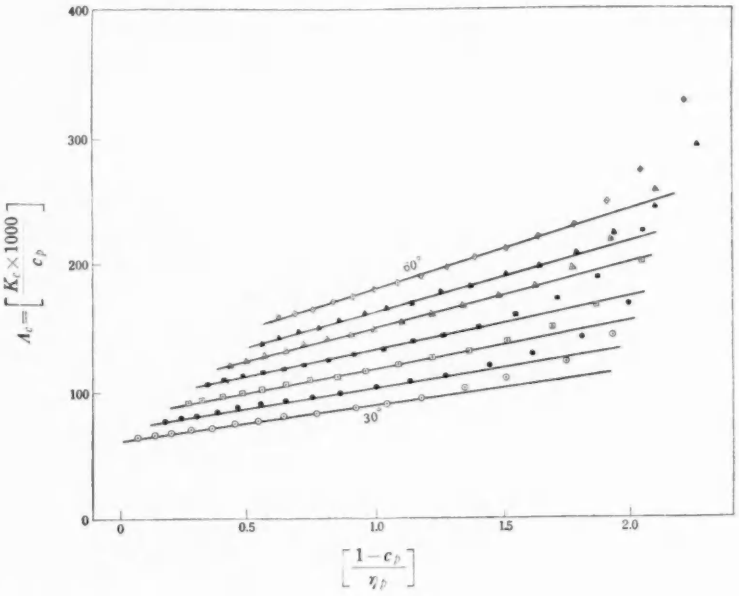

Fig. 1.

TABLE I
TEMPERATURE 30°C

Molality	Specific conductance $K_c \times 10^2$	Density	Relative viscosity	c_p	η_p	Λ_c	$\left[\frac{1-c_p}{\eta_p}\right]$
0.0992	0.9661	1.011	1.042	0.0673	0.4818	143.5	1.936
0.1965	1.638	1.027	1.070	1.1332	0.4946	122.9	1.752
0.2921	2.179	1.042	1.131	0.1977	0.5231	110.2	1.508
0.3862	2.673	1.057	1.182	0.2609	0.5468	102.4	1.352
0.4785	3.042	1.071	1.246	0.3228	0.5762	94.26	1.175
0.5693	3.413	1.085	1.288	0.3833	0.5958	89.04	1.035
0.6586	3.842	1.098	1.326	0.4428	0.6132	86.76	0.9088
0.7463	4.075	1.110	1.403	0.5009	0.6488	81.34	0.7693
0.8326	4.482	1.124	1.485	0.5581	0.6869	80.32	0.6433
0.9175	4.719	1.136	1.539	0.6141	0.7117	76.85	0.5423
1.0010	5.003	1.149	1.602	0.6688	0.7408	74.82	0.4471
1.0830	5.253	1.161	1.675	0.7231	0.7747	72.64	0.3575
1.1640	5.502	1.172	1.738	0.7759	0.8037	70.92	0.2788
1.2440	5.650	1.184	1.827	0.8273	0.8448	68.28	0.2044
1.3210	5.825	1.195	1.908	0.8780	0.8824	66.34	0.1382
1.3980	5.977	1.205	2.009	0.9281	0.9290	64.40	0.0774
1.5100 (Satd.)	—	1.223	2.162	1.0000	1.0000	—	—

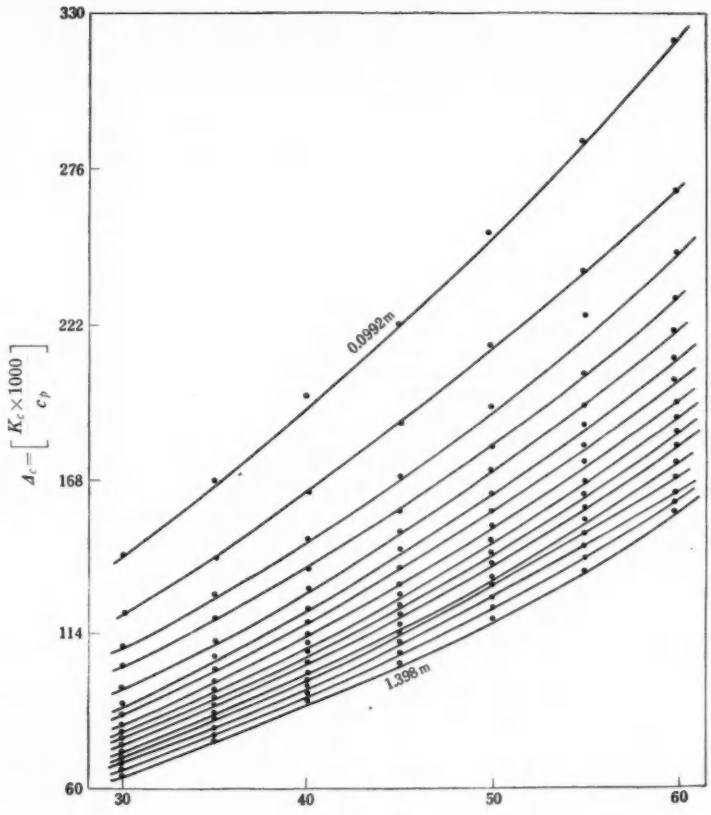

Fig. 2.

TABLE II
TEMPERATURE 35°C

Molality	Specific conductance $K_c \times 10^2$	Density	Relative viscosity	c_p	η_p	Λ_c	$\left[\frac{1-c_p}{\eta_p}\right]$
0.0992	1.041	1.009	1.047	0.0618	0.4722	168.6	1.9870
0.1965	1.738	1.025	1.078	0.1222	0.4863	142.2	1.8050
0.2921	2.343	1.040	1.124	0.1813	0.5069	129.2	1.6150
0.3862	2.874	1.054	1.172	0.2393	0.5286	120.0	1.4390
0.4785	3.321	1.068	1.225	0.2961	0.5525	112.1	1.2750
0.5693	3.778	1.082	1.273	0.3517	0.5741	107.4	1.1290
0.6586	4.151	1.095	1.318	0.4061	0.5944	102.2	0.9993
0.7463	4.482	1.109	1.385	0.4595	0.6247	97.54	0.8652
0.8326	4.872	1.121	1.442	0.5119	0.6504	95.17	0.7504
0.9175	5.172	1.133	1.502	0.5632	0.6775	91.83	0.6443
1.0010	5.508	1.146	1.555	0.6135	0.7013	89.78	0.5512
1.0830	5.821	1.158	1.619	0.6633	0.7318	87.76	0.4601
1.1640	6.009	1.170	1.687	0.7117	0.7608	84.43	0.3789
1.2440	6.169	1.181	1.760	0.7590	0.7938	81.28	0.3036
1.3210	6.341	1.192	1.830	0.8054	0.8254	78.74	0.2357
1.3980	6.528	1.203	1.914	0.8513	0.8632	76.67	0.1723
1.6500 (Satd.)	—	1.249	2.217	1.0000	1.0000	—	—

TABLE III
TEMPERATURE 40°C

Molality	Specific conductance $K_c \times 10^2$	Density	Relative viscosity	c_p	η_p	A_c	$\left[\frac{1-c_p}{\eta_p}\right]$
0.0922	1.143	1.007	1.047	0.0568	0.4619	201.3	2.042
0.1965	1.867	1.023	1.084	0.1123	0.4784	166.3	1.856
0.2921	2.504	1.038	1.119	0.1667	0.4937	150.2	1.689
0.3862	3.063	1.052	1.163	0.2200	0.5133	139.2	1.520
0.4785	3.576	1.066	1.207	0.2721	0.5325	131.4	1.367
0.5693	4.062	1.080	1.259	0.3232	0.5555	125.7	1.218
0.6586	4.482	1.093	1.305	0.3734	0.5757	120.0	1.088
0.7463	4.872	1.106	1.362	0.4224	0.6009	115.3	0.961
0.8326	5.253	1.119	1.417	0.4706	0.6252	111.6	0.847
0.9175	5.650	1.131	1.467	0.5177	0.6474	109.1	0.745
1.0010	5.942	1.143	1.520	0.5639	0.6707	105.4	0.650
1.0830	6.169	1.155	1.580	0.6096	0.6972	101.2	0.560
1.1640	6.441	1.167	1.640	0.6542	0.7236	98.47	0.478
1.2440	6.691	1.179	1.708	0.6976	0.7536	95.92	0.401
1.3210	6.901	1.190	1.771	0.7403	0.7814	93.22	0.332
1.3980	7.078	1.200	1.850	0.7807	0.8164	90.65	0.269
1.8000 (Satd.)	—	1.251	2.266	1.0000	1.0000	—	—

TABLE IV
TEMPERATURE 45°C

Molality	Specific conductance $K_c \times 10^2$	Density	Relative viscosity	c_p	η_p	A_c	$\left[\frac{1-c_p}{\eta_p}\right]$
0.0992	1.191	1.005	1.039	0.0525	0.4625	226.7	2.0480
0.1965	1.977	1.021	1.080	0.1040	0.4808	190.2	1.8630
0.2921	2.668	1.035	1.110	0.1543	0.4942	172.9	1.7120
0.3862	3.248	1.050	1.152	0.2036	0.5130	159.5	1.5520
0.4785	3.820	1.064	1.195	0.2519	0.5321	151.7	1.4060
0.5693	4.338	1.077	1.242	0.2991	0.5530	145.0	1.2680
0.6586	4.803	1.091	1.289	0.3455	0.5740	139.0	1.1400
0.7463	5.172	1.104	1.339	0.3909	0.5962	132.3	1.0220
0.8326	5.650	1.116	1.389	0.4355	0.6186	129.7	0.9126
0.9175	6.032	1.129	1.436	0.4792	0.6393	125.9	0.8147
1.0010	6.339	1.141	1.490	0.5219	0.6634	121.4	0.7206
1.0830	6.658	1.153	1.542	0.5643	0.6866	118.0	0.6346
1.1640	6.947	1.165	1.592	0.6054	0.7089	114.8	0.5567
1.2440	7.269	1.176	1.656	0.6457	0.7374	112.6	0.4805
1.3210	7.458	1.188	1.717	0.6852	0.7643	108.8	0.4118
1.3980	7.598	1.198	1.786	0.7243	0.7952	104.9	0.3466
1.9500 (Satd.)	—	1.268	2.246	1.0000	1.0000	—	—

A = a constant whose value is a function of temperature and dielectric constant of the medium.

The basis of the formulation of the concepts c_p and η_p has already been given[7].

In the present investigations the data collected for copper sulfate solutions are sought to be fitted into equation 1. We hoped to verify the equation of Wishaw and Stokes (loc. cit.) with the same data. Unfortunately, copper sulfate being an "intermediate electrolyte" and a bivalent salt with complications regarding ionic hydration in solution, and owing to uncertainty regarding the actual value of the mean distance of closest approach '$\dot{a}$', we could not test Wishaw and Stokes' equation or even that of Falkenhagen and Leist (loc. cit.). Equation 1 involves no such uncertain parameters since the very

7) C. V. Suryanarayana and V. K. Venkatesan, This Bulletin 31, 442 (1958).

TABLE V
TEMPERATURE 50°C

Molality	Specific conductance $K_c \times 10^2$	Density	Relative viscosity	c_p	η_p	Λ_c	$\left[\frac{1-c_p}{\eta_p}\right]$
0.0992	1.254	1.003	1.042	0.0485	0.4535	258.7	2.0980
0.1965	2.094	1.019	1.082	0.0959	0.4710	218.4	1.9200
0.2921	2.802	1.033	1.113	0.1423	0.4844	196.9	1.7710
0.3862	3.448	1.047	1.149	0.1878	0.5001	183.6	1.6240
0.4785	4.051	1.061	1.191	0.2324	0.5184	174.4	1.4800
0.5693	4.605	1.075	1.239	0.2759	0.5393	166.9	1.3430
0.6586	5.093	1.088	1.282	0.3187	0.5581	159.8	1.2210
0.7463	5.556	1.101	1.330	0.3606	0.5790	154.1	1.1040
0.8326	6.003	1.114	1.382	0.4017	0.6016	149.5	0.9945
0.9175	6.343	1.127	1.418	0.4420	0.6172	143.5	0.9040
1.0010	6.733	1.139	1.468	0.4814	0.6392	139.8	0.8114
1.0830	7.191	1.150	1.519	0.5205	0.6612	138.1	0.7252
1.1640	7.401	1.162	1.565	0.5585	0.6813	132.5	0.6480
1.2440	7.640	1.173	1.628	0.5955	0.7086	128.3	0.5709
1.3210	7.854	1.185	1.690	0.6320	0.7357	124.3	0.5001
1.3980	8.004	1.195	1.753	0.6680	0.7630	119.8	0.4351
2.1200 (Satd.)	—	1.285	2.296	1.0000	1.0000	—	—

TABLE VI
TEMPERATURE 55°C

Molality	Specific conductance $K_c \times 10^2$	Density	Relative viscosity	c_p	η_p	Λ_c	$\left[\frac{1-c_p}{\eta_p}\right]$
0.0992	1.311	1.001	1.039	0.0448	0.4401	292.5	2.1700
0.1965	2.172	1.016	1.076	0.0886	0.4560	245.0	1.9980
0.2921	2.936	1.030	1.108	0.1316	0.4693	223.1	1.8500
0.3862	3.634	1.045	1.140	0.1737	0.4831	209.2	1.7110
0.4785	4.241	1.059	1.180	0.2148	0.5000	197.4	1.5700
0.5693	4.838	1.073	1.223	0.2552	0.5182	189.5	1.4370
0.6586	5.379	1.086	1.266	0.2947	0.5365	182.5	1.3140
0.7463	5.898	1.098	1.311	0.3334	0.5555	176.9	1.2000
0.8326	6.284	1.111	1.355	0.3715	0.5741	169.2	1.0950
0.9175	6.723	1.124	1.398	0.4087	0.5926	164.5	0.9979
1.0010	7.145	1.136	1.437	0.4451	0.6088	160.5	0.9104
1.0830	7.471	1.148	1.486	0.4812	0.6298	155.2	0.8237
1.1640	7.782	1.160	1.530	0.5164	0.6483	150.7	0.7457
1.2440	8.082	1.170	1.582	0.5507	0.6705	146.8	0.6701
1.3210	8.289	1.182	1.641	0.5843	0.6953	141.9	0.5977
1.3980	8.405	1.192	1.702	0.6177	0.7206	136.1	0.5306
2.3000 (Satd.)	—	1.302	2.360	1.0000	1.0000	—	—

approach in its derivation was from a new angle (loc. cit.). Hence, equation 1 is now tested with the data of copper sulfate.

Experimental

All solutions were made by weight using "Analar" (British Drag House) variety of copper sulfate ($CuSO_4 \cdot 5H_2O$). A Jones and Bollinger type cell[8] of cell constant 0.6723 was used for conductivity determinations for all concentrations at different temperatures. The measurement of conductance was made by a Philip's GM 4249/01 bridge at a frequency of 1000 cycles/sec. Owing to the high concentration range in which measurements were made, the correction for conductance of pure solvent was quite negligible owing to high specific conductance in all the solutions and the correction was ignored. All connecting wires were heavily insulated, rigid, and well separated so that errors of poor insulation and induction effect were avoided. In the

8) G. Jones and G. M. Bollinger, *J. Am. Chem. Soc.*, 53, 411 (1931).

TABLE VII
TEMPERATURE 60°C

Molality	Specific conductance $K_c \times 10^2$	Density	Relative viscosity	c_p	η_p	Λ_c	$\left[\frac{1-c_p}{\eta_p}\right]$
0.0992	1.367	0.9988	1.034	0.0415	0.4319	329.3	2.219
0.1965	2.256	1.014	1.076	0.0822	0.4495	274.7	2.042
0.2921	3.063	1.028	1.099	0.1220	0.4592	251.1	1.912
0.3862	3.757	1.042	1.131	0.1609	0.4725	233.4	1.776
0.4785	4.438	1.056	1.169	0.1991	0.4884	222.9	1.640
0.5693	5.036	1.070	1.210	0.2364	0.5055	213.0	1.510
0.6586	5.603	1.083	1.251	0.2731	0.5225	205.1	1.391
0.7463	6.112	1.095	1.293	0.3089	0.5401	197.8	1.279
0.8326	6.560	1.109	1.331	0.3442	0.5560	190.5	1.180
0.9175	7.078	1.121	1.368	0.3787	0.5715	186.9	1.087
1.0010	7.521	1.133	1.411	0.4125	0.5893	182.4	0.997
1.0830	7.818	1.144	1.457	0.4460	0.6087	175.3	0.910
1.1640	8.175	1.157	1.502	0.4785	0.6275	170.8	0.831
1.2440	8.405	1.168	1.552	0.5102	0.6483	164.7	0.755
1.3210	8.735	1.180	1.600	0.5416	0.6683	161.3	0.686
1.3980	9.086	1.190	1.654	0.5724	0.6910	158.8	0.619
2.4900 (Satd.)	—	1.319	2.394	1.0000	1.0000	—	—

range of measurement of resistance the instrumental error was ±2.00%. The conductivity cell was immersed in a Gallenkamp b-12210 thermostat giving an accuracy of ±0.05°C.

The viscosities were determined using an Ostwald viscometer immersed in the same thermostat. After attainment of equilibrium the saturated solution was sucked through a tube plugged with cotton wool into a pipette which was kept at the same temperature as the thermostat to avoid crystallization of the saturated solution and transferred into the viscometer. The densities of all the solutions were also measured. Solubility data were obtained from Seidell[9].

Results obtained are given in the tables.

Discussion

A test of equation 1 consists in obtaining a linear plot when Λ_c is plotted against $(1-c_p)/\eta_p$. Fig. 1 shows that such a plot is a straight line at all the temperatures betweem 30° and 60°C, with a few points (right hand side)toward low concentrations going off the straight line at each temperature. This indicates that equation 1 is valid in the range of concentrations from 0.3862 M to saturation (1.5 to 2.5 M). Since the actual resistance measured at saturation at different temperatures happened to be small, attempt is not made here to compare the extrapolated value of Λ_s with that found experimentally owing to the limitations of the instrument used. This aspect is postponed to a future date.

Pearce and Pumplin[10] found out the partial molal volumes of copper sulfate in aqueous solutions upto saturation at 25°C. They observed that the data on copper sulfate solutions are especially interesting because of the negative values of the partial molal volumes in dilute aqueous solutions, quite similar to the phenomenon observed for lithium hydroxide, sodium hydroxide and magnesium sulfate solutions. The very low values in general for copper sulfate indicate a very large amount of electrostriction of the solvent produced by the cupric ion, the water dipoles being compressed around the cupric ion by the intense electrostatic field produced by the high charge density of the ion. Absence of any discontinuity in the curve and a constancy of the law of variation throughout the curve upto saturation indicate that no sudden changes occur either in the total number of water molecules surrounding the ion or the type of bonding between the ion and the water molecules. Stewart[11] observed that the variation of the partial molal volume of ions with concentration is closely linked with the change in structure of water in the same solutions, as revealed by X-ray studies.

9) Seidell "Solubilities of Organic and Inorganic Compounds," Van Nostrand Co., New York (1940), Vol. I.

10) J. N. Pearce and G. G. Pumplin, *J. Am. Chem. Soc.*, 59, 1221 (1937).

11). G. W. Stewart, *J. Chem. Phys.*, 7, 869 (1939).

Fig. 2 shows the temperature variation of Λ_c for all the sixteen concentrations of copper sulfate solutions investigated upon. The curves are not perfect straight lines but are slightly bent convex toward the X-axis. Usually the two factors that determine the form of the temperature conductance curve are: (1) the increase in the viscosity of the solution, and the corresponding decrease in the mobility of the ions, with decreasing temperature; and (2) the effect of temperature on association of ions. With complications of ionic hydration and uncertainties regarding the predominance of one or the other of the above two factors, it is difficult to explain the non-linear variation of Λ_c against temperature.

Equation 1 was originially derived for fully dissociated strong electrolytes based on the principle that the difference in the mobilities of an ion at two different concentrations is a function of the difference in the respective internal pressures at the two concentrations. Copper sulfate is known to be an intermediate electrolyte[12] and the above mentioned observations show that equation 1 holds well even with a bibivalent electrolyte like copper sulfate.

Summary

The electrical conductance of aqueous solutions of copper sulfate has been measured over a wide range of concentrations up to saturation. The equation connecting conductance and concentration in the range of high concentrations recently formulated by Suryanarayana and Venkatesan has been tested with the data obtained for copper sulfate solutions. The equation is found to be valid over a wide range of concentration from 0.3862 M to saturation at temperatures ranging from 30° to 60°C. Slight deviations have been observed at lower concentrations.

Physico-Chemical Laboratory
Annamalai University
Annamalainagar, South India

12) S. Glasstone, "The Electrochemistry of Solutions", Methuen and Co., London (1945), p. 67.

Substituent Effects on the Ultraviolet Absorption Spectrum of 1,3,5-Trinitrobenzene in Some Solvents

By Takehiro ABE

(Received August 22, 1958)

The near ultraviolet absorption spectrum of 1,3,5-trinitrobenzene shows an intense band at 223 mμ and two shoulders at about 300 and 340 mμ in ethanol[1,2]. The maximum absorption band has a shorter wavelength of 223 mμ and a greater molar absorbancy than that of nitrobenzene[2], which has been interpreted by Nagakura and Tanaka[3], in terms of the intramolecular charge transfer.

In the present paper, an attempt has been made to investigate the effects of four substituents on the spectra of 1,3,5-trinitrobenzene in some solvents. The ultraviolet absorption spectra of 1,3,5-trinitrobenzene (TNB), 2,4,6-trinitrotoluene (TNT), picryl chloride (PC), 2,4,6-trinitrophenylmethylnitramine (Tetryl) and picric acid (PA) have been compared in solvents like water, water-sodium hydroxide, ethanol, benzene and acetone, together with the solvent effects upon the spectra of PC, Tetryl and PA. The spectra of TNB and TNT, measured in the previous work[2], have been used here.

1) E. F. Caldin and G. Long, *Proc. Roy. Soc.*, **A228**, 263 (1955).
2) T. Abe, This Bulletin, **31**, 904 (1958).
3) S. Nagakura and J. Tanaka, *J. Chem. Phys.*, **22**, 236 (1954).

Experimental

Materials.—Trinitrobenzenes of commercial extra pure grade were purified by recrystallizing several times. PC: m. p. 82.5°C, Tetryl: m. p. 129.9°C, PA: m. p. 122.6°C. Commercial guaranteed solvents were fractionally distillated after usual treatments.

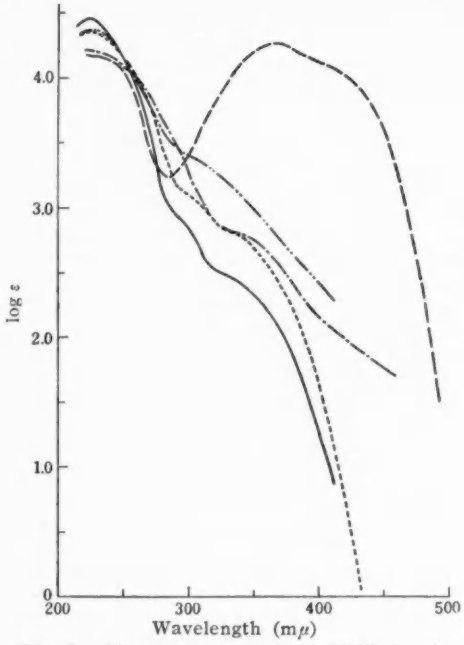

Fig. 1. Absorption spectra of TNB (——), TNT (------), PC (—·—·), Tetryl (—··—··) and PA (— —), all in ethanol.

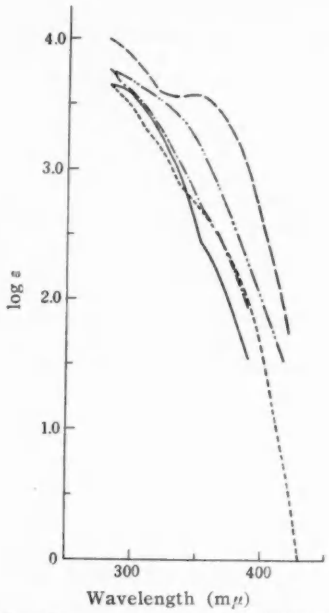

Fig. 3. Absorption spectra of TNB (——), TNT (------), PC (—·—·), Tetryl (—··—··) and PA (— —), all in benzene.

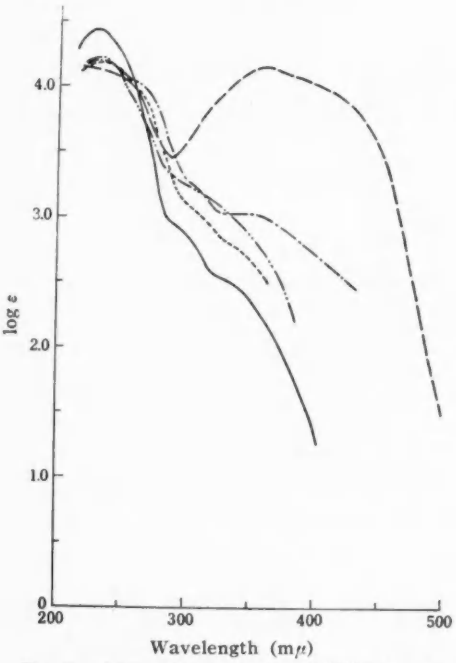

Fig. 2. Absorption spectra of TNB (——), TNT (------), PC (—·—·), Tetryl (—··—··) and PA (— —), all in water.

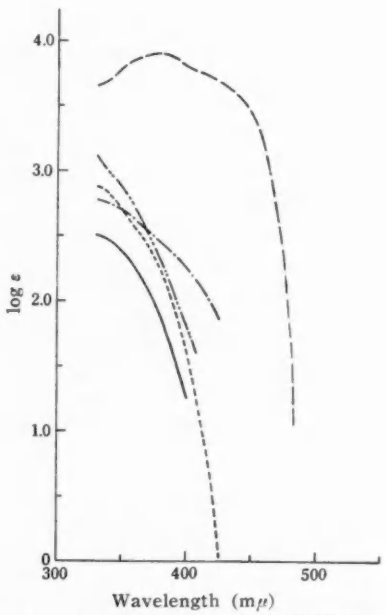

Fig. 4. Absorption spectra of TNB (——), TNT (------), PC (—·—·), Tetryl (—··—··) and PA (— —), all in acetone.

Spectra.—The spectra of the solution were measured with a Hitachi Model EPU-2 spectrophotometer at room temperature. Path length of absorption cells was 1 cm.

Results and Discussion

Spectra of Trinitrobenzenes in Some Solvents.—*In ethanol* (Fig. 1).—By substituting a group like $-CH_3$, $-Cl$, $-N(CH_3)NO_2$ or $-OH$, the 223 mμ band of TNB shifts to the red and its molar absorbancy decreases in the following order: TNB> Tetryl> TNT> PC> PA. Molar extinction coefficients of 300 and 340 mμ bands of the substituted trinitrobenzenes are greater than those of TNB, except those of PA that gives intense absorption bands at 350~450 mμ.

In the previous paper[2], it has been described that a benzene nucleus of polynitro-substituted benzene possesses some positive charge owing to the strong electron-attracting nature of nitro groups, and that the greater this positive charge, the greater becomes the blue shift of the maximum absorption band of the nitro compound. A benzene nucleus of each derivative of TNB possesses a less positive charge tnan that of TNB, because the electron of the $-CH_3$, $-Cl$, $-N(CH_3)NO_2$ or $-OH$ substituent can migrate to some extent toward the benzene nucleus in the direction opposite to the electron migration of the nitro groups, as indicated in Fig. 5. It is, therefore, known that the maximum absorption bands of the substituted trinitrobenzenes, benzene nuclei of which possess less positive charges than that of TNB, shift to the red with decreasing molar absorbancies, compared with the band of TNB.

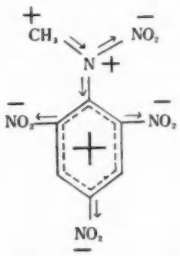

Fig. 5. Charge distribution of Tetryl.

In water (Fig. 2).—The substituted trinitrobenzenes show similar spectra as in ethanol, but give their maximum absorption bands at longer wavelengths and the smaller molar absorbancies in water than in ethanol. Both in ethanol and in water the molar absorbancies of their maximum absorptions are in the following order: TNB> Tetryl> TNT> PC> PA.

In benzene (Fig. 3).—The molar absorbancy of the 350 mμ shoulder of each substituted TNB is greater than that of TNB. Especially PA shows intense bands in this region.

In acetone (Fig. 4).—The molar absorbancies of the 340 mμ shoulders of the substituted trinitrobenzenes are greater than that of TNB. In addition to this shoulder, PA shows intense bands at 370~440 mμ. In all solvents the molar absorbancies of the 340 mμ bands of the trinitrobenzenes increase in the order of TNB, TNT, PC, Tetryl and PA, except the absorbancies of PC in water and in acetone.

It has been found that the visible absorption bands of TNB in acetone, indicated in the previous paper[2], are owing to the action of visible light on the trinitrobenzene used, because TNB that gives no visible absorption bands in acetone as shown in Fig. 4, shows such visible absorption spectra as indicated in the previous paper, after being irradiated by an usual incandescent lamp for a long time.

Solvent Effects on the Spectra of PC, Tetryl and PA (Figs. 1~4).—PC, Tetryl and PA give greater molar absorbancies of absorption bands near 300 mμ in benzene than in ethanol or in water. These great absorbancies in benzene seem probably to be due to formations of molecular complexes between the trinitrobenzenes and benzene, as TNB and TNT form complexes with benzene[2,4].

The absorption curves of PC and Tetryl in ethanol are not so closely resemble those in water as the curves of TNB and TNT. Only the 350 mμ band of PC exceptionally gives a greater molar absorbancy in water than in ethanol.

PA shows similar absorption curves in all three solvents like ethanol, water and acetone. This similarity seems to show that PA dissociates in negative ion not only in water, but also in ethanol and in acetone, losing a proton, because PA is known to be strongly acidic in water.

Spectra of Trinitrobenzenes in Aqueous Sodium Hydroxide Solution (Figs. 6~8).—In Fig. 6, visible absorption spectra of

4) G. Briegleb and J. Czekalla, *Z. Elektrochem.*, **59**, 184 (1955).

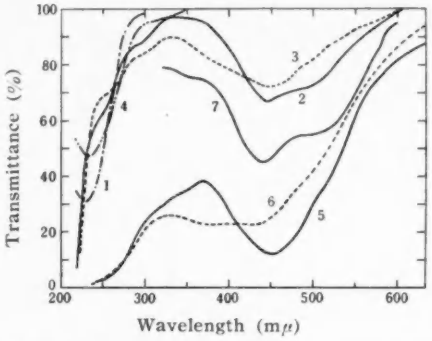

Fig. 6. Absorption curves of:
1. An aqueous solution of TNB;
2. A solution measured immediately after a few drops of 2 N sodium hydroxide solution were added into the solution (1);
3. A solution obtained by boiling the solution (2);
4. An aqueous solution of TNT;
5. A solution measured immediately after a few drops of 2 N sodium hydroxide solution were added into the solution (4);
6. A solution obtained by boiling the solution (5);
7. An aqueous solution of Tetryl, in which a few drops of 2 N sodium hydroxide solution were added.

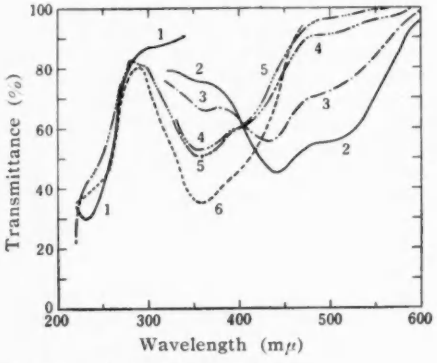

Fig. 7. Absorption curves of:
1. An aqueous solution of Tetryl;
2. A solution measured immediately after a few drops of 2 N sodium hydroxide solution were added into the solution (1);
3. A solution obtained by standing the solution (1) for about half an hour;
4. The solution (2) after an hour and forty minutes;
5. The solution (2) after two hours and a half;
6. An aqueous solution of PA.

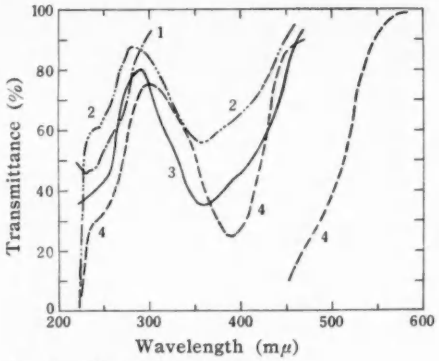

Fig. 8. Absorption curves of:
1. An aqueous solution of PC;
2. A solution in which a red color produced by adding a little of dilute sodium hydroxide solution into the solution (1), already discolored;
3. An aqueous solution of PA;
4. A solution obtained by adding a concentrated sodium hydroxide solution into the solution (3).

sodium hydroxide solutions of TNB, TNT and Tetryl are compared one another, and the absorption curves of the rather stable alkaline solutions of TNB and TNT, boiled to accelerate the rates of reactions between the trinitrobenzenes and alkali, are also indicated. The spectrum of TNB (curve 2) in sodium hydroxide solution closely resembles to that of Tetryl (curve 7). The spectrum of TNT (curve 5) in this solution also resembles them. These red colors are reversively decolorized by addition of weak acids.

On standing for two hours, the red color of the sodium hydroxide solution of Tetryl changes slowly to yellow, as described in Fig. 7. A spectrum of the yellow solution (curve 5) that yields no red color again by adding alkali, closely resembles that of PA (curve 6).

On treating an aqueous solution of PC with sodium hydroxide solution, a red color is produced and fades in a few minutes. By adding a concentrated solution of sodium hydroxide, a solution of PA at once gives a brownish orange color, which disappears in a moment. Absorption curves of yellow solutions to which these alkaline solutions of PC and PA change finally through red solutions, are given in Fig. 8. In a concentrated solution of sodium hydroxide, PA shifts a position of its maximum absorption band to the red by about 30 mμ, and shows a weak shoulder at about 500 mμ (curve 4).

From the above results, the red colors of the aqueous sodium hydroxide solutions of the substituted trinitrobenzenes are stable at room temperature in the following order: TNB and TNT> Tetryl> PC> PA. It is noticed that the substituted trinitrobenzenes that form the labile colors with sodium hydroxide, contain electron-donating substituents like $-N(CH_3)NO_2$, -Cl and -OH.

On boiling with dilute sodium hydroxide solution, TNB yields 3,3',5,5'-tetranitroazoxybenzene and 3,5-dinitrophenol[5]. On standing in the cold with methanolic sodium methylate, TNB yields 3,5-dinitroanisol[6] and on boiling with alcoholic soda solution, it undergoes a partial reduction to form 3,3',5,5'-tetranitroazoxybenzene[7]. The first product of the reaction of methanolic caustic alkali on TNB is a red crystalline addition product having the experimental composition, $TNB \cdot CH_3ONa \cdot 1/2H_2O$, isolated by Bruyn and Leent[8]. From these experimental results, the red product between TNB and sodium hydroxide seems probably to be an intermediate in the reaction of TNB to 3,5-dinitrophenol. The red products of TNT and Tetryl with sodium hydroxide may be also intermediates in their reactions. The transient colors of the sodium hydroxide solutions of PC and PA, absorption spectra of which have not been determined owing to their rapid discolorations, seem to be due to the same complexes as those of TNB, TNT and Tetryl. Actually, it has been reported that a methanol solution of TNT, treated with potassium methylate, yields a red product of an empirical composition, $TNT \cdot CH_3OK \cdot H_2O$[9]. A methanol solution of picryl chloride, treated with an excess of sodium methylate or of strong sodium hydroxide solution, also turns dark red and deposits red crystals of the empirical composition, $trinitroanisol \cdot NaOCH_3$[10]. The color reaction of sodium ethoxide with TNT and TNB in ethanol has been interpreted by Caldin and his co-workers[1,11] in terms of a proton-transfer reaction for TNT and in terms of an addition reaction for TNB.

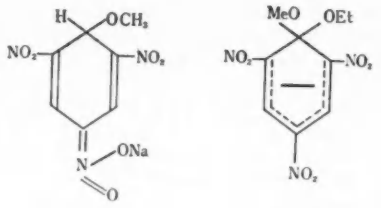

(a) (b)

Fig. 9. Meisenheimer's structure for $TNB \cdot CH_3ONa$(a) and $TNA \cdot OEt^-$(b).

A structure of the red product of $TNB \cdot CH_3ONa$ was presented by Meisenheimer[12], as indicated in Fig. 9 (a). His structure seems to be doubtful in the following point. If the red product between TNB and sodium hydroxide has such a structure as given in Fig. 9 (a), PA may be produced from it at the end of the reaction, while 3,5-dinitrophenol is experimentally obtained as mentioned above. The absorption band of PA is not found also in the spectrum (curve 3) of the boiled alkaline solution of TNB in Fig. 6. It has been, by Nagakura[13], suggested to the present author that TNB should react with sodium hydroxide as follows:

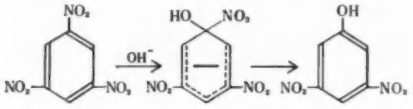

Pale yellow Red Yellow

It was suggested also by Meisenheimer[14] that a red product between 2,4,6-trinitroanisol (TNA) and sodium ethoxide had the probable constitution indicated in Fig. 9(b). In this case, he isolated as solids the products of the reaction of TNA with potassium ethoxide and of 2,4,6-trinitrophenetole with potassium methoxide, obtained a mixture containing trinitrophenetole on decomposing each of these solids with dilute sulfuric acid, and concluded that both red products consisted of the potassium salt of the anion (Fig. 9(b)). The structure presented by Meisenheimer for the complex between TNA and ethoxide ion, has been recently supported by Hamick and Foster[15,16], and by Nagakura and Tsubomura[13,17], who

5) L. de Bruyn and van Leent, *Rec. trav. Chim.*, **13**, 151 (1894).
6) L. de Bruyn, ibid., **9**, 208 (1890).
7) L. de Bruyn and van Leent, ibid., **13**, 148 (1894).
8) L. de Bruyn and van Leent, ibid., **14**, 150 (1895).
9) A. Hantzsch and H. Kissel, *Ber.*, **32**, 3140 (1899).
10) Jackson, *Am. Chem. J.*, **20**, 455 (1898); **23**, 294 (1901).
11) J. B. Ainscough and E. F. Caldin, *J. Chem. Soc.*, **1956**, 2528, 2540, 2546.
12) J. Meisenheimer, *Ann.*, **323**, 214, 241 (1902).
13) S. Nagakura, Private communication.
14) J. Meisenheimer, *Ann.*, **323**, 205 (1902).
15) D. L. Hamick and R. Foster, *J. Chem. Soc.*, **1954**, 2153.
16) R. Foster, *Nature*, **175**, 746 (1955).
17) H. Tsubomura, Private communication.

have succeeded in measuring an energy of activation for a decomposition reaction of a red complex of 2,4-dinitroanisol and hydroxyl ion to dinitrophenol.

In the reaction of Tetryl with sodium hydroxide PA seems to be finally produced through an intermediate, as indicated below, because the final absorption curve (5) of the reaction closely resembles that of PA (6) in Fig. 7. Although the red

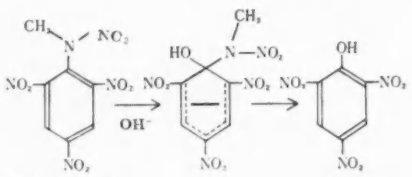

Pale yellow Red Yellow

products of TNB and Tetryl with alkali finally yield the different substances, that is, 3,5-dinitrophenol and PA, respectively, the resemblance between their spectra (curves 2 and 7 in Fig. 6) suggests that the structure of the red product of TNB may be similar to that of the red product of Tetryl. This is, thus, considered to support Meisenheimer's structure, since the resemblance of their spectra can be interpreted by assuming his structures in Fig. 9 (a), although the question pointed out above remains still.

Summary

(1) In ethanol and in water the maximum absorption bands of the substituted trinitrobenzenes are observed at longer wavelengths and possess smaller molar absorbancies than 1,3,5-trinitrobenzene, a benzene nucleus of which possesses some greater positive charge than those of the derivatives.

(2) Picric acid shows similar absorption curves in solvents like ethanol, water and acetone. This similarity seems to show that picric acid dissociates in all solvents.

(3) On treating the trinitrobenzenes with aqueous sodium hydroxide solution, the red colors are produced. The colors given by the trinitrobenzenes having substituents like $-N(CH_3)NO_2$, -Cl and -OH, are labile, while those produced from trinitrobenzene and 2,4,6-trinitrotoluene are rather stable. The spectrum of the red color of trinitrobenzene closely resembles that of Tetryl.

The author is particularly indebted to Professor Y. Nomura for his suggestion and encouragement of the present work. Thanks are also due to Associate Professor S. Maeda for use of the spectrophotometer.

Department of Chemistry
Defense Academy
Yokosuka, Kanagawa

---

*Penetration of Liquids into Filter Paper Used in Paper Chromatography**

By Masayuki NAKAGAKI and Kyoko OSAGAWA

(Received August 21, 1958)

The velocity of liquids ascending in filter paper, which is hung in a closed vessel and whose lower end is dipped in a liquid, is interesting from two viewpoints. The one is as the basis of the paper chromatography, in which the knowledge on the mechanism of the ascending of the developer liquid in a filter paper and on the properties of the filter paper seems to be fundamental to understand the physico-chemical details in the process of paper chromatography. The other standpoint is as a part of the studies of the penetration of liquids into porous materials. The latter, for example, the penetration of detergent solutions into clothes, is important when we consider the treatment of textiles in water.

The phenomenon can be treated by assuming that the penetration of liquids is due to the capillary force under the

* Presented before the Himeji Meeting held by the Chemical Society of Japan on May 31, 1958.

resistance by the viscosity and the hydrostatic pressure. Many theoretical and experimental investigations have already been made from this standpoint. Brittin[1] and Ikeda and Soeya[2] studied the ascending of liquids in capillary tubes. Lucas[3], Peek and McLean[4] and Fujita[5] studied the penetration into filter paper. Wolkowa[6] studied the penetration of liquids into a tube packed with powdered material. Carman[7] also studied the layer of powders on the basis of Kozeny's theory.

According to these investigations, the velocity of ascending, dh/dt, is given by[3,4]

$$dh/dt = (1/8\eta h)(2r\gamma \cos\theta - r^2 h\rho g) \quad (1)$$

and the equation for the initial stage of penetration is[3,4,6]

$$h^2 = kt \quad (2)$$

with $$k = r\gamma \cos\theta/2\eta \quad (2a)$$

In the present paper, a model of laminar capillary gaps will be used besides the model of tubular gaps already used by investigators cited above. Moreover, parameters will be used to take into account the winding of the gaps and the adsorption of liquids by the fibre. Finally, the penetration of liquids into the filter paper actually used in the paper chromatography will be studied.

Experimental

Organic Liquids.—Ethanol was boiled for 4 hours on a water bath with calcium oxide and distilled. The fraction distilled out at 78°C was dehydrated with sodium metal and distilled to collect the fraction at 78°C. Finally, it was again distilled on calcium oxide and the fraction of 78°C was used.

Benzene of the guaranteed reagent grade was distilled and the fraction at 80°C was used.

Acetone of the extra pure reagent grade was distilled and the fraction at 56.3°C was used.

Carbon tetrachloride of the extra pure reagent grade was treated with potassium hydroxide solution in an alcohol water mixture (KOH: H_2O: Alcohol = 1:1:2) and shaken on a water bath for 30 min. at 50~60°C. Then it was washed with water, dehydrated with sodium metal and distilled to collect the fraction at 76.7°C.

Method of the Measurement.—Toyo filter paper No. 50 (for chromatography) was cut in pieces of 1 cm. in width and 25 cm. in length, and marked every 1 cm. with a pencil to show the distance from one end. A piece of the filter paper was hung in a measuring cylinder of 200 cc. closed with a cork stopper. In the cylinder, 10 cc. of liquid for study was placed in advance. The filter paper was hung so that its lower end was just 1 cm. below the surface of the liquid. The time when the front of the liquid passed every pencil mark was measured by a stop watch. All measurements were made in a thermostat held at 20°, 30° or 40°±0.02°C.

Theoretical Consideration of the Penetration

It may be natural to assume that liquid goes up in a piece of filter paper owing to the capillary force, under the resistance by the viscosity and the hydrostatic pressure. The shape of the capillary gap may be assumed to be one dimensional (tube like) or two dimensional (laminar).

In the case of the one dimensional gap, the amount of the liquid which penetrates into the gap per unit time, Q (cc./sec.), is given by Poiseuille's law,

$$Q = (\pi r^4/8\eta l)p \quad (3)$$

where η is the viscosity of the liquid, r the radius of the gap, p the pressure difference and l the length of the capillary filled with the liquid. The value of l may be different from the height of the liquid penetrated, because the capillary may be curved or wound. Therefore, the factor f is introduced here to indicate the degree of winding of the capillary by the equation,

$$f = l/h \quad (4)$$

where h is the height to which the liquid has gone up.

Now, the pressure difference p is the difference of the pressure by the surface tension and the hydrostatic pressure by the gravity,

$$p = (2\gamma \cos\theta)/r - h\rho g \quad (5)$$

where γ is the surface tension of the liquid, θ is the advancing contact angle and ρ is the density of the liquid and g is the constant of the gravity. At the equilibrium, $h = h_\infty$ and $p = 0$, so that

$$h_\infty = 2\gamma \cos\theta/r\rho g \quad (6)$$

Then, another factor must be introduced here. If it is assumed that a fraction of the liquid which penetrates into the filter paper, α, is absorbed in fiber and $(1-\alpha)$ remains in the capillary gap, then,

$$(1-\alpha)Q = \pi r^2(dl/dt) = \pi r^2 f(dh/dt) \quad (7)$$

1) W. E. Brittin, *J. Appl. Phys.*, **17**, 37 (1946).
2) Y. Ikeda and T. Soeya, *J. Phys. Soc. Japan*, **4**, 306 (1949).
3) R. Lucas, *Kolloid-Z.*, **21**, 105 (1917); **23**, 15 (1918).
4) R. L. Peek and D. A. McLean, *Ind. Eng. Chem., Anal. Ed.*, **6**, 85 (1934).
5) H. Fujita, *J. Phys. Chem.*, **56**, 625 (1952).
6) Z. W. Wolkowa, *Kolloid-Z.*, **67**, 280 (1934).
7) P. C. Carman, *J. Soc. Chem. Ind.*, **57**, 225 (1938); **58**, 1 (1939).

Integrating this equation with Eqs. 2 and 4,

$$t/\tau = -h/h_\infty - \ln(1-h/h_\infty) \tag{8}$$

is obtained, where

$$\tau = 8\eta f^2 h_\infty/(1-\alpha)r^2\rho g \tag{9}$$

On the other hand, if the gap is two dimensional and its width is w and the half distance of the gap is a, ($w \gg a$), then Eqs. 3, 5, 6, 7 and 9 should be replaced by

$$Q = (2wa^3/3\eta l)p \tag{3a}$$

$$p = \gamma\cos\theta/a - h\rho g \tag{5a}$$

$$h_\infty = \gamma\cos\theta/a\rho g \tag{6a}$$

$$(1-\alpha)Q = 2awf\mathrm{d}h/\mathrm{d}t \tag{7a}$$

and

$$\tau = 3\eta f^2 h_\infty/(1-\alpha)a^2\rho g \tag{9a}$$

respectively. However, the final equation 8 holds also in this case, although the interpretation of the constants h_∞ and τ is different from the former case. The assumption of two-dimensional gaps seems to be more reasonable than the one-dimensional gaps in the case of the filter paper.

On the basis of Eq. 8, it is easily seen that h^2 is proportional to the time, t, at the initial stage of the penetration,

$$h^2/t = 2h_\infty{}^2/\tau \quad (h/h_\infty \ll 1) \tag{9}$$

which agrees with Eq. 2 if $2h_\infty{}^2/\tau$ is equal to k.

According to the experimental data, the h^2-t curve is, however, straight only in the very initial range. The curve is not straight in the later stage. It is, therefore, desirable to expand Eq. 8 in a power series. It can be done in two ways:

$$h^2/t = (2h_\infty{}^2/\tau)\{1-(2/3)(h/h_\infty) - (1/18)(h/h_\infty)^2 - \cdots\cdots\} \tag{11a}$$

and

$$t/h^2 = (\tau/2h_\infty{}^2)\{1+(2/3)(h/h_\infty) + (1/2)(h/h_\infty)^2 + \cdots\cdots\} \tag{11b}$$

These equations show that the plot of h^2/t or t/h^2 against h should be almost linear if h is sufficiently small compared to h_∞. These equations also show that the deviation from the linearity should be smaller in h^2/t than in t/h_2, because the coefficient of the term of $(h/h_\infty)^2$ is smaller in Eq. 11a than in Eq. 11b. This is shown in Fig. 1, where curve I shows Eq. 11a and curve II shows Eq. 11b. The straight lines I′ and II′ are the initial slope of these curves. The symbols a and b show the deviation of curves I or II from the linearity by 1% and 5%, respectively.

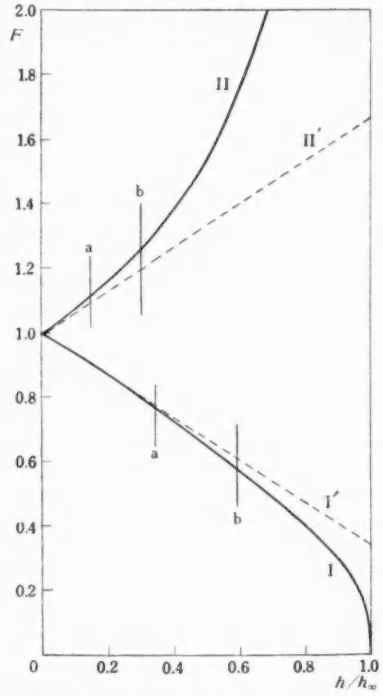

Fig. 1. Theoretical curves and their deviation from the linearity.

I: $F=(\tau/2h_\infty{}^2)(h^2/t)$
I′: $F=1-(2/3)(h/h_\infty)$
II: $F=(2h_\infty{}^2/\tau)(t/h^2)$
II′: $F=1+(2/3)(h/h_\infty)$
a: 1% deviation
b: 5% deviation

On the basis of the fact that curve I can be approximated by a straight line I′ in a fairly wide range of (h/h_∞), it is proposed to plote experimental values of (h^2/t) against h. The initial slope of this plot will give the values of A and B in the equation

$$h^2/t = A - Bh \tag{12}$$

and A and B are related to h_∞ and τ by the relations:

$$h_\infty = 2A/3B \tag{13}$$

and

$$\tau = 8A/9B^2 \tag{14}$$

as easily derived from Eq. 11a.

Results and Discussion

The height of the ascent of water and ethanol against time is shown in Fig. 2. The curves in this figure are the theoretical curves by Eq. 8, using the values of h_∞ and τ obtained by (h^2/t) vs. h plots on the basis of Eqs. 12, 13 and 14. These values are shown in Table I together with the

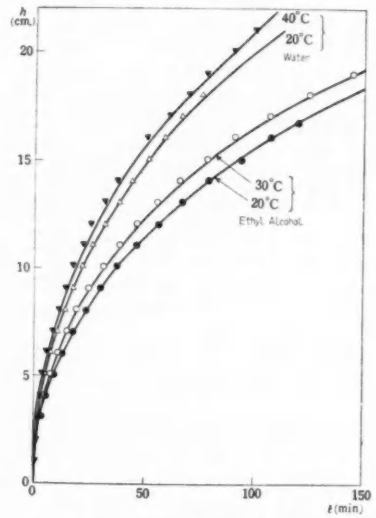

Fig. 2. The $h-t$ plot for water and ethanol.

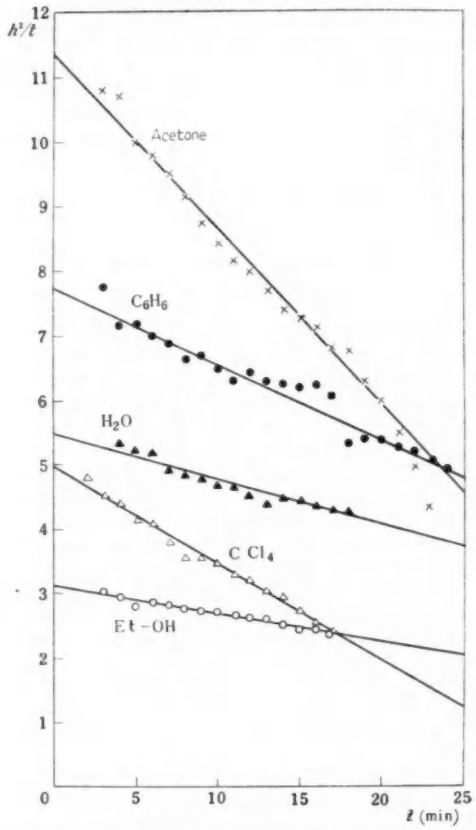

Fig. 3. The $h^2/t-h$ plot for acetone, benzene, water, carbon tetrachloride and ethanol.

TABLE I
CONSTANTS FOR THE PENETRATION OF WATER AND ETHANOL

	Water		Ethanol	
	20°C	40°C	20°C	30°C
A (cm²/min.)	5.45	6.10	3.10	3.87
B (cm./min.)	0.070	0.075	0.044	0.069
h_∞ (cm.)	51.9	54.2	47.5	37.4
τ (min.)	990	965	1460	722
x (μ)	14.3	13.1	6.09	7.50
y (μ)	1.65	1.37	1.59	1.84

TABLE II
CONSTANTS FOR THE PENETRATION OF SEVERAL LIQUIDS AT 20°C

	Acetone	Benzene	Water	CCl_4	Ethanol
A (cm²/min.)	11.37	7.71	5.45	4.95	3.10
B (cm./min.)	0.271	0.117	0.070	0.150	0.0435
η (c. p.)	0.323	0.647	1.009	0.970	1.200
γ (dyne/cm.)	23.70	28.88	72.75	26.77	22.27
ρ	0.7901	0.8788	0.9982	1.594	0.7893
x (μ)	10.9	7.65	14.3	7.78	6.09
y (μ)	2.06	1.82	1.65	1.88	1.59
$\cos\theta$	0.559	0.797	0.426	0.783	(1.00)
θ	55.0°	37.2°	64.8°	38.5°	(0°)
Two dimensional gap (a=6.09 μ)					
f (α=0.16)	2.71	3.06	3.38	2.95	3.50
f (α=0)	2.96	3.34	3.69	3.22	3.83
One dimensional gap (r=12.2 μ)					
f (α=0.16)	3.33	3.75	4.15	3.63	4.30
f (α=0)	3.64	4.10	4.54	3.96	4.70

values of A and B of Eq. 12.

In order to eliminate the factors depending on the properties of the liquid penetrating and in order to obtain the parameters depending mostly on the properties of the filter paper, two quantities, x and y, are introduced, both of which are proportional to the half distance, a, in the case of two-dimensional gap and are proportional to the radius, r, of the gap in the case of the one-dimensional gap. That is,

$$x=\gamma/\rho g h_\infty = a/\cos\theta \text{ or } r/2\cos\theta \qquad (15)$$

and

$$y=(3/2)(\eta B/\rho g)^{1/2}=(1-\alpha)^{1/2}a/f \text{ or } (3/8)^{1/2}(1-\alpha)^{1/2}r/f \qquad (16)$$

The values of x and y are cited in Table I. The values of x for water and ethanol are different from each other, while the values of y are approximately the same for both water and ethanol.

The relationship between (h^2/t) and h are shown in Fig. 3 for acetone, benzene, water, carbon tetrachloride and ethanol at 20°C. The linearity expected from Eq. 12 is satisfied. The values of A and B obtained from this linearity are listed in Table II. Using the values of the viscosity, surface tension and density of these liquids listed also in Table II, the values of x and y are calculated and shown in the same table. It is seen that the value x varies widely depending on the nature of the liquid, while the value of y is roughly the same.

According to Eq. 15, the difference of the value of x should be due to the difference of the contact angle. If the contact angle is assumed to be zero in the case of the smallest value of x, that is the case of ethanol (this corresponds to the assumption that $a=6.09\,\mu$ or $r=12.2\,\mu$), then, the largest possible values of $\cos\theta$ and the smallest possible values of the advancing contact angle, θ, are calculated as shown in Table II. For fat-free filter paper, it is said that the value of θ was zero for many liquids[4], but it is not so for the filter paper used in the actual paper chromatography.

In order to make further estimation, the value of α is assumed to be as follows. In the case of water, the amount of water contained in 1 cm^2 of the filter paper was 0.0165 g./cm^2, and the weight of the dried filter paper was 0.0133 g./cm^2. Therefore, the amount of water contained in 1 g. of the filter paper was 1.24 g. On the other hand, the amount of water adsorbed by 1 g. of the fiber of the filter paper may be about 0.2 g., referring to the data by Marshall and Peters[8]. Therefore, the value of α is assumed to be 0.16. If a liquid other than water is adsorbed less in the fiber, the value of α should be smaller than this. The values of f calculated under this assumption were listed in Table II. Assuming the value of $a=6.09\,\mu$ in the case of two-dimensional gap model, the mean value of f is 3.12 if $\alpha=0.16$ and 3.41 if $\alpha=0$. In the case of one-dimensional gap model of $r=12.2\,\mu$, the mean value of f is 3.85 if $\alpha=0.16$ and 4.21 if $\alpha=0$. Therefore, the length of the gap is three to four times larger than the length of the filter paper.

The value of $6.09\,\mu$ for the half distance of the gap seems to be reasonable, because the diameter of fibers of the filter paper measured under a microscope was about $15\,\mu$. In this connection, it may be good to point out the generally accepted fact that the dimension of the gap obtained by the measurement of the permeability of liquid is usually five to fifteen times greater than the value obtained by the measurement of the permeability of particles.

Summary

The penetration of liquid into a piece of filter paper hung vertically above a liquid is studied theoretically and experimentally. The height of the ascent of the liquid is proportional to the square root of the time at the initial stage of the penetration, but the proportionality does not hold in a wide range of time. The equation which describes this relationship between the height and time has been derived. The values of the parameters in the equation have been determined for acetone, benzene, water, carbon tetrachloride and ethanol. It is concluded that the capillary gap in the filter paper is about $6\,\mu$ in the half distance and the length of the gap is about 3 times larger than the length of the filter paper, if the gap is assumed to be two dimensional.

Faculty of the Science of Living
Osaka City University
Nishi-ku, Osaka

8) W. J. Marshall and R. H. Peters, *J. Soc. Dyers and Colourist*, **63**, 446 (1947).

The Aconite Alkaloids. XXIV.* Oxidation of Miyaconitine and Miyaconitinone

By Shichiro KAKIMOTO

(Received September 4, 1958)

Miyaconitine (I) $C_{23}H_{29}O_6N$ and miyaconitinone (II) $C_{23}H_{27}O_6N$ were isolated from *Aconitum miyabei*, Nakai, and the following extended formulae were given to them, respectively, in Part XVI[1].

$$C_{16}H_{20}\begin{cases}OCOCH_3\\OH\\(CO)_3\\N\text{-}C_2H_5\end{cases} \qquad C_{15}H_{19}\begin{cases}OCOCH_3\\(CO)_4\\N\text{-}C_2H_5\end{cases}$$

I II

Since these alkaloids were relatively unstable to oxidation with either potassium permanganate or nitric acid, no crystalline oxidation product could be isolated even by the best method[2] found for the aconite alkaloids by H. Suginome. But, when miyaconitinone was oxidized with potassium permanganate under milder conditions, oxomiyaconitinone (III) $C_{20}H_{20}O_6$ ($-CO\text{-}N\text{-}C_2H_5$) was obtained only in a small yield.

In Part XVI[1] it was shown that an α-diketone group exists in these two alkaloids, and it seemed that oxidation with hydrogen peroxide would be successful. But all attemps of oxidative ring opening under the vigorous conditions described, for instance, by Holleman[3] and by Boeseken[4], to open the ring of *o*-camphorquinone, were unsuccessful. The present author has established a milder method to oxidize *o*-camphorquinone almost quantitatively to camphoric acid and these alkaloids have been oxidized successfully to dibasic acids by this method.

Namely, oxidation of miyaconitine with dilute alkaline hydrogen peroxide gave a basic substance, oxymiyaconitine (IV) $C_{23}H_{29}O_7N$, and an acid, miyaconinic acid (V) $C_{21}H_{29}O_7N$. It was determined that miyaconinic acid retains the original ethylimino group but not the acetyl group. It was titrated as a monobasic acid and gave a monomethyl ester (VI) $C_{22}H_{31}O_7N$ by esterification with diazomethane, while the dimethyl ester (VII) $C_{23}H_{33}O_7N$ could be derived with dimethyl sulfate in a concentrated potassium hydroxide solution. Acetylation of the dimethyl ester afforded a diacetyl compound (VIII) $C_{27}H_{37}O_9N$. Miyaconinic acid as well as these derivatives could not be hydrogenated by the method[1] described as a method for comparison of miyaconitine with miyaconitinone. These experiments showed that miyaconitine was hydrolyzed and then oxidized at the α-diketone group to give a dibasic acid V and its transformations into the above-mentioned derivatives are represented by the following schema:

$$\text{I} \rightarrow C_{16}H_{20}\begin{cases}(OH)_2\\CO\\(COOH)_2\\N\text{-}C_2H_5\end{cases} \quad \text{V} \quad \rightarrow C_{16}H_{20}\begin{cases}(OH)_2\\CO\\COOH\\COOCH_3\\N\text{-}C_2H_5\end{cases} \quad \text{VI} \quad \rightarrow$$

$$C_{16}H_{20}\begin{cases}(OH)_2\\CO\\(COOCH_3)_2\\N\text{-}C_2H_5\end{cases} \quad \text{VII} \quad \rightarrow C_{16}H_{20}\begin{cases}(OCOCH_3)_2\\CO\\(COOCH_3)_2\\N\text{-}C_2H_5\end{cases} \quad \text{VIII}$$

Oxidation of miyaconitinone by the same method gave miyaconinic acid and miyaconitinonic acid (IX) $C_{23}H_{29}O_8N$. The formation of miyaconinic acid from miyaconitinone is analogous to the alkaline hydrolysis of miyaconitine and miyaconitinone to miyaconine. Miyaconitinonic acid had an acetyl group and absorbed 1 mole of hydrogen, so that its relation to miyaconinic acid may be similar to the relation of miyaconitinone to miyaconine. Accordingly, formula IX is given to miyaconitinonic acid.

$$C_{15}H_{19}\begin{cases}OCOCH_3\\(CO)_2\\(COOH)_2\\N\text{-}C_2H_5\end{cases}$$

IX

* This constitutes a part of a series entitled "The Aconite Alkaloids" by H. Suginome. The report, "On Lucaconine" presented in *Proc. Japan Acad.*, **22**, 122(1946) will be called Part XXIII. Part XXII is H. Suginome and S. Umezawa, *J. Fac. Sci. Hokkaido Univ., Ser. III Chem.*, **4**, 44 (1950).

1) H. Suginome, S. Furusawa, Y. Chiba and S. Kakimoto, ibid., **4**, 1 (1950).

2) H. Suginome, ibid., **2**, 95 (1937): *Ann.*, **533**, 172 (1931).

3) M. A. F. Holleman, *Rec. trav. chim.*, **23**, 169 (1904).

4) M. J. Boeseken, ibid., **30**, 142 (1911).

Miyaconinone that had been obtained by acid hydrolysis of miyaconitinone was oxidized to miyaconinic acid. This relation also had the same resemblance as observed previously. Miyaconine was oxidized to isomiyaconinic acid (X) differing from miyaconinic acid in melting point, optical rotation and crystalline form, but possessing the same formula $C_{21}H_{29}O_7N$ and the same chemical properties.

When miyaconitinonic acid was treated with acetic anhydride or heated under a reduced pressure, carbon dioxide and water were split off, producing a weak base, anhydrodecarboxymiyaconitinonic acid (XI) $C_{22}H_{27}O_5N$. It absorbed 1 mole of hydrogen, and had still an acetyl group. It could be distilled in high vacuum and it corresponded to a base resulting from original miyaconitinone by loss of one carbonyl group. It would be the most useful substance for succeeding degradation to clarify the constitution of the original alkaloid. The same treatment of miyaconinic acid with acetic anhydride afforded a weak base, diacetyldecarboxymiyaconinic acid (XII) $C_{24}H_{33}O_7N$. From isomiyaconinic acid, diacetyldecarboxyisomiyaconinic acid (XIII) $C_{24}H_{33}O_7N$ was obtained.

These acids and derivatives were produced by opening of one ring containing the α-diketone group just as expected. Further, anhydrodecarboxy compound XI was derived by closing the ring and splitting off carbon dioxide and water.

As the acids were titrated as monobasic, the ring opening might have occurred in the neighborhood of the ethylimino group. Accordingly, it was expected that the ethylimino group would be changed in its chemical properties and attacked in the ordinary degradation process. But, methiodides of their esters returned readily with alkali to the original substances such as miyaconitine and miyaconitinone.

Experimental

Oxomiyaconitinone (III).—Two g. of miyaconitinone was added to a solution of 0.15 g. of potassium permanganate and 5 cc. of glacial acetic acid in 30 cc. of acetone and the solution was allowed to stand for 24 hr. After filtration to remove manganese dioxide, the solution was evaporated to dryness and the residue was dissolved in water. The crude oxomiyaconitinone was extracted from the aqueous solution with chloroform and recrystallized from ethanol. Yield, 0.2 g. White needles, m. p. 210°.

Anal. Found: C, 64.86; H, 6.10; (N)-C_2H_5, 7.49. Calcd. for $C_{21}H_{29}O_7N$-C_2H_5: C, 64.62; H, 5.90; (N)-C_2H_5, 6.80%.

A Modified Method for Preparation of Camphoric Acid.—To a mixture of 2.5 cc. of 3 percent hydrogen peroxide, 2.5 cc. of N potassium hydroxide solution and 5 cc. of water, 0.2 g. of *o*-camphorquinone was added and the mixture was shaken for 24 hr. The reaction mixture was acidified and concentrated to give 0.2 g. of camphoric acid. m. p. 186~187°. $[\alpha]_D^{10}$ +57.3° (acetone).

Anal. Found: C, 59.90; H, 7.99. Calcd. for $C_{10}H_{16}O_4$: C, 59.98; H, 8.06%.

Oxidation of Miyaconitine with Hydrogen Peroxide.—*a*) *Oxymiyaconitine (IV).*—A suspension of 1.7 g. of powdered miyaconitine in a mixture of 8 cc. of 3 percent hydrogen peroxide, 10 cc. of N potassium hydroxide solution and 20 cc. of water, was shaken for 24 hr. The mixture of unchanged miyaconitine and oxymiyaconitine was collected and fractionally recrystallized from ethanol; 0.25 g. of oxymiyaconitine was obtained. m. p. 244~245° (decomp.). $[\alpha]_D^{9.5}$ +44.6° (N acetic acid).

Anal. Found: C, 64.33; H, 6.69. Calcd. for $C_{23}H_{29}O_7N$: C, 64.02; H, 6.78%.

b) *Miyaconinic acid (V).*—The basic filtrate from miyaconitine and oxymiyaconitine, was acidified with dilute hydrochloric acid and dried up under a reduced pressure. The residue was extracted with ethanol, the extract was evaporated to dryness and the residue was treated with dilute acetic acid. The crude acid thus obtained was dissolved in dilute ammonia water and reprecipitated with dilute acetic acid. Yield, 0.17 g. Needles, m. p. 295° (decomp.). $[\alpha]_D^{15}$ +17.7° (N ammonia). It contained 1 mole of water of crystallization.

Anal. Found: H_2O, 4.18. Calcd. for $C_{21}H_{29}O_7N$-H_2O: H_2O, 4.25. Found: C, 61.79; H, 6.96; N, 3.65; COOH*, 12.41. Calcd. for $C_{21}H_{29}O_7N$: C, 61.90; H, 7.18; H, 3.44; COOH, 11.08%.

c) *Monomethyl ester of miyaconinic acid (VI).*—To a suspension of 0.1 g. of miyaconinic acid in 25 cc. of ether, 0.1 g. of diazomethane was added and the mixture was allowed to stand for 24 hr. The precipitate was dissolved in dilute acetic acid and reprecipitated with dilute ammonia water. The precipitate was recrystallized from methanol. Yield, 0.1 g., m. p. 285° (decomp.). It contained 2 moles of water of crystallization.

Anal. Found: H_2O, 7.52. Calcd. for $C_{22}H_{31}O_7N \cdot 2H_2O$: H_2O, 7.88. Found: C, 62.73; H, 7.41; OCH_3, 7.76. Calcd. for $C_{22}H_{31}O_7N$: C, 62.69; H, 7.41; OCH_3 7.36%.

Its perchlorate melted at 210° with decomposition.

Anal. Found: Cl, 6.49. Calcd. for $C_{22}H_{31}O_7N \cdot HClO_4$: Cl, 6.80%.

Its methiodide melted at 271~272° with decomposition.

Anal. Found: C, 48.50; H, 5.51; I, 23.87. Calcd. for $C_{22}H_{31}O_7N \cdot CH_3I$: C, 48.90; H, 6.03; I, 23.53%.

d) *Dimethyl ester (VII).*—To a solution of 0.2 g. of miyaconinic acid in 1.3 cc. of 15 percent

* Titrated with 0.01 N potassium hydroxide (Indicator: Phenolphthalein).

potassium hydroxide solution, 1 cc. of dimethyl sulfate was added and the mixture was warmed at 60°. The reaction mixture was acidified with dilute sulfuric acid and filtered. The solution was alkalized with dilute ammonia water, producing 0.19 g. of the dimethyl ester. It melted at 296～297° with decomposition and formed a perchlorate and a methiodide.

Anal. Found: C, 63.58; H, 7.10; OCH_3, 14.08; (N)-C_2H_5, 7.18. Calcd. for $C_{23}H_{33}O_7N$: C, 63.41; H, 7.41; OCH_3, 14.24; (N)-C_2H_5, 6.67%. Found: Cl, 6.47. Calcd. for $C_{23}H_{33}O_7N\ HClO_4$; Cl, 6.62%.

e) Diacetyl dimethyl ester (VIII).—To a solution of 0.2 g. of dimethyl ester in 2 cc. of glacial acetic acid, 2 cc. of acetic anhydride and 2 cc. of pyridine were added. After 24 hr., the solvent was distilled off under a reduced pressure. The residue was dissolved in water, and dilute ammonia water was added to give 0.2 g. of diacetyl dimethyl ester. It was recrystallized from methanol. m. p. 167～168°.

Anal. Found: C, 62.65; H, 7.34; OCH_3, 11.12; (N)-C_2H_5, 5.43; $COCH_3$, 16.39. Calcd. for $C_{27}H_{37}O_9N$: C, 62.41; H, 7.18; OCH_3, 11.94; (N)-C_2H_5, 5.59; $COCH_3$, 16.57%.

Oxidation of Miyaconitinone.— Three g. of miyaconitinone was oxidized by the above-described method. After the separation of 0.32 g. of crude miyaconinic acid from the reaction mixture, chloroform was added to the filtrate and the mixture was stirred for several minutes. The semicrystalline product, presumably containing chloroform, was separated and warmed in water to remove the contained chloroform. From the concentrated solution, 0.17 g. of crude miyaconitinonic acid crystallized out in white needles. It was recrystallized from ethanol, m. p. 259° (decomp.). $[\alpha]_D^{10}$ −84.7° (N ammonia water).

Aanl. Found: C, 61.28; H, 6.57; COOH, 10.16; $COCH_3$, 9.83. Calcd. for $C_{23}H_{29}O_8N$: C, 61.73; H, 6.54; COOH, 10.05; $COCH_3$, 9.62%. 8.120 Mg. of sample absorbed 0.442 cc. of hydrogen (1.04 mol.).

Oxidation of Miyaconine.— Oxidation of 0.7 g. of miyaconine afforded 0.2 g. of isomiyaconinic acid. It melted at 268° with decomposition. White plates, $[\alpha]_D^{9.3}$ +27.3° (N ammonia water).

Anal. Found: H_2O, 4.55; C, 59.53; H, 7.06; COOH, 10.53. Calcd. for $C_{21}H_{29}O_7N\cdot H_2O$: H_2O, 4.25; C, 59.28; H, 7.35; COOH, 10.53%.

Oxidation of Miyaconinone.— From 0.45 g. of miyaconinone, 0.05 g. of miyaconinic acid was obtained, m. p. 295°.

Anal. Found: C, 62.69; H, 6.88. Calcd. for $C_{21}H_{29}O_7N$: C, 61.90; H, 7.18%.

Anhydrodecarboxymiyaconitinonic Acid (XI).—Miyaconitinonic acid (0.2 g.) was heated at 259° in a high vacuum for a few minutes. After cooling, the residue was recrystallized from ethanol to give anhydrodecarboxymiyaconitinonic acid. Yield, 0.13 g., m. p. 164～165°, $[\alpha]_D^{10}$ −117.0° (chloroform). XI was soluble in dilute hydrochloric acid, but almost insoluble in dilute acetic acid, and it was precipitated with ammonia water from the acidic solution. XI was also obtained from 0.1 g. of the original acid by heating with a mixture of 0.5 cc. of glacial acetic acid and 3 cc. of acetic anhydride for 1 hr., evaporating the solvent and adding water. XI was recrystallized from ethanol. Yield, 0.04 g.

Anal. Found: C, 67.43; H, 6.77; N, 3.74; $COCH_3$, 11.54. Calcd. for $C_{22}H_{27}O_6N$: C, 68.55; H, 7.06; N, 3.63; $COCH_3$, 11.09%. 8.533 Mg. of sample absorbed 0.442 cc. of hydrogen (1.15 mol.).

When this base was heated with 45 per cent ethanol for 2 hr., it was converted into a weak base, m. p. 194～195°, $[\alpha]_D^{10}$ −142.4° (chloroform). The latter base corresponded to decarboxymiyaconitinonic acid.

Anal. Found: C, 65.63; H, 6.94; $COCH_3$; 10.63. Calcd. for $C_{22}H_{29}O_6N$: C, 65.50; H, 7.25; $COCH_3$, 10.67%. 8.637 Mg. of sample absorbed 0.446 cc. of hydrogen (0.93 mol.).

Diacetyldecarboxymiyaconinic Acid (XII).—When 0.22 g. of miyaconinic acid was treated with acetic anhydride as mentioned above, 0.11 g. of diacetyldecarboxymiyaconinic acid was obtained in white prisms, m. p. 215～216°.

Anal. Found: C. 63.57; H, 6.39; $COCH_3$, 18.98. Calcd. for $C_{24}H_{33}O_7N$: C, 64.41; H, 7.43; $COCH_3$, 19.68%.

Diacetyldecarboxyisomiyaconinic Acid (XIII).—From 0.1 g. of isomiyaconinic acid, 0.01 g. of diacetyldecarboxyisomiyaconinic acid was obtained in white needles, m. p. 200～202°.

Anal. Found: C, 63.73; H, 6.50; $COCH_3$, 19.80. Calcd. for $C_{24}H_{33}O_7N$: C, 64.41; H, 7.43; $COCH_3$, 19.68%.

The author wishes to express his thanks to Professor Harusada Suginome, President of Hokkaido University, for his exceedingly kind direction throughout this work.

Department of Chemistry
Faculty of Science
Hokkaido University
Sapporo

The Aconite Alkaloids. XXV. Selenium Dehydrogenation of Miyaconitinone and Lucidusculine*

By Harusada SUGINOME and Shichiro KAKIMOTO

(Received September 4, 1958)

Miyaconitinone[1], $C_{23}H_{27}O_6N$, which has been isolated from *Aconitum miyabei*, Nakai, belongs to the aconine group that may be derived from the fundamental base, $C_{19}H_{29}N$; while lucidusculine[2], $C_{24}H_{35}O_4N$, which has been isolated from *Aconitum luciduscul*um, Nakai, may be derived from the fundamental base, $C_{20}H_{31}N$, similar to atisine. These two aconite alkaloids, belonging to different fundamental bases, were subjected to dehydrogenation by selenium, producing the following results:

Miyaconitinone → $C_{21}H_{38}$ (unsure), phenanthrene, anthracene

Lucidusculine → phenanthrene, 3-methylphenanthrene, pimanthrene (unsure)

Hetisine, atisine, napelline and staphisine all yielded neutral fractions consisting of complex mixtures of phenanthrene hydrocarbons, some of which were identified to be phenathrene, 1-methyl-, 1,7-dimethyl-, 1-methyl-6-ethylphenanthrene, 3-methylretene, and $C_{17}H_{16}$ or $C_{18}H_{18}$[3].

The conditions, employed at first, to dehydrogenate miyaconitinone were rather more vigorous than Lowson's procedure, but a good result was not obtained. Only an oily mixture of unsaturated hydrocarbons and a saturated hydrocarbon, which melted at 60° and seemed not to be pure but near to $C_{21}H_{38}$, were obtained.

When miyaconitinone was dehydrogenated under more drastic conditions, e. g., heated in a sealed tube at 300~320° for 24 hr. and then at 370~380° for 24 hr., an oily mixture of unsaturated hydrocarbons was yielded. High vacuum distillation of the mixture afforded crystalline hydrocarbons from which pure phenanthrene and anthracene were separated by means of recrystallization. Each of them was determined by observation of ultraviolet absorption spectrum and preparation of quinone and picrate.

Under the same condition, giving phenanthrene and anthracene from miyaconitinone, lucidusculine was dehydrogenated. The main part of mixture of crystalline hydrocarbons was phenanthrene, and two other hydrocarbons were obtained in small quantities. One of them was determined to be a methylphenanthrene by elementary analysis. It melted at 62° and was converted into the picrate, bright yellow needles, m. p. 130°, and into the quinone, orange plates, m. p. 204°. Therefore, it was decided to be a 3-methylphenanthrene[4]. The other hydrocarbon melted at 80° and was converted into the picrate, yellow needles, m. p. 125°, and into the quinone, reddish needles, m. p. 182°. It seemed to be 1,7-dimethylphenanthrene (pimanthrene)[5]. From lucidusculine no anthracene derivative was yielded, but only the derivatives of phenanthrene.

It has not yet been reported that anthracene is obtained from other aconite alkaloids. The authors have been able to obtain anthracene from miyaconitinone. But it may be too early to conclude that the aconite alkaloid, having the fundamental base, $C_{20}H_{31}N$, has a constitution with a skeleton that yields both phenanthrene and anthracene, because miyaconitinone has so many oxygen atoms that it is very unstable to oxidation (cf. Part XXIV) and because it requires a drastic condition for dehydrogenation. It is of interest that some cholestanediols can be converted readily into anthracene ring system[6].

* Part XXIV, S. Kakimoto, This Bulletin, **32**, 349(1959).

1) H. Suginome, S. Furusawa, Y. Chiba and S. Kakimoto, *J. Fac. Sci. Hokkaido Univ., Ser. III Chem.*, **4**, 1 (1950).

2) H. Suginome, S. Kakimoto and J. Sonoda, ibid., **4**, 25 (1950); R. Majima and S. Morio, *Ber.*, **65**, 599 (1936).

3) A. Lowson and J. E. C. Toops, *J. Chem. Soc.*, **1937**, 1640; W. A. Jacobs and L. C. Craig, *J. Biol. Chem.*, **143**, 589 (1942); L. C. Craig and W. A. Jacobs, ibid., **152**, 645, 651 (1944); W. A. Jacobs and C. F. Huebner, ibid., **170**, 189 (1947); C. F. Huebner and W. A. Jacobs, ibid., **169**, 211 (1946); **170**, 203 (1947).

4) R. D. Haworth, *J. Chem. Soc.*, **1932**, 1125.

5) L. Ruzicka and Fr. Balas, *Helv. Chim. Acta.*, **6**, 689 (1923).

6) K. Tsuda and R. Hayatsu, *J. Am. Chem. Soc.*, **77**, 3089 (1955).

Experimental

Dehydrogenation of Miyaconitinone. — A mixture of 3 g. of miyaconitinone and 15 g. of selenium was divided into four portions. Each of them was sealed in a hard glass tube and heated at 320° for 35 hr. The reaction mixtures were combined and extracted with ether, and from the extract, basic substances from which no crystalline substance could be isolated, were removed by extraction with dilute hydrochloric acid. After ether was distilled off, the residue was fractionated by high vacuum distillation (over 10^{-3} mm.). Three hundred mg. of first fraction, distilled at 80~130°, was treated with glacial acetic acid. The insoluble part was recrystallized three times from methanol to give 13 mg. of white leaflets, m. p. 60°. The material has no color reaction with tetranitromethane and may be $C_{21}H_{38}$ or hydrocarbon near $C_{21}H_{38}$.

Anal. Found: C, 85.36; H, 14.38. Mol. Wt. 294 (Rast's method). Calcd. for $C_{21}H_{38}$: C, 86.79; H, 13.21%. Mol. Wt. 290.

When water was added to the solution of unsaturated hydrocarbon in glacial acetic acid, oil was separated. It was distilled to give 230 mg. of oil which was colored by tetranitromethane. It seemed to be a mixture of unsaturated hydrocarbons.

Anal. Found: C, 89.64; H, 7.98%.

Since it was not possible to isolate the pure substance in the above described experiment, more drastic conditions were employed as the following.

A mixture of 20 g. of miyaconitinone and 80 g. of selenium was divided into ten portions. Each of them was heated at 300~320° for 24 hr., and then at 370~380° for the same period in a sealed tube. The reaction mixtures were combined and extracted with ether. Ethereal extract was washed with dilute hydrochloric acid, next with dilute sodium bicarbonate solution and then with water. After removal of the ether, the residue was distilled under a high vacuum to give one part of oil and 460 mg. of crystalline part. The latter was fractionally recrystallized from methanol into three parts, i) melted at 90~100°, ii) melted at 190~200°, iii) melted at 120~150°. Recrystallization through picrate and chromatographic separation of crude substance was not effective to obtain pure compounds. The part i thus separated was able to be purified through the picrate which was recrystallized from ethanol, and then the derived free hydrocarbon was recrystallized from methanol again to yield 25 mg. of phenanthrene, m. p. 99~100°. The substance was characterized by the observation of ultraviolet absorption spectrum and by preparing the picrate, m. p. 144° and phenanthrenequinone, m. p. 205°, which was derived by oxidation with chromic trioxide in glacial acetic acid. These derivatives gave no depression of the melting points on admixture with the corresponding derivatives of pure phenanthrene.

Anal. Found: C, 94.33; H, 5.24. Calcd. for $C_{14}H_{10}$: C, 94.34; H, 5.66. Found: C, 80.70; H, 3.66. Calcd. for $C_{14}H_8O_2$: C, 80.69; H, 3.87%. Found: C, 59.37; H, 2.71. Calcd. for $C_{14}H_{10}$. $C_6H_3O_7N$: C, 58.97; H, 2.80%.

The part ii, mentioned above, was recrystallized from methanol to yield 20 mg. of an anthracene, m. p. 215°. The derived anthraquinone melted at 283°.

Anal. Found: C, 94.35; H, 5.65. Calcd. for $C_{14}H_{10}$: C, 94.34; H, 5.66. Found: C, 80.41; H, 3.62. Calcd. for $C_{14}H_8O_2$: C, 80.69; H, 3.87%.

The part iii was found to be a mixture of i and ii. Recrystallization through picrate and chromatographic separation afforded no good result. Therefore, the mixture was oxidized with chromic trioxide in glacial acetic acid. The oxidized substance was dissolved in alcohol and the product was adsorbed on neutral alummina and eluted with benzene; 20 mg. of pure phenanthrenequinone and 15 mg. of anthraquinone could be separated.

Dehydrogenation of Lucidusculine. — The conditions of dehydrogenation were the same as those used for miyaconitinone to obtain phenanthrene and anthracene. Neutral oil in an amount of 1.731 g. was obtained from 20 g. of lucidusculine. From the oil, 426 mg. of crystalline hydrocarbon mixture was separated by high vacuum distillation. The mixture was repeatedly recrystallized from methanol, but only 45 mg. of phenanthrene, m. p. 98°, (its picrate, m. p. 142°, the quinone, m. p. 204°) was isolated and no anthracene could be obtained. Other parts of hydrocarbon mixture were converted into picrate. The recrystallization was repeated again to give phenanthrene picrate and two other picrates. One of them was in the form of bright yellow needles, m. p. 130° and the other of yellow needles, m. p. 125°. From the former, 38 mg. of 3-methylphenanthrene, m. p. 62° was obtained and it was oxidized to the quinone, m. p. 204°. Orange plates.

Anal. Found: C, 93.58; H, 6.06. Calcd. for $C_{15}H_{12}$: C, 93.71; H, 6.26%. Found: C, 80.92; H, 4.79. Calcd. for $C_{15}H_{10}O_2$: C, 81.10; H, 4.54%.

From the latter, 9 mg. of hydrocarbon, m. p. 80° was obtained. Five mg. of this substance was oxidized to quinone which was recrystallized from methanol and melted at 182°. Reddish needles. But its yield was too small to be recrystallized repeatedly for analysis. It seemed to be pimanthrene (1,7-dimethylphenanthrene).

Department of Chemistry
Faculty of Science
Hokkaido University
Sapporo

The Aconite Alkaloids. XXVI. On Lucaconine and Monoacetyllucaconine*

By Harusada SUGINOME and Sijô FURUSAWA**

(Received September 4, 1958)

In Part XXIII[1] of this series, it was reported that a new alkaloid, lucaconine, $C_{21}H_{33}O_6N$, was isolated from the roots of *Aconitum luciduscul*um, Nakai and it was suggested that it had two methoxyl, four hydroxyl, and a secondary amino group. One of the present authors with Amiya[2] found that diacetyllucaconine had two active hydrogens. Therefore, *N*-alkyl and other functional groups had to be determined more precisely. As the results of repeated examinations, it was found that the base had an *N*-ethyl and three methoxyl groups, and, therefore, the older molecular formula of lucaconine, $C_{21}H_{33}O_6N$, should be revised to $C_{24}H_{39}O_7N$***.

On the other hand, a new alkaloid was isolated from the roots of the above mentioned *Aconitum* species, viz., on the basis of the difference of solubility in benzene from the crude bases containing lucaconine. The content of the base was about one-tenth of that of lucaconine and was about 0.012 per cent that of dried roots. The new alkaloid was purified through a perchlorate, from which the free base was liberated and recrystallized from ethanol. The purified base had m.p. 187°, $[\alpha]_D^{18}+42.7°$, and molecular formula $C_{26}H_{41}O_8N$. On hydrolysis with alcoholic potassium hydroxide it split off one mole of acetic acid and produced the alkamine, lucaconine.

$$C_{26}H_{41}O_8N+H_2O\rightarrow CH_3COOH+C_{24}H_{39}O_7N$$

Therefore, this new base was named monoacetyllucaconine.

Acetylation of lucaconine I and monoacetyllucaconine II with acetic anhydride gave the same diacetyl compound, diacetyllucaconine III, $C_{28}H_{43}O_9N$, m. p. 124°, $[\alpha]_D^{16}+15.3°$, which afforded lucaconine on hydrolysis with alcoholic potassium hydroxide.

From these results the formulae of lucaconine I and monoacetyllucaconine II may be extended as follows:

$C_{19}H_{21}$ (OCH$_3$)$_3$, (OH)$_4$, N-C$_2$H$_5$ — Lucaconine (I)

$C_{19}H_{21}$ (OCH$_3$)$_3$, OCOCH$_3$, (OH)$_3$, N-C$_2$H$_5$ — Monoacetyllucaconine (II)

Lucaconine and monoacetyllucaconine are assumed to have hexacyclic structure based on the skeletal formula, $C_{19}H_{29}N$[3].

Experimental

Isolation of Lucaconine.—As described in the previous reports[1,4], 293.6 kg. of dried roots of *Aconitum luciduscul*um, Nakai was treated. The percolate thus obtained was divided into three fractions, which were named fraction I, fraction II, and fraction III as previously described[4]. The yield of fraction III was 1,062 g. (0.36% of dried roots). Treatment of fraction II with acetone gave 357 g. of crystalline material, which was recrystallized from ethanol to give 210 g. of crude lucaconine, melting at 197°.

From 5.5 g. of this crude lucaconine, 6.8 g. of crystalline perchlorate was prepared, which was recrystallized from ethanol to give 5.1 g. of pure perchlorate, m. p. 210° (decomp.). From this salt, 3.9 g. of a free base melting at 198° was liberated; on three recrystallizations from ethanol, the base melted at 200°, and showed no depression of the melting point on admixture with an authentic sample of lucaconine[1]. $[\alpha]_D^{16}+57.1°$ (chloroform).

Anal. Found: C, 63.48; H, 8.39; N, 3.55; OCH_3, 20.86; (N)-C_2H_5, 6.59. Calcd. for $C_{24}H_{39}O_7N$: C, 63.55; H, 8.45; N, 3.09; 3-OCH_3, 20.53; (N)-C_2H_5, 6.19%.

Determination of N-ethyl group[5].—Lucaconine was treated in the usual manner for Willstätter's *N*-alkyl determination. Trimethyl ethyl ammonium iodide thus obtained was analyzed.

* Part XXV, H. Suginome and S. Kakimoto, This Bulletin, **32**, 352 (1959).

** Present address, Faculty of Technology, Chû-ô University, Tokyo, Japan.

1) H. Suginome, S. Kakimoto, J. Sonoda and S. Noguchi, *Proc. Japan Acad.*, **22**, 122 (1946).

2) H. Suginome and T. Amiya, unpublished work.

*** The compositions calculated for these two formulae are nearly identical as follows: Calcd. for $C_{21}H_{33}O_6N$: C, 63.77; H, 8.41; N, 3.57%. Calcd. $C_{24}H_{39}O_7N$: C, 63.55; H, 8.45; N, 3.09%.

3) H. Suginome and K. Ohno, *J. Fac. Sci., Hokkaido Univ., Ser. III. Chem.*, **4**, 36 (1950).

4) H. Suginome, S. Furusawa, Y. Chiba and S. Kakimoto, ibid., **4**, 1 (1950).

5) R. Willstätter and M. Utzinger, *Ann.*, **382**, 148(1911); R. Majima and K. Tamura, ibid., **526**, 116 (1936).

Anal. Found: I, 60.38. Calcd. for $(CH_3)_3(C_2H_5)NI$: I, 59.02%.

The pure lucaconine was also obtained by treatment of the crude base melting at 197° with ethanolic potassium hydroxide, followed by recrystallization from ethanol.

Perchlorate.—m. p. 210° (decomp.).

Anal. Found: C, 51.68; H, 7.08; Cl, 6.39. Calcd. for $C_{24}H_{39}O_7N \cdot HClO_4$: C, 52.01; H, 7.75; Cl, 6.36%.

Hydrochloride.—m. p. 216~217° (decomp.) (from abs. ethanol).

Anal. Found: C, 58.81; H, 8.31; Cl, 7.32. Calcd. for $C_{24}H_{39}O_7N \cdot HCl$: C, 58.80; H, 8.22; Cl, 7.24%.

Hydrobromide.—m. p. 223° (decomp.) (from abs. ethanol).

Anal. Found: C, 54.30; H, 7.54; Br, 14.81. Calcd. for $C_{24}H_{39}O_7N \cdot HBr$: C, 53.91; H, 7.54; Br, 14.93%.

Methiodide.—m. p. 174° (from water).

Anal. Found: C, 49.23; H, 7.29; OCH_3, 16.36; I, 19.51. Calcd. for $C_{24}H_{39}O_7N \cdot CH_3I$: C, 50.40; H, 7.11; 3-$OCH_3$, 15.91; I, 21.32%.

The methiodide readily returned to the original base by means of alkali.

Isolation of Monoacetyllucaconine.—On being left to stand in a refrigerator, the mother liquor, obtained by removal of the lucaconine-rich base, gave 90 g. of crystalline substance melting at 168~172°. This substance was recrystallized from benzene and then from ethanol to give a crystalline base melting at 186°. Yield 12.8 g. From this base perchlorate was obtained, which after three recrystallizations from ethanol showed m. p. 202~202.5° (decomp.). Yield, 9.0 g. Free base, obtained from this perchlorate, showed m. p. 187°, $[\alpha]_D^{18}$ +42.7° (ethanol) after recrystallization from ethanol. Yield, 3.75 g.

Anal. Found: C, 63.11; H, 8.22; N, 2.85; OCH_3, 18.90; (N)-C_2H_5, 5.05; $COCH_3$, 10.80. Calcd. for $C_{26}H_{41}O_8N$: C, 63.07; H, 8.34; N, 2.83; 3-OCH_3, 18.79; (N)-C_2H_5, 5.86; $COCH_3$, 8.68%.

This base, monoacetyllucaconine, was easily soluble in methanol and in ethanol and moderately so in benzene but sparingly so in water and in petroleum ether.

Perchlorate.—m. p. 202~202.5° (decomp.).

Anal. Found: Cl, 5.85. Calcd. for $C_{26}H_{41}O_8N \cdot HClO_4$: Cl, 5.95%.

Hydrobromide.—m. p. 190~191° (decomp.).

Anal. Found: H_2O, 2.42. Calcd. for $C_{26}H_{41}O_8N \cdot HBr \cdot 3/4H_2O$: H_2O: 2.29%.

Anal. (anhydrous) Found: Br, 13.21. Calcd. for $C_{26}H_{41}O_8N \cdot HBr$: Br, 13.85%.

Hydrolysis of Monoacetyllucaconine.—After monoacetyllucaconine was hydrolyzed with 0.5 N ethanolic potassium hydroxide, a crystalline substance was obtained. After recrystallization from ethanol, it was identified as lucaconine by the mixed melting point test.

Anal. Found: C, 63.34; H, 8.77. Calcd. for $C_{24}H_{39}O_7N$: C, 63.55; H, 8.45%.

Acetic acid produced on hydrolysis of monoacetyllucaconine was identified as silver salt.

Anal. Found: Ag, 64.67. Calcd. for CH_3CO_2Ag: Ag, 64.64%.

Diacetyllucaconine (III).—*a) From Lucaconine (I).*—Lucaconine was heated in acetic anhydride for 30 min., and the reaction mixture was treated in the usual manner. After recrystallization from dilute ethanol, diacetyllucaconine was obtained in colorless needles, m. p. 124°, $[\alpha]_D^{16}$ +15.3° (94% ethanol).

Anal. Found: C, 62.40; H, 8.01; N, 2.69; $COCH_3$, 15.93. Calcd. for $C_{28}H_{43}O_9N$: C, 62.55; H, 8.05; N, 2.61; 2-$COCH_3$, 15.9%.

b) From Monoacetyllucaconine (II).—Upon the same treatment as in the case of lucaconine described above, monoacetyllucaconine afforded the same diacetyllucaconine, m. p. and mixed m. p. 124°.

After being heated at 145° for 10 min. under reduced pressure (1×10^{-5} mmHg), diacetyllucaconine was recovered unchanged.

Hydrolysis of Diacetyllucaconine (III).—Diacetyllucaconine was hydrolyzed by heating with 0.5 N ethanolic potassium hydroxide. After removal of most of the ethanol, the reaction mixture was extracted with chloroform and then the chloroform extract was evaporated to give lucaconine, which melted at 198° after recrystallization.

Anal. Found: C, 63.58; H, 8.67; N, 3.44. Calcd. for $C_{24}H_{39}O_7N$: C, 63.55; H, 8.45; N, 3.09%.

Department of Chemistry
Faculty of Science
Hokkaido University
Sapporo

The Molecular Cross-sectional Areas for the Determination of Specific Surface Areas of Solids. I. Carbon Black

By Kumasaburo KODERA and Yoshito ONISHI

(Received September 11, 1958)

Various methods have been developed to estimate the specific surface areas of solids from the theory of physical adsorption. Among them, most widely used is the Brunauer-Emmett-Teller, or B. E. T. method[1]. In this method, the number of adsorbed molecules necessary to cover the surface of 1 g. of a solid completely with a monomolecular layer is evaluated by so-called B. E. T. equation, i. e.,

$$\frac{P}{V(P_s-P)} = \frac{1}{V_mC} + \frac{(C-1)}{V_mC}\cdot\frac{P}{P_s} \qquad (1)$$

where P is the equilibrium pressure, P_s the saturation pressure of the adsorbate gas, V the volume of the gas adsorbed at S. T. P., V_m that necessary to cover the surface with a monomolecular layer, and C a constant.

Specific surface area is then obtained by multiplying V_m with the molecular cross-sectional area, σ, which is given by the following equation:

$$\sigma = 1.091(M/N\rho)^{2/3} \qquad (2)$$

where M is the molecular weight, ρ the density in the liquid (or solid) state of the adsorbate, and N Avogadro number. If the number of molecules in a monomolecular layer and the cross-section obtained above were correct, the calculation would give an absolute surface area, and the values obtained by different adsorbates should agree. But it is well known, generally, that this is not the case. For instance, Jacobs and Tompkins[2] stated that most adsorbates yield surface areas that require multiplication by a factor of between 1.2 and 1.5, and in extreme cases 2 or 3, to give areas agreeing with those calculated from the nitrogen isotherms. This disagreement may arise from either of two reasons: (1) the B. E. T. equation cannot be applied satisfactorily for the isotherms; and (2) equation 2 for σ fails to give a correct cross-section of an adsorbate molecule on the surface. Existence of chemisorption, active spots, and pores or cracks on the surface mainly affects the type of isotherm while packing of adsorbate molecules on the surface affects σ because the factor 1.091 in equation 2 is calculated from the assumption that the adsorbate molecules on the surface is spherical closest packing, i. e., three dimensionally 12 co-ordination and two dimensionally 6 co-ordination. Therefore, it is very difficult to know the absolute value of the surface area by this method. Thus, to compare surface areas using different gases, relative values of cross-sections should be determined beforehand.

On the other hand, Harkins and Jura[3] have developed the absolute calorimetric method to measure the absolute surface area without the knowledge of the cross-section of the adsorbate molecule. But this method has not been employed generally, because it can not be applied to solids which have pores and cracks and the method of measurement is so difficult that its applicability is rather limited.

Livingston[4] examined published data about the measurements of the specific surface areas of oxides by the B. E. T. method and assigned the cross-sections of adsorbate molecules which might give the consistent areas for oxides. He took the case of adsorption of nitrogen at $-195°$ as a standard process and assigned the value 15.4 Å^2 for the cross-section of a nitrogen molecule instead of widely used value, 16.2 Å^2, obtained from equation 2 using liquid density of nitrogen. Cross-sections of the other gas molecules were, then, determined so as to give equal surface area with nitrogen. These values are shown in Table V, column 5. These values, however, can not necessarily give consistent surface areas for other solids than oxides. In the experiments described below, adsorption of several gases on carbon black samples was measured by the same

1) S. Brunauer, P. H. Emmett and E. Teller, *J. Am. Chem. Soc.*, **60**, 301 (1938).

2) P. W. M. Jacobs and F. C. Tompkins, "Chemistry of the Solid State", edited by W. E. Garner, Butterworth Scientific Publications, London (1955), p. 91.

3) W. D. Harkins and G. Jura, *J. Am. Chem. Soc.*, **66**, 1362 (1944).

4) H. K. Livingston, *J. Colloid Sci.*, **4**, 447 (1949).

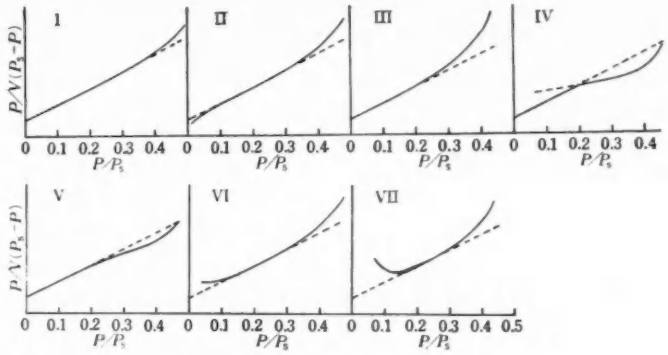

Fig. 1. Types of B. E. T. curves.

apparatus under similar experimental conditions. The specific surface areas of the adsorbents were then calculated and by comparing them with each other and with the values obtained from the electron microscopy, and taking into consideration of the two dimensional van der Waals' constant of argon, the molecular cross-section for each adsorbate gas which would give consistent surface area was determined. Gases were also examined to discover whether they were suitable for this purpose or not.

Experimental Method and Results

A series of 8 commercial carbon blacks listed in column 2, Table I, were used in this experiment. Nitrogen, argon, oxygen, carbon dioxide and *n*-butane were chosen as adsorbate gases.

The apparatus for the adsorption measurement was an ordinary volumetrical type. Temperatures of the adsorbents were measured by a vapor-pressure thermometer with suitable vapors. Samples of carbon black were heated at 200°C in the apparatus and evacuated until pressure in the apparatus reached 1×10^{-5} mmHg every time before the adsorption was measured. In most cases adsorption isotherms were taken between the relative pressures of 0.02 to 0.35, and in some cases up to 0.90. Measured values of $P/V(P_s-P)$ were plotted as a function of P/P_s, according to equation 1. Curves obtained were classified in 7 types as shown in Fig. 1.

Curves I and III have similar forms, but the former has a longer linear portion which extends over 0.35 of P/P_s. Curve II is the most general form which has the linear part from 0.05 to 0.2 or more, and below 0.5 deflects downwards. Curves IV to VII are of special types which appear in a few cases.

In Table I, types of curves obtained are listed together with the appearance of the hysteresis in the measured pressure range.

V_m was calculated from the linear parts of these curves and shown in Table II. From these values of V_m, specific surface areas of the adsorbent were calculated using molecular cross-sections in column 4, Table V, which were calculated by equation 2 using the liquid density of each gas at measured temperatures[5]. The values are shown in Table III. The ratio S_{N_2}/S is that between surface area measured by nitrogen and that of the other gas. Surface areas measured by the absolute method by Okuda and Tanaka[6] and from electron microscopy by Suito and Arakawa[7] are shown for comparison. It should be remembered that the latter values were calculated from average particle diameter $d_1=\sum nd/\sum n$, assuming the density of carbon black to be 1.8, whereas values from the adsorption correspond to $S=K(\sum nd^2/\sum nd^3)$, where K is a shape factor.

Discussion

As are shown in Table III, the ratios of surface area by nitrogen adsorption to that by argon adsorption (S_{N_2}/S), for both adsorption temperatures are 1.14 and their standard deviations are small. For oxygen and *n*-butane, the standard deviations in area ratios are greater and for carbon dioxide the greatest, even with the exclusion of No. 6.

Applicability of the B.E.T. isotherm can be judged from the range of the linear part on the curve. From Fig. 1 and Table I, it is seen that argon (−183°C) and oxygen show largest range of linear part and then follow nitrogen and argon (−196°C). Of

5) P. H. Emmett and S. Brunauer, *J. Am. Chem. Soc.*, **59**, 1153 (1937).

6) S. Okuda and N. Tanaka. The report to be published soon in *J. Ceramic Association, Japan.* (*Yogyo Kyokai Shi*).

7) E. Suito and M. Arakawa, "Collaborative Research Reports of the Ministry of Education." (Chemistry), p. 120 (1956). Data given by the authors were average particle diameter d_1, from which the surface areas shown in the table were calculated.

TABLE I
TYPES OF B. E. T. CURVES

No.	Black	N_2(−196°C)		Ar(−196°C)		Ar(−183°C)		O_2(−183°C)		CO_2(−78°C)		n-C_4H_{10}(0°C)	
		Type	Hyst.	Type	Hyst.	Type	Hyst.	Type	Hyst.	Type	Hyst.	Type	Hyst
1	Peerless II A	III	−	III	−	III	−	III	−	III	−	III	+
2	Philblack-E	I	−	I	−	I	−	I	−	II	+	I	−
3	Tokai S. 285	III	−	III	−	II	−	I	−	II	+	I	+
4	Denka 2000	III	−	III	−	I	−	I	−	II	−	I	−
5	Mi-ike 20	II	−	I	−	I	−	II	−	II	−	IV	+
6	P-33	III	−	I	−	I	−	II	−	II	−	II	+
7	Denka granular	IV	−	V	−	II	−	II	−	VII	−	II	+
8	Witoco	III	−	III	−	I	−	II	−	II	−	II	+

TABLE II
VALUES OF V_m

No.	N_2 cc./g.	Ar(−196°C) cc./g.	Ar(−183°C) cc./g.	O_2 cc./g.	CO_2 cc./g.	n-C_4H_{10} cc./g.
1	80.7	85.4	80.3	89.6	58.5	27.5
2	30.6	30.6	29.5	32.4	19.6	11.3
3	21.1	22.0	21.2	23.8	14.5	7.58
4	9.93	10.1	9.76	10.0	6.21	3.83
5	3.97	4.15	3.88	3.88	2.69	1.51
6	3.67	3.66	3.62	3.53	1.12	1.38
7	14.6	16.0	14.7	15.2	10.3	5.98
8	27.1	27.1	26.2	33.1	20.8	9.23

TABLE III
SPECIFIC SURFACE AREAS MEASURED BY VARIOUS GASES

No.	N_2(−196°C) S_{N_2} m²/g.	Ar(−196°C) S m²/g.	S_{N_2}/S	Ar(−183°C) S m²/g.	S_{N_2}/S	O_2(−183°C) S m²/g.	S_{N_2}/S	CO_2(−78°C) S m²/g.	S_{N_2}/S	n-C_4H_{10}(0°C) S m²/g.	S_{N_2}/S	Electron microscope	Absolute method
1	351.5	317.3	1.11	311.0	1.13	340.0	1.03	267.7	1.31	237.0	1.48	99.0	
2	133.0	113.4	1.17	114.2	1.16	123.0	1.08	89.7	1.47	97.2	1.38	112.2	
3	91.9	81.6	1.13	81.9	1.12	90.3	1.02	66.4	1.38	65.4	1.41	60.6	46.4
4	43.2	37.6	1.15	37.8	1.14	37.9	1.14	28.4	1.52	33.0	1.31	81.3	
5	17.4	15.4	1.13	15.0	1.16	14.7	1.18	12.3	1.41	13.0	1.34	17.9	
6	16.0	13.6	1.18	14.0	1.14	13.4	1.19	5.1	(3.14)	11.9	1.35	22.8	
7	63.6	59.2	1.08	57.0	1.12	57.6	1.10	47.0	1.35	51.6	1.23	49.2	
8	118.0	100.5	1.17	101.4	1.16	125.5	0.94	95.3	1.34	79.6	1.48	91.6	109
Avarage			1.14		1.14		1.09		1.38		1.37		
Standard deviation			0.03		0.02		0.08		0.09		0.08		

The value in parentheses is excluded from the average.

TABLE IV
COMPARISON OF SURFACE AREA FROM B. E. T. METHOD AND ELECTRON MICROSCOPY

No.	N_2	Ar(−196°C)	Ar(−183°C)	O_2	CO_2	n-C_4H_{10}
1	(3.54)	(3.20)	(3.14)	(3.44)	(2.10)	(2.40)
2	1.18	1.01	1.02	1.10	0.80	0.87
3	1.52	1.35	1.35	1.49	1.10	1.08
4	(0.53)	(0.46)	(0.46)	(0.47)	0.35	(0.41)
5	0.97	0.86	0.84	0.82	0.69	0.73
6	0.70	0.60	0.61	0.59	(0.22)	0.52
7	1.29	1.20	1.16	1.17	0.96	1.05
8	1.29	1.10	1.11	1.37	1.04	0.87
Average	1.16	1.02	1.02	1.09	0.823	0.853
Mol. cross-section	14.0	13.5	14.2	12.9	20.7	37.6 Å²

these two, argon (−196°C) has longer linear portions though not listed in the table. By *n*-butane, linear parts are also large but in most cases isotherms show hysteresis. Carbon dioxide is inferior to the other gases. Among the adsorbents used, No. 7 exhibits anomalous isotherms for all gases.

From the above facts, nitrogen and argon turned out to be the most suitable adsorbates for the surface area measurement of carbon black, while oxygen and *n*-butane are seen to be somewhat inferior to the former two. Carbon dioxide is not suitable for this purpose. From the surface ratio values in Table III, except for No. 6 by carbon dioxide, it is possible to eliminate the differences in surface areas measured by different gases by assigning a proper molecular cross-section for each gas. In doing this, a gas which might be considered to give the specific surface area nearest to the absolute surface should be chosen as a standard gas; then, the cross-section of other gases could be determined to give the equal surface area as the standard gas. Generally, nitrogen is used for the B. E. T. method with the cross-section of 16.2 Å^2, but it generally gives a larger surface area when compared with that by the other gases and also with the value obtained by electron microscopy or the absolute method. To compare surface area values by the B. E. T. method with those by electron microscopy, ratio of the values by the two methods was calculated for each carbon black with various gases and listed in Table IV*. It is seen from the table that the agreement of values between the two methods is best for argon, whereas nitrogen adsorption gives somewhat greater values. The molecular cross-section of each gas used for the evaluation of the surface area was divided by the respective average ratio and shown in the bottom of the table. These are cross-sections which will give surface areas in agreement with those from electron microscopy. For carbon black, Anderson and Emmett[8] concluded that 16.2 Å^2 is better than 13.8 Å^2 calculated from the solid density. On the other hand, Arnell and Henneberry[9] compared the surface areas of carbon blacks measured by permeability, electron microscopy, and the B. E. T. method using nitrogen cross-section of 16.2Å^2. The results revealed that the surface areas measured by the B. E. T. method was 30% larger in average than those by the other methods (except for samples which had pores and cracks as mentioned by Arnell et al.).

From the above considerations, the value 16.2 Å^2 for nitrogen cross-section would be too large. The concept of two dimensional gas of adsorbed molecules suggests that the molecular cross-section should be nearly equal to the two-dimensional van der Waals' constant[10]. For nitrogen this value is 15.4 Å^2; Livingston used this value as a standard and estimated the cross-section of other gases from this value. In the above experiment both nitrogen and argon proved to be suitable for this method, but from Table IV, it is seen that argon gives surface areas more consistent with those by electron microscopy than nitrogen does. In addition, the following facts point to the superiority of argon to nitrogen, i. e., in the plot of equation 1, generally, the former has longer linear part than the latter. Moreover, argon shows no chemisorption and exhibits more ideal packing state on the surface as it consists of monoatomic molecules and has no quadruple moment which nitrogen has to some extent[11]. The fact that the agreement between the two dimensional van der Waals' constant and the value from the equation 2 is better in argon than in nitrogen, seems to show that the former exhibits more ideal packing state on the surface than the latter does. Therefore, argon was taken as a standard. For the molecular cross-section of argon, three values were obtained, i. e., 13.5 Å^2 from comparison with electron microscopy, 13.8 Å^2 from equation 2 using liquid density at −195°C, and 13.6 Å^2 from the van der Waals' constant. Among these three values, 13.8 Å^2 from equation 2 was employed as a standard, because the differences among these values are rather small and there is no serious reason to change the generally employed value from equation 2. The molecular cross-section thus determined, those given by Livingston,

* Values in parentheses are the largest and the smallest ratios for each gas and are excluded from the average, because corresponding samples might have some undesirable surface states or particle size distributions for this comparison.

8) R. B. Anderson and P. H. Emmett, *J. Applied Phys.*, **19**, 367 (1948).

9) J. C. Arnell and G. O. Henneberry, *Canadian J. Res.*, **A, 26**, 29 (1948).

10) J. H. de Boer, "Dynamical Character of Adsorption", Oxford (1953), p. 172.

11) W. V. Smith and R. Howard, *Phys. Rev.*, **77**, 132 (1950).

TABLE V

MOLECULAR CROSS-SECTIONAL AREAS

Gas	Temp.	van der Waals' const.	Eq. 2 Liq. state.	Livingston's	Present Authors'
N_2	−196°C	15.4 Å²	16.2 Å²	15.4 Å²	14.2 Å²
Ar	−196	13.6	13.8	14.6	13.8
Ar	−183	13.6	14.4	15.5	14.4
O_2	−183	13.5	14.1	14.6	13.5
CO_2	− 78	16.5	17.0	19.5	20.8
n-C_4H_{10}	0	33.0	32.1	44.6	38.6

TABLE VI

SPECIFIC SURFACE AREAS

No.	N_2 S m²/g.	Ar(−196°C) S m²/g.	Ar(−183°C) S m²/g.	O_2 S m²/g.	CO_2 S m²/g.	n-C_4H_{10} S m²/g.	Elec. micro.	Abs. method
1	304.0	317.3	311.0	325.0	327.0	285.0	99.0	
2	116.7	113.4	114.2	117.7	109.6	116.7	112.2	
3	80.5	81.6	81.9	86.3	81.1	78.8	60.6	46.4
4	37.9	37.6	37.8	36.3	34.7	39.7	81.3	
5	15.3	15.4	15.0	14.1	15.0	15.6	17.9	
6	14.0	13.6	14.0	12.8	6.2	14.3	22.8	
7	55.8	59.2	57.0	55.1	57.5	62.1	49.2	
8	103.5	100.5	101.4	120.0	116.6	95.8	91.6	109

ordinary values from equation 2 and the two dimensional van der Waals' constants are shown in Table V. It is seen that the values agree surprisingly well with those in Table IV except oxygen. The value for oxygen agrees with that of van der Waals' constant. The value for nitrogen becomes smaller than that from equation 2 and of Livingston. Livingston said that according to the results of Arnell and Henneberry for 9 carbon blacks, nitrogen adsorption surfaces are about 12% higher than the values by permeability and electron microscopy. It is not clear how Livingston estimated the value of 12%, but if nitrogen cross-section 16.2 Å² used by Arnell and Henneberry is reduced by 12%, it gives 14.5 Å² which nearly agrees with the present value.

The specific surface areas calculated by these cross-sections are listed in Table VI. Comparison with the values by the absolute method shows good agreement in case of No. 8, while in No. 3, the absolute method gives a far smaller value. The electron microscopy also gives a smaller value for the latter sample. If there were small pores and cracks on the surface of the latter, unobservable by the electron microscope, these would be covered by the adsorbate in the case of the absolute method, so that both methods might give lower values than the B. E. T. method does. Other small values by electron microscopy are also explainable by the existence of pores and cracks. Thus, Nos. 1, 3 and 8 show somewhat lower values also by n-butane adsorption which suggest the existence of small pores, into which rather large n-butane molecules can not penetrate.

In electron microscopy, as is described above, the surface areas were calculated from $d_1=\sum nd/\sum n$, assuming all the particles to be spherical. Calculation from d_1 gives correct surface area only when all the particles have the same size. Generally, this is not the case, and owing to the particle size distribution, this calculation gives too large a surface area. Moreover, as was pointed out by Arnell and Henneberry, if a small number of large particles were overlooked in measuring particle size by the electron microscope, surface area estimated from the results would give also higher value. Therefore, larger values than those by the B. E. T. method are not unexplainable.

No. 6 shows a remarkably small surface for carbon dioxide. The surface area of this sample for carbon dioxide increased as the temperature of heating before the adsorption rose above 200°C, although it remained constant for nitrogen and argon. This effect of heating temperature was seen only in this sample. This might be explained as the heat treatment above 200°C changed surface state of this sample, and also changed the state of adsorption of carbon dioxide molecules, but the

adsorption of nitrogen and argon, which should be purely physical, would not be affected.

Conclusions

For the measurement of the specific surface areas of solid adsorbents, argon and nitrogen are most suitable for adsorbate gases. Oxygen and *n*-butane are also applicable but carbon dioxide may give unreliable results in some cases. The cross-sectional areas of adsorbed molecules listed in Table V, column 6, were determined to give consistent surface areas for different gases. The anomaly for carbon dioxide may be explained by the surface state of the carbon black.

Department of Chemistry, Faculty of Industrial Arts, Kyoto Technical University, Sakyo-ku, Kyoto

---

*Studies on 3-(Anthraquinon-1-yl)oxazolidin-2-ones. I. 3-(Methylanthraquinon-1-yl)oxazolidin-2-ones and Their Related Compounds**

By Kō Naiki

(Received September 18, 1958)

In a previous paper[1], it was reported that 1-aminoanthraquinone reacted with 2-chloroethyl chloroformate and formed 2-chloroethyl anthraquinon-1-yl carbamate. The chloroethyl anthraquinonyl carbamate was converted into 1-*N*-2-hydroxyethylaminoanthraquinone by the action of potassium hydroxide, and 3-(anthraquinon-1-yl)oxazolidin-2-one could not be separated from reaction mixture by fractional recrystallization. The reactions are explained as follows (Scheme I).

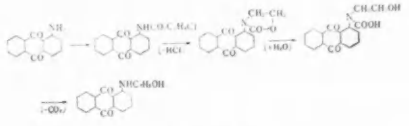

Sheme 1

In another paper[2], it was found that 2-chloroethyl anthraquinon-1-yl carbamates which contain 2-substituent in anthraquinone nucleus were converted into 2′-substituted 3-(anthraquinon-1-yl)oxazolidin-2-ones by the action of potassium hydroxide.

The result of these investigations suggests the existence of a steric hindrance of 2′-substituent in the anthraquinonyl-oxazolidinones which plays an important part in the stability of the anthraquinonyl-oxazolidinones in aqueous solution of potassium hydroxide. Similarly, an electronic effect of substituent should be considered to be important and this is being investigated in the author's laboratory.

In the present study, 3-(methylanthraquinon-1-yl)-oxazolidin-2-ones, 1-*N*-2-hydroxyethylaminomethylanthraquinones and 2-chloroethyl methylanthraquinon-1-yl carbamates were synthesized and the effect of the methyl group by its position on the stability of the anthraquinonyloxazolidinones was investigated. None of them has yet been prepared, so far as is known.

Preparation and Results

The syntheses of the compounds were carried out according to the following processes (Scheme II).

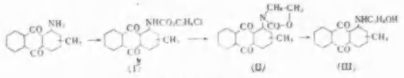

Scheme II

2-Chloroethyl 2-methylanthraquinon-1-yl carbamate (Ia), 3-methylanthraquinon-1-yl carbamate (Ib) and 4-methylanthraquinon-1-yl carbamate (Ic) were obtained from the corresponding 1-aminomethylanthraquinones by the action of 2-chloroethyl

* Presented at the 11th Annual Meeting of the Chemical Society of Japan, April, 1958.

1) K. Naiki, *J. Soc. Org. Syn. Chem. Japan*, (*Yūki Gōsei Kagaku Kyokaishi*), **12**, 364 (1954).

2) K. Naiki, ibid., **14**, 84 (1956).

chloroformate in the presence of sodium carbonate in boiling xylene. 1-*N*-2-Hydroxyethylamino-2-methylanthraquinone(IIIa), 1-*N*-2-hydroxyethylamino-3-methylanthraquinone(IIIb) and 1-*N*-2-hydroxyethylamino-4-methylanthraquinone(IIIc) were obtained from the corresponding 2-chloroethyl methylanthraquinonyl carbamates by the action of 20% aqueous solution of potassium hydroxide at 105~107°. Mixtures of the hydroxyethylaminomethylanthraquinones, the 3-(methylanthraquinon-1-yl)-oxazolidin-2-ones(II) (IIa, 2′-methyl; IIb, 3′-methyl; IIc, 4′-methyl) and the unchanged 2-chloroethyl methylanthraquinonyl carbamates were obtained from the corresponding 2-chloroethyl methylanthraquinon-1-yl carbamates by the action of 20% aqueous solution of potassium hydroxide at 98~99° for 1 hour.

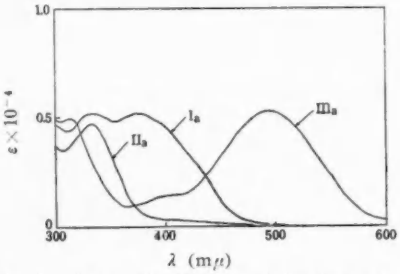

Fig. 1. Absorption spectra of the derivatives of 1-amino-2-methylanthraquinone (in toluene)
Ia: 2-Chloroethyl 2-methylanthraquinon-1-yl carbamate
IIa: 3-(2-Methylanthraquinon-1-yl) oxazolidin-2-one
IIIa: 1-*N*-2-Hydroxyethylamino-2-methylanthraquinone

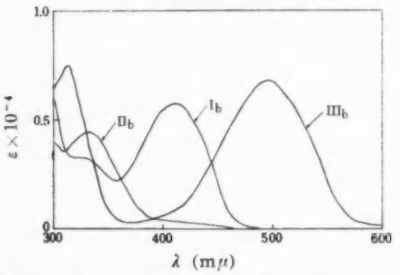

Fig. 2. Absorption spectra of the derivatives of 1-amino-3-methylanthraquinone (in toluene)
Ib: 2-Chloroethyl 3-methylanthraquinon-1-yl carbamate
IIb: 3-(3-Methylanthraquinon-1-yl) oxazolidin-2-one
IIIb: 1-*N*-2-Hydroxyethylamino-3-methylanthraquinone

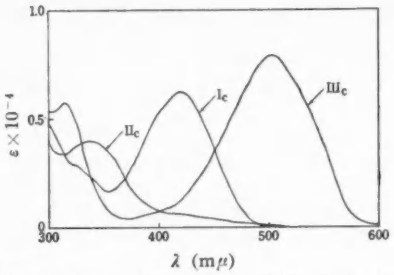

Fig. 3. Absorption spectra of the derivatives of 1-amino-4-methylanthraquinone (in toluene)
Ic: 2-Chloroethyl 4-methylanthraquinon-1-yl carbamate
IIc: 3-(4-Methylanthraquinon-1-yl) oxazolidin-2-one
IIIc: 1-*N*-2-Hydroxyethylamino-4-methylanthraquinone

The proportion of the constituents of the reaction mixtures was determined by spectrophotometry. These results are shown in Table I. Each of the constituents was separated from the reaction mixtures by column chromatography from benzene on alumina.

Absorption spectra of the compounds obtained above are shown in Figs. 1, 2 and 3, respectively. Absorption maxima and extinction coefficients are given in Table III.

Discussion

Effects of the Methyl Group According to its Position on the Stability of the Methylanthraquinonyloxazolidinones.— On account of aqueous dispersion of solid materials, various difficulties may be introduced in the discussion when their stabilities are compared with one another. Nevertheless, it may probably be considered that there exists some close relation between the stability and the factors such as electronic and steric effects of groups. Table I shows clearly that the 2′-methyl group increases the stability of

TABLE I
THE PROPORTION OF THE CONSTITUENTS OF THE REACTION PRODUCT FROM THE 2-CHLOROETHYL METHYLANTHRAQUINON-1-YL CARBAMATES AND 20% AQUEOUS SOLUTION OF POTASSIUM HYDROXIDE*

Position of CH_3	I %	II %	III %
2	7	77	16
3	13	23	64
4	14	51	35

* Determined by the spectrophotometry.

the anthraquinonyloxazolidinone in aqueous solution of potassium hydroxide. In other words, it shows the existence of steric hindrance of the methyl group in the hydrolysis process (cf. Scheme I).

The reaction mixture obtained from the chloroethyl methylanthraquinonyl carbamates and potassium hydroxide can be separated into the constituents by the column chromatography from benzene on alumina. It is observed, however, that the unreacted 2-chloroethyl methylanthraquinonyl carbamates are gradually converted into the corresponding methylanthraquinonyloxazolidinones on alumina in the column. For this reason, the use of the column chromatography to determine exactly the proportion of the constituents is not desirable in a strict sense. Thus, the determination of the proportion of the constituents was attempted by the spectrophotometry. Since the principal absorption bands of the constituents are apart from one another as shown in Figs. 1, 2 and 3, the determination of the proportion of the constituents was carried out exactly.

The Effect of the 2-Methyl Group on Absorption Spectra.—A marked difference in intensity of light absorption between mono- and dimethylated 1-aminoanthraquinones was explained by the steric hindrance of the *N*-methyl group with the adjacent carbonyl group[3]. Accordingly, it may be expected that another substituent at 2-position provides a further steric effect. This expectation agrees with the experimental result of the 1-amino-2-methoxyanthraquinones shown in Table II[4].

TABLE II
ABSORPTION SPECTRA OF 1-AMINO-2-METHOXYANTHRAQUINONES

Compound	Principal absorption band (in ethanol)
1-Amino-2-methoxyanthraquinone	478 mμ
1-Methylamino-2-methoxyanthraquinone	520 mμ
1-Dimethylamino-2-methoxyanthraquinone	506 mμ

It is now apparent that the steric hindrance of the methyl group of the compounds discussed here plays an important part. It has been known that the first absorption band of the 1-substituted anthraquinones can be attributed to resonance hybrid of the normal and the extreme ionic form (IV). The explanation of the formation of the ionic form is given by the well-known mechanism (V) which shows a mesomeric shift of the electrons from the 1-substituted group to the carbonyl oxygen atom. Thus, the contribution of the ionic form will be further increased by the 1-substituent with the greater electron-donating ability, resulting in the stronger the donating power, the longer the wave length of absorption maxima. This is illustrated in the case of the hydroxyethylaminoanthraquinones (Table III). However, in the 2-chloroethyl anthraquinonyl carbamates, another electron shift may be introduced in the opposite sense (VI). This alternative effect will counter the shift of the electrons to the anthraquinone ring and lower the wave length of absorption.

TABLE III
ABSORPTION SPECTRA OF 1-AMINOMETHYLANTHRAQUINONES*

Compound	$\lambda_{max.}$ (mμ)		$\varepsilon_{max.} \times 10^{-4}$	
Ia	336	378	0.518	0.520
Ib	320	414	0.335	0.580
Ic	~325	421	(0.271)	0.618
IIa	332	~400	0.469	(0.021)**
IIb	333	~405	0.443	(0.040)**
IIc	337	~420	0.388	(0.052)**
IIIa	312	492	0.501	0.518
IIIb	313	497	0.768	0.687
IIIc	315	504	0.580	0.792

Bracketed values are absorption bands of low intensity.
~ denotes point of inflexion.
* Measured by a Shimadzu QB-50 Electrophotometer. Solvent: toluene; concn. 1×10^{-4} mol./l.
** Concn. 1×10^{-3} mol./l.

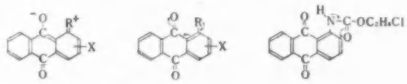

The further effect will come into play if such a group as methyl is introduced in the 2-position, for the steric hindrance from both the carbonyl and the methyl group forces atoms attached to the substituting group out of the plane of the anthraquinone nucleus. Consequently, in the case of the spectrum of 2-chloroethyl 2-methylanthraquinon-1-yl carbamate, the intensity of the corresponding absorption band (336 mμ) to that of anthraqinone becomes stronger and the primary band (378 mμ)

3) R. H. Peters et al., *J. Chem. Soc.*, **1953**, 2101.
4) K. Naiki, *J. Org. Syn. Chem. Japan* (*Yūki Gōsei Kagagu Kyokaishi*), **11**, 113 (1953).

becomes weaker than the other methylanthraquinonyl carbamates. If a more bulky group such as the oxazolidinonyl group is at the 1-position of the anthraquinone nucleus, the steric effect inhibits the shift of the electrons from the nitrogen atom to the anthraquinone nucleus, and spectra of the anthraquinonyloxazolidinones are very similar to that of anthraquinone itself.

In the case of the methylanthraquinonyloxazolidinones, it seems that the 2-methyl group in the anthraquinone nucleus increases the steric inhibition and the absorption intensity at about 400 mμ becomes weaker than the other methylanthraquinonyloxazolidinones.

Experimental

2-Chloroethyl 2-Methylanthraquinon-1-yl carbamate (Ia).—The synthesis of the compound was reported in the previous paper[2]. The product was recrystallized from ethanol, giving yellow needles, m. p. 173~174°.

2-Chloroethyl 3-Methlanthraquinon-1-yl carbamate (Ib).—A mixture of 1.08 g. of 1-amino-3-methylanthraquinone (m. p. 185~189°), 0.76 g. of 2-chloroethyl chloroformate, 0.54 g. of sodium carbonate and 70 ml. of xylene was refluxed with stirring for 2 hours. Insoluble substance was removed by hot filtration and the filtrate was evaporated to a volume of about 20 ml. for crystallization. Yield, 1.27 g. (83% of the theory) of yellow needles, m. p. 198~200°. The product was recrytallized from ethanol, giving yellow needles, m. p. 201~202°. *Anal.* Found: N, 4.34. Calcd. for $C_{18}H_{14}O_4NCl$: N, 4.07%.

2-Chloroethyl 4-Methylanthraquinon-1-yl carbamate (Ic).—A mixture of 1.88 g. of 1-amino-4-methylanthraquinone (m. p. 180~182°), 1.24 g. of 2-chloroethyl chloroformate, 0.95 g. of sodium carbonate and 18 ml. of xylene was refluxed with stirring for 6 hours. The insoluble substance was removed by hot filtration and the filtrate was cooled. The crystal formed was collected and dried. Yield, 2.45 g. (90% of the theory) of yellow needles, m. p. 187~188°. It was recrystallized from ethanol, giving yellow needles, m. p. 190~191°. *Anal.* Found: N, 4.25. Calcd. for $C_{18}H_{14}O_4NCl$: N, 4.07%.

Behavior of 2-Chloroethylmethylanthraquinon-1-yl carbamates on Alumina.—2-Chloroethyl 3-methylanthraquinon-1-yl carbamate (0.40g., m. p. 198~199°) was dissolved in benzene, then adsorbed on alumina, stood overnight and eluted by the use of ethanol. The substance (0.30 g., m. p. 213~215°), consisting of 3-(3-methylanthraquinon-1-yl)oxazolidin-2-one and unchanged 2-chloroethyl 3-methylanthraquinon-1-yl carbamate, was obtained. It was separated into the constituents by means of chromatography on alumina from benzene. 2-Chloroethyl 3-methylanthraquinon-1-yl carbamate passed through the column; 3-(3-methylanthraquinon-1-yl)oxazolidin-2-one was eluted by the use of ethanol. Pure 3-(3-methylanthraquinon-1-yl)oxazolidin-2-one was obtained.

Similar treatment of 2-chloroethyl 2-methylanthraquinon-1-yl carbamate and 4-methylanthraquinon-1-yl carbamate gave 3-(2-methylanthraquinon-1-yl)oxazolidin-2-one and 3-(4-methylanthraquinon-1-yl)oxazolidin-2-one, respectively.

3-(2-Methylanthraquinon-1-yl)oxazolidin-2-one (IIa).—The synthesis was reported in the previous paper[2]. Pale yellow needles, m. p. 226~227°.

3-(3-Methylanthraquinon-1-yl)oxazolidin-2-one (IIb).—A mixture of 1.00 g. of finely powdered 2-chloroethyl 3-methylanthraquinon-1-yl carbamate (m. p. 198~199°) and 30 g. of 20% aqueous solution of potassium hydroxide was heated in a boiling water bath with vigorous stirring for 1 hour. After being diluted with water, the precipitate was collected, washed with water and dried. Yield, 0.82 g. of reddish powder. The product, consisting of unchanged 2-chloroethyl 3-methylanthraquinon-1-yl carbamate, 3-(3-methylanthraquinon-1-yl)oxazolidin-2-one and 1-*N*-2-hydroxyethylamino-3-methylanthraquinone, was dissolved in benzene and chromatographed on alumina. 1-*N*-2-Hydroxyethylamino-3-methylanthraquinone is most strongly adsorbed and 3-(3-methylanthraquinon-1-yl)oxazolidin-2-one is more strongly adsorbed than 2-chloroethyl 3-methylanthraquinon-1-yl carbamate. The red band, containing 1-*N*-2-hydroxyethylamino-3-methylanthraquinone, was eluted by the use of ethanol. Yield, 0.38 g. of red needles, m. p. 234~235°. The pale orange band, containing 3-(3-methylanthraquinon-1-yl)oxazolidin-2-one, was eluted by the use of ethanol. Yield, 0.18 g. of pale orange needles, m. p. 235~236°. It was recrystallized from ethanol, giving pale orange needles, m. p. 235~236°. *Anal.* Found: N, 4.50. Calcd. for $C_{18}H_{13}O_4N$: N, 4.56%. The yellow eluate, containing 2-chloroethyl 3-methylanthraquinon-1-yl carbamate, was evaporated for crystallization. Yield, 0.14 g. of yellow needles, m. p. 198~199°

3-(4-Methylanthraquinon-1-yl)oxazolidin-2-one (IIc).—A mixture of 0.50 g. of finely powdered 2-chloroethyl 4-methylanthraquinon-1-yl carbamate (m. p. 187~188°) and 15 g. of 20% aqueous solution of potassium hydroxide was heated with vigorous stirring in a boiling water bath for 1 hour. After being diluted with water, the precipitate was collected, washed with water and dried. Yield, 0.33 g. of reddish brown powder. It was fractionally recrystallized from ethanol, giving pale brown needles, m. p. 201~202°. *Anal.* Found: N, 4.58. Calcd. for $C_{18}H_{13}O_4N$: N, 4.56%.

The chromatographic separation of the reaction product obtained above, consisting of 1-*N*-2-hydroxyethylamino-4-methylanthraquinone, 3-(4-methylanthraquinon-1-yl)oxazolidin-2-one and unchanged 2-chloroethyl 4-methylanthraquinon-1-yl carbamate, was carried out in the same with the 3-methyl derivative. Yield, 0.100 g. of 1-*N*-2-hydroxyethylamino-4-methylanthraquinone, m. p. 153~154°, 0.130 g. of 3-(4-methylanthraquinon-1-yl) oxazolidin-2-one, m. p. 201~202°, and 0.060 g. of

2-chloroethyl 4-methylanthraquinon-1-yl carbamate, m. p. 189~190°.

Determination of the Proportion of the Constituents of the Reaction Product Obtained from the 2-Chloroethyl Methylanthraquinon-1-yl Carbamates and 20% Aqueous Solution of Potassium Hydroxide.—A mixture of 0.20 g. of finely powdered 2-chloroethyl methylanthraquinon-1-yl carbamate and 6.00 g. of 20% aqueous solution of potassium hydroxide was heated with vigorous stirring in a boiling water bath for 1 hour. After being diluted with water, the precipitate was collected, washed with water and dried. Yield, 0.16 g. of pale red powder, m. p. 192~201°, from 2-chloroethyl 2-methylanthraquinon-1-yl carbamate; 0.15 g. of brownish red powder, m. p. 139~149°, from 2-chloroethyl 3-methylanthraquinon-1-yl carbamate; 0.16 g. of reddish brown powder, m. p. 148~167°, from 2-chloroethyl 4-methylanthraquinon-1-yl carbamate.

The proportion of the constituents of the products obtained above were determined by the use of a Shimadzu QB-50 Electrophotometer. Optical densities (D) of the benzene solutions of the products are shown in Tables IV, V and VI. It was found by simple caluculation that the reaction product obtained from 2-chloroethyl 2-methylanthraquinon-1-yl carbamate contains 21 mg. of 1-*N*-2-hydroxyethylamino-2-methylanthraquinone, 124 mg. of 3-(2-methylanthraquinon-1-yl) oxazolidin-2-one and 12 mg. of 2-chloroethyl 2-methylanthraquinon-1-yl carbamate; the product obtained from 2-chloroethyl 3-methylanthraquinon-1-yl carbamate contains 91 mg. of 1-*N*-2-hydroxyethylamino-3-methylanthraquinone, 33 mg. of 3-(3-methylanthraquinon-1-yl)oxazolidin-2-one and 26 mg. of 2-chloroethyl 3-methylanthraquinon-1-yl carbamate; the product obtained from 2-chloroethyl 4-methylanthraquinon-1-yl carbamate contains 51 mg. of 1-*N*-2-hydroxyethylamino-4-methylanthraquinone, 82mg. of 3-(4-methylanthraquinon-1-yl)oxazolidin-2-one and 27 mg. of 2-chloroethyl 4-methylanthraquinon-1-yl carbamate.

TABLE IV

OPTICAL DENSITIES OF THE PRODUCT OBTAINED FROM 2-CHLOROETHYL 2-METHYLANTHRAQUINON-1-YL CARBAMATE* AND EXTINCTION COEFFICIENTS OF THE CONSTITUENTS

λ (mμ)	D	$\varepsilon\times10^{-4}$		
		Ia	IIa	IIIa
330	0.670	0.511	0.469	0.346
380	0.086	0.511	0.037	0.109
490	0.128	0.004	0.003	0.518

* Solvent: toluene; conc. 47 mg./l.

TABLE V

OPTICAL DENSITIES OF THF PRODUCT OBTAINED FROM 2-CHLOROETHYL 3-METHYLANTHRAQUINON-1-YL CARBAMATE*AND EXTINCTION COEFFICIENTS OF THE CONSTITUENTS

λ (mμ)	D	$\varepsilon\times10^{-4}$		
		Ib	IIb	IIIb
340	0.475	0.318	0.401	0.685
420	0.147	0.538	0.036	0.124
500	0.357	0.005	0.007	0.672

* Solvent: toluene; concn. 48 mg./l.

TABLE VI

OPTICAL DENSITIES OF THE PRODUCT OBTAINED FROM 2-CHLOROETHYL 4-METHYLANTHRAQUINON-1-YL CARBAMATE* AND EXTINCTION COEFFICIENTS OF THE CONSTITUENTS

λ (mμ)	D	$\varepsilon\times10^{-4}$		
		Ic	IIc	IIIc
340	0.472	0.206	0.378	0.197
420	0.254	0.618	0.051	0.119
500	0.438	0.002	0.015	0.778

* Solvent: toluene; concn. 48 mg./l.

1-*N*-2-Hydroxyethylamino-2-methylnathraquinone (IIIa).—The synthesis was reported in the previous paper[2]. It was purified by means of chromatography from benzene on alumina and recrystallized from toluene, giving red needles, m. p. 141~142°.

1-*N*-2-Hydroxyethylamino-3-methylanthraquinone (IIIb).—A mixture of 1.00 g. of finely powdered 2-chloroethyl 3-methylanthraquinon-1-yl carbamate (m. p. 198~199°) and 30 g. of 20% aqueous solution of potassium hydroxide was refluxed with stirring in an oil bath for 1 hour. After being diluted with water, the precipitate was collected, washed with water, dried and recrystallized from toluene. Yield, 0.67 g. (83% of the theory) of red needles, m. p. 180~181°. It was recrystallized from toluene, giving red needles, m. p. 180.5~181.0°. *Anal.* Found: N, 5.21. Calcd. for $C_{17}H_{15}O_3N$: N, 5.02%.

1-*N*-2-Hydroxyethylamino-4-methylanthraquinone (IIIc).—A mixture of 0.50 g. of finely powdered 2-chloroethyl 4-methylanthraquinon-1-yl carbamate (m. p. 187~188°) and 15 g. of 20% aqueous solution of potassium hydroxide was refluxed with stirring in an oil bath for 1 hour. After being diluted with water, the precipitate was collected, washed with water, dried and recrysatllized from toluene. Yield, 0.30 g. (73% of the theory) of brownish red needles, m. p. 163~164°. It was recrystallized from toluene, giving brownish red needles, m. p. 164~165°. *Anal.* Found: N, 5.04. Calcd. for $C_{17}H_{15}O_3N$: N, 5.02%.

The writer is indebted to Mr. Yoshié Tanizaki for his advice.

The Laboratory of Dyestuff Chemistry
Tokyo Institute of Technology
Meguro-ku, Tokyo

Polyterpenes. II[1]. *Oxidation of Thujopsene with Lead Tetra-acetate**

By Shizuo NAGAHAMA, Hiroshi KOBAYASHI and Saburo AKIYOSHI

(Received September 19, 1958)

It has been reported by Kawamura[2] and recently by Nozoe et al.[3], that thujopsene, the main constituent of Hiba (*Thujopsis dolabrata Sieb. et Zucc.*) wood oil, affords a glycol, m. p. 91°, by the oxidation with permanganate in acetone containing water. On the other hand, the authors obtained a ketonic acid, m. p. 165° as a main product and no glycol was found when the oxidation was carried out in acetone solution without addition of water[1].

To obtain the glycol by an alternate route, oxidation of this sesquiterpene with lead tetra-acetate was attempted. However, contrary to the expectation, a ketone and its enol acetate were found to be the main products.

It is well known that the olefines, when oxidized with lead tetra-acetate, usually give a mixture of acetates produced partly by the addition of acetoxyl group to the double bond and partly by the substitution to the alpha position of the double bond or simultaneous occurrence of these cases[4]. As a single example of ketone formation, there are some reports concerning the formation of R-homocamphenylone from camphene[5,6], which accompanied by ring-enlargement**. In the present case, however, the oxidation was considered to be accompanied by ring-contraction, a novel reaction which seems not to have appeared in literature. The reaction was carried out in two ways. (1) To the benzene solution of the terpene was added solid lead tetra-acetate in portions. (2) The minium was added to the mixture of the terpene and acetic acid. The reaction product was fractionated by distillation under reduced pressure, and the main fraction was found to be the same in both cases. As an example, one of the results obtained by method 1 is shown in Table I.

TABLE I

Frn.	b. p.	mm.	Yield g.	n_D^{25}	d_4^{25}	E. V.*
1	92~102°	8	3.25	1.4984	0.9296	—
2	~105°	7.5	2.90	1.5025	0.9232	—
3	~106°	7.5	3.31	1.5045	0.9355	—
4	~119°	7	1.15	1.5050	0.9517	16.5
5	~127°	7	13.25	1.4870	0.9802	68.5
6	~137°	6	2.97	1.4909	0.9897	97.7
7	~144°	6	3.81	1.4934	1.0026	174
8	~155°	6	2.45	1.4970	1.023	204

* Ester value. Calcd. for $C_{17}H_{26}O_2$: 214

The infrared spectra were examined concerning all fractions, and no appreciable band was found in 3400 cm^{-1} region. Fraction 5 had an infrared band at 1708 cm^{-1} (cf. Fig. 1) and its greater part proved to be a ketone I which gave a semicarbazone m. p. 214° (decomp.) and a 2,4-dinitrophenylhydrazone m. p. 170°. The highest boiling fraction showed a band at 1745 cm^{-1} suggesting that it was probably a mixture of normal ester (1735~1740 cm^{-1}) and enol ester (1755 cm^{-1}). This was confirmed by the fact that the saponification product of this fraction showed bands at 3450 and 1708 cm^{-1} and gave a 2,4-dinitrophenylhydrazone, m. p. 168°, which was identified with that of ketone I by mixed melting-point test and infrared spectrum. In the spectra of fractions 6 and 7, rather weak bands were observed at 1825 and 1666 cm^{-1}.

Since ketone I, $C_{15}H_{24}O$ gave an acid $C_{14}H_{22}O_2$, m. p. 102° (II) by hypohalite oxidation, it was presumed to be a methyl ketone. Alkaline permanganate oxidation

* Partly presented before the Kyushu Local Meeting of the Chemical Society of Japan held at Kumamoto, October 29, 1957, and before the Symposium on Perfumery, Terpene and Essential Oil Chemistry held at Fuse City November 30, 1957.

1) Part I, This Bulletin, **30**, 886 (1957).

2) J. Kawamura, *Bull. Govt. Forest Expt. Station*, **30**, 59 (1930).

3) T. Ozeki, S. Seto and T. Nozoe, 10th Annual Meeting of the Chemical Society of Japan, April, 1957.

4) R. Criegee, *Ann.*, **481**, 263 (1930).

5) M. Ishidate, N. Inoue, and H. Fukushima, This Bulletin, **17**, 491 (1942): *J. Pharm. Japan* (*Yakugaku Zasshi*), **63**, 104 (1943).

6) Y. Matubara, *J. Chem. Soc. Japan, Pure Chem. Sec.* (*Nippon Kagaku Zasshi*), **76**, 1088, 1092 (1955), ibid., **78**, 726, 730 (1957).

** Added in proof: Another example of this type of reaction had been reported by P. Naffa and G. Ourisson (*Bull. soc. chim. France* **1954**, 1115., *C. A.*, **49**, 12386h (1955)), where longihomocamphenylone was obtained from longifolene by this reagent.

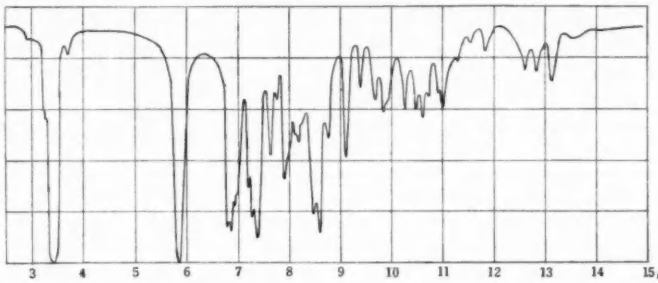

Fig. 1. Ketone I (regenerated from semicarbazone. Spectrum of Fraction 5 was essentially identical with this.)

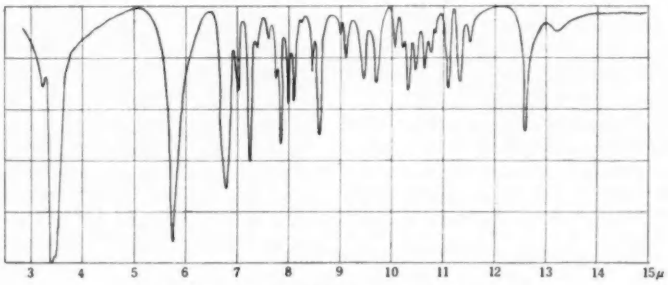

Fig. 2. Ketone VII (Nujol).

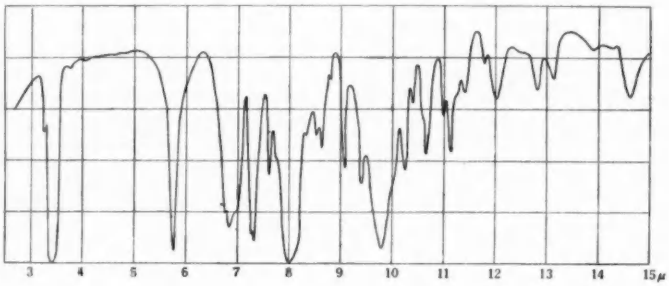

Fig. 3. Ester V.

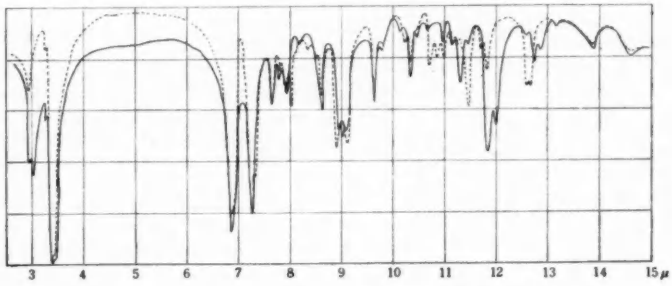

Fig. 4. —— Peroxide X, ------ Peroxide XI (Nujol).

of I gave mainly a dicarboxylic acid $C_{13}H_{20}O_4$ (III) accompanied by a small amount of acid II. Acid III was readily converted into an anhydride, m. p. 211~212° (IV) by heating or treating with acetic anhydride. Since this anhydride shows infrared absorption at 1799 and 1754 cm^{-1} (in carbon tetrachloride) and is stable toward heating, it may be considered to be of glutaric anhydride type.

Peracetic acid oxidation of ketone I followed by saponification and alumina chromatography gave an alcohol $C_{13}H_{22}O$, m.p. 78° (VI), and a ketone $C_{13}H_{20}O$, m.p. 118.5~121° (VII) (Fig. 2). When chromatographic separation was performed prior to the saponification, an ester V (Fig. 3) was obtained. Saponification of ester V gave alcohol VI, which in turn gave ketone VII by the chromic acid oxidation***. It is noticeable that ketone VII shows infrared absorption at 1727 cm^{-1} (in carbon tetrachloride) which is intermediate value of cyclopentanone (1745 cm^{-1}) and cyclohexanone (1715 cm^{-1}). Alcohol VI was oxidized with permanganate under a condition similar to the oxidation of ketone I, giving the same dicarboxylic acid III.

It has been reported[1] that the dicarboxylic acid obtained from thujopsene by permanganate oxidation followed by hypobromite treatment, gave an anhydride VIII, m. p. 110°, to which a glutaric anhydride was suggested from the infrared spectrum. However, an adipic anhydride IX from methyl vouacapenate showed anhydride bands at 1808 and 1764 cm^{-1} (in chloroform)[7]. Furthermore, Ozeki, Seto and Nozoe[3] obtained the "pyroketone" m. p. 121° by treating the dicarboxylic acid with acetic anhydride, followed by heating to 310°. On reexamining the experiment, it was confirmed that the pyroketone was identical with the above-mentioned ketone VII. Therefore, it must be considered that the anhydride VIII is of an adipic anhydride type, and the ring containing double bond in thujopsene is of a six-member type.

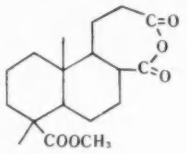

IX

The result mentioned above is formulated as Scheme I, assuming the cyclopentyl methyl ketone structure I for ketone I. Infrared absorption at 1708 cm^{-1} supports the validity of this inference.

In the case of the peracetic acid oxidation of ketone I, two kinds of crystalline ketone peroxide were separated. One of them $C_{15}H_{26}O_4$ (X) was obtained in 47% yield when the reaction was carried out below 20°. By means of iodometric titration, it was proved that two -OOH groups are present in X. When the acetic acid solution of X was warmed, the peroxide was decomposed and the original ketone I was regenerated. When the oxidation

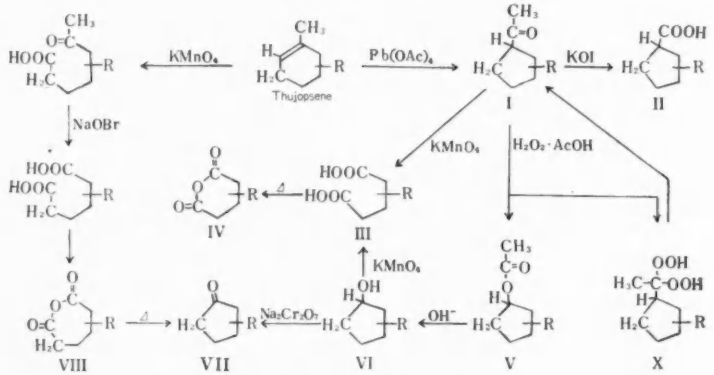

Scheme I. R = C_9H_{18}

*** The same ketone VII was separated from the neutral parts of permanganate oxidation products of thujopsene.

7) M. Arakawa, Private communication.

was conducted at about 25°, another peroxide XI was obtained in a poor yield. It decomposed at 135~138°, but it was not studied further owing to lack of material. The infrared spectra of X and XI are shown in Fig. 4.

Further investigations on the structure of thujopsene are being carried on.

Experimental

Thujopsene was obtained by the fractionation of Hiba wood oil as previously described[1].

Reaction of Thujopsene with Lead Tetra-acetate.—(a) Thujopsene (35 g.) was dissolved in 165 cc. of dry benzene, and lead tetra-acetate (prepared from 305 g. of acetic acid, 105 g. of minium, and recrystallized from acetic acid) was added portionwise with stirring for half an hour. The flask was immersed now and then in the water bath to keep the temperature below 40°. Stirring was continued for an additional one and a half hours. The reaction mixture was filtered, sodium bicarbonate solution was added to the filtrate and the organic layer was separated. This was washed twice with water, again with diluted sodium bicarbonate solution and finally with water and dried over sodium sulfate. Solvent was removed and the residue was fractionated. The result of a typical run is shown in Table I. Fraction 5 which boiled mainly at 125~127°/7 mm., gave a yellow 2, 4-dinitrophenylhydrazone m. p. 170~170.5°, and a semicarbazone, m. p. 213~214°C (decomp.).

Anal. Found: C, 69.53; H, 9.83; N, 15.41. Calcd. for $C_{16}H_{27}ON_3$: C, 69.27; H, 9.81; N, 15.15%.

Regenerated ketone from the semicarbazone showed the following constants. B. p. 132~133°/9 mm. n_D^{20} 1.4920, d_4^{20} 0.979, M. R. 65.1. Calcd. for $C_{15}H_{24}O$, 64.91. Infrared spectrum, Fig. 1. The ketone separated in another run on the second distillations gave the following constants. B. p. 125°/5 mm. n_D^{26} 1.4897, d_4^{26} 0.9762, $[\alpha]_D^{30}$ +1.23°.

(b) To a mixture of 35 g. of thujopsene, 305 g. of acetic acid and 105 g. of acetic anhydride, was added 160 g. of minium in portions for 1.5 hours, the temperature being kept below 60°. Stirring was continued for one additional hour. Water was added, and the solution was neutralized with sodium carbonate, filtered and extracted with benzene. Fractionation gave 13.3 g. of ketone I, b. p. 125~127°/7 mm.

Hypohalite Oxidation of Ketone I.—The ketone (1 g.) was dissolved in 10 cc. of dioxane and oxidized with the hypobromite solution prepared from 4.8 g. of sodium hydroxide, 75 cc. of water and 2.1 cc. of bromine. When the mixture was warmed gradually, the reaction set in at about 80°. The crude acid II was precipitated by acidification of the alkaline solution, yield 850 mg. Repeated crystallization from methanol-water and final sublimation under reduced pressure gave a sample of m. p. 101~102°. The same acid was obtained by potassium hypoiodite oxidation according to the procedure of Heer and Miescher[8].

Anal. Found: C, 75.72; H, 10.10. Calcd. for $C_{14}H_{22}O_2$: C, 75.63; H, 9.97%.

Permanganate Oxidation of I.—The ketone (1 g.) was suspended in 40 cc. of 5% sodium hydroxide solution and 100 cc. of 4% potassium permanganate solution was added portionwise with stirring at 50~60°. Permanganate was consumed in 7 hours. On dissolving manganese dioxide with sodium bisulfite and hydrochloric acid, an acid mixture was precipitated, which was collected and dissolved in benzene. The benzene solution was extracted with sodium bicarbonate and sodium hydroxide solution successively. Acid III (122 mg.) was obtained from the former extract and recrystallized from methanol-water.

Anal. Found: C, 65.37; H, 8.05. Calcd. for $C_{13}H_{20}O_4$: C, 64.98; H, 8.39%.

The sodium hydroxide extract gave 4 mg. of crude acid II m. p. 98~99°.

Anhydride IV.—Acid III (192 mg.) was heated with 5 cc. of acetic anhydride for 3 hours and acetic anhydride was removed under reduced pressure. The residue was crystallized by rubbing and recrystallized from acetic anhydride, m. p. 211~212°, yield 80 mg. When acid III was heated in a small tube, dehydration occurred at about 190° and melted at 211°. After being cooled, the contents solidified, and this solid also melted at 211°. The infrared spectrum coincided with that of the anhydride obtained by acetic anhydride treatment. Mixed melting point of III and IV showed no appreciable depression. Though the anhydride was heated to 450°, evolution of carbon dioxide was not observed practically and the anhydride could be recovered.

Peracetic Acid Oxidation of Ketone I.—(a) Ketone I (3.0 g.) was dissolved in 30 cc. of acetic acid (treated with chromium trioxide) and 24 cc. of hydrogen peroxide (30%) was added with swirling. After being kept at room temperature (about 25°) for 38 hours, the mixture was diluted with water and extracted with ether, and the ether extract was washed three times with sodium bicarbonate solution and then twice with water. On evaporation of ether, 1.95 g. of reaction product was obtained. This was dissolved in 5 cc. of methanol, and sodium hydroxide solution (1 g. in 5 cc. of water) was added to it and the mixture was allowed to stand overnight; then it was poured into water, and extracted with ether. Ether was removed and the residue was dissolved in petroleum ether and chromatographed with alumina column of 1.8×10 cm. The petroleum ether eluate was an oil (0.5 g. n_D^{20} 1.4965) and the infrared spectrum suggested the presence of unchanged I. The benzene and ethyl acetate eluates gave a crystalline alcohol, 0.42 g., m. p. 74~76°. An analytical sample was prepared by purification with the aid of sublimation under reduced pressure, m. p. 78°.

8) J. Heer and K. Miescher, *Helv. Chim. Acta*, **28**, 156 (1945).

Anal. Found: C, 80.10; 11.64. Calcd. for $C_{13}H_{22}O$: C, 80.35; H, 11.41%.

In another run where the reaction mixture was allowed to stand for 3 days, the product was distilled under reduced pressure, saponified and chromatographed; the petroleum ether eluate gave crystalline ketone, m. p. 113~114° (100 mg. from 2.9 g. of I) and its infrared spectrum was identical with that of ketone VII obtained by chromic acid oxidation of alcohol VI.

(b) The ketone (5.4 g.) was oxidized for 5 days as before and a solid substance XI (195 mg.) was separated from the reaction mixture. This was filtered and recrystallized from benzene-petroleum ether mixture, which decomposed at 135~138°. The infrared spectrum is shown in Fig. 4. The attempted elementary analysis failed because of an explosion. The filtrate was treated as before (without distillation and saponification) and the product was chromatographed. Petroleum ether eluate (0.4 g. n_D^{26} 1.4863, d_4^{22} 0.9957) and benzene eluate (1.3 g. n_D^{20} 1.4858, d_4^{22} 1.044, infrared spectrum Fig. 3) were combined and saponified with methanolic sodium hydroxide solution, and alcohol VI was obtained in quantitative yield. Although ethyl acetate eluate (0.5 g. n_D^{22} 1.5000) did not crystallize, its infrared spectrum was essentially identical with that of VI.

(c) The ketone (3.67 g.) was dissolved in 45 cc. of acetic acid, to which 30 cc. of hydrogen peroxide (30%) was added. When the reaction mixture being kept below 20° overnight, a large quantity of crystalline substance X separated out. This was collected on a glass filter, recrystallized from benzene, yield 2.11 g. (47%), decomposed at about 120°.

Anal. Found: C, 66.78; H, 9.69. Calcd. for $C_{15}H_{28}O_4$: C, 66.63; H, 9.69%.

A 13.2 mg. and a 15.0 mg. portion of the sample required 1.98 cc. and 2.19 cc. of 0.1 N sodium thiosulfate solution (f=1.008). Calcd. for $C_{15}H_{24}\cdot 2OOH$: 1.93 and 2.19 cc.

Acetic acid solution of X was warmed and water was added. On cooling there separated out an oil, from which a semicarbazone of m. p. 214° (decomp.) was obtained. The infrared spectrum of this semicarbazone was identical with that of semicarbazone of I.

Chromic Acid Oxidation of VI.—Sodium dichromate (100 mg.) was dissolved in 0.5 cc. of acetic acid and alcohol VI (194 mg.) in 0.5 cc. of acetic acid was added. The mixture was warmed for a few minutes and allowed to stand for one day. Water was added and the oil which separated was extracted with ether. Ether was evaporated and residue was crystallized by rubbing. Yield 148 mg. Recrystallization from methanol-water and sublimation under reduced pressure gave a sample of m. p. 118.5~121°C.

Anal. Found: C, 81.46; H, 10.37. Calcd. for $C_{13}H_{20}O$: C, 81.20; H, 10.48%.

2, 4-Dinitrophenylhydrazone orange m. p. 215~216°.

Permanganate Oxidation of VI.— Alcohol VI (1.0 g.) was suspended in 40 cc. of 5% sodium hydroxide solution and 50 cc. of 4% permanganate solution was added to it dropwise with vigorous stirring. The temperature was kept below 55° by cooling with a water bath. After being stirred for 4 hours, the reaction mixture was acidified with hydrochloric acid and sodium bisulfite was added to it. The precipitate which separated was dissolved in sodium bicarbonate solution, filtered and reprecipitated with hydrochloric acid; yield 647 mg. The infrared spectrum of it was identical with that of III obtained from ketone I. It gave the anhydride of m. p. 211~212°.

The authors wish to express their gratitude to Professor M. Hamana and Professor H. Saikachi of the Pharmaceutical Department of this University for elementary analysis and measurement of rotation. They are also indebted to Mr. M. Shido for elementary analysis.

Department of Synthetic Chemistry
Faculty of Engineering
Kyushu University
Hakozaki, Fukuoka

Phenothiazine Derivatives. V[1]*. Synthesis of Hydroxyphenothiazines*

By Manabu FUJIMOTO

(Received September 24, 1958)

Of the theoretically possible four hydroxyphenothiazines, the 3-hydroxy compound I only has been reported[2,3]. By treating 4-hydroxydiphenylamine with sulfur and iodine, Houston et al.[2] prepared the compound as a dark greenish brown solid with m. p. 170~175°C and with a tendency to be easily oxidized in air to 3-phenothiazone (II) (Chart I).

Before Houston et al., Hilditch and Smiles already prepared the supposed 3-hydroxyphenothiazine[3] by an intramolecular rearrangement of phenothiazine 5-oxide in acetic acid. It was a purple crystalline mass that defied purification. They submitted it to reduction with zinc and hot acetic acid and obtained a colorless soft crystalline substance which rapidly recovered purple color in the presence of air.

Chart I

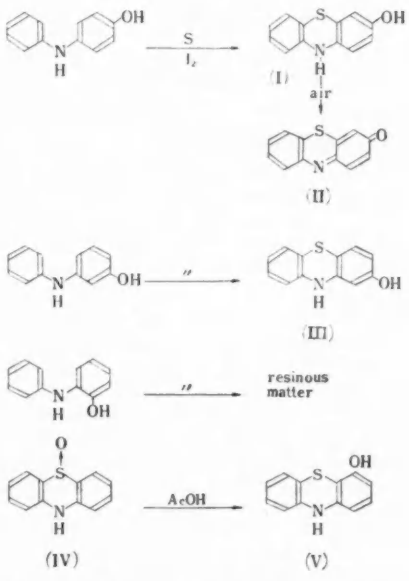

The present author repeated the experiment of Hilditch and Smiles and obtained a reddish-violet substance in fine powder melting at 141~143°C. It showed a distinct depression of the melting point on admixture either with 3-hydroxyphenothiazine (I) or with 3-phenothiazone (II), prepared according to the method of Houston et al[2]. Although the rearranged product was chromatographically pure and phenolic in nature, it was evidently different from the substances of Houston et al.

The investigation described below presents a contribution to the solution of the problem concerned. In the first place, an attempt was made to synthesize all of the unknown hydroxyphenothiazines.

It was reported by Charpentier et al.[4] that the reaction of a *meta* substituted diphenylamine with sulfur and a small amount of iodine as a catalyst gives a mixture of a 2-substituted phenothiazine and its 4-isomer, although the 2-substituted product is formed in a greater yield, and that 3-methoxydiphenylamine gives only 2-methoxyphenothiazine.

The present author obtained one hydroxyphenothiazine by thionation of 3-hydroxydiphenylamine, but could not isolate the expected isomeric product. Therefore, the hydroxyphenothiazine is supposed to be 2-hydroxyphenothiazine (III). As a very unstable compound, 2-hydroxydiphenylamine gave only a black resinous matter by a similar treatment. If 1-hydroxyphenothiazine, were obtained by the reaction of 2-hydroxydiphenylamine it would have a tendency to form 1-phenothiazone similarly to the 3-hydroxy isomer I.

As an alkaline solution of the substance, obtained by the intramolecular rearrangement of phenothiazine 5-oxide IV with acetic acid according to Hilditch and Smiles resists aeration, it is considered to be a phenol with the hydroxyl group in a *meta* position to the nitrogen atom. Two such hydroxyphenothiazine are possible,

1) Part IV: This Bulletin, **32**, 296 (1959).
2) D. F. Houston et al., *J. Am. Chem. Soc.*, **71**, 3818 (1949).
3) T. P. Hilditch and S. Smiles, *J. Chem. Soc.*, **101**, 2295 (1912).
4) P. Charpentier et al.: *Compt. rend.*, **235**, 59 (1952).

namely, 2-hydroxy- and 4-hydroxy-phenothiazines. As the substance from the rearrangement of the 5-oxide (IV) differs conspicuously from 2-hydroxyphenothiazine (III) described above, it must be 4-hydroxyphenothiazine (V). The position 4 is quite a reasonable place where the sulfoxide oxygen atom may migrate.

Experimental

3-Hydroxyphenothiazine (I) and 3-Phenothiazone (II). — Essentially the method of Houston et al.[5] was followed.

2-Hydroxyphenothiazine (III). — A mixture of 3.7 g. of 3-hydroxydiphenylamine and 1.4 g. of sulfur was ground in a mortar and placed in a 100 ml. flask. Then 0.04 g. of iodine was added, and the flask was stoppered and placed in a metal bath preheated to 190°C. The bath temperature was kept at 190~200°C during 30 min., while hydrogen sulfide was evolved, and then for additional 10 min. The reaction mass was poured into a porcelain dish and allowed to cool. It solidified to a greenish-yellow cake. Yield, 4.2 g. Fractional recrystallization from benzene gave 3.2 g. of the pure substance III in dark yellow powder, m. p. 270~272°C. It gives cobalt-blue coloration with sulfuric acid.

Anal. Found: C, 67.11; H, 4.09; N, 6.40. Calcd. for $C_{12}H_9ONS$: C, 66.85; H, 4.21; N, 6.50%.

4-Hydroxyphenothiazine (V). — Acetic acid (20 ml.) was added to phenothiazine 5-oxide (IV) (1.0 g.), and the reddish-violet solution was refluxed for 3 hr. Acetic acid was evaporated in vacuo, and the residue was recrystallized from absolute ethanol. The yield was quantitative. It forms reddish-violet fine powder, m. p. 141~143°C, and gives sepia-brown coloration with sulfuric acid. It is soluble in 10% aqueous caustic soda. The benzene solution showed a single adsorption band in the chromatogram on alumina.

Anal. Found: C, 67.01; H, 4.08; N, 6.45. Calcd. for $C_{12}H_9ONS$: C, 66.85; H, 4.21; N, 6.50%.

Summary

The phenolic compound resulting from the rearrangement of phenothiazine 5-oxide in acetic acid was found to be 4-hydroxyphenothiazine, and to be different from 2- and 3-hydroxyphenothiazines which were derived from 3- and 4-hydroxydiphenylamines, respectively, by fusion with sulfur and iodine.

The author expresses his thanks to Professor Y. Urushibara, Tokyo University, for his helpful guidance throughout this work, to Dr. K. Takeda, Director of the Laboratory, for his permission to complete this research, and also to the members of the Center of Microanalytical Services, Shionogi and Co., Ltd., for the elementary analyses.

Research Laboratory
Shionogi & Co., Ltd.
Imafuku, Amagasaki

*Heat of Solution of Methanolized Cellulose**

By Yoshizo TSUDA

(Received September 19, 1958)

In our previous papers[1,2], the lateral order distribution of cellulose was determined and discussed. In our laboratory the lateral order distribution has been determined from the solubility data of methanolized cellulose in aqueous sodium hydroxide solution of various concentrations.

Recently it has been shown that the solubility of methanolized cellulose depends on the degree of polymerization of the methanolized cellulose and that distribution obtained by such a method gives rather a longitudinal order distribution of crystallites. On the other hand, it has been shown that the effect of the degree of polymerization of hydrolyzed cellulose on its solubility is smaller than that of the lateral order[3].

The present investigation of heat of solution of methanolized cellulose was undertaken to obtain some informations

* This paper was presented at the 11th Annual Meeting of the Chemical Society of Japan, April, 1958.

1) Y. Tsuda and S. Mukoyama, This Bulletin, **29**, 748 (1956).

2) Y. Tsuda and S. Mukoyama, *Textile Research J.*, **27**, 945 (1957).

3) H. Sobue, S. Fukuhara and M. Moriya, *J. Chem. Soc. Japan, Ind. Chem. Sec.* (*Kogyo Kagaku Zasshi*), **61**, 1015 (1958).

about the dependency of the solubility of methanolized cellulose on the cohesive energy of crystallites.

Experimental

Cellulose Samples. — Cuprammonium rayon, Shin-toramomen, BX-yarn[4], viscose rayon, tire-cord rayon A (conventional) and tire-cord rayon B (all-skin type) were used.

Methanolysis. — Methanolysis of the samples was performed at 40° for 24 hours with 1 N hydrogen chloride in absolute methyl alcohol. After methanolysis, the residue was filtered, washed with methanol until it became chloride-free and then dried.

Measurement of Heat of Solution. — The apparatus was a simple non-adiabatic calorimeter composed of a 100 ml. pyrex vacuum bottle, a Beckmann thermometer (in 0.01° division), a stirring rod and a sample inlet tube, as shown in Fig. 1.

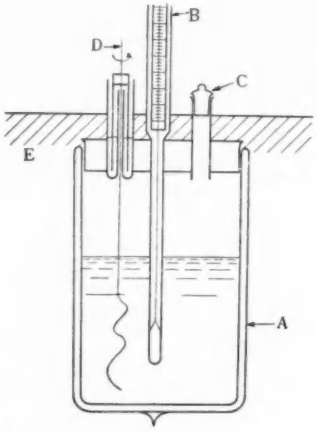

Fig. 1. Calorimeter.
A, 100 ml. pyrex vacuum bottle
B, Beckmann thermometer
C, Sample inlet tube
D, Stirrer
E, Thermostat

The apparatus was immersed in a thermostat kept at 20°. Methanolized sample (50 mg.) was bone-dried and kept at 20°. The solvent was 50 ml. of 11% aqueous sodium hydroxide solution, which was kept at 20° in the calorimeter. The stirring was done at a constant speed because constancy of the mechanical generation of heat was necessary for the measurement of small heat change. Under these experimental conditions observed temperature rise was about 0.05°, which was estimated to 0.001°. The dissolution of methanolized cellulose in the alkaline solution was a relatively rapid reaction. The heat capacity of calorimeter was determined experimentally under working conditions by measuring the heat of solution of potassium chloride in water.

Degree of polymerization was measured using cuprammonium solvent. Lateral order distribution was obtained by the same method as described in a previous paper[2].

Results

In Table I are shown the values of the heat of solution together with the statistical quantities which indicate their reliability. Degree of polymerization of methanolized cellulose is also shown in Table I. It is evident from Table I that the heats of solution of samples I, II and III are smaller than the others and those of samples V and VI are larger than the rest. The lateral order distribution of these samples is shown in Fig. 2.

TABLE I
HEAT OF SOLUTION

	Methanolized	Heat of solution cal./g.	95% Confidence limit	Degree of polymerization
I	Cuprammonium Rayon	27.6	±1.3	50
II	Shin-toramomen	27.8	±1.2	45
III	BX-yarn	29.2	±1.3	40
IV	Viscose Rayon	31.4	±1.2	33
V	Tire-cord Rayon A	33.4	±1.3	28
VI	Tire-cord Rayon B	34.3	±1.1	25

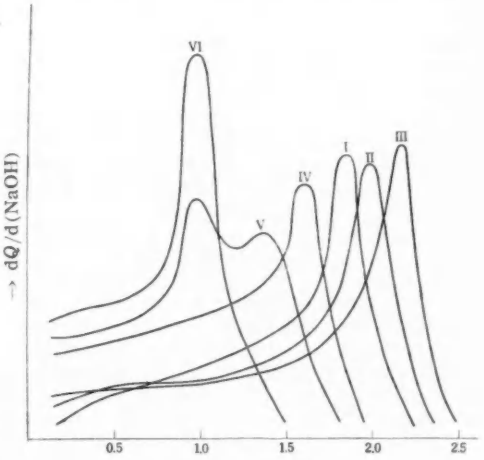

Fig. 2. Lateral order distribution (types identified in Table I).

Discussion

The heat of solution of the cellulose sample, H_s, can be separated in two parts as follows;

4) N. Drisch and L. Soep, *Textile Research J.*, **23**, 513 (1953).

$$H_s = H_a - E_c$$

where H_a is the heat of solution of amorphous cellulose in the alkaline solvent and E_c is the cohesive energy of the cellulose sample. H_a is a constant value with respect to all cellulose samples under a given experimental condition. Therefore the difference in the heat of solution of two samples can be regarded as the difference in their cohesive energies; that is, the larger the heat of solution, the smaller the cohesive energy. It will be seen from the results in Table I that the methanolysis residue of Shin-toramomen, Bx-yarn and cuprammonium rayon have large cohesive energy values and tire-cord rayons have rather low values. On the other hand, as shown in Fig. 2, the former shows high lateral order distributions and the latter shows low lateral order distributions. These relationships indicate that the distribution obtained from the fractional dissolution of methanolized cellulose corresponds to the distribution of cohesive energy. Although the degree of polymerization can be regarded as another factor of the fractional dissolution, its effect would be relatively small in comparison with the effect of cohesive energy.

It may be accepted from these relationships that the length of crystallite depends on the lateral order of crystallite and a portion of high lateral order can form a long crystallite, and therefore the dependency of lateral order distribution on the degree of polymerization has been observed.

If it is assumed that methanolysis destroys only the aggregated portion of very low cohesive energy, the cohesive energy of the methanolysis residue would be almost identical with that of the original cellulose.

Summary

The heat of solution of methanolysis residue of cellulose fibers was measured and then the difference in the cohesive energy of different samples was estimated. It was elucidated that the cohesive energy of methanolized cellulose corresponds to the experimentally evaluated lateral order.

Research Center, Toyo Rayon Co. Ltd., Otsu, Shiga

Effects of Dry Grinding on Talc

By Hiroshi TAKAHASHI

(Received October 2, 1958)

In the previous papers, the effects of dry grinding on kaolin minerals were studied, and the mechanism of the structural change caused by dry grinding was presented[1]. That is, there are two ways of change in structure. One is the production of a non-crystalline material attended with disordering of a crystalline portion, and the other is the reaggregation process. Finally, the kaolin mineral changes into a completely amorphous substance through a formation of a zeolitic substance. The mechanism of the dry grinding on kaolin minerals must be common somewhat to any substances with layered structure. In the ball-milling of graphite, too, a remarkable disordering in structure was observed by Bacon[2]. However, the effects of grinding for substances with the layered structure have not been studied very much heretofore, with the exceptions of kaolinite and mica[3]. The mechanism of dry grinding on kaolin minerals is somewhat common to that of other clay and related minerals, for example, such as montmorillonite, mica, attapulgite, pyrophyllite, serpentine and chrysotile. The results of the grinding

1) H. Takahashi, "Proc. Sixth Natl. Conference on Clay and Clay Minerals", Natl. Res. Council-Natl. Acad. Sci., (in press); H. Takahashi, This Bulletin, **32**, 235, 245, 252 (1959).

2) G. E. Bacon, *Acta Cryst.*, **5**, 392 (1952).

3) M. L. Jackson and E. Truog, *Soil Sci. Soc. Am., Proc.*, **4**, 136 (1939); R. C. Mackenzie and A. A. Milne, *Min. Mag.*, **32**, 178 (1953); R. C. Mackenzie and A. A. Milne, *Clay Min. Bull.*, **2**, 57 (1953).

effects on these clay and related minerals are reported in the following papers. Talc is an end-member of clay mineral with three-layered structure. In this study, the effects of a mechanical-mortar dry grinding on talc are discussed in the structural change, and compared with those of kaolin minerals.

Experimental

The sample used in this study is talc from Kanjun, China. The dry grinding was done in the same manner as for kaolin minerals. That is, 30 g. of original sample was charged and ground by a mechanical-mortar (15.2 cm. in dia. and 8.4 cm. in depth). Experimental specimens were taken out at intervals of 48 hours and examined by X-ray diffraction, differential thermal and electron microscopic methods. The density was also measured.

X-ray powder diagrams were recorded by an X-ray diffractometer (Geigerflex). Experimental conditions are as follows. Filtered Cu radiation (Cu $K\alpha$: 1.5418Å), at 35 kV and 15 mA is used, scanning speed is 1° or 1/4° 2θ per minute, time constant is 4 seconds, receiving slit is 0.2 mm. or 0.1 mm., angular aperture is 1° or 1/2° were used. The differential thermal analysis curves were recorded by the apparatus described by Sudo et al.[4]. Care was taken to pack a specimen into the sample block in the homogeneous manner and also to keep the weight of specimen constant. The mean heating rate is 12.5°C per minute. The density was measured by pycnometer in carbon tetrachloride. It was done after it had been dried at 110°C in order to avoid the effect of the adsorbed water. Electron micrographs were obtained by the Hitachi HU-10A type Electron Microscope.

Results and Discussion

X-Ray Diffraction Studies.—X-ray diffractometer traces and data are given in Fig. 1 and Table I. In this table, the interplaner spacing and the relative intensity measured from the X-ray trace are shown and the values described in ASTM Card are given for reference.

Generally, as the grinding progresses, even though the X-ray diagram is similar to that of the original sample, a decrease in the intensity of reflections except for some reflections and an increase in the background are observable. The intensity of reflections belonging to the basal reflections come to decrease sharply as compared with that of the original sample during the early stage of grinding. Another distinct feature observable in the X-ray

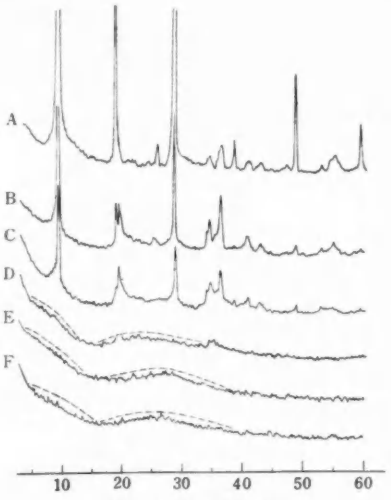

Fig. 1. X-ray diffractometer traces of ground specimens of talc.
A, original talc
B, ground 96 hours
C, ground 192 hours
D, ground 240 hours
E, ground 384 hours
F, ground 528 hours

diagram is that the reflection of 4.60Å spacing comes to be remarkably distinctive as the reflection of 4.69Å spacing weakens due to the progress of grinding. The profile of this reflection becomes an assymmetric broad band which is similar to the (02,11) band found in the X-ray diagram of halloysite. It seems that this reflection is related to the structure of talc and has (020) index rather than a spurious line[5]. The above-mentioned two characteristics with respect to the intensities of reflection line and background observed in the early stage of grinding become more and more distinct as the grinding progresses up to 192 hours. After 192 hours in grinding, the change of the interplaner spacing is not so remarkable. When the grinding progresses further, the X-ray diagram changes remarkably in contrast with that observed thus far. In the 240-hour-ground specimen, the X-ray diagram scarcely has any distinct reflection, but only two very diffuse bands. It is clear that a non-crystalline substance is produced by dry grinding. In the process of the grinding of talc, a remarkable change

4) T. Sudo et al., *J. Geol. Soc. Japan*, (*Chishitsu-Gaku-Zasshi*), 58, 679 (1952).

5) D. M. C. MacEwan, "X-Ray Identification and Crystal Structures of Clay Minerals", Mineralogical Society (London), Edited by G. W. Brindley, p. 311 (1951).

TABLE I
POWDER DATA OF GROUND TALC

A.S.T.M. Index (No. II-1238)		Original Talc		Ground 96 hr.		Ground 192 hr.		Ground 240 hr.		Ground 384 hr.		Ground 528 hr.	
d(*kX*)	*I*	*d*(Å)	*I*	*d*	*I*	*d*	*I*	*d*	*I*	*d*	*I*	*d*	*I*
9.4	8	9.4	VS	9.3	VS	9.3	MS	9.8	W vbr	9.8	VW vbr	9.8	VW vbr
4.69	4	4.69	S	4.70	M	4.69	W						
		4.60	VW	4.59	M	4.58	M br	4.55	VW				
3.88	1b												
3.37	3	3.45	MW	3.50	W			3.8	W vbr	3.3	W vbr	3.4	W vbr
3.11	10	3.12	VS	3.11	MS	3.12	M						
2.70	1	2.63	W	2.63	MW	2.64	VW						
2.59	2	2.60	W	2.60	MW	2.60	MW	2.60	VW				
2.47	5	2.48	MW	2.49	MS	2.49	M br						
2.32	1	2.34	MW	2.34	VW	2.34	VW						
2.20	3	2.21	W br	2.21	W br	2.22	W br						
2.09	2	2.11	W br	2.11	W br	2.12	W br						
1.92	0.5	1.927	W										
1.86	3	1.870	MS	1.870	W	1.873	W						
1.725	2	1.731	W	1.73	W	1.73	VW br						
1.67	4	1.665	MW br	1.67	MW br	1.68	VW br						
1.652	1—2												
1.632	1b												
1.55	3	1.560	M	1.56	W br	1.56	VW br						

Key to abbreviatin: VS: very strong, S: strong, MS: medium strong, MW: medium weak, W: weak, VW: very weak, br: broad, vbr: very broad.

occurs in the structure at the period between 192 hours and 240 hours under the experimental condition of this experiment. In the 384-hour-ground specimen, the X-ray diagram is nearly similar to that of the 240-hour-ground specimen. As the grinding progresses, the maximum points of diffuse bands in the X-ray diagram gradually become more and more indistinct, and the intensity of the background at the small angle part of a scattering angle increases progressively.

That a zeolitic substance is formed in the dry grinding of kaolin minerals can be supported on the basis of the X-ray diagram of the ground specimen treated with a weak alkali- and acid-solution as described in the previous papers[1]. These procedures were used for some ground specimens of talc. A part of these X-ray traces are shown in Fig. 2.

From a comparison of these X-ray traces with those of the original ground specimen, the following conclusions are drawn. In the alkali-treated specimen of 192-hour-ground talc, only a slight increase in the intensity of background is observable in the X-ray diagram, as compared with that of the original ground specimen. The X-ray pattern of the acid-treated specimen after being treated with the above weak alkaline solution is almost similar to that of

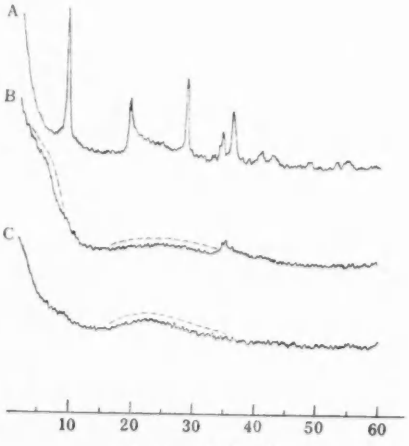

Fig. 2. X-ray diffractometer traces of alkali- and acid-treated specimens of ground talc.
A, 192-hour-ground talc treated with 0.1 N HCl after treated with 0.1 N NaOH
B, 240-hour-ground talc treated with 0.1 N NaOH
C, 240-hour-ground talc treated with 0.1 N HCl after treated with 0.1 N NaOH

TABLE II
THERMAL DATA OF GROUND TALC
(ALL TEMPERATURES ARE DEGREES CENTIGRADE)

Grinding time (hr.)	E_{N1}		E_X		E_{N2}	
	Temp. at peak (°C)	Height of peak	Temp. at peak (°C)	Height of peak	Temp. at peak (°C)	Height of peak
0	—	—	—	—	990	13
48	—138—	6	807	9	980	8
96	—135—	9	805	20	970	6
192	—140—	14	807	50<	968	4
240	—150—	13	807	8	945	2
528	—140—	15	825	1	—	—

the original ground specimen, however, the pattern becomes somewhat distinct owing to a dissolution of an amorphous substance produced by dry grinding. In the X-ray diagram of the weak alkali-treated 240-hour-ground specimen, two very diffuse bands are noticeable as is clear by comparison of Fig. 1-D and Fig. 2-B. The positions of the maximum points of these bands are about 14.7Å and 3.5Å in the interplaner spacings. In addition to these diffuse bands, a very remarkable scattering is also observable in the region of a scattering angle as low as six degrees. To dissolve the amorphous substance produced by dry grinding, acid treatement was given. The X-ray diagram of the residual part has a broad band with a maximum of 3.86Å in spacing. The background decreases below that before acid treatment. This fact indicates that in the 192-hour-ground specimen, the disordering in the talc structure is observable but the production of an amorphous substance is yet remarkable. In this stage, a zeolitic substance is not to be formed. In the 240-hour-ground specimen, the crystalline substance is not present. This fact is ascertained by the X-ray diagram of a residual substance treated with alkali and acid. Therefore, it is considered that the structure of this specimen is not perfectly amorphous, but it is related somewhat to the original structure though the original talc structure disintegrates due to dry grinding. In the light of the X-ray data, the structure of the 384-hour-ground specimen is considerably similar to that of the 240-hour-ground specimen. In the 528-hour-ground specimen, the amorphous substance dissoluble by the alkali-acid treatment considerably increases. This means an increase of the amorphous substance by dry grinding.

Consequently, it is concluded that in the dry grinding of talc, the disordering of structure is remarkable up to a certain stage of grinding, and past this stage, the specimen changes wholly into a non-crystalline substance and then gradually changes into a completely amorphous substance. Therefore, the formation of a zeolitic substance is not remarkable as compared with that of kaolin mineral.

Differential Thermal Analysis. — Differential thermal analysis curves of the specimens in the various periods of grinding are shown in Fig. 3, and thermal data measured from these curves are given in Table II.

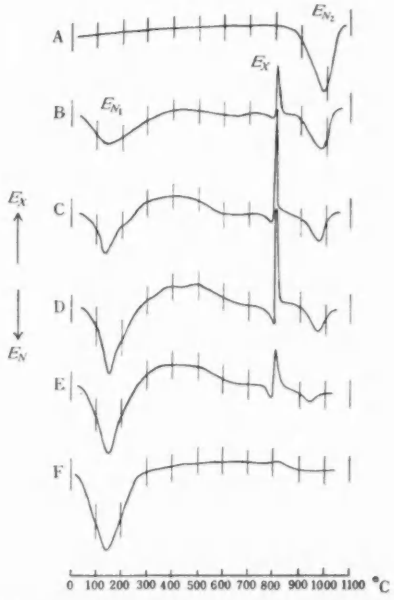

Fig. 3. Differential thermal analysis curves of ground talc.
A, original talc
B, ground 48 hours
C, ground 96 hours
D, ground 192 hours
E, ground 240 hours
F, ground 528 hours

The original sample has only an endothermic reaction (E_{H2}) associated with the loss of lattice water. The peak temperature of the endothermic reaction is 990°C, which is nearly equal to the value given in literature[6]. In the 96-hour-ground specimen, the first endothermic reaction (E_{H1}) associated with the loss of adsorbed water is apparent. This fact means that a non-crystalline substance is produced by dry grinding. As that of a kaolin mineral, a lowering in the peak temperature and a decrease in the height are observable in the second endothermic reaction (E_{H2}). It seems that these characteristics are related to the partial disintegration of the original structure. In the differential thermal analysis curve of this specimen, another important characteristic is observable. That is, a sharp exothermic reaction (E_X) is apparent at about 800°C, and there is the presence of a slight but distinct endothermic reaction immediately before this reaction. In the 192-hour-ground specimen, all features observed in the differential thermal analysis curves of the 48- and 96-hour-ground specimens become all the more distinct. An increase in the height of the first endothermic reaction, a remarkable increase in the intensity of the exothermic reaction, a lowering in the peak temperature and a decrease in the height of the second endothermic reaction are observable. Moreover the endothermic reaction just before the exothermic reaction becomes more distinct. The first endothermic reaction of ground specimens up to 192 hours is considered to be caused by a non-crystalline substance produced by grinding rather than by the water which gets into the inter-layers of talc as an inter-layer water, because the basal spacing of these specimens does not change much. In the 240-hour-ground specimen, the height of the exothermic reaction sharply decreases and the height of the second endothermic reaction decreases remarkably as compared with those of the 192-hour-ground specimen. In a many-hour-ground specimen, for example, the 528-hour-ground specimen, the reaction which is present in the original specimen is absent. Only the first endothermic reaction associated with the loss of the adsorbed water, and the weak and broad exothermic reaction at 825°C are observable. Then the endothermic reaction just before the exothermic reaction has already disappeared.

On the differential thermal analysis curves of the ground specimens, an important and interesting phenomenon is observable. That is, a new phase different from the original structure is apparent in the course of dry grinding. To ascertain this new phase, the X-ray traces of the 192-hour-ground specimen taken out just before and after the exothermic reaction on the differential thermal analysis curve are compared. A difference is observable in that only a reflection of 2.885Å spacing is apparent. From the facts that all reflections of the original 192-hour-ground specimen remain in the X-ray diagram of the specimen taken out just after the exothermic reaction and that a new reflection appears, it is supposed that the exothermic reaction on the differential thermal analysis curve is not based on the structural change of original talc. And from the fact that this exothermic reaction disappears again in many-hour-ground specimens, it is supposed that this exothermic reaction is not also based on the structural change of a perfectly amorphous substance produced by dry grinding. Therefore, it is clear that this exothermic reaction is based on crystallization from the new phase formed by dry grinding which is not the talc structure and is not a perfectly amorphous structure. This sort of structural change is not found at all in the case of kaolin minerals. The appearance of a new phase

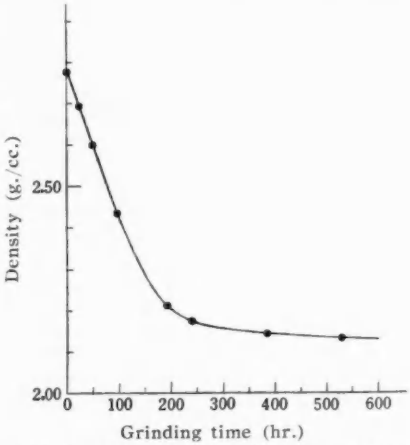

Fig. 4. Curve showing the change of the density with the time of grinding.

6) M. M. Taboadela and V. A. Ferrandis, "Differential Thermal Investigation of Clays", Mineralogical Society (London), Edited by R. C. Mackenzie (1957), p. 176.

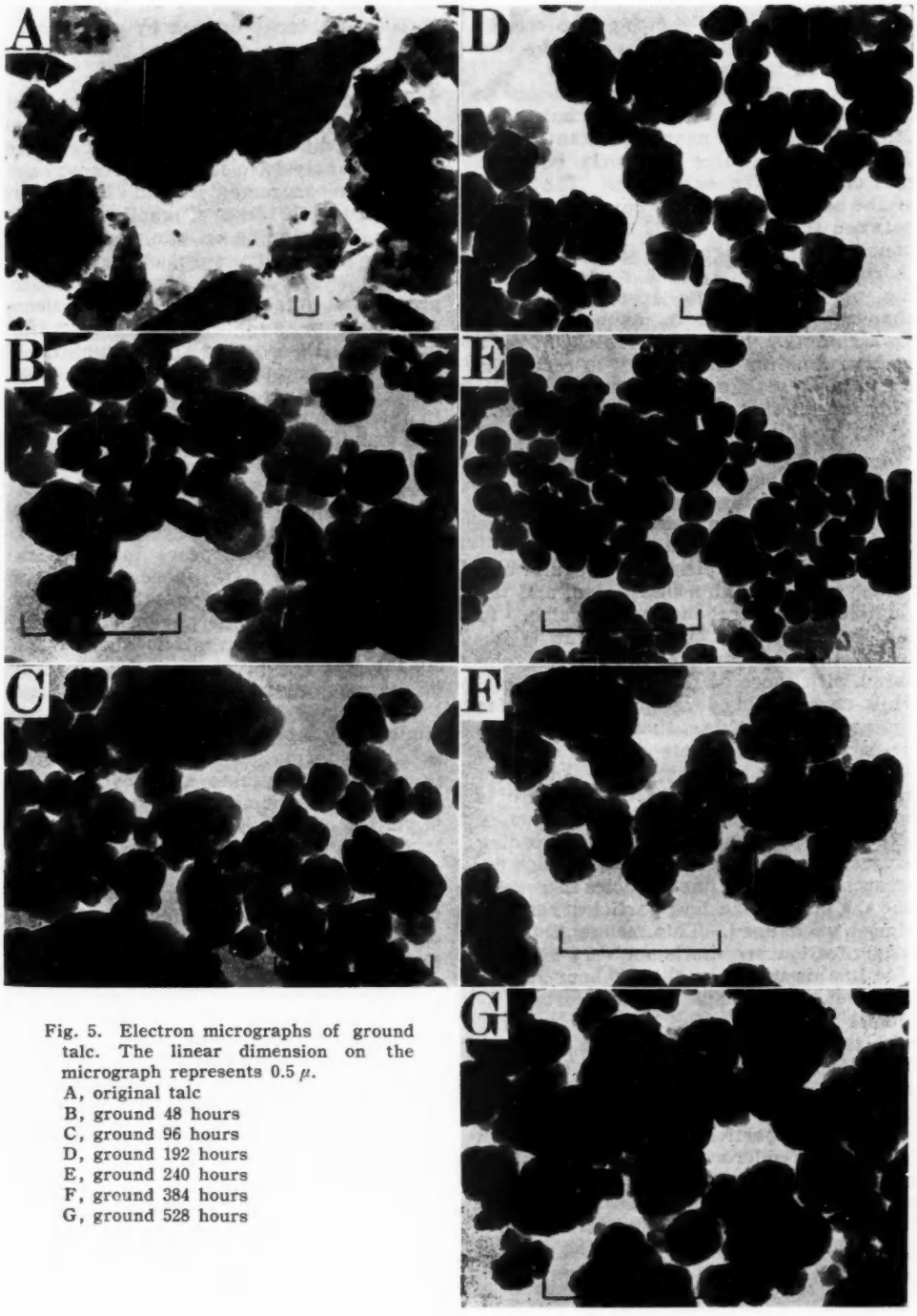

Fig. 5. Electron micrographs of ground talc. The linear dimension on the micrograph represents 0.5 μ.
A, original talc
B, ground 48 hours
C, ground 96 hours
D, ground 192 hours
E, ground 240 hours
F, ground 384 hours
G, ground 528 hours

by dry grinding is an important characteristic of talc.

Density.—A curve showing the change of the density in the process of the dry grinding on talc is shown in Fig. 4.

The density sharply decreases up to about 200 hours in the grinding, but thereafter it reaches a nearly constant value. This constant value is nearly equal to that of a gel-like substance. The point of the bend in the density curve is existent between the points of 192 hours and 240 hours. In the light of the X-ray and thermal data, this point corresponds to the point where the structure of talc changes wholly into a new structure by dry grinding. In talc, grinding takes a longer time for the density to reach the constant value than that of kaolin minerals. This means that talc suffers the effects of dry grinding less than kaolin minerals do, for the structure of talc is stronger than that of kaolin minerals.

Electron Microscopic Studies. — Fig. 5 shows the electron micrographs in the process of grinding on talc.

The original sample is an irregular and platty particle with a sharp edge, and the particle has several microns in size. In the 48-hour-ground specimen, it is observed that the particles are fine as compared with those of the original particle, while considerably large particles are also observable. It seems that the fine particles do not aggregate unlike the fine particles in the grinding process of kaolin minerals, and the edge of this particle is not sharp. The shape of the considerably large particle is spherical. As the grinding progresses, number of large particles decreases and that of fine particles increases, but the size of the fine particles remains almost unchanged. This means that the reaggregation process is not very remarkable in this case. In the 240-hour-ground specimen, the shape of the particle is almost uniformly spherical as compared with that of the 192-hour-ground specimen but it is not so spherical as the shape of particles found in the process of dry grinding of kaolin minerals. The mean value of the particle size of this specimen is about 0.1 micron. Past this stage in grinding, the particle size increases as compared with that of the 240-hour-ground specimen. As the grinding further progresses, an irregular growth of the particle is observable. This corresponds to the fact that the completely amorphous substance has been produced by grinding.

Summary

The several-hundred-hour mechanical-mortar dry grinding on talc was examined by X-ray diffraction method, differential thermal analysis, electron microscopy and density measurements, and they were compared with those of kaolin minerals. In the dry grinding on talc, some characteristics in the structural changes by dry grinding were found. As the grinding progresses, the original crystals cleave and fracture and then split into fine crystals. Disordering in structure of these fine crystals is observable before the talc structure disintegrates completely. In talc, a new substance is produced by dry grinding, which is somewhat related to but different from the original talc structure. The appearance of this new phase is most remarkable in the stage of grinding where the crystalline pattern of talc entirely disappears in the X-ray diagram. This new phase has a non-crystalline structure, but the strurcture is not completely amorphous. It crystallizes into a new crystal at about 800°C. As the grinding progresses, the structure of this new phase gradually disintegrates to a completely amorphous structure similar to that of a silica-magnesia mixed gel. The formation of a zeolitic structure is not so remarkable; also, even if this structure is formed, the period of its stage is very short. It is an important characteristic that talc wholly changes into a new non-crystalline substance by dry grinding. It is generally supposed that talc does not easily suffer the effects of dry grinding because the structure is stronger than that of kaolin minerals.

The author wishes to express his hearty thanks to Professor H. Akamatu for his continuous advice and encouragement. Thanks are due to Professor T. Sudo of the Tokyo University of Education and Professor R. E. Grim of the University of Illinois for their valuable suggestions and discussions.

Department of Chemistry
Faculty of Science
the University of Tokyo
Hongo, Tokyo

Wet Grinding on Kaolin Minerals

By Hiroshi TAKAHASHI

(Received October 2, 1958)

In the previous studies, the effects of dry grinding on the structural change of kaolin minerals have been presented[1]. It was concluded that the effect of dry grinding depends on the internal degree of crystallinity of the original kaolin mineral, and there are two processes in the structural change. One is the production of a non-crystalline material attended by disordering of the crystalline portion, and the other is the reaggregation process. At a certain period in the grinding, a zeolitic structure is formed; then finally, kaolin mineral changes into a completely amorphous substance like a silica-alumina mixed gel.

Considerable work has been done on the dry grinding of kaolinite, but comparatively little is known on the wet grinding. It was found by Shaw that the wet grinding of kaolinite causes a shearing along the cleavage plane[2]. This will lead to weakening the stacking force between kaolin unit layers. The wet grinding of kaolinite has been made heretofore using ball-mill with water or organic liquid such as benzene. Judging from the fact that wet grinding causes a shearing stress, it is obvious that a higher viscous liquid is more effective in the grinding process than the lower one. Therefore, glycerol was used in the present experiment, combined with a mechanical-mortar as it is very effective in causing a change in structure as discussed in the previous papers[1].

The purpose of this study is to know the correlation between the effect of the wet grinding and that of the dry grinding from the point of view of the degree of the crystallinity of kaolin minerals. It is hoped that this will lead to the fundamental information concerning kaolin minerals.

1) H. Takahashi, "Proc Sixth Natl. Conference on Clay and Clay Minerals", Natl. Res. Council-Natl. Acad. Sci., (in press). H. Takahashi, This Bulletin, **32**, 235, 245, 252 (1959).

2) B. T. Shaw, *J. Phys. Chem.*, **46**, 1032 (1942).

Experimental

The following kaolin minerals were investigated: Kaolinite from Mesa Alta, N. M., U. S. A.; Halloysite from Spruce Pine, N. C., U. S. A.; Halloysite from Tintic, Utah, U. S. A.. These specimens are API Standard Clay Minerals. The structural characteristics of these specimens were discussed in the previous paper[3]. Of all kaolin minerals, Mesa Alta kaolinite has the highest degree of crystallinity, of all halloysites, Spruce Pine halloysite has the highest degree of crystallinity, and Tintic halloysite has a lower degree of crystallinity than Spruce Pine halloysite.

30 g. of each original kaolin mineral was charged, mixed with 100 cc. glycerol. The mixture was wet-ground by a mechanical-mortar (15.2 cm. dia. and 8.4 cm. in depth). The specimen was taken out at intervals of 48 hours and washed with water throughly and then air-dried. The experimental specimen thus prepared was examined by X-ray, thermal and electron microscopic methods. In parallel with these examinations, its density was measured.

X-ray powder diagrams were recorded by an X-ray diffractometer (Geigerflex). Experimental conditions are as follows. Filtered Cu radiation (Cu K_α: 1.5418 Å) at 35 kV and 15 mA is used, scanning speed is 1° or 1/4° 2θ per minute, time constant is 4 seconds, receiving slit is 0.2 mm. or 0.1 mm., angular aperture 1° or 1/2° were used. The differential thermal analysis curves were recorded by the apparatus described by Sudo et al.[4]. Care was taken to pack the specimen into the sample block in a homogeneous manner and also to keep the weight of the specimen constant. The mean heating rate is 12.5°C per minute. The density was measured by pycnometer in carbon tetrachloride. The electron micrographs were obtained by the Hitachi HU-10A type Electron Microscope.

Results and Discussion

X-Ray Diffraction Studies. — X-ray diffractometer traces in the wet grinding process of kaolin minerals are given in Fig. 1. Fig. 1-a and Table I show the X-ray traces and the data of Mesa Alta kaolinite in their various stages of the wet grinding.

3) H. Takahashi, This Bulletin, **31**, 275 (1958).

4) T. Sudo et al., *J. Geol. Soc. Japan(Chishitu-Gaku-Zasshi)*, **58**, 679 (1952).

TABLE I
POWDER DATA OF WET-GROUND KAOLINITE (MESA ALTA, N. M.)

Brindley and Robinson			Original Kaolinite		Ground 96 hr.		Ground 192 hr.		Ground 384 hr.	
d	*I*	*hkl*	*d*	*I*	*d*	*I*	*d*	*I*	*d*	*I*
7.15	10+	001	7.14	VS	7.15	VS	7.16	VS	7.165	S
4.45	4	020	4.46	M	4.46	M	4.46	M	4.46	W
4.35	6	$1\bar{1}0$	4.35	S	4.35	M	4.36	W	4.36	W
4.17	6	$11\bar{1}$	4.18	S	4.18	M	4.18	W		
4.12	3	$1\bar{1}\bar{1}$	4.13	M						
3.837	4	$02\bar{1}$	3.84	M	3.84	W				
3.734	2	021	3.73	W	3.73	VW				
3.566	10+	002	3.57	VS	3.57	VS	3.58	VS	3.58	S
3.365	4	111	3.37	M						
3.138	2	$11\bar{2}$	3.14	W						
3.091	2	$1\bar{1}\bar{2}$	3.09	W						
2.748	2	022	2.75	W						
2.553	8	$20\bar{1}, 1\bar{3}0, 130$	2.55	S	2.56	M	2.56	M	2.56	W
2.521	4	$13\bar{1}, 1\bar{1}2$	2.53	M	2.53	W	2.53	W	2.53	VW
2.486	9	$1\bar{3}1, 200, 112$	2.49	S	2.49	M	2.49	M	2.49	M
2.374	7	003	2.37	M	2.38	W	2.38	W	2.39	W
2.331	10	$20\bar{2}, 1\bar{3}1, 11\bar{3}$	2.33	S	2.33	S	2.34	S	2.34	M
2.284	9	$1\bar{1}\bar{3}, 131$	2.29	S	2.29	M	2.29	M	2.29	M
2.243	1	$13\bar{2}, 040$	2.24	W						
2.182	3	$1\bar{3}\bar{2}, 220$	2.18	W						
2.127	2	$02\bar{3}, 041$	2.13	W						
3.057	1	$22\bar{2}$	2.06	W						

Key to abbreviation: VS: very strong, S: strong, M: medium, W: weak, VW: very weak, br: broad, vbr: very broad.

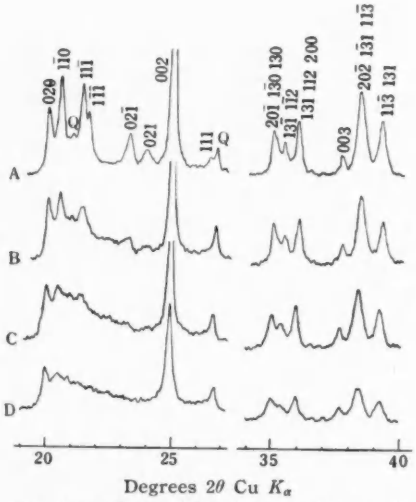

Fig. 1-a. X-ray diffractometer traces of wet-ground specimens of Mesa Alta kaolinite.
A, original kaolinite
B, ground 96 hours
C, ground 192 hours
D, ground 384 hours

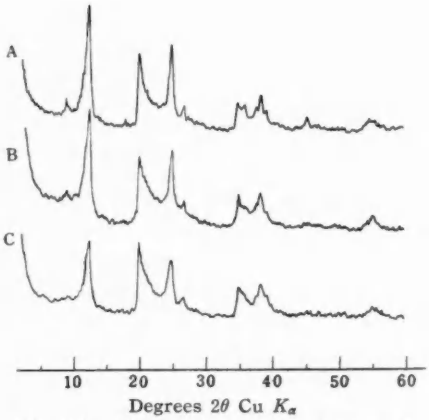

Fig. 1-b. X-ray diffractometer traces of wet-ground specimens of Spruce Pine halloysite.
A, original halloysite
B, ground 192 hours
C, ground 384 hours

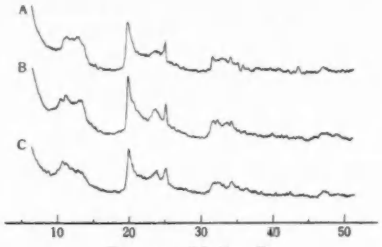

Fig. 1-c. X-ray diffractometer traces of wet-ground specimens of Tintic halloysite.

A, original halloysite
B, ground 192 hours
C, ground 528 hours

As the grinding progresses, the intensities of all reflections decrease and those of the background increase slowly. The X-ray diffraction diagram of the 48-hour-ground kaolinite is not much different from that of the original kaolinite. However, all the reflection lines become broad, $(1\bar{1}\bar{1})$ reflection becomes weak and the resolution of $(20\bar{1}, 130, 1\bar{3}0)$ reflection and $(13\bar{1}, 11\bar{2})$ reflection slightly fall. In the 96-hour-ground specimen, $(11\bar{1})$ and $(1\bar{1}\bar{1})$ reflections become broad, and they are hardly resolved at all with each other. The intensities of $(02\bar{1})$ and (021) reflections decrease and $(11\bar{2})$, $(1\bar{1}\bar{2})$ and (022) reflections disappear. These facts mean that the unit layers are displaced slightly in parallel to *b*-axis. In the 192-hour-ground specimen, a decrease in the intensity and a broadening of (020) and $(1\bar{1}0)$ reflections are observable, but $(02\bar{1})$ reflection can scarcely be detected. From these phenomena, it can be seen that a displacement occurs in this specimen, which is more random than the displacement by $b_0/3$ in parallel to *b*-axis. In the X-ray diagram of the 288-hour-ground specimen, the lowering in the resolution of (020) and (110) reflections is observable, but the broad $(1\bar{1}\bar{1})$ line can not be seen. In the X-ray diagram of the 384-hour-ground specimen, a wedge-like (02, 11) band is observable, but (003), $(20\bar{2}, 1\bar{3}1, 11\bar{3})$ and $(1\bar{1}\bar{3}, 131)$ reflections resolve distinctly with one another. The structure of the 384-hour-ground specimen becomes similar to that of fireclay[5]; however, it has still more regular displacement comparing with that of fireclay. As shown in Table I, in the process of wet grinding, the value of the basal spacing grows gradually, though slightly, as the grinding progresses. This means that the local water gets into the space between the kaolin unit layers as the inter-layer water, or that the stacking of the unit layers becomes looser owing to the shearing stress. From the above results, it is clear that the structural change of kaolinite caused by wet grinding results from cleavages in the kaolin crystal.

In the case of halloysite, however, the features observed in kaolinite are not so remarkable. Figs. 1-b and -c show the X-ray traces in various stages of wet grinding of Spruce Pine halloysite and Tintic halloysite, respectively. As seen in these figures, the X-ray traces for various stages of wet grinding are only slightly different from one another. In the wet-ground specimen of Spruce Pine halloysite, all reflections become slightly broad; only the intensity of (00*l*) reflection decreases and the background increases, as the grinding progresses. In Tintic halloysite, the changes in X-ray traces due to wet grinding are similar to that of Spruce Pine halloysite. In the 528-hour-ground specimen, it is observable that the halloysite-glycerol complex is formed.

The reflection lines generally become slightly broad by wet grinding. To ascertain the broadening of the reflections, crystallite dimensions in the wet grinding process of Tintic halloysite are measured from (001) reflection and (02, 11) band[6], as reported in the previous papers[1,7]. Their values are shown in Table II.

The crysatllite dimensions thus obtained

TABLE II
CRYSTALLITE DIMENSIONS IN THE VARIOUS STAGES OF WET GRINDING OF TINTIC HALLOYSITE

Grinding time (hr.)	Crystallite dimension (Å)	
	L_c (from 001 reflection)	L_a (from 02, 11 band)
0	80	155
192	76	141
288	70	118
384	66	110
528	58	105

5) G. W. Brindley and K. Robinson, *Trans. Farad. Soc.* **42B**, 198 (1946).
6) W. L. Bragg, "The Crystalline State", I, 189 (1933); B. E. Warren, *Phys. Rev.*, **59**, 693 (1941); C. W. Brindley and K. Robinson, *Min. Mag.*, **28**, 393 (1948); C. R. Houska and B. E. Warren, *J. Appl. Phys.*, **25**, 1503 (1054).
7) H. Takahashi, This Bulletin, **32**, 17 (1959).

are, of course, not accurately real crystallite sizes but relative values. The change of the basal spacing in the process of wet grinding of halloysite is not so remarkable as that of kaolinite. This indicates that the cleavage caused by wet grinding is not very remarkable in halloysite compared with that of kaolinite. The dry grinding is in general more effective than the wet grinding in causing the structural change. However, it is observable that there is a great difference in the wet grinding effects between kaolinite and halloysite. As clearly shown in X-ray data, kaolinite is subjected to its effects more than halloysite though its degree of crystallinity is originally higher. In kaolinite, the shearing stress acts in parallel to the layer planes, as kaolinite is made of stacking of parallel unit layers. On the other hand, in halloysite, its crystal has a tubular shape, resulting from the rolling up of the unit layers[8]. So, it is hard to make cleavage by shearing stress through wet grinding. Furthermore, as halloysite has originally a two-dimensional structure; even if a small displacement takes place along the unit layers, it does not affect its X-ray diagram.

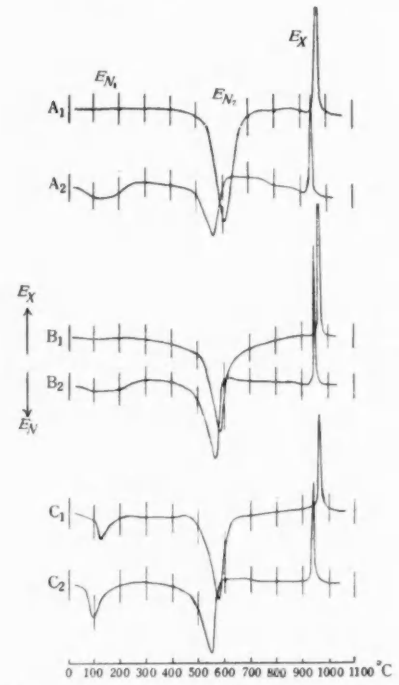

Fig. 2. Differential thermal analysis curves of wet-ground specimens of kaoiin minerals.
A_1, original Mesa Alta kaolinite
A_2, ground 384 hours
B_1, original Spruce Pine halloysite
B_2, ground 384 hours
C_1, original Tintic halloysite
C_2, ground 528 hours

Differential Thermal Analysis.—Differential thermal analysis curves and data in the process of wet grinding of kaolin minerals are shown in Fig. 2 and Table III.

In ground specimens of kaolinite, the the first endothermic reaction (E_{n1}) associated with the loss of the inter-layer or adsorbed water becomes apparent and its height increases as the grinding progresses. This means that the water gets locally into the increased spaces between kaolin layers because of cleavages through wet grinding, and it becomes the interlayer water, and/or that the non-crystalline material which adsorbs some amounts of water is produced by wet grinding. For the second endothermic reaction (E_{n2}) associated with the loss of the lattice water, as the grinding progresses, the lowering in its peak temperature and the decrease in its peak height and area are observable. In the final exothermic reaction (E_x) due to the mullite nucleation, as the grinding progresses, the lowering in the peak temperature, the increase in the peak breadth and the decrease in the peak height and area are observable. However, in halloysite, these features observed in this reaction are not so remarkable compared with that of kaolinite. This fact corresponds to the fact that kaolinite is more liable to suffer the effects of wet grinding than halloysite as shown in X-ray data. That is, in halloysite, although a lowering in the peak temperature is observable, the peak breadth decreases and the peak height is either invariable or increases. These phenomena indicate that the effect of wet grinding of halloysite is nearly the same as the effect at the early stage of dry grinding[1].

Density.—In Fig. 3 is shown the density at various periods of grinding. Measurements were made after the specimens had been dried at 110°C in order to avoid the effect of the adsorbed water.

In halloysite, the density gradually decreases at first; after reaching a certain point of grinding, it rapidly decreases. On

8) T. F. Bates, F. A. Hildebrand and A. Swineford, *Am. Mineral.*, **35**, 463 (1950).

TABLE III
THERMAL DATA OF WET-GROUND KAOLIN MINERALS
(ALL TEMPERATURES ARE DEGREES CENTIGRADE)

Specimen	E_{n1}			E_{n2}			E_x			
	Temp. (°C)	Height	Area	Temp. (°C)	Height	Area	Temp. (°C)	Height	Area	Breadth (°C)
Kaolinite (Mesa Alta, N.M.)										
Original	—	—	—	604	16	1080	966	39	220	5.1
Wet-Ground 384 hr.	120—170	2	230	566	13	660	947	31	190	8.4
Halloysite (Spruce Pine, N.C.)										
Original	125	1	70	583	17	1380	973	45	220	4.0
Wet-Ground 384 hr.	100—200	1	200	564	15	900	971	53	190	3.5
Halloysite (Tintic, Utah)										
Original	130	4	170	571	12	680	969	16	170	9.4
Wet-Ground 432 hr.	-110-	5	240	555	10	560	952	16	130	7.3

the other hand, in kaolinite, the decrease in the density is remarkable in the early stage of grinding, then the density slowly decreases, and finally it attains a nearly constant value. The rate of change in the density corresponds to the fact that kaolinite is more liable to suffer the effect of wet grinding than halloysite, at least in the early stage of grinding as indicated in previous sections.

The structure of kaolinite changes into a disordered structure due to cleavage caused by the wet grinding, while halloysite scarcely suffers the effect in the early stage of grinding. In a considerably long time of grinding, the structure of halloysite gradually decomposes due to fracturing and cleavage caused by grinding. This corresponds to the somewhat rapid decrease in the density.

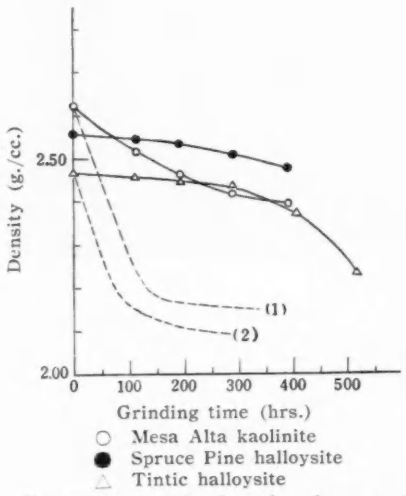

Fig. 3. Curves showing the changes of the density of wet-ground specimens of kaolin minerals with the time of grinding. (1), (2): Curves showing the changes in the process of dry grinding of Mesa Alta kaolinite and Tintic halloysite, respectively.

Electron Microscopic Studies.—The electron micrographs of some ground specimens are shown in Fig. 4.

In the early stage of grinding of kaolinite, it is seen that the edge of a kaolin crystal tends to curl. This tendency is interpreted in the light of the characteristic of the shape of kaolin unit layer by Bates et al.[8]. That is, kaolin mineral with a random displacement has generally the tubular shape like halloysite. The relation between the degree of crystallinity of a kaolin mineral and the shape of the crystal was presented in the previous paper[3]. As the grinding progresses, the shape of the kaolin crystal gradually change into a circular but platty shape. The particle size does not change remarkably. Finally, it changes into spherical aggregates of fine platty particles.

In halloysite, various shapes such as split tubular, platty, lath-shaped, cabbage-like and other variations are observable in the wet grinding process. From these phenomena, it seems that the force of wet grinding causes fracturing rather than shearing.

Mechanism of Structural Change of Kaolin Mineral due to Wet Grinding.—When kaolinite is wet-ground, the crystal

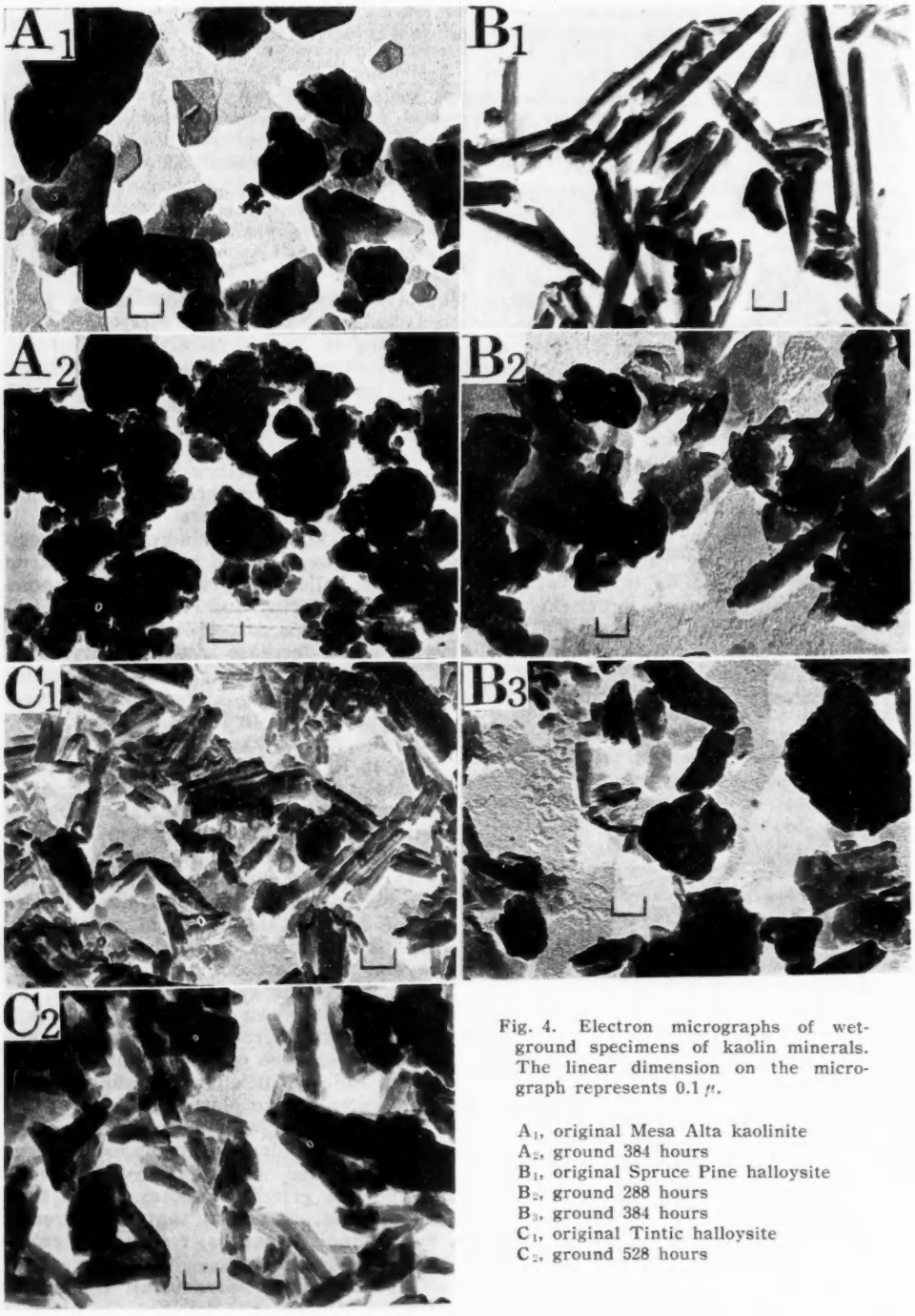

Fig. 4. Electron micrographs of wet-ground specimens of kaolin minerals. The linear dimension on the micrograph represents 0.1 μ.

A_1, original Mesa Alta kaolinite
A_2, ground 384 hours
B_1, original Spruce Pine halloysite
B_2, ground 288 hours
B_3, ground 384 hours
C_1, original Tintic halloysite
C_2, ground 528 hours

cleaves along the layer plane owing to shearing stress. In consequence, displacement of layers takes place in parallel to *b*-axis. As the grinding progresses for a long time, the structure of the original kaolinite with a triclinic in symmetry change into the more disordered structure. These displacements are remarkable in the early stage of grinding. The change of the particle shape due to wet grinding is observable as the gradual formation of fine and radial platty particles though it is not so remarkable in the early stage. When the grinding further progresses, kaolinite with a higher degree of crystallinity gradually changes into kaolin with a random displacement similar to that of halloysite.

In the early stage of grinding of halloysite, the original crystal splits and fractures owing to the fracturing force. Therefore, the change on the X-ray diagram is not so remarkable and the thermal data also indicate the same tendency. From the electron micrographs, too, it can be concluded that the force of wet grinding acts as a fracturing force, which results in splitting tubular crystal. The process of the structural change through wet grinding for the platty particle of halloysite produced by splitting is similar to that of kaolinite.

Summary

The effects of wet grinding on kaolin minerals were examined by X-ray diffraction method, differential thermal analysis, electron microscopy and density measurement. The effects of wet grinding of kaolin minerals are different from those of dry grinding, particularly at the early stage of grinding. It has been considered that the force of dry grinding acts as fracturing and cleaving forces, while the force of wet grinding acts as a weak cleaving force for kaolinite and as a weak fracturing force for halloysite in the early stage of grinding. It has been revealed that the effects of wet grinding depend on the shape of crystal in the original kaolin mineral in the early stage of grinding, and beyond a certain stage of grinding, they depend on the structural perfectness of the kaolin layer, that is, the internal degree of crystallinity of the original kaolin mineral.

The author wishes to express his hearty thanks to Professor H. Akamatu for his continuous advice and encouragement. Thanks are due to Professor T. Sudo of the Tokyo University of Education for his valuable suggestions and discussions.

Department of Chemistry
Faculty of Science
the University of Tokyo
Hongo, Tokyo

Formation and Aging of Precipitates. XI. An Electron Micro-Diffraction Study on Nucleation of Barium Sulfate Precipitate from Homogeneous Solution*

By Kazuyoshi TAKIYAMA

(Received October 6, 1958)

In the course of precipitate formation, the nucleation process is the idea generally accepted. The nucleation involves a process of formation of embryo, which is an unstable intermediate, and a process of the nucleus formation. When the precipitate is formed with direct mixing of ions, the growth of the nuclei formed in small numbers plays a predominant part in the region of the lower concentration, and the nucleation plays a predominant part in the higher concentration region[1,2]. When the precipitate is formed from a homogeneous solution, the nucleation occurs when a certain degree of supersaturation is attained[3]. During the

* The tenth paper of this series, This Bulletin, **32**, 68 (1959).

1) K. Takiyama, ibid., **31**, 950 (1958).
2) K. Takiyama, ibid., **32**, 68 (1959).
3) V. K. LaMer and R. H. Dinegar, *J. Am. Chem. Soc.*, **73**, 380 (1951).

precipitation process the crystal property of particles seems to appear after nucleation.

An attempt has been made in the present investigation to employ the electron micro-diffraction method with a view to observe the nucleation process during the formation of barium sulfate precipitate according to LaMer and Dinegar's method[3].

Experimental

Procedure.—Fifty ml. of 0.02 M ammonium persulfate solution was added to a 200 ml. beaker containing 50 ml. of 0.02 M barium nitrate solution. Barium sulfate formed from the sulfate in persulfate was filtered with a glass filter. Ten ml. of 0.1 M sodium thiosulfate solution was then added to the clear filtrate and the reaction solution thoroughly mixed was kept in a thermostat at 25°C. The precipitate, when examined with a beam of white light, exhibited Tyndal beam 7 minutes after the addition of thiosulfate.

The reaction mixture was poured into a spray bottle which was kept in the thermostat, and was sprayed on tiny Formvar films floating on the surface of distilled water 5, 6, 7, 8, 9 and 10 minutes after the addition of thiosulfate. A few minutes were allowed for diffusion of soluble salts from the drop of reaction mixture into the water below. The films were scooped with specimen grids for observation with an electron microscope.

Calculation of Size of Crystalline Nucleus.—From the Thomson's equation[4] on nucleation in the supersaturated vapor, the size of nucleus formed in the supersaturated sparingly soluble salt solution is expressed by the following equation,

$$r = \frac{2M\sigma}{i\boldsymbol{R}T\rho \ln S/S_\infty} \qquad (1)$$

where r is the radius of spherical nucleus, M the molecular weight, σ and ρ are the surface tension and the density of the crystal, $\boldsymbol{R}$ is the gas constant, T the absolute temperature, S the supersaturation concentration, S_∞ the solubility of the salt and i the van't Hoff factor. According to LaMer and Dinegar[3], the value of the supersaturation ratio, $\sqrt{K^\circ_{SS}/K^\circ_{SP}}$ (K°_{SS} and K°_{SP} are the activity products of both supersaturated and saturated solutions), is a constant and is 22 on an average at 25°C. The value of r is calculated in the present case, as 100 Å from the equation 1, when this limiting value, 22, is substituted for S/S_∞. On the other hand, the condition of concentration of reacting ions at the time that the precipitate begins to appear in the case of homogeneous solution method, seems to correspond to the limiting supersaturation concentration at which the precipitate appears without an induction period in the case of direct mixing method. This limiting supersaturation concentration is about 0.002 M[1]. The size of nucleus, r, is calculated as 60 Å according to the equation 1, when this value of 0.002 is substituted for S. It seems that the size of crystalline nucleus formed under the experimental condition mentioned above is in the range of 100 to 200 Å in diameter.

4) W. Thomson, *Phil. Mag.*, **42**, 448 (1871).

Results

The image of particles began to be observed with the electron microscope after 6 minutes and the particles grew gradually as the time passed. An electron micrograph and an electron diffraction pattern obtained from the six minutes' specimen are shown in Figs. 1 a and b. The diameter of particles shown in Fig. 1 a measures 30 to 80 Å and the particles looked like unstable embryos formed by aggregation of monomers. As the crystal structure of these particles is not perfect, the diffraction pattern is composed of a few broad rings. The particles in the seven minutes' specimen are nearly spherical and measure 100 to 200 Å in diameter as shown in Fig. 2 a. The size of these particles coincides with that obtained by the calculation from equation 1. The electron diffraction pattern obtained from these particles is composed of indistinct coarse rings as shown in Fig. 2 b. But the rings indicate that the crystal structure of particles is more perfect than that of particles shown in Fig. 1 a. The size of particles in the eight minutes' specimen is 300 to 400 Å in diameter as shown in Fig. 3 a. The electron diffraction pattern is composed of distinct coarse Debye-Scherrer rings as shown in Fig. 3 b. The crystal structure of particles seems to have been completed in this stage. The particles in the ten minutes' specimen are spindle-shaped and the length of the long axis is about 1000 Å as shown in Fig. 4 a. The electron diffraction pattern obtained from one of the particles arrow is N-pattern as shown in Fig. 4 b. Each particle is obviously a single crystal, and the long axis proves to be b-axis from the analysis of the pattern shown in Fig. 4 b. The shape of the particle grown completely is oval. The oval particle of barium sulfate seems to be formed through dendritic growth in every direction from a crystal nucleus and the particle has a single crystal structure. The growth along b-axis seems to be more or less marked.

The particles of barium sulfate began

Electron micrographs and diffraction patterns of barium sulfate presipitates.

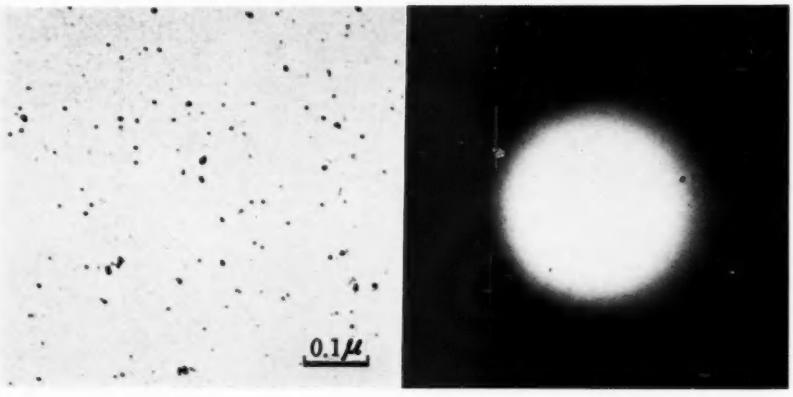

a b

(×100, 000)

Fig. 1. Embryos of barium sulfate precipitate sampled after 6 minutes.

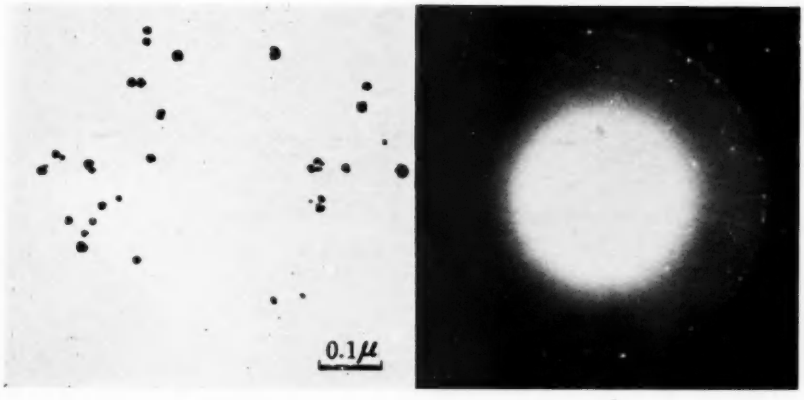

a b

(×100, 000)

Fig. 2. Crystal nuclei of barium sulfate precipitate sampled after 7 minutes.

Electron micrographs and diffraction patterns of barium sulfate presipitates.

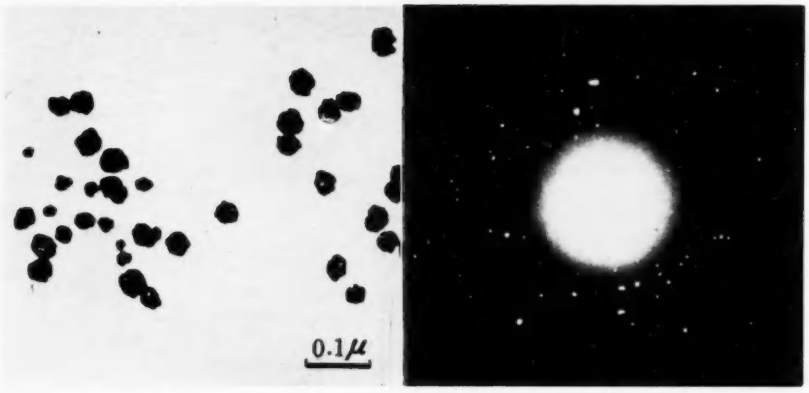

a b

(×100, 000)

Fig. 3. Crystals of barium sulfate precipitate sampled after 8 minutes.

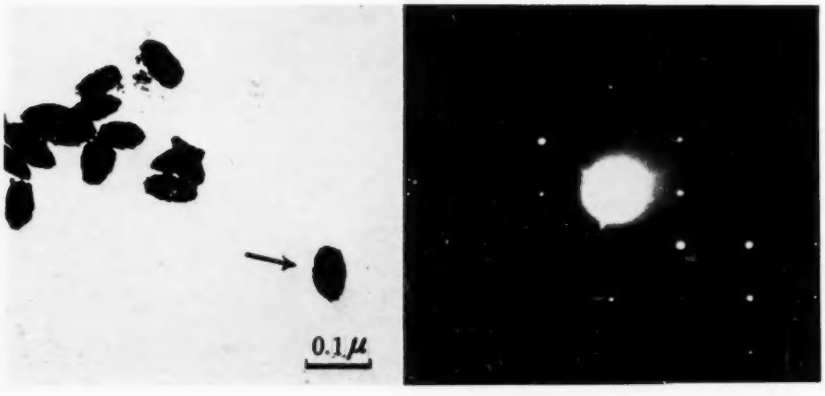

a b

(×100, 000)

Fig. 4 Single crystals of barium sulfate precipitate sampled after 10 minutes.

to appear after 6 minutes and grew up continuously into large crystals. During the precipitation process, the existence of the nucleus with a certain size can be logically proved from the standpoint of thermodynamics[3,4], but in fact only the continuous growth of a particle is observed by electron microscopy and the particle appears to form a distinct crystal structure when it has attained the size as large as that of the nucleus calculated thermodynamically.

Summary

The nucleation process of the precipitation of barium sulfate from the homogeneous solution of persulfate-thiosulfate system was observed by the electron micro-diffraction method. The particles grew continuously, but the distinct crystal structure began to appear in the particles having the length of 100 to 200 Å in diameter, corresponding to the nucleus calculated thermodynamically.

The author gratefully acknowledges the guidance of Professor Eiji Suito of Kyoto University. He also wishes to express his hearty thanks particularly to Professor Masayoshi Ishibashi of Kyoto University for his continuous advice and encouragement.

Institute for Chemical Research
Kyoto University
Takatsuki, Osaka

Studies on the Interaction of Surface Films with Solute in Solution. V Deposition of Monolayers of Several Amphipathic Compounds from Surfaces of Aqueous Solutions of Congo Red and Crystal Violet

By Mitsuo MURAMATSU

(Received September 18, 1958)

It has been shown by several investigators that useful knowledge could frequently be obtained for the surface interaction of the insoluble monolayer formed at air-water interface with the other additives, by investigating the nature of the built-up film obtained from the surface of aqueous substrate. Thus, the nature of the mixed monolayer of stearic acid and normal paraffin[1] or cetyl alcohol[2] has been studied by means of this method. In the latter case, formation of a stoichiometric complex of 1:1 ratio was suggested by the measurement of the surface potential, which was in agreement with the experimental result on the mixed monolayer of the same materials spread on the surface of water[3]. Such a method could sometimes be applied to study the interaction between the insoluble monolayer and the aqueous solute in the solution underlying the film. The present author[4] obtained the built-up film of stearic acid of low refractive index by transferring the monolayer from the surface of aqueous solutions containing copper, aluminum and thorium ions and discussed the structure of metal soap formed at the solution-air interface. A similar method could successfully be applied to the case of interaction between dicarboxyacids in aqueous phase and octadecylamine in the monolayer spread on it[5].

In the preceding reports[6,7] it has been shown that the addition of dye to aqueous substrate resulted in a remarkable expansion of the monolayer of amphipathic compound spread on it, when pH of the substrate was in a proper range where the binding of dye to the film material as well as the aggregation of the former

1) H. Sobotka and S. Rosenberg, *J. Colloid Sci.*, **5**, 581 (1950).
2) T. Isemura and R. Nakagawa, *Memoirs Inst. Sci. Ind. Research, Osaka Univ.*, **8**, 140 (1951).
3) J. Marsden and J. H. Schulman, *Trans. Faraday Soc.*, **34**, 748 (1938).
4) M. Muramatsu and T. Sasaki, This Bulletin, **25**, 21, 25 (1952).
5) T. Sasaki and M. Muramatsu, ibid., **26**, 96 (1953).
6) M. Muramatsu, ibid., **31**, 878 (1958).
7) M. Muramatsu, ibid., **32**, 114 (1959).

was remarkable. This could be ascribed to the interaction between the dye and the amphipathic compound, involving ionic, dipolar and van der Waals' forces. A similar conclusion was obtained by Matuura[8] in the case of the monolayer of stearic acid. To obtain further confirmations for such an interaction, the present author has intended to study the nature of the built-up films of several amphipathic compounds transferred from the surfaces of aqueous solutions of Congo red and Crystal violet.

Experimental

Materials. — Amphipathic compounds and dyes were purified thoroughly by the methods similar to those used in the former experiments[6,7]. Oleic acid and castor oil as piston oils were pure grade commercial products of Kahlbaum and Takeda, respectively, which were used without any further purification. Tri-*p*-cresyl phosphate was synthesized by the reaction of *p*-cresol and phosphorus pentachloride[9] and was distilled three times in vacuo.

Method.—Monolayers were spread from the benzene solutions of amphipathic compounds onto the aqueous substrates, containing or lacking the dyes. They were built up onto the base echelon of successive Y-multilayers of barium stearate deposited on a highly polished slide of stainless steel, by means of Langmuir-Blodgett technique[10] under the spreading pressure, F, of either of tri-*p*-cresyl phosphate ($F=10$ dyn./cm.), castor oil (15 dyn./cm.) or oleic acid (30 dyn./cm.), unless otherwise mentioned. The spacing of the built-up film was determined by means of the simplified optical method[11], assuming the same refractive index of 1.462 for the film as that of the base echelon, spacing of which was reported to be 24.4Å[10].

Concentration of the dye solution was kept to 10^{-4}mol./l. The acidity of the substrate was adjusted simply by twice-distilled hydrochloric acid and ammonia using the Beckman glass electrode. In the case of dye solution, experiments were conducted under the pH of largest expansion of each monolayer[7,8].

Results

Ease of Building-up of the Films.— Successive Y-multilayer of stearic acid could easily be obtained in pH range of 4～7 by transferring the monolayer under the spreading pressure of oleic acid or castor oil from the surface of water containing no dye. When pH of water was less than 4, however, the monolayer adherred neither to the bare surface of the slide nor to the base echelon of barium stearate. These facts are in agreement with what was reported[10]. In contrast with this, the successive Y-multilayer was obtained from the surface of the aqueous solution of Congo red the pH of which was 3.2. Deposition of the monolayer was clearly favored by the addition of the dye at least in the region of low pH, presumably owing to an increased stability of the film. From the surface of the solution of Crystal violet, we could obtain the Y-multilayer only when the monolayer was compressed by oleic acid and the slide was dried thoroughly after each transfer of the film.

Attempts were made to build the multilayers of cholesterol from the substrates of water and solution of Congo red. In the former case the substrate water of pH 5.8 proved to be favorable for obtaining the successive Y-layer for any piston oil used, while deposition of the monolayer was unsuccessful on the substrate of pH 2.0. Here, the addition of Congo red to the substrate resulted in promoting the easiness of building-up of the film even at pH 2.0. In this case the use of oleic acid and castor oil as piston oil effected Y-layer and occasionally X-layer.

The monolayers of cetyl alcohol, ethyl *n*-hexadecyl ether and ethyl stearate adhered neither to the bare surface of the slide nor to the base echelon, irrespective of the addition of Congo red to the substrate. This was indeed the fact under the spreading pressure of any piston oil used. Further efforts were also made to build up the multilayers under the spreading pressure of benzene solutions of film material placed near the slide covered with the base echelon. This method proved to be suitable for the deposition of such monolayers as copper, aluminum and thorium stearate, to which the ordinary technique of Langmuir-Blodgett method failed to apply[4]. However, it was unsuccessful in the present case even with this method.

The monolayer of octadecylamine could be deposited onto the base echelon only when the fiilm was compressed by tri-*p*-cresyl phosphate, under the substrate pH of 5～9. This was in agreement with the results reported in a former paper[5]. When Crystal violet was added to the aqueous substrate, no monolayer could be deposited in many cases onto the solid surface. Even when it could be built up,

8) R. Matuura, This Bulletin, **24**, 282 (1951).
9) W. Autenrieth and A. Geyer, *Ber.*, **41**, 146 (1908).
10) K. B. Blodgett and I. Langmuir, *Phys. Rev.*, **51**, 964 (1937), etc.
11) T. Tachibana, *J. Japanese Biochem. Soc.* (*Seikagaku*), **20**, 8 (1948).

TABLE I

BUILT-UP FILMS OF STEARIC ACID, CHOLESTEROL AND OCTADECYLAMINE TRANSFERRED FROM THE SURFACES OF AQUEOUS SUBSTRATES CONTAINING OR LACKING DYE

Film material	Conditions of building-up: Substrate sol.		Piston oil*	Nature of the built-up film: Type of the film	Apparent spacing, Å	Wetting toward	
	Dissolved dye	pH				water	benzene
Stearic acid	none	4~7	C or O	Y	23.1±0.2	hydrophobic	oleophobic
〃	Congo red	3.2	C or O	Y	22.1±0.4	〃	oleophilic
〃	Crystal violet	7.2	O	Y	29.2±2.9	〃	〃
Cholesterol	none	5.8	T, C or O	Y	18.4±0.2	〃	〃
〃	Congo red	2.0	C or O	Y or X	25.8±0.3	〃	〃
Octadecylamine	none	5~9	T	Y	24.4±0.5	〃	oleophobic
〃	Congo red	5.5	T	Y	22.4±0.4	〃	oleophilic

* C, castor oil; O, oleic acid; T, tri-*p*-cresyl phosphate

we merely obtained optically heterogeneous films, irrespective of the nature of the piston oil and of the substrate pH. In contrast with this, homogeneous Y-multilayer was obtained successively from the surface of the solution of Congo red of pH 5.5, when the monolayer was compressed by tri-*p*-cresyl phosphate and the built-up film was dried after each transfer of the film.

The conditions for the successful deposition of the film were summarized in the columns of Table I from the first to the fourth columns. In this table the fifth column expresses the types of the multilayers thus obtained.

Spacing of the Built-up Films. — In Table I, the sixth column shows the spacing of the built-up films of stearic acid, cholesterol and octadecylamine, transferred from the surfaces of aqueous substrates containing or lacking dye. They are expressed in average values of 5—12 independent experiments. When the monolayer was deposited from the surface of water, the spacing depended only a little on the acidity of substrate throughout the whole region of pH investigated and on the choice of piston oil. The latter condition was valid also in the case of the solution of dye as substrate. This might come from the low compressibility of these films[7].

Wettability of the Films. — As is cited in the seventh column of Table I, all built-up films were of hydrophobic character when they were once dried. Of these films, the film of stearic acid was reported to be wetted profoundly by aqueous solutions of copper, aluminum and thorium ions[4,12]. Such an effect of metal ions was observed in the present experiments for the built-up films of stearic acid transferred from the surfaces of water, solution of Congo red and of Crystal violet. However, there were some differences between the three films in their behaviors towards the subsequent procedure. For the first film, the solid surface remained in its hydrophilic condition for at least two minutes after final rinsing with water. For the second and the third films, the procedure under the same condition resulted in peeling-back of rinsing water. After the films were once dried, the subsequent conditioning by aqueous metal ions gave rise to no wetting of the first film, while it rendered the remaining two films wettable.

The last column of Table I represents the wettability of these films toward a drop of benzene placed on them. Though the test was merely qualitative, the result was sufficient to classify the film into two groups with respect to their wetting characters. Benzene showed a large contact angle toward the films of stearic acid and of octadecylamine both transferred from the surface of water. When the slide was tilted, the drop slid on the film on which less color change was observed at the track. On the contrary, the contact angle was very small for the rest of the films and the sliding of the drop resulted in a remarkable change in color, showing the profound dissolution of film materials into the benzene drop.

Discussion

As mentioned in the preceding section, the monolayers of cetyl alcohol, ethyl *n*-hexadecyl ether and ethyl stearate spread on the surfaces of water adhered neither to the metal surface nor to the base echelon of barium stearate. Isemura

12) I. Langmuir, *Science*, **87**, 493 (1938); A. Inaba, This Bulletin, **26**, 43 (1953).

and Nakagawa[2] have obtained a similar result for the case of cetyl alcohol. In the case of ethyl stearate it was reported[13] that the monolayer could be deposited successively only under the delicate control of substrate pH, speed of down- and up-trip of the slide. The built-up film thus obtained however seems to consist of large crystals transferred heterogeneously on the slide, as was pointed out by the microscopic observation[14]. All these phenomena, as well as the present results, seem to show the difficulty of building up a non-ionic monolayer spread on water. A similar result was obtained for the monolayers of these compounds spread on aqueous solutions of Congo red. Under the present conditions of pH of substrate, the majority of dye molecules were considered to be in a zwitterion form as pointed out in a preceding report[7]. Therefore, there is no net charge in the molecules either of film materials or of dye.

On the other hand, building-up was successful in the cases of the monolayers of stearic acid, cholesterol and octadecylamine spread on the solutions of Congo red, and of stearic acid on the solution of Crystal violet. Of these films, it is noticeable that the building-up of the monolayers of stearic acid and cholesterol is facilitated by an addition of Congo red to the substrate. Here, because of Congo red being in the region more acidic than the isoelectric point, the molecules of the dye have a positive charge while the monolayers are not in a charged state[7]. In the remaining two cases, dye and film materials are charged oppositely to each other, as pointed out in the preceding reports[7,15]. These facts lead us to a presumption that a suitable attachment of charged dye to the film material does not decrease the easiness of obtaining a built-up film of its own.

As seen in Table I, the apparent spacing of the built-up film of stearic acid or octadecylamine is decreased by an addition of Congo red to the substrate of the monolayer. It has been reported that the monolayers of stearic acid[8] and octadecylamine[7] expanded remarkably when they were spread on aqueous solution of Congo red and were compressed to a surface pressure of piston oil used in the present experiment. This could be explained by an attachment of colloidal aggregates of dye to the monolayer. Therefore the attachment of Congo red to the film may cause an increase in film thickness, while it may result in a decrease in surface density of *n*-hydrocarbon chain of the amphipathic compound and consequently a decrease of refractive index of the film. These two effects contribute oppositely to each other to the apparent spacing which we actually measured assuming the same refractive index of the upper layer as that of the base echelon. In the present case, the effect of the former seems to be overwhelmed by that of the latter. A similar effect of solute was observed in the case of the built-up film of stearic acid obtained from the surface of aqueous solutions of copper, aluminum and thorium ions[4]. In contrast with this, an overwhelming contribution of the former is observed for the film of cholesterol spread on the solution of Congo red and for the film of stearic acid on the solution of Congo red and for the film of stearic acid on the solution of Crystal violet.

It is of interest to show that, though all the films studied exhibit hydrophobic property, they are wettable toward benzene, except for the films of stearic acid and octadecylamine transferred from the surface of water which proved to be oleophobic. Zisman et al.[16] obtained the oleophobic monolayers of methyl-rich surface being non-wettable toward methylene liquid such as *n*-hexadecane, benzene, etc. They explained the phenomenon by a difference between methyl-methyl and methylene-methylene attractions[17]. As was pointed out by several investigators[18], the oleophobic character toward methylene liquid seems to suggest the existence of the methyl-rich surface, in which the molecules are closely packed and orientate towards the contacting phase. In Table I the built-up films of stearic acid and octadecylamine show an oleophobic property while the cholesterol film proves to be oleophilic, when they are transferred from the surface of water. This can be explained by the greater difficulty of packing of methyl head for the case of cholesterol, as would be expected from the special structure of

13) E. Stenhagen, *Trans. Faraday Soc.*, **34**, 1328 (1938).
14) G. Knott, J. H. Schulman and A. F. Wells, *Proc. Roy. Soc.*, **A176**, 534 (1940).
15) M. Muramatsu, This Bulletin, **31**, 871 (1958).
16) W. A. Zisman et al., *J. Colloid Sci.*, **1**, 513 (1946); **2**, 563 (1947).
17) W. A. Zisman et al., ibid., **7**, 109, 166, 428, 465 (1952).
18) See, *Discussions Faraday Soc.*, **3**, 259 (1948).

cholesterol. Similarly, the oleophilic nature of the films taking up the dye can reasonably be explained by the structure of built-up film consisting of widely spaced *n*-hydrocarbon chain. We can find that this is also in a conformity with the effect of added dyes upon the limiting area of the monolayers of stearic acid, cholesterol and octadecylamine[7,8].

Summary

Attempts were made to obtain the built-up films of stearic acid, cholesterol, cetyl alcohol, ethyl *n*-hexadecyl ether, ethyl stearate and octadecylamine, by transferring each monolayer from the surfaces of water and aqueous solutions of Congo red and Crystal violet. Deposition of the monolayers of cetyl alcohol, ethyl *n*-hexadecyl ether and ethyl stearate was unsuccessful, irrespective of whether the substrate contained dye or not. On the other hand, the monolayers of the remaining compounds could easily be deposited onto the solid phase from the surfaces of water and dye solution.

The effect of added dye upon the apparent spacing of the film thus obtained seems to show an attachment of dye to the film substance, though the spacing varied from one case to another. This variation could be explained taking account of the balance of two contributing factors mutually opposite to the apparent spacing: one, increase of the film thickness due to the attachment of dye, and the other, decrease of the refractive index of the film due to the wide separation of *n*-hydrocarbon chain. Such a consideration was supported by the data on the wettability toward benzene. All these phenomena are in agreement with the data on the effect of dissolved dye upon the limiting area of the monolayer spread on it.

In conclusion the author expresses his hearty thanks to Professor T. Sasaki for his kind guidance in the course of this study. The cost of this research has been defrayed from the grant of the Ministry of Education given to the Professor.

Department of Chemistry
Faculty of Science
Tokyo Metropolitan University
Setagaya-ku, Tokyo

Remarks on the Molecular Calculation of Naphthalene and Anthracene

By Noboru MATAGA, Kichisuke NISHIMOTO and Shizuyo MATAGA

(Received September 22, 1958)

The calculations made by Pariser and Parr[1,2] and also by Pople[3] in terms of semi-empirical molecular orbital (MO) method, have made a remarkable progress in the interpretation of the spectra of π-eletron systems. However, the agreement between the experimental and the theoretical results on the spectra of naphthalene which should come to our attention naturally next to benzene, does not seem to be satisfactory as yet. Although the results of Pople's SCF calculation[3] and Pariser's ASMOCI calculation[2] seem to be fairly well founded experimentally, the results of SCF and ASMOCI calculations of Moser and Lefebvre[4] in various degrees of approximations are in rather an unfortunate disagreement with experimental observations. Such an undesired circumstance is not restricted only to the case of electronic spectra, but, for example, the calculated bond orders of naphthalene and anthracene seem to agree hardly at all with observed values. The bond orders of naphthalene calculated with naive MO's are in a serious discrepancy with experimental values, but those of anthracene calculated in the same way are in good cor-

1) R. Pariser and R. G. Parr, *J. Chem. Phys.*, **21**, 466, 767 (1953); ibid., **23**, 711 (1955).
2) R. Pariser, ibid., **24**, 250 (1956).
3) J. A. Pople, *Proc. Phys. Soc.*, **A68**, 81 (1955).
4) R. Lefebvre and C. Moser, *J. Chem. Soc.*, **1956**, 1557, 2734.

TABLE I
CALCULATED AND OBSERVED SPECTRA OF NAPHTHALENE

State	Calcd. (i)		(ii)		(iii)		Pople		Pariser		Obs.	
	$h\nu$(e.V.)	f	$h\nu$(e.V.)	f	$h\nu$(e.V.)	f	$h\nu$(e.V.)	f	$h\nu$(e.V.)	f	$h\nu$(e.V.)	f
$^1B_{3u}$	4.253	0.00	4.256	0.00	4.245	0.00	4.40	—	4.018	0.000	3.99	0
$^1B_{2u}$	4.503	0.33	4.465	0.25	4.680	0.29	4.65	—	4.493	0.256	4.30	0.18
$^1B_{3u}$	5.803	2.03	5.813	2.09	5.860	2.18	6.13	—	5.939	2.115	5.50	2.0
$^1B_{2u}$	6.337	0.46	6.415	0.83	6.490	0.89	6.20	—	6.309	0.699	7.30	0.6
$^3B_{2u}$	2.584	0.00	2.627	0.00	2.725	0.00	3.09	—	2.180	0.000	2.6	—
$^3B_{3u}$	3.758	0.00	3.762	0.00	3.740	0.00	4.09	—	3.639	0.000	3.7(?)	—
$^3B_{3u}$	4.253	0.00	4.256	0.00	4.245	0.00	4.40	—	4.018	0.000	—	—
$^3B_{2u}$	4.334	0.00	4.269	0.00	4.380	0.00	4.83	—	4.220	0.000	—	—

TABLE II
CALCULATED AND OBSERVED SPECTRA OF ANTHRACENE

State	Calcd. (i)		(iii)		Pople		Pariser		Obs.	
	$h\nu$(e.V.)	f	$h\nu$(e.V.)	f	$h\nu$(e.V.)	f	$h\nu$(e.V.)	f	$h\nu$(e.V.)	f
$^1B_{2u}$	3.279	0.26	3.481	0.39	3.72	—	3.648	0.386	3.30	0.1
$^1B_{3u}$	3.898	0.00	3.908	0.00	4.15	—	3.715	0.000	3.50	0
$^1B_{3u}$	5.098	2.74	5.185	3.00	5.64	—	5.499	3.229	4.80	2.20
$^1B_{2u}$	6.648	1.03	6.441	0.81	6.44	—	6.586	0.644	5.64	0.65
$^3B_{2u}$	1.713	0.00	1.691	0.00	2.23	—	1.660	0.000	1.8	—
$^3B_{3u}$	3.595	0.00	3.585	0.00	3.96	—	3.503	0.000	—	—
$^3B_{3u}$	3.898	0.00	3.908	0.00	4.15	—	3.715	0.000	—	—
$^3B_{2u}$	4.793	0.00	4.824	0.00	5.39	—	5.230	0.000	—	—

respondence with experiment. The application of the semiempirical SCFMO method of Pople to these molecules leads to a nice agreement with experiment in the case of naphthalene[5] but at the same time to a wrong prediction in the case of anthracene[6]. However, employing the values of molecular integrals which we have been using for studying the electrostructures of nitrogen heterocycles[7], the electronic spectra and other properties of naphthalene and anthracene seem to be satisfactorily interpreted. In the present report, the results of our calculation on the aromatic hydrocarbons will be described with some critical discussions comparing our results with those of other authors.

I. Electronic Spectra.—As indicated in Tables I and II, the calculated spectra of naphthalene and anthracene employing our parameters[7] are in a satisfactory agreement with experimental values. In these tables the results obtained by Pople and Pariser, respectively, are also given for the purpose of comparison. In both of these tables, "i" is the result of the ordinary Hartree-Fock SCF calculation with the approximation of zero differential overlap, and "ii" is obtained by an approximate SCF calculation in which $F_{\mu\nu}$'s for the neighbors more distant than the nearest are neglected, and in "iii" the naive MO's are used for the calculation of excitation energies and oscillator strengths. The calculated results in "iii" are close to those "i" or "ii", and the agreement with the observed values is satisfactory. This fact is in accordance with the circumstance that, as pointed out by Dewar and Longuet-Higgins[8], owing to the uniform charge distribution in aromatic hydrocarbons, their naive MO's themselves are fairly close to SCFMO's.

Now, the results obtained by Lefebvre and Moser are collected in Table III. In this table, A is the result of the calculation which involves the penetration integrals to hydrogen atoms, in addition to other parameters which are the same as used by Pariser and Parr. Accordingly, the pairing property between the bonding and the antibonding orbitals is lost in this

5) J. A. Pople, *Trans. Faraday Soc.*, **49**, 1375 (1953).
6) H. O. Pritchard and F. H. Sumner, *Proc. Roy. Soc.*, **A226**, 128 (1954).
7) N. Mataga and K. Nishimoto, *Z. physik. Chem. N. F.* **13**, 140 (1957); N. Mataga, This Bulletin, **31**, 453, 459, 463 (1958).
8) M. J. S. Dewar and H. C. Longuet-Higgins, *Proc. Phys. Soc.*, **A67**, 795 (1954).

case. In B, $F_{\mu\mu}$, the diagonal element of Fock's Hamiltonian in terms of AO, has been assumed to be constant regardless of the position of carbon atoms, resulting in the pairing property, and all the off-diagonal elements, $F_{\mu\nu}$'s for nearest neighbors have been assumed to be equal to each other. For more distant neighbors, $F_{\mu\nu}$ is calculated by $F_{\mu\nu}=H_{\mu\nu}-1/2\ P_{\mu\nu}\gamma_{\mu\nu}$, where $H_{\mu\nu}$ is the off-diagonal element of core Hamiltonian, $P_{\mu\nu}$ is the bond order and $\gamma_{\mu\nu}$ is the electronic Coulomb repulsion integral. In C, it has been assumed that all values of $H_{\mu\nu}$ for nearest neighbors are equal.

TABLE III

SPECTRA OF NAPHTHALENE CALCULATED BY LEFEBVRE AND MOSER (SINGLET STATES)

(A)

MO's state	$h\bar{c}\nu$(e.V.)			f		
	Hückel	Cyclic	SCF	Hückel	Cyclic	SCF
B_{3u}	4.668	3.819	4.696	0.02	0.02	0.13
B_{2u}	4.984	4.180	4.995	0.05	0.00	0.00
B_{3u}	6.655	6.799	6.333	2.47	3.43	1.51
B_{2u}	6.542	5.939	6.538	1.28	1.01	1.15

(B)

MO's state	$h\bar{c}\nu$(e.V.)		f	
	Hückel	Cyclic	Hückel	Cyclic
B_{3u}	4.722	4.586	0.00	0.00
B_{2u}	4.161	4.086	0.30	0.35
B_{3u}	7.563	7.466	2.54	3.80
B_{2u}	6.762	6.993	1.11	0.59

(C)

MO's state	$h\bar{c}\nu$(e.V.)		f	
	Hückel	Cyclic	Hückel	Cyclic
B_{3u}	4.403	4.120	0.00	0.00
B_{2u}	4.289	4.314	0.20	0.20
B_{3u}	6.343	7.000	2.36	3.56
B_{2u}	6.597	5.834	1.05	0.71

The most important difference of our calculation from Lefebvre's and Moser's is in the choice of parameters, especially of $\gamma_{\mu\nu}$ values. In this respect, some discussions will be given in the latter part of this paper.

II. Bond Orders.—As mentioned in the introductory part of the present paper, Pople's self-consistent treatment as applied to the calculation of bond orders gave good agreement with the experiment for naphthalene, but not for anthracene, whereas with the simple treatment without the inclusion of electronic interaction, the situation was reversed. In view of this circumstance, Pritchard and Sumner[9] tried to hit the experimental values calculating the bond orders of naphthalene and anthracene by various approximations. This was, however, a rather hard task. Among various approximations (six approximations), only one (their approximation 5) gave results for both molecules free from significant error. In this approximation, Pople's self-consistent MO method was used with variation of α, the diagonal element of core Hamiltonian in terms of μth AO; the correction used was $\Delta\alpha=\beta$ in the sense that atoms labelled 3 in Fig. 1 are more electronegative than other atoms in the system.

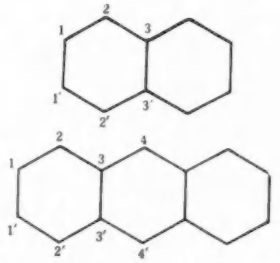

Fig. 1. Numbering of atoms in naphthalene and anthracene.

Now, as indicated in Table IV, the bond lengths calculated by the self-consistent field MO method using our parameters, are in good correspondence with experiment, where the results of Pritchard and Sumner by approximation 5 (abbreviated as P.S.) are also indicated for the purpose of comparison. In this table, the calculated

TABLE IV

CALCULATED AND EXPERIMENTAL BOND LENGTHS OF NAPHTHALENE AND ANTHRACENE (IN A)

Naphthalene

bond	Calcd. (i)*	(ii)*	P.S.	Expt.
1—2	1.374	1.369	1.369	1.365±0.006
2—3	1.414	1.417	1.420	1.425±0.005
3—3'	1.412	1.406	1.409	1.393±0.010
1—1'	1.405	1.412	1.413	1.404±0.009

Anthracene

bond	Calcd. (i)*	P.S.	Expt.
1—2	1.370	1.365	1.371±0.006
2—3	1.423	1.430	1.424±0.005
3—4	1.396	1.403	1.396±0.004
3—3'	1.436	1.432	1.436±0.007
1—1'	1.408	1.422	1.408±0.010

* The meaning of i and ii is the same as those in Tables I and II.

9) H. O. Pritchard and F. H. Sumner, *Trans. Faraday Soc.*, **51**, 457 (1955).

bond lengths were obtained from the bond orders using the equation

$$R_{\mu\nu}=S-\frac{S-D}{1+\kappa\left(\frac{1-P_{\mu\nu}}{P_{\mu\nu}}\right)}$$

where S is taken to be 1.54 Å, D=1.33 Å and κ=0.765.

None of the calculated values using our parameters differs from the experimental mean by more than two and a quater times the "estimated standard deviation," and may be regarded as correct.

III. Ionization Potentials and Electron Affinities.—The ionization potentials and electron affinities are important quantities for studying the molecular sturctures. We have examined whether our calculation can predict correctly the ionization potentials and electron affinities of naphthalene and anthracene. The calculated values have been standardized to the observed values of benzene, i.e., after adding $\Delta I=I^{\text{obs.}}_{\text{benz.}}-I^{\text{calc.}}_{\text{benz.}}$ or $\Delta A=A^{\text{obs.}}_{\text{benz.}}-A^{\text{calc.}}_{\text{benz.}}$ to the calculated ionization potentials or electron affinities, respectively; the theoretical values have been compared with experiment. As shown in Table V, the calculated values agree satisfactorily with observed values.

TABLE V
CALCULATED AND OBSERVED IONIZATION POTENTIALS OF NAPHTHALENE AND ANTHRACENE (IN e.V.)

Molecule	Ionization Potential Calcd. (i)*	(ii)*	(iii)*	Obsd.
Benzene	(9.24)			9.24
Naphthalene	8.116	8.125	8.068	8.12 (a)
Anthracene	7.414	—	7.400	—
Molecule	**Electron Affinity Calcd. (i)***	**(ii)***	**(iii)***	**Obsd.**
Benzene	(−0.54)			−0.54 (b)
Naphthalene	0.595	0.585	0.643	0.65 (b)
Anthracene	1.297	—	1.310	1.19 (b)

* The meaning of i, ii and iii is the same as in other tables.

(a) K. Watanabe and J. R. Mottl, *J. Chem. Phys.*, **26**, 1773 (1957).

(b) Blackedge and Hush, quoted in, N. S. Hush and J. A. Pople, *Trans. Faraday Soc.*, **51**, 600 (1955).

Discussion

As has been described so far, the electronic spectra, bond lengths, ionization potentials and electron affinities calculated with our parameters are in an excellent agreement with experimental values, and the main difference of our calculation from that of other authors' is in the choice of $\gamma_{\mu\nu}$ values. Our values are somewhat smaller than those used by Pariser and Parr and by Pople. The procedure employed by Pariser and Parr for evaluating $\gamma_{\mu\mu}$ is analogous to the Moffitt's method of "atoms in molecules"[10] which takes into account accurately the energy difference between the separated pairs of ions and neutral atoms. In other words, it may also be regarded as an appropriate consideration of the effect of electronic correlation for the one-center interaction integral $\gamma_{\mu\mu}$, by the use of the experimental values of atomic valence state ionization potential and electron affinity[11]. In Moffitt's method, $\gamma_{\mu\nu}$'s where $\mu\neq\nu$, are calculated theoretically using, for example, Slater type AO's. In the procedure used by Pariser and Parr, $\gamma_{\mu\nu}$'s for neighbors more distant than the nearest are calculated in terms of Slater type AO's or by uniform charge sphere approximation. $\gamma_{\mu\nu}$'s for nearest neighbors are evaluated by interpolation formula of the type: ar^2+br+c, where r is the interatomic distance and $c=\gamma_{\mu\mu}$. When atoms are combined to form a molecule, however, the effective charges for σ-electrons may be rather increased compared with the case of isolated atoms and the electron clouds associated with σ-bonds may somewhat contract.

In contrast to this, the effective changes for π-electrons may by decreased. Owing to this circumstance, one should use a little smaller values of $\gamma_{\mu\nu}$'s than those used by Pariser and Parr and by Pople, which may be a cause of the excellent agreement of our calculated results with experiment. In addition, our procedure for evaluating $\gamma_{\mu\nu}$'s is very simple and straightforward. One can easily obtain them if one can only know the values of valence state ionization potentials and electron affinities of the atoms involved. Another reason for the use of our $\gamma_{\mu\nu}$ values may be as follows, although it might be essentially the same as described above. When applied to some simple molecules such as hydrogen[12,13] and lithium molecules[14], the method of Moffitt gives

10) W. Moffitt, *Proc. Roy. Soc.*, **A210**, 245 (1951); *Report Progr. Phsics*, **17**, 173 (1954).
11) W. Kotos, *Acta Phys. Polon.*, **16**, 299 (1957).
12) C. W. Scherr, *J. Chem. Phys.*, **22**, 149 (1954).
13) A. C. Hurley, *Proc. Phys. Soc.*, **A68**, 149 (1955).
14) A. Rahman, *Physica*, **20**, 623 (1954).

rather unsatisfactory results. For example, it leads to the conclusion that the ground state of the hydrogen molecule is almost completely ionic[13]. A similar conclusion is also reached in the case of the diamond[15]. In the latter case, however, if one calculate non-empirically the energies and wave functions employing Slater AO's, one can obtain the result that the ground state is homopolar even if the agreement between the calculated and the observed cohesive energy is very unsatisfactory.

Then, one may be able to improve the results in the following way. For example, if $\gamma_{\mu\mu}$ calculated with Slater AO's is κ times the $\gamma_{\mu\mu}$ evaluated by Moffitt's method, one divides by κ all $\gamma_{\mu\nu}$'s calculated with Slater AO's and one uses $\gamma_{\mu\nu}=(1/\kappa)\gamma_{\mu\nu}$ (Slater) in the calculation of molecular energy and wave function. Actually, in the case of the diamond, a satisfactory improvement has been brought about in this way[15]. Although the real theoretical ground for doing it in this way is not very clear, the physically unsatisfactory results at which Moffitt's method arrives originate from the inconsistent use of, for example, $\gamma_{\mu\mu}$ values which are obtained empirically on the one hand and $\gamma_{\mu\nu}$ $(\mu\neq\nu)$ values which are calculated with ordinary orbital functions on the other hand. Thus, even if the interatomic part of energy is very small compared with its intra-atomic part, the former still affects the calculated results to such an extent as described above.

When studing the π-electronic structures, such a circumstance may not be very serious as in the case of σ-electronic structures. Nevertheless, our calculation in the present paper seems to indicate that such a circumstance still exists in the case of π-electronic structures. Actually, the ratio $\gamma_{\mu\nu}$ (Slater)$/\gamma_{\mu\nu}$, where $\gamma_{\mu\nu}$ is the value we have used, is approximately constant and close to κ when μ-th and ν-th atoms are one or two bond distances apart from each other and approaches gradually to unity as they become more distant.

Summary

Electronic structures of naphthalene and anthracene have been studied by the self-consistent field MO method employing our semiempirical parameters. The calculated electronic spectra, bond lengths, ionization potentials and electron affinities are in a good agreement with expriment. Some discussions have been given in connection with the method of "atoms in molecules" and others.

We are grateful to Professor R. Fujishiro for his encouragement. One of the authors (N.M.) expresses with pleasure his cordial thanks to Mr. T. Yamaguchi of Osaka University for his helpful discussions.

Institute of Polytechnics
Osaka City University
Kita-ku, Osaka

15) T. Yamaguchi, Private communication.

The Aconite Alkaloids. XXVII. On Lucaconine*

By Sijô FURUSAWA**

(Received September 4, 1958)

In the previous paper[1] the extended formulae of lucaconine (I), $C_{24}H_{39}O_7N$, and monoacetyllucaconine (II), $C_{26}H_{41}O_8N$, were given as follows:

$C_{19}H_{21}\begin{cases}(OCH_3)_3\\(OH)_4\\N\text{-}C_2H_5\end{cases}$ Lucaconine (I)

$C_{19}H_{21}\begin{cases}(OCH_3)_3\\OCOCH_3\\(OH)_3\\N\text{-}C_2H_5\end{cases}$ Monoacetyllucaconine (II)

The present paper describes further experiments, undertaken with the object of characterizing the hydroxyl groups of lucaconine. Acetylation of lucaconine (I)

* This constitutes a part of a series entitled "The Aconite Alkaloids" by H. Suginome. Part XXVI, cf. foot note 1).

** Present address, Faculty of Technology, Chûô University, Tokyo, Japan.

1) H. Suginome and S. Furusawa, This Bulletin, **32**, 354.

with acetic anhydride gave diacetyllucaconine(III), $C_{28}H_{43}O_9N$[1], while, on treatment with acetyl chloride, lucaconine (I) yielded anhydrodiacetyllucaconine(IV), $C_{28}H_{41}O_8N$, m. p. 156°, $[\alpha]_D^{27}+20.0°$. This anhydrodiacetyl-compound IV was obtained also from monoacetyllucaconine (II) and diacetyllucaconine (III) by the similar treatment. Anhydrodiacetyllucaconine (IV) decolorized bromine in acetic acid and absorbed one mole of hydrogen over platinum catalyst, showing the presence of a double bond. A small quantity of isodiacetyllucaconine, $C_{28}H_{43}O_9N$, m. p. 188° (decomp.), $[\alpha]_D$ 0°, was isolated as a by-product when lucaconine (I) was treated with a large quantity of acetyl chloride.

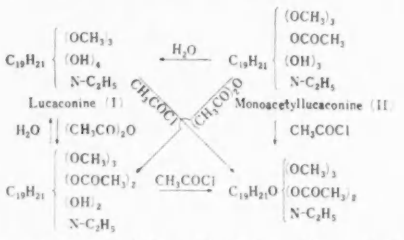

Oxidation of diacetyllucaconine (III) with potassium permanganate in acetone, followed by hydrolysis, gave two neutral products, oxolucaconine (V), $C_{24}H_{37}O_8N\cdot 1\,^3/_4\ H_2O$, m. p. 132°, $[\alpha]_D^{16.2}+24.2°$, as a main product and isooxolucaconine (VI), $C_{24}H_{37}O_8N$, m. p. 242°, $[\alpha]_D^{22.6}+44.8°$, as a by-product. The latter compound VI was also obtained by heating V at about 150° for 10 minutes under reduced pressure (1×10^{-5} mmHg) and VI was partly converted reversely into V on action of methanolic hydrogen chloride or alcoholic sodium hydroxide in a sealed tube. Treatment of oxolucaconine V with acetyl chloride, followed by hydrolysis, gave anhydrooxolucaconine (VII), m. p. 256°, $[\alpha]_D^{27}-25.0°$. This compound VII was also obtained directly from anhydrodiacetyllucaconine(IV)by oxidation with potassium permanganate, followed by hydrolysis.

Acetylation of isooxolucaconine(VI) and of anhydrooxolucaconine (VII) by acetic anhydride gave no crystalline product, but the determination of acetyl groups of these amorphous products showed the production of diacetyl-compounds by these reactions.

On treatment with chromic acid in glacial acetic acid lucaconine (I) was converted into lucaconinone-I (VIII), $C_{24}H_{37}O_7N$, m. p. 210°, $[\alpha]_D^{27}+15.0°$, which showed bands in the infrared spectrum at 2.99 and 5.72 μ, corresponding to hydroxyl and five-membered ring ketone group[2], and formed a monoxime melting at 223~224° (decomp.). Oxolucaconine(V)was converted by the same procedure into a diketo-compound, oxolucaconinedione(IX), $C_{24}H_{33}O_8N$, m. p. 209°, $[\alpha]_D^{26.7}+139°$, which showed bands in the infrared spectrum at 2.90, 5.72, 5.83 and 6.08 μ, characteristic of hydroxyl, five-membered ring ketone, six-membered ring ketone and lactam carbonyl group, respectively[2], and further furnished

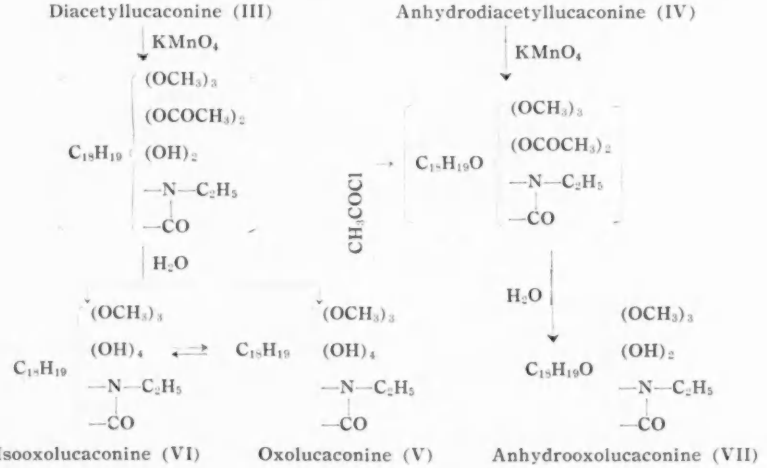

2) H. Suginome, T. Amiya and T. Shima, unpublished work.

a monoxime melting at 246~248° (decomp.). In this case, a by-product, isooxolucaconinedione (X), $C_{24}H_{33}O_8N \cdot H_2O$, m. p. 136° (decomp.), $[\alpha]_D^{26}$ +33.7°, which formed the same monoxime (m. p. 246~248°) as described above, was obtained***. Isooxolucaconine(VI) gave only isooxolucaconinedione(X) by similar procedure. Anhydrooxolucaconine(VII) was similarly oxidized into a diketo-compound, anhydrooxolucaconinedione (XI), $C_{24}H_{31}O_7N$, m. p. 272°, $[\alpha]_D^{26.5}$ −84.2°, which showed bands in the infrared spectrum at 5.72 and 5.83 μ[2], and gave a monoxime melting at 268° under decomposition.

Upon treatment with acetyl chloride, both oxolucaconinedione (IX) and isooxolucaconinedione (X) gave the same monoacetyloxolucaconinedione (XII), $C_{26}H_{35}O_9N$, m. p. 269° (decomp.), $[\alpha]_D^{26.7}$ +113°. On hydrolysis with methanolic sodium hydroxide, this compound XII afforded nearly an equal amounts of IX and X.

Selenium was liberated on heating lucaconinone-I (VIII) and oxolucaconinedione(IX) with selenium dioxide in glacial acetic acid. On the contrary, lucaconine(I) and oxolucaconine(V) did not give selenium under similar conditions. That may probably be due to the presence of a methylene group adjacent to a keto group in VIII and IX.

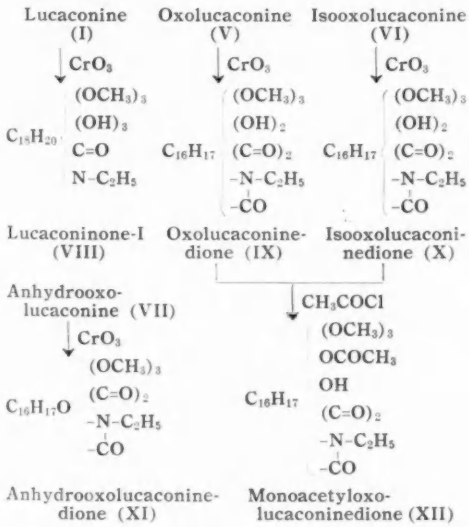

On the basis of these facts, it may be reasonably concluded that, of four hydroxyl groups of lucaconine, two can be acetylated or oxidized to oxo groups, one being attached to a five-membered ring and the other to a six-membered ring, but the remaining two hydroxyl groups can be neither acetylated nor oxidized under usual conditions. Furthermore, it is to be noted that the latter two hydroxyl groups split off one mole of water on treatment with acetyl chloride. These observations will be discussed in a later paper.

In conclusion mention will be made of the action of nitric acid on lucaconine. Upon treatment with concentrated nitric acid, lucaconine(I) was converted into nitro-nitrosolucaconinic acid (XIII), $C_{16}H_{19}O_9N_3$, m. p. 214° (decomp.), $[\alpha]_D^{27}$ −117°. This compound contained two methoxyl groups but no *N*-ethyl group and was soluble in alkali with a pale yellowish green color.

Experimental

Anhydrodiacetyllucaconine (IV).—*a) From Lucaconine.*—A mixture of 2.0 g. of lucaconine and 10 cc. of acetyl chloride was allowed to stand in a sealed tube for ten days. After removal of the excess of acetyl chloride, the residue was treated with ice-water and made alkaline with aqueous ammonia to give a white precipitate. This material was recrystallized from ethanol to obtain anhydrodiacetyllucaconine in colorless plates, m. p. 156°, $[\alpha]_D^{27}$ +20.0° (94% ethanol). Yield 1.5 g.

Anal. Found: C, 64.63; H, 7.83; N, 2.90; OCH_3, 19.73; $COCH_3$, 18.14. Calcd. for $C_{28}H_{41}O_8N$: C, 64.72; H, 7.95; N, 2.70; OCH_3, 17.90; 2-$COCH_3$, 16.56%. 6.459 mg. of the substance absorbed 2.84 cc. of hydrogen (1.04 mol.).

When a mixture of 1.0 g. of lucaconine and 10 cc. of acetyl chloride was refluxed for 40 min., and treated in the usual manner, it yielded 0.4 g. of anhydrodiacetyllucaconine and a small quantity (ca. 0.01 g.) of a crystalline substance, isodiacetyllucaconine, m. p. 188° (decomp.), $[\alpha]_D$ 0°.

Anal. Found: C, 62.69; H, 8.37; N, 2.80; OCH_3, 16.84; $COCH_3$, 16.81. Calcd. for $C_{28}H_{43}O_9N$: C, 62.55; H, 8.05; N, 2.61; 3-OCH_3, 17.31; 2-$COCH_3$, 16.02%.

b) From Monoacetyllucaconine (II).—A mixture of 0.5 g. of monoacetyllucaconine and 4.5 cc. of acetyl chloride was refluxed for 40 min. The reaction mixture was treated in the usual manner to give 0.38 g. of anhydrodiacetyllucaconine.

c) From Diacetyllucaconine (III).—A mixture of 0.25 g. of diacetyllucaconine and 5 cc. of acetyl chloride was allowed to stand at room temperature for a week. After treatment as described above, 0.2 g. of anhydrodiacetyllucaconine was obtained.

Oxolucaconine (V).—To a solution of 3.2 g. of diacetyllucaconine in 100 cc. of acetone, 3.5 g. of powdered potassium permanganat was gradually added under stirring and chilling. Manganese

*** There is a possibility that isooxolucaconinedione (X) is a hydrate of oxolucaconinedione(IX), but it is preferable to call it an "iso-" compound because of difference in optical activities.

dioxide was filtered off and the filtrate was evaporated to dryness. The residue was treated with boiling ethanolic potassium hydroxide for 30 min. After cooling, the solution was made slightly acidic with hydrochloric acid and was evaporated up. The residue was then extracted with absolute ethanol and the ethanolic extract was evaporated to give ca. 1.8 g. of colorless crystals which were recrystallized from ethanol. Oxolucaconine was obtained in colorless crystals, m. p. 132°, $[\alpha]_D^{16.2}$+24.2° (94% ethanol). This material was insoluble in water, diluted hydrochloric acid and diluted aqueous ammonia, and it seemed to be neutral.

Anal. Found: C, 57.54; H, 7.96; N, 2.72; H_2O, 6.06; (N)-C_2H_5, 4.32. Calcd. for $C_{24}H_{37}O_9N$. $1^3/_4$ H_2O: C, 57.75; H, 8.18; N, 2.81; H_2O, 6.32; (N)-C_2H_5, 5.82%.

From the mother liquor of the above recrystallization, a small quantity of a crystalline substance, m. p. 242°, identical with isooxolucaconine mentioned next, was obtained.

Isooxolucaconine (VI).—When 0.2 g. of oxolucaconine was heated at 150° for 5 min. under reduced pressure (1×10^{-5} mmHg), it decomposed under foaming, became glassy and crystallized on cooling. On recrystallization from ethanol, isooxolucaconine was obtained in colorless needles, melting at 242°, $[\alpha]_D^{22.6}$+44.8° (94% ethanol).

Anal. Found: C, 61.17; H, 8.16; OCH_3, 20.73. Calcd. for $C_{24}H_{37}O_9N$: C, 61.65; H, 7.98; 3-OCH_3, 19.93%.

Upon heating with methyl iodide in a sealed tube, isooxolucaconine could not be methylated but yielded oxolucaconine. The same substance was also produced when isooxolucaconine was heated in a sealed tube with ethanolic potassium hydroxide or with methanolic hydrogen chloride.

Acetylation of Isooxolucaconine (VI).—A solution of isooxolucaconine in a mixture of pyridine and acetic anhydride (1:1) was allowed to stand at room temperature overnight. After removal of the solvents, an amorphous product was treated with aqueous ammonia and extracted with ether. An amorphous residue, obtained on evaporating the ethereal extracts, was purified by repeated precipitation from dilute ethanol.

Anal. Found: $COCH_3$, 16.85. Calcd. for $C_{24}H_{35}O_9N(COCH_3)_2$: 2-$COCH_3$, 15.60%.

Anhydrooxolucaconine (VII).—*a*) *From Anhydrodiacetyllucaconine (IV).*—To a solution of 0.6 g. of anhydrodiacetyllucaconine in 20 cc. of acetone, 0.4 g. of powdered potassium permanganate was added. After being kept for 24 hr. manganese dioxide was filtered off and the filtrate was evaporated to give 0.5 g. of an amorphous residue. This product was treated with ethanolic potassium hydroxide and then crystallized from ethanol. On repeated recrystallization from ethanol, anhydrooxolucaconine, m. p. 256°, $[\alpha]_D^{27}$−25.0° (94% ethanol) was obtained. It was soluble in methanol and slightly so in acetone, ether and water.

Anal. Found: C, 64.32; H, 7.91; N, 3.27; OCH_3, 20.69; (N)-C_2H_5, 4.72. Calcd. for $C_{24}H_{35}O_7N$: C, 64.17; H, 7.85; N, 3.12; 3-OCH_3, 20.72; (N)-C_2H_5, 6.46%.

b) *From Oxolucaconine (V).*—A mixture of 2.0 g. of oxolucaconine and 20 cc. of acetyl chloride was refluxed for 30 min. After removal of the excess of acetyl chloride, the residue was treated with alkali to give 1.0 g. of a crystalline substance. On recrystallization from ethanol, anhydrooxolucaconine, m. p. 257°, was obtained.

Acetylation of Anhydrooxolucaconine (VII).—A mixture of 0.05 g. of anhydrooxolucaconine, 0.5 cc. of pyridine and 0.2 cc. of acetyl chloride was allowed to stand at room temperature overnight. After removal of the solvent, the residue was treated with aqueous ammonia to give a white precipitate. This precipitate was dissolved in ethanol and was reprecipitated by addition of water. After repetition of this treatment, the precipitate was dried and analyzed.

Anal. Found: $COCH_3$, 17.64. Calcd. for $C_{24}H_{33}O_7N(COCH_3)_2$: 2-$COCH_3$, 16.15%.

Lucaconinone-I (VIII).—To a solution of 2.0 g. of lucaconine in 25 cc. of glacial acetic acid, a solution of 0.7 g. (2 mol.) of chromic trioxide in 15 cc. of acetic acid was dropped in under stirring and coolling. After standing overnight and after the removal of the solvent, a glassy substance was obtained. This material was dissolved in water; the solution was made alkaline and was extracted with chloroform. On evaporation of the chloroform solution, 0.64 g. of a crystalline residue was yielded, which was recrystallized from 99% ethanol to give crystals melting at 200~201°. Yield 0.4 g. This substance was converted into perchlorate, melting at 236° after being recrystallized from ethanol. It was transformed into the free base by the usual method. The base, lucaconinone-I, thus obtained melted at 210°, $[\alpha]_D^{27}$+15.0° (94% ethanol).

Anal. Found: C, 63.82; H, 8.31; N, 3.18. Calcd. for $C_{24}H_{37}O_7N$: C, 63.83; H, 8.26; N, 3.11%.

Perchlorate.—m. p. 236° (decomp.) (from ethanol).

Anal. Found: Cl, 6.92. Calcd. for $C_{24}H_{37}O_7N\cdot HClO_4$: Cl, 6.79%.

Oxime.—m. p. 223~224° (decomp.) (from ethanol).

Anal. Found: N, 6.12. Calcd. for $C_{24}H_{38}O_7N_2$: N, 6.01%.

Oxolucaconinedione (IX).—To a solution of 0.8 g. of oxolucaconine in 10 cc. of glacial acetic acid, a solution of 0.28 g. (2.2 mol.) of chromic anhydride in 10 cc. of the same solvent was added slowly under stirring and cooling. After the mixture was set aside overnight, it was treated in the usual manner to give 0.3 g. of a crystalline product which was recrystallized from ethanol. Oxolucaconinedione was obtained as colorless needles melting at 209°, $[\alpha]_D^{26.7}$+139° (94% ethanol).

Anal. Found: C, 62.10; H, 7.40; N, 3.11. Calcd. for $C_{24}H_{33}O_9N$: C, 62.13; H, 7.18; N, 3.02%.

Oxime.—m. p. 246~248° (decomp.) (from ethanol).

Anal. Found: N, 5.91. Calcd. for $C_{24}H_{34}O_8N_2$: N, 5.86%.

The mother liquor from which the above mentioned crystals were separated was extracted with chloroform and the chloroform extracts were evaporated to dryness. The residue was crystallized from ethanol to give 0.1 g. of a colorless crystalline substance, m. p. 136~137° (decomp.), which was identified with isooxolucaconinedione mentioned below.

Isooxolucaconinedione (X).—Isooxolucaconine was oxidized with chromic anhydride in glacial acetic acid by the method described above to give isooxolucaconinedione, colorless crystals melting at 136~137° (decomp.), $[\alpha]_D^{26}$+33.7° (94% ethanol).

Anal. Found: C, 59.77; H, 7.43; N, 3.17; H_2O, 3.62. Calcd. for $C_{24}H_{33}O_8N \cdot H_2O$: C, 59.82; H, 7.34; N, 2.91; H_2O, 3.75%.

The oxime prepared from isooxolucaconinedione melted at 246~248° (decomp.) and showed no depression of the melting point on admixture with the above-mentioned oxolucaconinedione oxime.

When isooxolucaconinedione was heated in an oil bath at 160~170° for 10 min. under reduced pressure (1×10^{-5} mmHg), it melted under foaming and crystallized on cooling. Recrystallization from ethanol gave a crystalline substance, m. p. 136° (decomp.), which showed no depression of the melting point on admixture with the starting material.

Anhydrooxolucaconinedione (XI). — With 0.08 g. of chromic anhydride in acetic acid, 0.25 g. of anhydrooxolucaconine was oxidized as described above to give 0.2 g. of anhydrooxolucaconinedione, which was recrystallized from ethanol, m. p. 272°, $[\alpha]_D^{26.5}$−84.2°. It was sluble in methanol, ethanol and acetone and sparingly soluble in ether and benzene.

Anal. Found: C, 64.30; H, 7.50; N, 3.27. Calcd. for $C_{24}H_{31}O_7N$: C, 64.70; H, 7.01; N, 3.14%.

Oxime.—m. p. 268° (decomp.).

Anal. Found: N, 6.52. Calcd. for $C_{24}H_{32}O_7N_2$: N, 6.08%.

Monoacetyloxolucaconinedione (XII).—A mixture of 0.26 g. of oxolucaconinedione and 3 cc. of acetyl chloride was heated under reflux for 30 min. After removal of the solvent, the residue was treated with aqueous ammonia to give white precipitate which was crystallized from ethanol. Monoacetyloxolucaconinedione melted at 269° (decomp.), $[\alpha]_D^{26.7}$+113° (ethanol). It was soluble in methanol and ethanol and sparingly soluble in acetone, benzene and water.

Anal. Found: C, 62.62; H, 7.56; $COCH_3$, 8.79. Calcd. for $C_{24}H_{32}O_8N(COCH_3)$: C, 61.80; H, 6.98; $COCH_3$, 8.51%.

This substance was also obtained from isooxolucaconinedione by the same procedure as described above.

Hydrolysis of Monoacetyloxolucaconinedione (XII).—A solution of 0.1 g. of monoacetyloxolucaconinedione in 2 cc. of N-methanolic sodium hydroxide was heated for 20 min. After removal of the solvent, the residue was treated with water and the precipitate was fractionally recrystallized from ethanol. Isooxolucaconinedione melting at 132° (decomp.) and oxolucaconinedione melting at 207° were yielded in nearly equal amounts.

Nitronitrosolucaconinic Acid (XIII).—A mixture of 3.0 g. of lucaconine and 20 cc. of nitric acid (*d*: 1.43) was heated on a water bath at 80° for 1 hr. with stirring. After cooling, 30 cc. of water was added and yellow precipitate was collected, which was repeatedly precipitated from diluted ethanol and finally crystallized from diluted acetone. Nitronitrosolucaconinic acid was obtained in pale yellow plates, melting at 214°, $[\alpha]_D^{27}$−117°. It was easily soluble in acetone and sparingly so in water, methanol, ethanol, ether and chloroform.

Anal. Found: C, 48.60; H, 4.81; N, 10.83; OCH_3, 15.32; COO-, 24.64; (N)-C_2H_5, neg. Calcd. for $C_{12}H_{13}O_3N_3(OCH_3)$-$(COO)_2$: C, 48.47; H, 4.78; N, 10.57; 2-OCH_3, 15.62; 2-COO-, 22.66%.

The author wishes to express his sincere thanks to Professor Harusada Suginome, President of Hokkaido University, for his kind guidance throughout this work.

Department of Chemistry
Faculty of Science
Hokkaido University
Sapporo

The Study of Adsorption of Detergents at a Solution-Air Interface by Radiotracer Method. II. The Kinetics of Adsorption of Sodium Alkyl Sulfates

By Ryohei MATUURA, Hideo KIMIZUKA, Shigeru MIYAMOTO, Ryosuke SHIMOZAWA and Katsumasa YATSUNAMI

(Received September 24, 1958)

It is usual in the case of the solution of detergents that a considerable time is required to attain true equilibrium of adsorption at the solution-air interface. The process has been studied chiefly from the measurement of the change in surface tension with time. The suggestion that the diffusion of solute to the surface is a cause of the alteration of surface tension with time was first made by Milner[1], and equations to describe the phenomena in terms of diffusion have been deduced by Bond and Puls[2], Ross[3], Ward and Tordai[4], Bartholomé and Schäfer[5], Lange[6] and Fordham[7]. However, it has been proved that there are many cases in which the process can not be explained in terms of simple diffusion alone, and the factors governing the adsorption rate other than diffusion have been proposed. For example, the concept of energy barrier has been introduced by Doss[8], Blair[9] and Addison[10].

In the preceding paper[11] the Gibbs adsorption equation has been checked in the case of sodium dodecyl sulfate, tetradecyl sulfate and hexadecyl sulfate at the solution-air interface. It is perfectly clear that the Gibbs equation refers only to the adsorption equilibrium. It has nothing to do with the process of reaching the equilibrium, and so to calculate the surface excess at the stage of non-equilibrium from surface tension by using the Gibbs equation is incorrect. In order to study the kinetics of adsorption, therefore, it is preferable to measure the change in the adsorbed amount with time directly. By using radioisotopes this can easily be done. The method is simple and accurate, and is most suitable since the adsorption can be measured at a liquid surface without any mechanical disturbances. It is the purpose of the present experiment to measure the rate of adsorption of sodium alkyl sulfates at the solution-air interface by radiotracer method and to make discussions as to the theories of the adsorption rate presented by earlier authors.

Experimental

Surface active substances used in the present experiment were the same as those in the preceding paper[11], i.e., sodium dodecyl sulfate (SDS), sodium tetradecyl sulfate (STS), and sodium hexadecyl sulfate (SHS). Labelling these compounds with S-35 was described earlier[11].

The counting apparatus was also the same as that used in the preceding paper[11]. After the formation of a fresh plane surface of a detergent

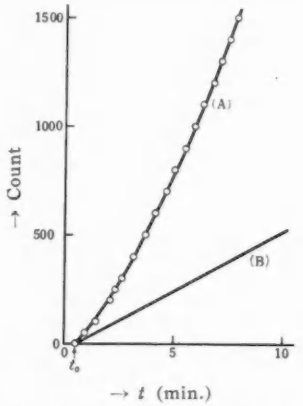

Fig. 1. Count vs. time curves for the solution of SHS (A) and sulfuric acid (B). Concentration, 4.24×10^{-6} mole/l.

1) S. R. Milner, *Phil. Mag.*, (6), **13**, 96 (1907).
2) W. N. Bond and H. O. Puls, ibid., (7), **24**, 864 (1937).
3) S. Ross, *J. Am. Chem. Soc.*, **67**, 990 (1945); *J. Phys. Chem.*, **49**, 377 (1945).
4) A. F. H. Ward and L. Tordai, ibid., **14**, 453 (1946).
5) E. Bartholomé and K. Schäfer, *Melliand Textilber.*, **31**, 487 (1950).
6) H. Lange, *Kolloid-Z.*, **121**, 130 (1951); **136**, 136 (1954).
7) S. Fordham, *Trans. Faraday Soc.*, **50**, 593 (1954).
8) K. S. G. Doss, *Kolloid-Z.*, **86**, 205 (1939); **87**, 272 (1939).
9) C. M. Blair, Jr., *J. Chem. Phys.*, **16**, 113 (1948).
10) C. C. Addison and S. K. Hutchinson, *J. Chem. Soc.*, **1949**, 3387.
11) R. Matuura, H. Kimizuka, S. Miyamoto and R. Shimozawa, This Bulletin, **31**, 532 (1958).

solution, the measuring arrangement was quickly set in and the count from the solution was measured with time. An example is shown in Fig. 1 (curve A). The curve B in the same figure shows a change in the counting with time of a sulfuric acid solution with the same concentration and specific activity as the detergent solution. The two series of measurements should be done under exactly the same conditions. t_0 in Fig. 1 is the starting time of counting. The tangent of the curve at any time t is clearly the intensity of radiation from the bulk of the solution, I_i, plus that from the adsorbed layer at that time, $I_{s(t)}$. The intensity of radiation from sulfuric acid solution does not show any change with time and it can be regarded as equal to I_i since no surface adsorption will take place with sulfuric acid solution of so low a concentration as in the present experiment. Then,

$$I_{s(t)} = (I_i + I_{s(t)}) - I_i \quad (1)$$

i.e., the counting rate at time t of the surface layer can be obtained from the difference between the counting rate of the detergent solution at that time and that of sulfuric acid solution. The surface excess at time t, Γ_t, is calculated from $I_{s(t)}$ by using the following relation;

$$\Gamma_t = I_{s(t)}/SA \quad (2)$$

where S is the specific activity of the radioactive substance and A is the surface area of the solution. S can be determined as in the preceding paper[1].

Results

The change in adsorption with time of SDS, STS and SHS at the solution-air interface is plotted in Figs. 2, 3 and 4, respectively. The abscissa is represented as the square root of time for the convenience of discussions.

Discussions

It is seen from Figs. 2, 3 and 4 that at the initial stage of adsorption the surface excess of the detergents is proportional to the square root of time, i.e., the adsorption at constant temperature can be expressed by the relation,

$$\Gamma_t = Kt^{1/2} \quad (3)$$

were, t is the time of aging and K is a constant independent of time but dependent on the concentration of the detergent solution. When K is plotted against concentration, C, approximately linear relation can be found as shown in Fig. 5, i.e.,

$$K = K_0 C \quad (4)$$

where K_0 is a constant characteristic of each detergent. From Eqs. 3 and 4 the

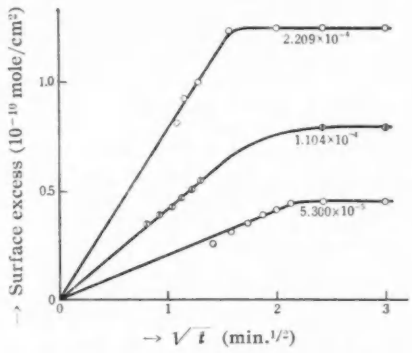

Fig. 2. Surface excess vs. time curves of SDS, at 28±1°C. Numericals of each curve represent the concentration of the detergent solution in mole/l.

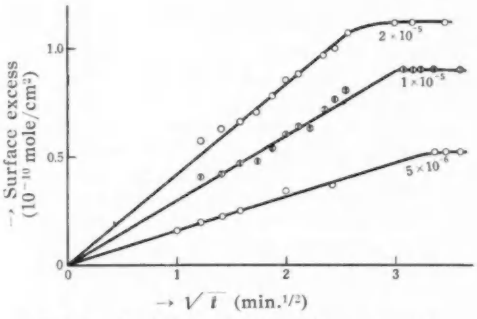

Fig. 3. Surface excess vs. time curves of STS, at 28±1°C. Numericals of each curve represent the concentration of the detergent solution in mole/l.

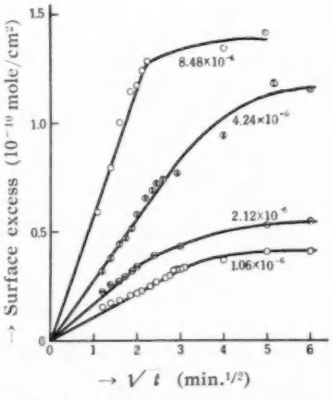

Fig. 4. Surface excess vs. time curves of SHS, at 28±1°C. Numericals of each curve represent the concentration of the detergent solution in mole/l.

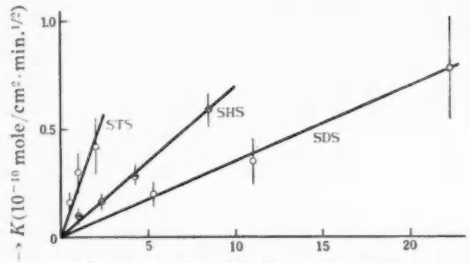

Fig. 5. K vs. concentration of detergents at 28±1°C.

following relation is obtained;

$$\Gamma_t = K_0 C t^{1/2} \tag{5}$$

Now the simple diffusion theory[4] tells us that the surface excess at time t, Γ_t, is given by the relation,

$$\Gamma_t = 2C(Dt/\pi)^{1/2} \tag{6}$$

where D is the diffusion coefficient of the solute molecules. At first sight it is seen that Eq. 6 is similar in form to Eq. 5, and this similarity of the two equations may seem to lead to the conclusion that the rate of adsorption is determined solely by the diffusion of solute molecules from the bulk phase to the surface layer. But further insight makes it clear that discrepancy is involved in the simple diffusion theory. If the simple diffusion theory could be applied to the present case, K_0 in Eq. 5 should be equal to $2(D/\pi)^{1/2}$ in Eq. 6. Then we should be able to calculate the diffusion coefficient from the experimental values of K_0. The calculated values of diffusion coefficient of three alkyl sulfates used are shown in Table I as D_{calc}. In order to check the diffusion theory it is necessary to compare these values of D_{calc} with the observed values of diffusion coefficient. We could not find in any literature the experimental values of diffusion coefficient of sodium alkyl sulfates in aqueous solutions, but we can estimate the values from conductivity data of Lottermoser and Püschel[12] by using the Nernst's equation,

$$D = \Lambda_0 RT/|Z|F^2 \tag{7}$$

where Λ_0 is the conductivity at infinite dilution of surface active ion with the valency Z and F, R and T are Faraday constant, gas constant and absolute temperature, respectively. The estimated values of diffusion coefficient for three alkyl sulfate ions used are shown in Table I as D_{est}. These values are, of course, diffusion coefficients at infinite dilution, but the concentrations so small as in the present experiment would not alter the values appreciably.

TABLE I
COMPARISON OF DIFFUSION COEFFICIENTS

Detergents	SDS	STS	SHS
Temp. (°C)	28±1	28±1	28±1
D_{calc}(cm^2/sec.)	1.60×10^{-9}	7.69×10^{-8}	6.32×10^{-7}
D_{est}(cm^2/sec.)	6.80×10^{-6}	4.54×10^{-6}	4.01×10^{-6}

As seen from Table I the calculated values of the diffusion coefficient are in general much smaller than the estimated ones. Moreover, the most embarrassing point is that the diffusion coefficient calculated by the simple diffusion theory decreases considerably with decrease in the chain length of the detergent molecule. This is quite unreasonable. Therefore, we can conclude that the simple diffusion theory can not explain the rate of adsorption of sodium alkyl sulfates at the solution-air interface under the conditions of the present experiment.

Salley et al.[13] measured the rate of adsorption of Aerosol OTN at the solution-air interface by radiotracer method and obtained the rate equation,

$$\Gamma_t = kt^n \tag{8}$$

where k and n are constants. They found that n is nearly 1/2. They calculated the diffusion coefficient of sulfosuccinate ion from the experimental values of k by making use of the simple diffusion equation. The calculated diffusion coefficient was $0.7\sim2.2\times10^{-4}$ cm^2/min., which was, according to them, comparable to the observed value, $3\sim4\times10^{-4}$ cm^2/min. However, we suppose that the agreement is not so good as to confirm the validity of the simple diffusion theory, and various surface active compounds, especially with varying chain length, should be examined in order to check the diffusion theory.

In the case of the adsorption of surface active electrolytes, such as those used in the present experiment, it is reasonable to take the energy barrier idea into consideration. Let λ be the energy barrier to the adsorption, then the rate equation[9] may be given by

$$\Gamma_t = 2C(Dt/\pi)^{1/2}\exp(-\lambda/RT) \tag{9}$$

12) A. Lottermoser and F. Püschel, *Kolloid-Z.*, **63**, 175 (1933).

13) D. J. Salley, A. J. Weith, Jr., A. A. Argyle and J. K. Dixon, *Proc. Roy. Soc.*, **A203**, 42 (1950).

in which the simple diffusion equation is combined with the idea of energy barrier. Tentatively we applied Eq. 9 to the present case and calculated the energy barrier to the adsorption of three alkyl sulfates used in the present experiment. That is, from Eqs. 5 and 9

$$K_0 = 2(D/\pi)^{1/2} \exp(-\lambda/RT) \qquad (10)$$

Using the value of D, estimated from the conductivity data of Lottermoser and Püschel, and K_0, obtained in the present experiment, the values of energy barrier were calculated*. They are shown in Table II.

TABLE II

ENERGY BARRIER, λ, TO THE ADSORPTION

Detergents	SDS	STS	SHS
Temp. (°C)	28±1	28±1	28±1
Energy barrier, λ, (kcal./mole)	2.5	1.2	0.6

We could not compare the calculated energy barrier with the observed one, and therefore the validity of the energy barrier theory has not been established. This point will be discussed by further study of the adsorption rate, especially in the presence of inorganic electrolytes.

* Strictly speaking, we should calculate λ from the slope of $\ln K_0/2(D/\pi)^{1/2}$ vs. $1/T$ plot.

Summary

The rate of adsorption of sodium dodecyl sulfate, sodium tetradecyl sulfate and sodium hexadecyl sulfate at the solution-air interface has been measured by radiotracer method. It has been found that the surface excess of a detergent is proportional to the concentration of the solution and the square root of time of aging at the initial stage of adsorption. The simple diffusion theory has been checked and it has been found that the results of the present experiment can not be explained by the simple diffusion theory. The idea of energy barrier has tentatively been applied and the values of energy barrier have been calculated.

The authors wish to express their thanks to Professor Tunetaka Sasaki of Tokyo Metropolitan University for his kind advice and encouragement throughout this study. The expenses of this research were defrayed from the Scientific Research Grant of the Ministry of Education, to which the authors' thanks are also due.

Department of Chemistry
Faculty of Science
Kyushu University
Hakozaki, Fukuoka

The Different Distribution of Rubidium and Cesium in Natural Plants

By Noboru YAMAGATA, Toshiko YAMAGATA and Shunji MATSUDA

(Received October 9, 1958)

The uptake of rubidium and cesium by plants in relation to potassium absorption was studied by several investigators. Collander[1] found that the differences between the plant species, the eleven phanerogams studied, were only moderate for potassium, rubidium and cesium contents; all plants absorbed rubidium and cesium with almost the same rapidity as for potassium. The data of Collander and the experiments of other investigators[2-4] suggested the possible use of radioactive rubidium-86 as a tracer for potassium in plant growth experiments, since an isotope of potassium having a suitable half-life was not readily available. On the other hand, cesium-137 is one of the principal long-lived products of nuclear fission and its absorption by cultured plants is a matter of keen interest.

If cesium is hardly differentiated in uptake by plants as in the case of rubidium, and its translocation up to the aerial part is similar to that of rubidium, the distribution of these elements in the leaves of natural plants must be of the same nature. The present paper points

1) R. Collander, *Plant Physiol.*, **16**, 691 (1941).
2) E. Epstein, *Proc. Fourth Ann. Oak Ridge Summer Sym.*, **TID-5115**, 418 (1952).
3) F. J. Richards, *Ann. Bot.*, **8**, 323 (1945).
4) J. C. Martin et al., *Soil Sci. Soc. Amer. Proc.*, **10**, 94 (1946).

TABLE I
RUBIDIUM AND CESIUM CONTENT OF NATURAL PLANT
(Dry basis)

Name	Location	K %	Rb p.p.m.	Cs p.p.m.
Usnea longissima	Ozegahara, forest	0.249	0.8	0.01
〃	〃 , 〃	0.256	0.7	0.004
Thelypteris oligophlebia	Ōmine-mine	2.92	50	0.05
Lepisorus Thumbergianus	Ozegahara, forest	1.07	4	0.1
Dicranopteris glauca	Mt. Ōdaigahara	0.631	20	0.01
Osmunda cinnamomea	Ozegahara, bog	1.61	5	0.1
〃	〃 , forest	1.83	6	0.3
Equisetum arvense	Ōmine-mine	5.02	30	0.01
〃	〃	2.27	20	0.05
Abies Mariesii	Mt. Zaō	0.287	3	0.05
Tsuga Sieboldii	Ozegahara, forest	0.601	2	0.03
Pinus densiflora	Tsubaki, sea-shore	0.378	2	0.01
P. pumira	Mt. Zaō	0.346	3	0.05
P. parvifolia	Mt. Shibutsu	0.347	1	0.01
Myrica gale var. tomentosa	Ozegahara, bog	0.354	2	0.08
Ostrya Japonica	Mt. Zaō	0.802	10	0.02
Fagus japonica	〃	0.514	10	0.05
Quercus crispula	Mt. Ōdaigahara	0.816	5	0.02
〃	Ozegahara, forest	0.707	2	0.4
〃	Mt. Shibutsu	0.531	2	0.01
Reynoutria japonica	Mt. Shibutsu	0.837	3	0.6
Dianthus superbus var.	Mt. Shibutsu	0.964	4	0.3
Nuphar pumilum var. ozeense	Ozegahara, bog	0.887	10	0.05
Nymphaea tetragona	〃 , 〃	0.743	10	0.05
Ranunculus nipponicus var.	〃 , 〃	1.91	5	0.3
Magnolia obovata	Mt. Zaō	0.866	10	0.02
〃	Ōmine-mine	2.01	20	0.004
Hydrangea hirta	〃	1.22	10	0.3
Saxifraga Fortunei	Mt. Shibutsu	0.801	1	0.01
Sorbus commixta	〃	0.987	4	0.002
Sanguisorba sitchensis	〃	1.15	4	0.03
Sieversia pentapetala	〃	0.310	2	0.05
Skimmia japonica	Mt. Ōdaigahara	0.726	6	0.2
Empetrum nigrum var. japonicum	Mt. Shibutsu	0.233	1	0.05
Acer Tschonoskii	Mt. Zaō	0.677	6	0.05
A. Mono	Ozegahara, forest	1.39	4	0.05
Aesculus turbinata	〃 , 〃	1.20	3	0.02
Tilia japonica	〃 , 〃	1.71	5	0.03
Kalopanax pictus	〃 , 〃	1.90	6	0.07
Phyllodoce aleutica	Mt. Zaō	0.338	3	0.02
Rhododendron sp.	〃	0.677	6	0.05
R. Tchonoskii	Mt. Shibutsu	0.324	0.8	0.05
R. Fauriae	〃	0.300	1	0.05
Andromeda Polifolia var. grandiflora	Ozegahara, bog	0.456	1	0.05
Arcterica nana	Mt. Shibutsu	0.173	0.6	0.1
Menyanthes trifoliata	Ozegahara, bog	1.81	6	0.4
Adenophora nikoensis	Mt. Shibutsu	2.64	8	1
〃	〃	2.10	3	0.1
Cirsium spicatum	Mt. Zaō	1.25	30	0.3
〃	Ōmine-mine	1.90	20	0.04
Sasa paniculata	Mt. Ōdaigahara	0.490	4	0.01
S. oseana	Ozegahara, bog	1.34	8	0.1

Name	Location	K %	Rb p.p.m.	Cs p.p.m.
Miscanthus sinensis	Gunma-mine	0.171	1	0.1
〃	Mt. Zaō	0.934	30	0.2
〃	Ozegahara, bog	0.869	20	1
Phragmites communis	〃 , 〃	1.37	4	0.5
Lisichiton camtschatcense	〃 , 〃	6.45	25	0.5
Veratrum stamineum	〃 , 〃	4.35	30	0.01
〃	Mt. Shibutsu	2.71	8	0.05
Narthecium asiaticum	Ozegahara, bog	1.98	10	0.1
Iris laevigata	〃 , 〃	1.63	4	0.05

out the different distribution of rubidium and cesium in natural plants and deals with the discussion of the different nature of these elements in the biological cycle from soil to plant.

Distribution of Rubidium and Cesium in Natural Plants.—The distribution studies on the rare alkali elements in soil, plants, and waters have been carried out and reported by one of the authors[5]. Sixty-one samples of natural plants consisting of fifty different species were collected from various districts in Japan and analyzed for leaves by a spectrographic method by use of cathode-layer arc excitation. The plant species consist of two mosses, seven ferns, five gymnosperms, and eleven monocotyledons, the rest being dicotyledons. The analytical data are summarized in Table I. Rubidium varied from 0.6 to 50 p.p.m. and cesium from 0.002 to 1 p.p.m. on the dried material.

The determination of rubidium and cesium in plants has been reported by G. Bertrand and D. Bertrand[6]. The values for land plants examined by them ranged from 2.1 to 81 (average, 20.3) p.p.m. of rubidium and from 3 to 88.5 (average, 22) p.p.m. of cesium for phanerogams on the dried material. The values for rubidium are in good agreement with those given by the authors; however, the values for cesium given by Bertrand et al. are an order similar to the values for rubidium, showing surprisingly high values. Recently, Smales and Salmon analysed seaweed and the ratios of $0.55\sim1.4\times10^{-2}$ (average, 1.0×10^{-2}) were given for the ratio Cs/Rb[7]. Rubidium is more abundant than cesium by factors of approximately 100 in rocks, soils, seaweeds, and other natural materials; the land plants could not be the only exception. The result of the authors' determination indicates the variation of the Cs/Rb ratio from 2×10^{-4} to 2×10^{-1} and the average 3×10^{-2}.

Relationships between the potassium content and the rubidium or the cesium content of natural plants were examined;

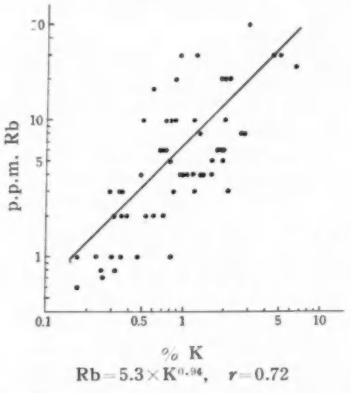

$Rb=5.3\times K^{0.94}$, $r=0.72$

Fig. 1. Relation between potassium and rubidium contents of natural plant.

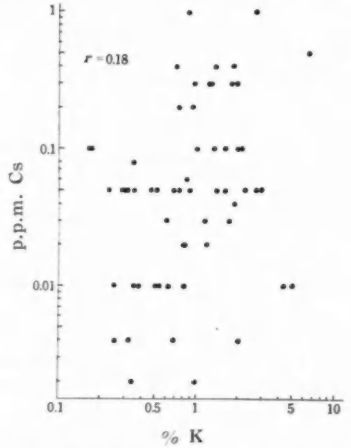

Fig. 2. Relation between potassium and cesium contents of natural plant.

5) N. Yamagata, *J. Chem. Soc. Japan, Pure Chem. Sec.* (*Nippon Kagaku Zasshi*), **71**, 288, 567 (1950); **72**, 154, 157, 247, 299, 530, 610, 753 (1951); N. Yamagata and T. Kurobe, ibid., **72**, 944 (1951).

6) G. Bertrand and D. Bertrand, *Compt. rend.*, **219**, 325 (1944); **229**, 453 (1949).

7) A. A. Smales and L. Salmon, *Analyst*, **80**, 37 (1955).

TABLE II
RUBIDIUM AND CESIUM CONTENTS OF SOIL IN JAPAN
(Dry basis, hot conc. HCl soluble)

Soil Type	Location	K %	Rb p.p.m.	Cs p.p.m.
Kwantō loam	Meguro, Tokyo	0.04	0.8	0.02~0.2
〃 , uppon layer	Nishigahara, Tokyo	0.05	0.8	0.1 ~1
〃 , lower layer	〃 〃	0.04	0.6	0.01~0.1
Volcanic ashy soil	Hokkaido	0.02	0.3	0.06~0.6
Bog soil, upper layer	Aomori Pref.	0.13	20	0.5
Meadow soil, upper layer	Akita Pref.	0.08	8	0.1 ~1
〃 , middle layer	〃	0.07	40	0.4
〃 , lower layer	〃	0.05	10	0.2
Volcanic ashy soil	Ibaragi Pref.	0.01	2	0.03
Tertiary diluvium, upper layer	Aichi Pref.	0.04	3	0.03~0.3
〃 lower layer	〃	0.06	10	0.2
Alluvial paddy soil	Shiga Pref.	0.11	80	0.3 ~3
Granitic alluvium	Shiga Pref.	0.07	20	0.2 ~2
Sandy alluvium (I)	Kagawa Pref.	0.07	10	0.03
〃 (II)	〃	0.07	2	0.04~0.4
Average		0.06	14	(0.3)

the Rb/K ratio varied from 1.2×10^{-4} to 3.2×10^{-3} and the average was 7.3×10^{-4} for sixty-one samples. The variation of Cs/K ratio was greater than that of Rb/K and covered from 2×10^{-6} to 1×10^{-3}. Fig. 1 is a plot in logarithmic scale of the potassium content in percent versus the rubidium content in p.p.m. The existence of a linear relationship between rubidium and potassium contents can easily be seen; the coefficient of correlation (r) is 0.72. Fig. 2 is a plot in logarithmic scale of the potassium versus the cesium content. In this case, the existence of a linear relationship is doubtful (r=0.18). The coefficient of correlation between rubidium and cesium contents was also calculated and the value of 0.0073 appears to indicate no relation between the contents of these elements in the examined plants.

The variation of the Cs/K ratio greater than the Rb/K ratio and the doubtful existence of correlation between cesium and potassium contents may be accounted for by one or several reasons as under described.

(1) The variation of total cesium content of the soils on which the plants were growing is greater than that of rubidium.

(2) The uptake of cesium into the aerial portions of the plants is irregular as compared with that of rubidium; for example, the uptake tends to increase at the higher concentrations of cesium in soil solution.

(3) The ion-exchange or adsorption mechanism between soil and solution that makes the release of cesium and rubidium for soil colloids and minerals is different.

Distribution of Rubidium and Cesium in Soil.—Soils usually contain 20~500[8] or 5~100 (average, 60[9] or 100[10]) p.p.m. of total rubidium and only less than 1 to 25.7 (max.) p.p.m.[8] of total cesium in contrast with 1.36% of total potassium on the average[9]. Although the data for cesium are too incomplete to guess the average content, Vinogradov gave a value of approximately 5 p.p.m.[9,10]. The average ratio of Rb/K is $4\sim7\times10^{-3}$ and the average Cs/K is approximately 4×10^{-4}. Those data appear to be reasonable in accordance with Horstman's recent work[11]. He gave 240~460 for the average ratios K/Rb of various rocks (Rb/K=$2.2\sim4.2\times10^{-3}$) and 6700 for K/Cs of granitic rocks (Cs/K=1.5×10^{-4}). On the weathering of rocks, absolute loss of the three elements occurs with the fastest leaching and the least adsorption of potassium, as the result, the ratios of Rb/K and Cs/K increase. However, the above-mentioned data indicate that soils differ not so much from fresh rocks in the averaged ratios of Rb/K and Cs/K.

No biological activities can ever extend to the complete decomposition of soil forming silicate minerals, although the total elements existing in soil are reserved

8) D. J. Swaine, "Trace-Element Content of Soils", Commonwealth Bureau of Soil Sci. Tech. Comm., No 48 (1955) p. 34, 88.
9) V. I. Vernadsky, "Selected Papers" (in Russian), ed. by A. P. Vinogradov, Acad. Sci. U. S. S. R. Moscow (1954) Vol. I, p. 365.
10) A. P. Vinogradov, "Geochemistry of Rare and Disperse Chemical Elements in Soil" (in Russian), Acad. Sci. U. S. S. R. Moscow (1957) p. 86-94, 216.
11) E. L. Horstman, *Geochim. et. Cosmochim. Acta*, 12. 1-28 (1957).

for living matter to be utilized in far future. In this respect, we often consider the amount of elements extractable with mineral acid as a measure for the availability by plants in the near future.

Fifteen representative Japanese soils were extracted with hot hydrochloric acid (31%) and analyzed; the result[12] has been recalculated and summarized in Table II. The variation of rubidium and cesium covered from 0.3 to 80 and from 0.01 to 3 p.p.m. respectively when potassium varied from 0.01 to 0.13%. The Rb/K ratio varied from 1.5×10^{-3} to 7×10^{-2} and the Cs/K ratio varied from 4×10^{-5} to 1×10^{-3}. These values indicate that the variations of levels of rubidium and cesium in soil are of the same order and it appears to us that the first reason (1) for the different distribution of these elements in natural plants fails to elucidate the fact.

Culture Experiment.—Many investigators carried out the culture experiments with solutions of various concentrations of rubidium and cesium; an example is shown in Table III. When the uptake by natural or cultivated plants growing in soil comes into question, we must consider the natural levels of rubidium and cesium concentrations in soil. Indeed, the culture experiment with higher concentrations may serve for certain physiological purposes, however, for the present purpose, it will be desirable to make the levels of these elements in culture solution as close as possible to those in natural soil conditions.

TABLE III
RUBIDIUM, CESIUM AND POTASSIUM LEVELS IN CULTURE SOLUTION USED BY SEVERAL INVESTIGATORS

	Rb meq./l.	Cs meq./l.	K meq./l.
Collander[11]	0.1 2	0.1	2
Menzel and Heald[13]	0.054 0.0054	0.054 0.0054	0.54
Murphy et al.[14]	Rb/K (weight) 1/1, 1/2, 1/5, 1/10		

It is not the total or acid soluble but only a fraction of the elements that the root of a plant can readily absorb. It is well known that rubidium and cesium are more firmly held by the clay fraction of soil than potassium, probably on account of their greater ionic polarizability. We can therefore assume that the Rb/K and the Cs/K ratios in the neutral ammonium acetate extract of soil or in the actual soil solution are probably smaller respectively than the ratios of the total or strong acid soluble elements in soil.

As the concentrations of available or active rubidium and cesium in soil had not been estimated when the present cultue experiment was undertaken, the standard ratios of Rb/K and Cs/K were temporarily fixed to approximately 10^{-2} and 2×10^{-4} respectively except where varied as an experimental condition.

Experimental

The experiment was conducted in a greenhouse and cucumber, rice-plant, and soy-bean were chosen for the experiment plants. The seedlings were grown in nutrient solutions in 3 liter porcelain pots from 3rd July to 11th July when tracer isotopes were added. After that, a long period experiment was carried on for thirty days with occasional renewal of nutrient solution and radio isotopes.

The culture solution was prepared with extra pure chemicals and distilled water; the elementary composition was as follows[15]: (p.p.m. in solution)

NO_3-N: 130, NH_4-N: 23, K: 200, Ca: 200, Na: 20, Mg: 40, Si: 20, P: 50, Cl: 20, S: 50, Fe: 2, Mn: 0.4, B: 0.4, Zn: 0.4, Cu: 0.04, Mo: 0.002.

Two isotopes ^{137}Cs and ^{86}Rb were added together in a concentration of about 10 μc/l. each of nutrient solution. Another experiment to determine the uptake velocity of these elements by plants in a short period was conducted with higher concentrations of isotopes.

The harvested plant leaves were incinerated and counted for the total activity of ^{137}Cs and ^{86}Rb. After thirty-nine days the sample was recounted for the activity. As the difference was to be ascribed to the decay of a short-lived isotope ^{86}Rb (half-life: 19.5 days), each of the activities of these isotopes could be calculated. After the activity determination, the plant ash was analyzed for potassium by a chemical method. The ratio of counts from ^{137}Cs (or ^{86}Rb) and concentration of potassium in the plant were compared with the same ratio in the culture solution. The distribution factors between plant and solution were calculated by dividing the two ratios: (^{86}Rb/K in plant)/(^{86}Rb/K in solution) for rubidium, and (^{137}Cs/K in plant)/(^{137}Cs/K in solution) for cesium.

12) N. Yamagata, *J. Chem. Soc. Japan, Pure Chem. Sec.* (*Nippon Kagaku Zasshi*), **71**, 567 (1950).
13) R. G. Menzel and W. R. Heald, *Soil Sci.*, **80**, 287 (1955).
14) W. S. Murphy, A. H. Hunter and P. F. Pratt, *Soil Sci. Soc. Amer. Proc.*, **19**, 433 (1955).
15) N. Yamagata and T. Yamagata, Culture experiment with a universal solution. Presented at the Annual Meeting of the Society of the Science of Soil and Manure, Tokyo, Apr., 1958.

Results

A short period experiment was performed to examine whether there were any differences between rubidium and cesium of the transport velocity into the aerial part. The result of the experiment is shown for rice-plant (Fig. 3). The transport velocity is represented by plotting the increase of distribution factors against time, consequently, it does represent an increase of rubidium or cesium in the plant not absolutely but relatively to potassium. Rapid absorption is observed in several early hours and steeper slope for rubidium appears to indicate faster transport in the plant or rubidium than of cesium at the early stage of absorption, although the difference between these elements will have no connection with the absorption during the prolonged period.

A long period experiment was conducted with the three crop plants over a range of concentrations of rubidium and cesium from 0.02 to 20 and about 0.0001 to 4 p.p.m. respectively. The results are shown in Table IV. The effect of concentration was not clear except for rubidium in the case of soy-bean. The relatively small variation of distribution factors with concentration in nutrient solution indicates that the effect of concentration on rubidium and cesium uptake relative to potassium is small, by a factor of two or three at most. The results also indicate that a difference exists between plant species. It can be seen that the distribution factor for cesium is greater in leaves than roots only in the case of soy-bean. The rice-plant accumulates less cesium relative to potassium than the other plants. These results are in good agreement with Rediske and Selders' experiement with several other crop plants[16].

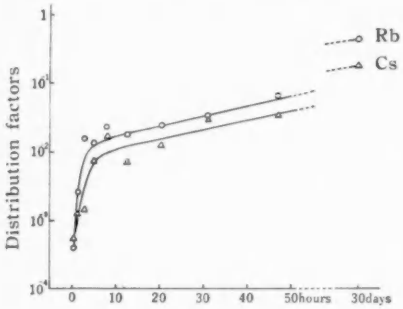

Fig. 3. Uptake velocity of cesium and rubidium by rice-plant as represented by distribution factor between solution and plant leaf.

Distribution of Rubidium and Cesium in Tobacco Leaf.—The analytical data for the distribution of the alkali elements in cultivated tobacco leaves were previously presented by one of the authors[17]. The recorded value for rubidium varied from 5 to 90 p.p.m. on the dried material and the average was 30 p.p.m. The Rb/K ratio varied from 5×10^{-4} to 3×10^{-3} and the average was 1×10^{-3}; these values are in good agreement with those of the natural plants.

On the other hand, the concentration of cesium in tobacco leaves was very low and for this reason it was only successfully determined quantitatively for one sample among seventeen (No. 10a in the original paper). This sample contained 0.17 p.p.m. cesium in ash or 0.02 p.p.m. in the dried material, and the Cs/K ratio for the whole leaf was 1.2×10^{-6}. The Cs/K ratios for the rest of the sample are considered to be less than this value. It can thus be concluded that the Cs/K ratios for cultivated tobacco leaves are surprisingly low as compared with those for the natural plants ($2\times10^{-6}\sim1\times10^{-3}$).

According to the experiment conducted by Menzel[18], the uptake of rubidium and cesium by plants was inversely proportional to the available potassium in the soil, and the uptake of cesium was more affected than that of rubidium by the increase in available potassium. Thus, the remarkable discrimination in the cultivated tobacco plant of cesium from potassium will be accounted for by the possible existence of a greater quantity of available potassium in the soil as compared with the case of natural plants.

Another interesting phenomenon should be pointed out, that of the different distribution with in the tobacco leaf of cesium from rubidium and potassium. The tobacco leaf was divided into two portions, the principal vein and the remaining part, and separately analyzed. Qualitative examination indicated in every sample of tobacco leaves the considerable enrichment of potassium and rubidium in the vein and the inverse trend for cesium. Quantitative determinaion was made with the tobacco leaf No. 10a and the result is

16) J. H. Rediske and A. A. Selders, *U. S. Atomic Energy Comm.*, HW-35174 (1953).
17) N. Yamagata, *J. Chem. Soc. Japan, Pure Chem. Sec.* (*Nippon Kagaku Zasshi*), **71**, 288 (1950).
18) R. G. Menzel, *Soil Sci.*, **77**, 419 (1954).

TABLE IV

DISTRIBUTION FACTORS FOR Rb-K AND FOR Cs-K IN LEAF AND ROOT OF PLANTS OF SEVERAL CROP SPECIES

(K: 200 p.p.m. in nutrient solution)

Pot No.	Ratios in Nutrient soln. (in weight)		Part	Distribution Factors					
				Cucumber		Rice-plant		Soy-bean	
	Rb/K	Cs/K		Rb/K	Cs/K	Rb/K	Cs/K	Rb/K	Cs/K
1	10^{-4}	5×10^{-7}	L	0.30	0.66	0.35	0.31	0.17	0.40
			R	*0.14*	*0.62*	*0.26*	*0.33*	*0.72*	*0.28*
2	10^{-3}	2×10^{-5}	L	0.56	0.91	0.57	0.23	0.24	0.82
			R	*0.13*	*1.75*	*0.50*	*0.49*	*0.65*	*0.40*
3 (standard)	10^{-2}	2×10^{-4}	L	0.32	0.40	0.45	0.18	0.39	0.54
			R	*0.18*	*0.81*	*0.45*	*0.46*	*0.65*	*0.33*
4	10^{-1}	2×10^{-3}	L	0.50	0.52	0.88	0.57	0.48	0.57
			R	*0.30*	*1.25*	*0.32*	*0.25*	*0.42*	*0.30*
5	10^{-2}	2×10^{-2}	L	0.72	0.57	0.17	0.15	0.72	0.72
			R	*0.35*	*0.76*	*0.22*	*0.58*	*0.24*	*0.33*
Average			L	0.48	0.61	0.48	0.29	0.40	0.61
			R	*0.22*	*1.04*	*0.35*	*0.42*	*0.54*	*0.33*

TABLE V

THE DIFFERENT DISTRIBUTION IN TOBACCO LEAF OF CESIUM FROM RUBIDIUM AND POTASSIUM

(Sample No. 10a, recalculated from the previous report[17])

	K %	Rb p.p.m.	Cs p.p.m.	Rb/K	Cs/K
Whole leaf	1.77	40	0.02	2×10^{-3}	1.2×10^{-6}
Principal vein	3.70	90	0.006	2.5×10^{-3}	1.5×10^{-7}
The remaining part	1.35	20	0.02	1.5×10^{-3}	1.5×10^{-6}

shown in Table V. The Rb/K ratio is similar in the principal vein and in the rest. On the other hand, the Cs/K ratio in the former is approximately one tenth of the ratio in the latter, that is to say, the cesium is relatively enriched in the latter as compared with potassium and rubidium. These results appear to be inconsistent with the conclusions by Glueckauf[19] who considered the possible enrichment of cesium and strontium occurring in flowers, leaf veins and root substrate.

Conclusion

1. The greater variation of cesium in natural plants than that of rubidium could not be attributed to the variations of total or acid soluble elements in the soil.

2. The relative uptake by plants of rubidium and cesium to potassium was only slightly affected by the concentrations of these elements in nutrient solution. It appears that a difference does exist between plant species in their ability to accumulate cesium and rubidium relative to potassium.

3. The greater variation of the Cs/K ratio and the doubtful existence of correlation between cesium and potassium contents of natural plants may be principally attributed to the complicated mechanisms of ion-exchange or adsorption between soil and solution.

Fixation by soils and uptake by plants of cesium have been investigated by several authors[20-22] in connection with the problems of radioactive contamination from nuclear fission explosions and also with a view to the ultimate disposal of fission products. The fate of cesium-137 in the biogeochemical cycle from soil to plant has usually been considered likely to follow that of potassium. This appears not to be true after both the results ascertained by us and other investigators. When consideration is taken of the difference of the ionic radii between rubidium (1.49Å) and cesium (1.63Å), we can not expect that cesium can replace potassium (1.33Å) as freely as rubidium does. In this regard, the concept of the "Cesium Unit" temporarily adopted by U.N. authorities to evaluate the concentration of cesium-137 in natural

19) E. Glueckauf, *Atomic Energy Research Establishment*, Harwell, **SPAR/7** (1956).

20) C. B. Amphlett, *Research*, **8**, 335 (1955).

21) C. B. Amphlett and L. A. McDonald, *J. Inorg. & Nuclear Chem.*, **2**, 403 (1956).

22) H. Nishita et al., *Soil Sci.*, **81**, 317 (1956).

materials relatively to potassium has little meaning. We believe that the future burden of mankind with radioactive cesium-137 will properly be estimated on the basis of the concept of isotopic dilution.

Kiriu College of Technology
Gunma University, Kiriu

Stereochemistry of Some Steroidal Ketones

By Ken-ichi MORITA

(Received November 12, 1958)

According to Barton's rule[1a] for calculating the relative degrees of steric hindrance of carbonyl groups, the degree of steric hindrance of a $C_{(6)}$-carbonyl group must be the same whether it is in a 5α-steroid or in a 5β-steroid[2]. However, the fact that reduction of a $C_{(6)}$-carbonyl group in a 5α-steroid (I) with lithium aluminum hydride gives exclusively an axial isomer[3] whereas reduction of a $C_{(6)}$-carbonyl group in a 5β-steroid (II) with the same reagent gives a considerable amount of an equatorial isomer[4] suggests[1b,5] that the degrees of steric hindrance of the two carbonyl groups may be different. In the two compounds, the geometrical circumstances around the carbonyl groups are equal except the $C_{(4)}$-methylene groups (see I and II). The expressions A and B show the views[6] looking down the $C_{(5)}$-$C_{(6)}$-axes of a 5α-6-ketone (I) and a 5β-6-ketone (II), respectively. The angle between the $C_{(6)}$-oxo-group and the $C_{(4)}$-methylene group is much greater in II than in I. The interaction between the oxo-group and the $C_{(4)}$-methylene group may be smaller in II than in I. Thus the oxo-group in II must be less hindered[7]. This postulation is well in line with the results of the hydride reduction, if we accept the generalization[1b,5] that the more hindered ketone gives the more axial hydroxyl group by lithium aluminum hydride reduction.

This view may be extended to carbonyl groups in other positions. As far as the steroid nucleus of 5α-series is concerned, the angular methyl groups at positions $C_{(10)}$ and $C_{(13)}$ are axial with respect to A and C ring, respectively. Therefore the degrees of steric hindrance of the carbonyl groups at positions $C_{(1)}$ and $C_{(12)}$ may be less[8] than Barton's degree[1a]. If we

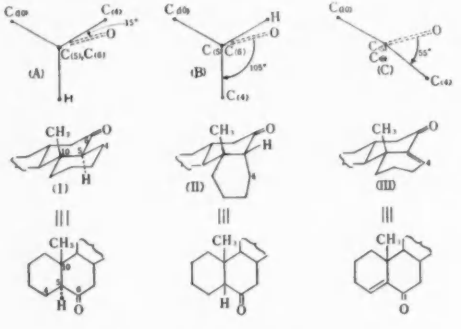

1) D. H. R. Barton, *J. Chem. Soc.*, **1953**, 1027, (a) p. 1034, (b) p. 1029 footnote 23.
2) Barton has stated that systems having cis-fused rings may prove more complex.
3) C. W. Shoppee and G. H. R. Summers, *J. Chem. Soc.*, **1952**, 3361.
4) Y. Urushibara and K. Mori, This Bulletin, in press.
5) Cf. W. G. Dauben, E. J. Blanz, Jr., J. Tin and R. A. Micheli, *J. Am. Chem. Soc.*, **78**, 3752 (1956).
6) W. Klyne, *Experientia*, **12**, 119 (1956).

7) It may be noted that the conformation of 5α-6-ketone system (I) is still favored from a viewpoint of relative stability[6].
8) An axial methyl group attached at α-carbon atom may have less hindering effect than an axial methyl group attached at β-carbon atom, and steric effect by these axial methyl groups seems to be important in the intermediates. The expression D shows the necessary intermediates for the reactions with reagents like lithium aluminum hydride[9], semicarbazide, phenylhydrazines[10], and so on.

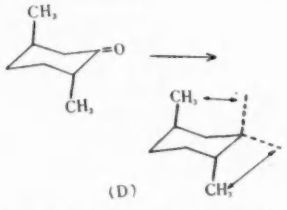

9) L. W. Trevoy and W. G. Brown, *J. Am. Chem. Soc.*, **71**, 1675 (1949).
10) See, e. g., Hammett, "Physical Organic Chemistry", McGraw-Hill Book Co., p. 333 (1940).

TABLE I

REDUCTION OF STEROIDAL KETONES WITH LITHIUM ALUMINUM HYDRIDE

Compounds	Position of carbonyl groups*	Relative degrees of steric hindrance		Products	Composition of products		Ref.
		Barton's degree	Modified degree		Equatorial (%)	Axial (%)	
cholestan-1-one	1	2^+	1^{++}	cholestan-1-ol	35	65	11
cholestan-2-one	2	1	1	cholestan-2-ol	37	52	5
cholestan-3-one	3	0	0	cholestan-3-ol	90	10	12, 13, 14
coprostan-3-one	3(5β)	0	0	coprostan-3-ol	94	4	12
cholest-5-en-3-one	3(5-ene)	0	0	cholest-5-en-3-ol	90	5	12
cholestan-4-one	4	2	2	cholestan-4-ol	7	86	15
cholest-5-en-4-one	4(5-ene)	—	less than 2	cholest-5-en-4-ol	main	—	16, 15
cholestan-6-one	6	2	2	cholestan-6-ol	6	93	3
coprostan-3, 6-dione	6(5β)	2	1^+	coprostan-3, 6-diol	considerable amount of 6α(equatorial)-compd.		4
cholest-4-en-6-one	6(4-ene)	—	less than 2	cholest-4-en-6-ol	main	—	16, 15
cholest-4-en-3β-ol-6-one acetate	6(4-ene)	—	less than 2	cholest-4-en-3β, 6-diol	75(crude)	—	17
cholestan-3β-ol-7-one acetate	7	1^+	1^+	cholestan-3β, 7-diol	45	55	5
4-chloro-17α-hydroxy-3,20-bisethylenedioxy-pregnan-11-one	11	3^+	3^+	4-chloro-11, 17α-dihydroxypregnane-3, 20-dione bisethylene-ketal	trace	90	18
25D, 5α-spirostan-3β-ol-12-one acetate	12	2^+	1^{++}	25D, 5α-spirostane-3β, 12-diol	50	50	19

* In 5α-steroids unless otherwise stated

arbitrarily indicate the degree of the steric effect by an axial substituent attached at α-carbon atom by the + sign, indicating a positive magnitude less than one unit, Barton's degrees may be modified as shown in IV (see also Table I). The results of reduction of steroidal ketones with lithium aluminum hydride (Cf. Table I) suggest[20] that the sum (indicated by the ++ sign)

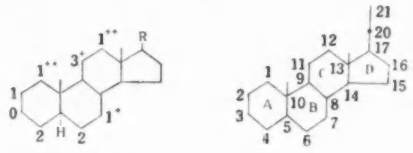

IV

of the steric effect by the γ-carbon atom which is bent round so as to hinder the carbonyl group and the steric effect by the axial substituent attached at α-carbon atom may be smaller than one unit in magnitude. If it is true, the order of relative degrees of steric hindrance of the $C_{(1)}$- or $C_{(12)}$-carbonyl group and of those of the $C_{(4)}$- or $C_{(6)}$-carbonyl group reverses in the two estimations.

Becker et al.[1,6] and Jones et al.[15] recorded that reduction of cholest-4-en-6-one with lithium aluminum hydride gave mainly cholest-4-en-6α-ol. Urushibara and Mori[17] reported that reduction of cholest-4-en-3β-ol-6-one acetate with lithium aluminum hydride gave mainly cholest-4-en-3β, 6α-diol. These facts are of interest in connection with the foregoing discussion.

11) H. B. Henbest and R. C. L. Wilson, *J. Chem. Soc.*, **1956**, 3289.
12) C. W. Shoppee and G. H. R. Summers, ibid., **1950**, 687.
13) H. R. Nace and G. L. O'Connor, *J. Am. Chem. Soc.*, **73**, 5824 (1951).
14) W. G. Dauben, R. A. Micheli and J. F. Eastham, ibid., **74**, 3852 (1952).
15) D. N. Jones, J. R. Lewis, C. W. Shoppee and G. H. R. Summers, *J. Chem. Soc.*, **1955**, 2876.
16) E. J. Becker and E. S. Wallis, *J. Org. Chem.*, **20**, 353 (1955).
17) Y. Urushibara and K. Mori, This Bulletin, in press.
18) R. H. Levin et al., *J. Am. Chem. Soc.*, **76**, 546 (1954). Cf. L. H. Sarett et al., ibid., **73**, 1777 (1951).
19) R. Hirshmann, C. S. Snoddy, Jr., C. F. Hiskey and N. L. Wendler, ibid., **76**, 4013 (1954).
20) It may be necessary to study the relative degrees of steric hindrance of t[illegible]e carbonyl groups by using carbonyl reagents such as ethyleneglycol, ethanedithiol, semicarbazide and the phenylhydrazines, etc., since the degrees of steric hindrance of the carbonyl groups may not exactly be reflected redution with lithium aluminum hydride[21].
21) Cf. K. D. Hardy and R. J. Wicker, ibid., **80**, 640 (1958).

Cholest-4-en-6-one and cholest-4-en-3β-ol-6-one acetate exhibit the maximum absorption bands at 243 mμ (ε=6,360)[22] and 236 mμ (ε=6,300)[23] in the ultraviolet region, respectively. A method of calculating the principal absorption band of α,β-unsaturated ketones was devised by Woodward[24] and was extended by Fieser and Fieser[25]. The calculated value of the absorption maximum for the 4-ene-6-ketone system is 242mμ, which is in agreement with the observed wavelengths within 6 mμ. In Woodward-Fieser-Fieser's method of calculation no steric factor is considered. We may thus assume[26] that the steric hindrance involved in the system does not cause an abnormal change in wavelength but causes a decrease in absorption intensity and is associated with the transition between the non-planar ground state and the near-planar excited state[27]. Hence, the interplanar angle θ between the $C_{(6)}$-carbonyl double bond and the 4,5-ethylenic bond in the ground state may be calculated[30] from Braude-Sondheimer's equation[26] as roughly 55°[31], if the value of intensity for the unhindered system is arbitrarily taken as 18,000[33]. The expression C shows the view looking down the $C_{(5)}$-$C_{(6)}$-axis of the 4-ene-6-ketone (III). The interaction between the carbonyl group and the $C_{(4)}$-methylene group may be smaller in III than in I; it means that the carbonyl group in III is less hindered, and then may be reduced to the stable form in a more proportion. The result of the hydride reduction corroborates the assumption. Jones et al.[15] reported that reduction of cholest-5-en-4-one, λ_{max} 242 mμ (calculated value; 242 mμ), ε=5,900, with lithium aluminum hydride gave mainly the 4α (equatorial)-hydroxy compound. This phenomenon may also be explained in a similar way ($\theta \simeq 55°$). Another example was recorded by Shapiro et al.[34] who reduced 5,16-pregnadien-3β-ol-20-one acetate with lithium aluminum hydride, obtaining the 20α-hydroxy compound (stable form). 16,17-Saturated $C_{(20)}$-ketones are exclusively reduced to 20β-isomers[35].

The author is indebted to Professor S. Mori, Tokyo Metropolitan University, Dr. M. Nakamura, Director of the Institute, and Mr. R. Mamine, the Institute, for their interest in the present study.

Sugiyama Chemical Research Institute
Mure, Mitaka, Tokyo

22) H. Reich, F. W. Walker and R. W. Collins, *J. Org. Chem.*, **16**, 1753 (1951).
23) E. R. H. Jones et al., *J. Chem. Soc.*, **1937**, 801; ibid., **1940**, 659.
24) R. B. Woodward, *J. Am. Chem. Soc.*, **63**, 1123 (1941); **64**, 76 (1942).
25) L. F. Fieser and M. Fieser, "Natural Products related to Rhenanthorene", 3rd. ed., Reinhold Publishing Corp., (1949) p. 190.
26) E. A. Braude and F. Sodheimer, *J. Chem. Soc.*, **1955**, 3754.
27) It should be noted that the wavelengths of the absorption maxima of the semicarbazone (253 mμ; ε, 7,050) and of the 2, 4-dinitrophenylhydrazone (375 mμ; ε, 24,900) of cholest-4-en-6-one are abnormally low[22,28,29] with low intensity. Steric hindrance involved in the systems seems to be strong, because of bulkiness of $=NNHCONH_2$ and $=NNHC_6H_3(NO_2)$-2,4 moieties, and to be associated with transitions between non-planar ground states and non-planar excited states.
28) L. Dorfman, *Chem. Revs.*, **53**, 86 (1953).
29) K. Hirayama, "Zikken Kagaku Koza", 1,I, Maruzen, Tokyo, (1957), p. 91, 97.
30) The rough interplanar angles for other α,β-unsaturated ketosteroids may also be calculated.
31) Turner and Voitle[32] ascribed the fact that compounds having the s-cis configuration exhibit diminished absorption intensity to the decrease in the distance separating the ends of the conjugated system.
32) R. B. Turner and D. M. Voitle, *J. Am. Chem. Soc.*, **73**, 1403 (1951).
33) Cf. K. Morita, This Bulletin, **31**, 379 (1958); see also Idem., *J. Chem. Soc. Japan, Pure Chem. Sec.* (*Nippon Kagaku Zasshi*), **78**, 1581 (1957).
34) E. L. Shapiro, D. Gould and E. B. Hershberg, *J. Am. Chem. Soc.*, **77**, 2912 (1955).
35) *Inter al.*, W. Klyne and E. Miller, *J. Chem. Soc.*, **1950**, 1972; H. Hirschmann et al., *J. Biol. Chem.*, **192**, 115 (1951); R. B. Turner and D. M. Voitle, *J. Am. Chem. Soc.*, **73**, 2283 (1951).

SHORT COMMUNICATIONS

Crystal Structures of Silicon Nitride

By Kiichi NARITA and Kenji MORI

(Received September 28, 1958)

Leslie, Carrol and Fisher[1] separated silicon nitride from nitrided silicon steel and, by studying the X-ray and the electron diffractions of the nitride, proposed an orthorhombic cell for Si_3N_4. More recently Turkdogan and Ignatowiez[2] reported that non-metallic inclusions extracted from the nitrided Iron-Silicon alloys are identical with one of the two silicon nitrides synthesized.

It has been established[2-5] that when silicon is nitrided at high temperatures varying from 1200 to 1400°C, a mixture of two phases (α and β) of nitrides is formed. Vassiliou and Wilde[3] mentioned that these two phases were regarded as orthorhombic (α) and hexagonal (β), respectively. But Popper and Ruddlesden[4] reported that one of them (β) can be indexed as rhombohedral, while both of the two phases were claimed to be hexagonal by Hardie and Jack[6]. More recently Forgeng and Decker[5] have come to the same view as Hardie and Jack's. The spacings, however, calculated by the various investigators are in good agreement with one another, notwithstanding that they differ in opinions on these two phases. Thus, it may not yet be concluded that the behavior of silicon nitride in steel is unequivocally solved.

The present authors prepared silicon nitrides in the following way and made a study on their X-ray and electron diffractions, using an electron microscope also at the same time. As it was difficult to obtain the appropriately large single crystal of silicon nitride for X-ray diffraction, the N-pattern obtained with a selected area electron diffraction was used for a study of the crystal structure of this material, in the place of the precession diagram in the X-ray diffraction study. This paper is to present a brief report of the results obtained.

The samples of silicon nitrides were prepared by heating the powdered elementary silicon in a current of ammonia* in the temperature range 1200° to 1500°C. Caution, however, was paid: at every several hours' interval the reaction product was taken out, ground into particles of about 150 mesh in size, and then submitted to the repeated reactions.

The final product is composed of the two specimens; the major part is grayish white powder, and the other of less quantity white mould growing on the former. When the mould-form product is ground, it changes into grayish white powder similar to that of the major part. It is to be noted that there is no distinguishable difference between these two specimens, as far as the X-ray diffraction spectra obtained with a diffractometer are concerned. This leads the present authors to a suggestion that both of these two specimens can be regarded as a mixture of α and β silicon nitride and others, as described below.

Table I shows the results from our studies of the X-ray diffraction (on both two specimens) and the selected area electron diffraction (on the material shown in Fig. 1). The spacings are in good agreement with those given by other investigators. One of the substances, which is more frequently found in the mould-form portion, is in the form of the flat needle as shown in Fig. 1. Its pattern of the selected area electron diffraction in the form of rectangle-shaped N-pattern is illustrated in Fig. 2. It is regarded that this pattern corresponds to the reciprocal lattice of $(11\bar{2}0)$ plane of hexagonal α-silicon nitride

1) W. C. Leslie, K. G. Carroll and R. M. Fisher, *Trans. Am. Inst. Mining Met. Engrs.*, **194**, 204 (1952).
2) E. T. Turkdogan and S. Ignatowiez, *J. Iron and Steel Inst.*, **185**, 200 (1957).
3) B. Vassiliou and F. G. Wilde, *Nature*, **179**, 435 (1957).
4) P. Popper and S. N. Ruddlesden, ibid., **179**, 1129 (1957).
5) W. D. Forgeng and B. F. Debker, *Trans. Am. Inst. Mining Met. Engrs.*, **212**, 343 (1958).
6) D. Hardie and K. H. Jack, *Nature*, **180**, 332 (1957).

* Purification of ammonia was made following the method of A. Farkas and H. W. Melville: "Experimental methods in Gas Reactions", Macmillan, London (1939), p. 162. Flow rate was regulated as 250 cc./min./3.14 cm^2.

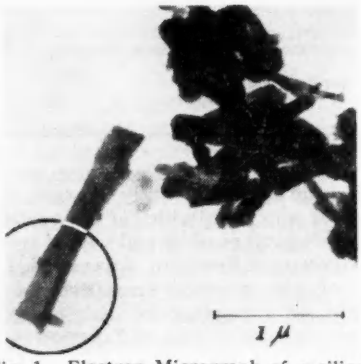

Fig. 1. Electron Micrograph of α-silicon nitride.

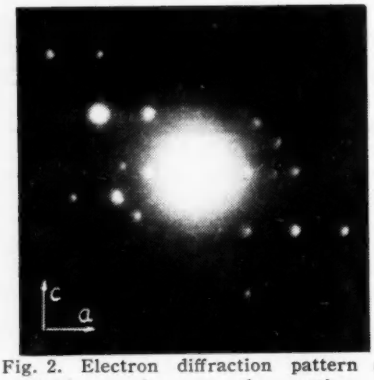

Fig. 2. Electron diffraction pattern of nitride, pertinent to the portion as enclosed by the circle in Fig. 1.

TABLE I

X-RAY DATA FOR THE SILICON NITRIDE

Electron diffraction	Diffractometer		α-Si_3N_4		β-Si_3N_4		Forgeng, Decker[5] Si_2ON	
d Obsd.	*d* Obsd.	Int.	*hkl*	*d* Calcd.	*hkl*	*d* Calcd.	*hkl*	*d*
6.68 Å	6.67 Å	13	100	6.74 Å				
	6.63	9			100	6.58 Å		
5.76			001	5.64				
	5.15	9						
	4.64	9					110	4.69 Å
	4.46	13					020	4.44
4.29	4.32	100	101	4.33				
	3.89	36	110	3.88				
	3.82	13			110	3.80		
	3.47	13						
3.34	3.37	36	200	3.37			111	3.38
	3.30	27			200	3.29		
2.84	2.89	82	201	2.89				
2.78	2.82	9	002	2.82				
	2.67	32			101	2.73	200	2.75_3
2.58	2.60	77	102	2.60				
	2.54	73	210	2.54				
	2.49	23			210	2.49		
	2.43	9					002	2.42_9
	2.39	13					201	2.39_4
	2.32	45	211	2.32	111	2.31	131	2.30_1
	2.28	9	112	2.28				
2.21	2.24	4	300	2.25			040	2.22_5
	2.18	9			201	2.19		
2.12	2.16	27	202	2.16			112	2.15_1
	2.13	5					022	2.12_9
2.05	2.08	32	301	2.08			221	2.10_7
			220	1.94				
					220	1.90		
	1.88_7	10	212	1.88_8	211	1.89_3		
1.87			003	1.88_0				
	1.86_7	13	310	1.86_5				
	1.80_8	9	103	1.81_3			202	1.81_9
	1.76_8	9	311	1.77_9			310	1.79_7
1.72	1.75_4	9	302	1.75_4	301	1.75_3	132	1.77_9

mentioned by the other investigators[5,6]. And it can not be indexed according to Leslie's[1] orthorhombic lattice.

In view of the above, the crystal structure of α-silicon nitride is regarded more likely as hexagonal. The selected area electron diffraction could not be applied to β-silicon nitride; however, considering the structure of β silicon nitride as hexagonal, as mentioned by the other investigators[5,6], the X-ray diffraction data shown in Table I can be explained as resulting from the mixture of α and β nitrides.

The parameters of these hexagonal cells of α and β silicon nitrides which are yielded from the X-ray diffraction data are as follows:

α-silicon nitride $a_0=7.76\pm0.05$ Å
$c_0=5.64\pm0.006$ Å $c/a=0.727$
β-silicon nitride $a_0=7.59\pm0.06$ Å
$c_0=2.92\pm0.008$ Å $c/a=0.385$

There are some discrepancies between the observed values for spacings obtained with the diffractometer and the calculated values. One of such discrepancies is also found in Leslie's data[1]. These discrepant spacings coincide with those of silicon oxynitride determined by Forgeng and Decker[5] as shown in Table I.

Research Department
Kobe, Steel Works, Ltd.
Fukiai-ku, Kobe

Chemical Shifts of Proton Resonance and Mesomeric Effects in Substituted Benzene

By Hiroshi SHIMIZU, Mikio KATAYAMA and Shizuo FUJIWARA

(Received December, 8, 1958)

In regard to the chemical shift phenomena of nuclear magnetic resonance, efforts have been made to correlate the observed values with the bond characters of the compounds including the resonating nuclei, and successful results have been obtained with the fluorine resonances in binary systems[1]. Further study for the dependence of the chemical shifts on the substituents in polyatomic molecules were made by Gutowsky et al. and showed that *mata* and *para* substituents in substituted fluorobenzenes produced fluorine shifts proportional, respectively, to the inductive and the resonance effects of the substituents as is inferred from chemical reactivities. They showed also that the substituent effects in polysubstituted fluorobenzenes are reasonably additive[2]. Since these results offer most valuable informations for the investigations of the reactions of simple organic molecules, further study of the problem has been made by Corio and Dailey for the proton shifts in monosubstituted benzenes[3], but the results are rather complicated and have been interpreted in terms of the polarization effects in aromatic substitution reactions.

As the last results are complicated by the electron coupling of the proton spins, we have planned here to make measurements of proton resonance in substituted benzenes at a moderate resolution, where the ring protons will give a sharp line, and to investigate the proton shifts in relation with the characters of the substituent groups. The apparatus used is the one constructed in this laboratory, being operated at 27.030 Mc and using a permanent magnet.

In the actual experiments of the measurements, each sample was mixed with cyclohexane at the ratio of 1:1 by volume and the shift was measured as the average of the separations between the sample and cyclohexane in several records. Then, as shown in Table I, the shift values were

TABLE I
CHEMICAL SHIFT OF PROTON MAGNETIC RESONANCE IN SUBSTITUTED BENZENES

Substance	Chemical shifts (ref. benzene)
C_6H_5-NO_2	+14.5±0.5 cps
-COCl	+14.5 〃
-CH_3	− 2.5 〃
-F	− 8.0 〃
-Cl	− 4.0 〃
-Br	− 3.5 〃
-I	− 0.5 〃
-OH	− 9.5 〃
-NH_2	−19.5 〃
resonance frequency:	27.030 Mc.

1) H. S. Gutowsky and C. J. Hoffman, *J. Chem. Phys.*, **19**, 1259 (1951).

2) H. S. Gutowsky, D. W. McCall, B. R. McGarvey and L. H. Meyer, *J. Am. Chem. Soc.*, **74**, 4809 (1952).

3) P. L. Corio and B. P. Dailey, ibid., **78**, 3043 (1956).

4) C. K. Ingold, "Strurcture and Mechanism in Organic Chemistry", G. Bell & Sons Ltd. (1953).

calculated taking benzene as the reference.

It is noted in Table I that there are observed very small but definite shifts for both bromo and chlorobenzene from benzene and, furthermore, our results in the table show a fine proportionality with the ability of each group to cause mesomeric effect[1].

Authors are very grateful to Professor Osamu Simamura of the University of Tokyo for valuable discussions. Our thanks are also due to Miss M. Nakahara who has made the purification of some of the samples.

University of Electrocommunications
Chofu, Tokyo

The Poisoning Effect of Lead Acetate and Quinoline

By Tosao Fukuda

(Received February 23, 1959)

As previously reported[1], when palladium-calcium carbonate catalyst was poisoned by lead acetate, the activity for the hydrogenation of 1, 4-butenediol decreased with increasing amount of lead acetate. It seems likely that, when it is poisoned by a large amount of lead acetate, the activity for the hydrogenation of 1, 4-butynediol as well as 1, 4-butenediol disappears completely. On the other hand, when palladium-calcium carbonate catalyst was poisoned by quinoline, the activity for the hydrogenation of 1, 4-butenediol disappeared almost completely, while that for the hydrogenation of 1, 4-butynediol decreased to about a half. Accordingly, it was suggested that the partial hydrogenation of 1, 4-butynediol can be achieved by using quinoline as a poison, but not by using lead acetate.

It is a well known fact that the catalyst properties may be changed complicatedly by the adsorption of the poisons[2]. It seems that the properties of palladium-calcium carbonate catalyst are also affected by the adsorption of lead acetate or quinoline. The effect of quinoline might be different from that of lead acetate. Accordingly, the partial hydrogenation of 1,4-butynediol takes place as observed.

However, it seems that the difference in the poisoning effect of lead acetate and quinoline originated also in the difference of the adsorbability between lead acetate and quinoline.

The experiments were carried out by using the aqueous solution of 1, 4-butynediol and 1, 4-butenediol, at 25°C. The concentration of 1, 4-butynediol and 1, 4-butene-

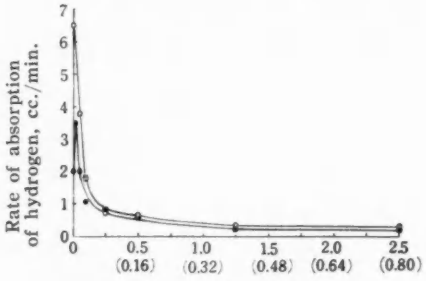

Fig. 1. The poisoning effect of acetate on the hydrogenation of 1,4-butynediol and 1,4-butenediol.
Pd-$CaCO_3$(5%) 300 mg.
Concentration of 1,4-butynediol (or 1,4-butenediol) 175 μmol./cc.
Oscilaltion 250 turns/min.
● 1,4-butynediol
○ 1,4-butenediol

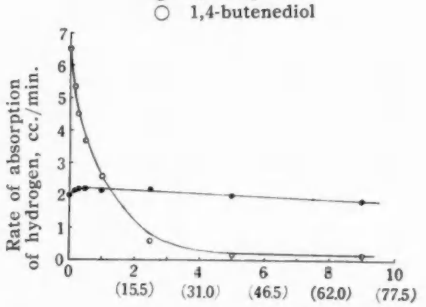

Fig. 2. The poisoning effect of quinoline on the hydrogenation of 1,4-butynediol and 1,4-butenediol.
Pd-$CaCO_3$(5%) 300 mg.
Concentration of 1,4-butynediol (or 1,4-butenediol) 175 μl./cc.
Oscillation 250 turns/min.
● 1,4-butynediol
○ 1,4-butenediol

1) T. Fukuda and T. Kusama, This Bulletin, **31**, 339 (1958).
2) R. Suhrman and K. Schultz, *Z. Phys. Chem. N. F.*, **1**, 69 (1954); W. H. Sachtler, *J. Chem. Phys.*, **25**, 751 (1956); L. E. Moore and P. W. Selwood, *J. Am. Chem. Soc.*, **78**, 697 (1956).

diol was 175 μ mol./cc. The results are shown in Fig. 1 and Fig. 2.

When lead acetate was added to the reactant, the activity of palladium-calcium carbonate catalyst disappeared almost completely with 0.4 μ mol./cc. of lead acetate. When quinoline was used with 0.4 μ mol./cc., the activity for the hydrogenation remained almost unchanged. When it was used 40 μ mol./cc. the activity for the hydrogenation of 1,4-butynediol decreased only a little, but that for the hydrogenation of 1,4-butenediol disappeared almost completely. It is interesting to note that, when the catalyst was poisoned by a small amount of quinoline, the activity for the hydrogenation of 1,4-butynediol increased at first and then decreased with increasing amount of quinoline.

When palladium-calcium carbonate catalyst was poisoned by the larger amount of lead acetate, the activity for the hydrogenation of 1,4-butynediol as well as 1,4-butenediol disappered completely. But, when it was poisoned by quinoline, the activity for the hydrogenation of 1,4-butenediol disappeared completely, while that for the hydrogenation of 1,4-butynediol decreased only a little. These results may explain clearly that lead acetate is adsorbed much more strongly than 1,4-butynediol, but quinoline is not. The catalyst properties are affected by quinoline. Quinoline might be adsorbed competitively with 1,4-butynediol and 1,4-butenediol. As a result, the hydrogenation of 1,4-butenediol is stopped by quinoline, while that of 1,4-butynediol is only retarded.

It may be concluded that the difference in the poisoning effect of lead acetate and quinoline originates also in the difference of the adsorbability between lead acetate and quinoline.

The author is grateful to Professor T. Kusama, Yokohama National University, for his unfailing kindness in encouraging this work.

Faculty of Engineering
Yokohama National University
Minami-ku, Yokohama

*Isomerization of Luciculine**

By Takashi Amiya

(Received February 25, 1959)

Lucidusculine (I) ($C_{24}H_{35}O_4N$) is one of the aconite alkaloids; upon hydrolysis it gives a trihydric amino alcohol, luciculine (II) ($C_{22}H_{33}O_3N \cdot H_2O$)[1]. In contact with palladium-carbon in the presence of hydrogen and methanol, compound II was found to isomerize to a ketone base, isoluciculine (III), m.p. 131~136C°, λ_{max} in MeOH 302 mμ, logε1.4 (*Anal.* Found: C, 71.22; H, 9.33; N, 332; H_2O, 2.33. Calcd. for $C_{22}H_{33}O_3N \cdot {}^1/_2H_2O$: C, 71.71; H, 9.30; N, 3.80; H_2O, 2.44%). Compound III showed a band at 5.82 μ in the infared spectrum, and was considered therefore to be a cyclic six-membered ketone. Since it was shown previously that a terminal methylene group exists in compound II[1], this isomerization seems to proceed similarly to that of Shimoburo base I[2], hypognavine[3] or napellonine[4,**] as follows:

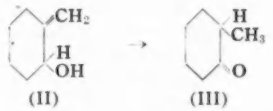

(II) (III)

On the basis of these observations, the presence of an allyl alcohol moiety in the structure of compound II may be claimed.

The author is grateful to Professor Harusada Suginome, President of Hokkaido University, for his unfailing kindness in encouraging this work.

Department of Chemistry
Faculty of Science
Hokkaido University
Sapporo

* This paper constitutes a part of a series entitled "The Aconite Alkaloids" by H. Suginome.

1) H. Suginome, T. Amiya and T. Shima, in preparation.

2) T. Sugasawa, *Pharm. Bull. Japan*, **4**, 6 (1956).

3) S. Sakai, ibid., **5**, 1 (1957).

4) K. Wiesner, Z. Valenta, J. F. King, R. K. Maudgal, L. G. Hamber and Shô Itô, *Chem. and Ind.*, **1957**, 173.

** It has been shown that napellonine is identical with Shimoburo base I[5].

5) K. Wiesner, Shô Itô and Z. Valenta, *Exper.*, **14**, 167 (1958).

Preparation of Chromium-51 of a High Specific Activity by the Szilard-Chalmers Process

By Nagao SHIBATA and Kenji YOSHIHARA

(Received January 16, 1959)

High specific activity ^{51}Cr has been prepared by neutron irradiation of electromagnetically enriched ^{50}Cr in a pile[1]; but this method offered only a small enrichment factor (about 23). The Szilard-Chalmers process of chromate or dichromate was investigated by Green and Maddock[2], and by Kahn, Freedman and Bryant[3], and it was found that about 30% and 8% tervalent chromium were formed from chromate, and dichromate, respectively (crystalline in both cases). This effect is applicable to the enrichment of ^{51}Cr but the yield is not very high.

In this paper, the authors studied the preparation of high specific activity ^{51}Cr by the Szilard-Chalmers process of neutron-irradiated, highly stable dye, Palatine Fast Blue GGN (Fig. 1), and succeeded in preparing highly enriched ^{51}Cr with a high yield.

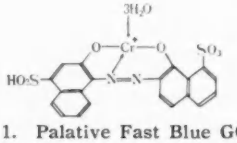

Fig. 1. Palative Fast Blue GGN.

This dye is water-soluble and slightly acid. It has an affinity to an anion- but not to a cation- exchange resin, whilst tervalent chromium is caught by the latter. The present separation is based on this difference.

The dye which was irradiated in the reactor, JRR-1 (neutron flux: 4×10^{11} n/cm^2 sec.), was dissolved in 0.01 N hydrochloric acid, passed through a resin column (10 mm. $\phi\times100$ mm. of Diaion SK#1, 100—200 mesh), and the column was washed with a sufficient volume of distilled water till the effluent became colorless. Then hydrochloric acid of various concentrations was passed through the column. The ^{51}Cr on the resin was eluted dy this procedure. Elution curve is shown in Fig. 2 in which many peaks appear. As the sample is dissolved in hydrochloric acid, complicated chloro-complexes of chromium may be formed. When the histogram is compared with the elution curves of a few chloro-aquo chromium ions, the first peak in Fig. 2 seems to be ascribed to the dichloro-tetra-aquo, the second to the monochloro-penta-aquo, and the third to the hexa-aquo chromium ion. It is not clear to which chemical forms the fourth and the fifth portion are to be assigned, but they were co-precipitated together with tervalent chromium. Thus 77~83% of the total activity was eluted from the resin in cationic forms.

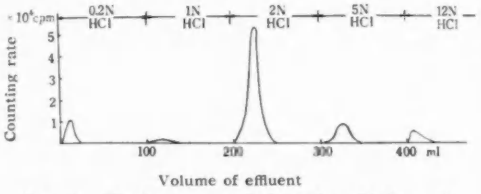

Fig. 2. Elution curve of chromium-51 formed in Palative Fast Blue GGN by hydrochloric acid.

Harbottle[4] investigated the Szilard-Chalmers process of some tervalent chromium salts, and found that about 10% of the neutron-captured atoms are present in sexivalent form. In the present case, whether tervalent chromium of Palatine Fast Blue GGN is oxidized to sexivalent or not was investigated as follows. Pottasium chromate carrier was added to the dye solution which had passed through the cation exchanger, as well as tervalent chromium as hold-back carrier. Lead acetate solution was added to this mixture to precipitate chromate as lead chromate. The activity observed in the procipitates was about 6 to 8% of the total activity. It is considered that this quantity corresponds to that of chromate formed on the present nuclear transformations.

For the preparation of high specific activity ^{51}Cr, it is considered to be convenient to utilize tervalent chromium which is caught by the cation exchanger, because it is difficult to separate the anionic part of chromium from the dye and from the contaminating activities (^{35}S and ^{32}P formed from the sulfonic sulfur).

1) Oak Ridge National Laboratory; "Radioisotopes, Special Material and Services".
2) J. H. Green and A. G. Maddock, *Nature*, **164**, 788 (1949).
3) M. Kahn, A. J. Freedman and E. A. Bryant, AECU-2329 (1949).
4) G. Harbbottle, *J. Chem. Phys.*, **22**, 1038 (1954).

The solution of neutron irradiated dye is passed through the cation exchanger column, and the column is washed with distilled water sufficiently. Tervalent chromium absorbed on the column is eluted by 200 ml. of 5N hydrochloric acid. Then, sulfric acid is added to the effluent and the mixture is dried up. This must be repeated decompose of micro quantities of organic substances. Then the sample is treated with silver peroxide to oxidise tervalent chromium to chromate. The product is sufficiently pure and impure activities were not detected by the inspection of its γ-ray spectrum and decay curve (by the Geiger tube). The yield is 69 to 75%, and the enrichment factor is 915 for 15 hr. irradiation and is 1150 for 5 hr. irradiation. This preparation method of enriched ^{51}Cr is considered to be useful. And the hot-atom chemistry of chromium complexes of diazo-compounds in detail is to be published at hand.

The authors wish to express their acknowledgement to Dr. K. Kimura for his kind encouragement and to Dr. T. Ishimori for his valuable suggestions and to Mr. I. Okubo for his helpful opinions.

Division of Isotope Applications
Japan Atomic Energy
Research Institute
Tokai, Ibaraki

Self-diffusion of Benzene under Pressure

By Hiroyuki HIRAOKA

(Received February 9, 1959)

Most of the works on diffusion in liquids have been made at atmospheric pressure. At atmospheric pressure, however, both the temperature and the density are varying simultaneously and so it is impossible to separate the effects of these two factors on diffusion. There has been no attempt to separate the two effects on self-diffusion of organic liquids except carbon tetrachloride[1] and carbon disulfide[2]. In advance of the present work, diffusion of iodine and sulfur in benzene under pressure was studied[3]. In this communication a study on the self-diffusion of benzene under pressure is presented.

Diffusion was measured by the capillary-cell method. The diffusion cells were accurately calibrated capillaries about 4 cm. in length and 0.02 ml. in volume and were filled with benzene containing carbon-14 sufficient to give 1900 counts per minute in a counting system used. The cells were immersed in a reservoir of pure inactive benzene in a thermostat constant to ± 0.01 °C. Diffusion was allowed to proceed for about 3 days, after which benzen in the cell was transferred into a combustion apparatus by a gas-phase sampling technique and was converted into barium carbonate by wet combustion method. The activity was measured by an α-β-γ proportional counter. Three to six determinations were carried out at each experimental conditions and the maximum deviation occurred was as large as 3.5 per cent from the mean. The results were presented in Table I with Graupner's data[4] at atmospheric pressure.

According to Eyring's theory[5], if the mechanism of activation in diffusion can be assumed identical with that of viscous flow, the relation between self-diffusion coefficient and viscosity in liquids is given by

$$D\eta/kT = \lambda_1/(\lambda_2\lambda_3) \qquad (1)$$

where the common notation is used. The constancy of the values of $D\eta/kT$ is shown in Table I, where at 35°C the values of λ_1 and $(\lambda_2\lambda_3)^{1/2}$, obtained on the assumption that $\lambda_1\lambda_2\lambda_3$ is equal to the mean molecular volume, are also given. The distance between two adjacent layers of graphite is 3.40 Å and the molecular diameter of benzene is 4.96 Å, and thus the values of λ_1 and $(\lambda_2\lambda_3)^{1/2}$ agree fairly well with the known dimensions of the molecule. From the self-diffusion coefficient of carbon-tetrachloloride determined by Hildebrand et al., $\lambda_1 = 2.24$ Å and $(\lambda_2\lambda_3)^{1/2} = 8.48$ Å at 25°C is obtained with the same assumption as used above. Although benzene is particularly amenable to Eyring's theory, because its geometry should lead to diffusion preferentially in the direction of benzene ring plane, it is strange that in the case

1) H. Watts, B. J. Alder and J. H. Hildebrand, *J. Chem. Phys.*, **23**, 659 (1955).
2) R. C. Koeller and H. G. Drickamer, ibid., **21**, 267 (1953).
3) H. Hiraoka, to be published in *J. Chem. Soc. Japan, Ind. Chem. Sec.* (*Kogyo Kagaku Zasshi*), **62** (1959).
4) K. Graupner and E. R. S. Winter, *J. Chem. Soc.*, **1952**, 1145.
5) S. Glasstone, K. J. Laidler and H. Eyring, "The Theory of Rate Processes", McGraw-Hill Co., New York, (1941), p. 477.

Table I

SELF-DIFFIUSION COEFFICIENTS OF BENZENE

	Temp. (°C)									
	15		25		35				45	
Pressure	$D\times10^5$	$D\eta/kT\times10^6$	$D\times10^5$	$D\eta/kT\times10^6$	$D\times10^5$	$D\eta/kT\times10^6$	λ_1	$(\lambda_2\lambda_3)^{1/2}$	$D\times10^5$	$D\eta/kT\times10^6$
(kg/cm²)	$\left(\frac{cm^2}{sec.}\right)$	$\left(\frac{1}{cm^2}\right)$	$\left(\frac{cm^2}{sec.}\right)$	$\left(\frac{1}{cm.}\right)$	$\left(\frac{cm^2}{sec.}\right)$	$\left(\frac{1}{cm.}\right)$	(Å)	(Å)	$\left(\frac{cm^2}{sec.}\right)$	$\left(\frac{1}{cm.}\right)$
1.03	1.83	3.23	2.13	3.12	2.42	2.99	2.12	8.42	2.86	3.00
	1.88[a]		2.15[a]		2.40[a]				2.67[a]	
250	1.47	3.19	1.69	3.02	1.97	2.96	2.09	8.39	2.29	2.93
500			1.39	3.04	1.59	2.92	2.06	8.38	—	—
660									1.64	2.88

a) ref. 4)

of carbontetrachloride λ_1 is much smaller than $(\lambda_2\lambda_3)^{1/2}$. It can not be concluded that the valuse of λ_1 and $(\lambda_2\lambda_3)^{1/2}$ thus calculated are true dimensions in liquid state, as Partington et al.[6] and other investigators did.

The relation between the experimental activation energy of diffusion at a constant volume, E_v, and the experimental activation energy at a constant pressure, E_p, is given by

$$E_v = E_p + (RT^2)(\alpha/\beta)(\partial \ln D/\partial P)_T \quad (2)$$

where α is the isobaric expansion coefficient and β the isothermal compressibility. From the values in Table I the following results are obtained: $E_p = 2{,}780$ cal./mole, $(RT^2)(\alpha/\beta)(\partial P \ln D/\partial)_T = 2{,}000$ cal./mole, $E_v = 780$ cal./mole. According to Eyring, the increase of internal energy for the activation process, ΔE^*, is given by

$$\Delta E^* = E_v - RT \quad (3)$$

This gives the value $\Delta E^* = 170$ cal./mole, which is so small that it is difficult to consider any high potential barrier for diffusion in benzene.

The author wishes to express his appreciation to Dr. Jiro Osugi for his interst in this work.

Department of Chemistry
Faculty of Science
Kyoto University
Sakyo-ku, Kyoto

6) J. R. Partington, R. F. Hudson and K. W. Bagnall, *J. Chem. Phys.*, **55**, 77 (1958).